1-1-1998

# Macrocyclic polymers from cyclic oligomers of poly(butylene terephthalate).

Samuel Miller
*University of Massachusetts Amherst*

# MACROCYCLIC POLYMERS FROM CYCLIC OLIGOMERS OF POLY(BUTYLENE TEREPHTHALATE)

A Dissertation Presented

by

SAMUEL MILLER

Submitted to the Graduate School of the
University of Massachusetts Amherst in partial fulfillment
of the requirements for the degree of

DOCTOR OF PHILOSOPHY

May 1998

Polymer Science and Engineering

# MACROCYCLIC POLYMERS FROM CYCLIC OLIGOMERS OF POLY(BUTYLENE TEREPHTHALATE)

A Dissertation Presented

by

SAMUEL MILLER

Approved as to style and content by:

William J. MacKnight, Chair

Roger P. Kambour, Member

James A. Donovan, Member

Richard J. Farris, Department Head
Polymer Science and Engineering

This work is dedicated with love to my wife of 25 years,

Marlene M. Miller,

for her continuing support and perseverance.

# ACKNOWLEDGEMENTS

I wish to thank Dr. Roger P. Kambour, who has been a friend and mentor for over twenty five years, for encouraging me to return to graduate school and pursue this degree under his guidance and supervision. His continuing quest for scientific truths, his careful attention to details, and his constant admonitions that sound science must be irrefutable, have provided a standard against which I shall try to measure my future scientific career.

A special thanks is given to Dr. William J. MacKnight for inviting me to enter the academic curriculum after an extended period in industry, and serving as chair of my thesis committee. The university experience has been much more rewarding by virtue of his continuing support, respect, and encouragement in reaching my academic goal.

And thanks to Dr. James A. Donovan for serving on my thesis committee and giving a fresh approach to the mechanical aspects of the work. As a mechanical engineer with an interest in polymeric materials, he has provided me with a broader outlook for interpreting the fundamental results in this work.

I also wish to thank Dr. Jean M. Heuschen for granting and securing the GE Leave of Absence which has allowed me to pursue this degree, and Dr. Frank J. Williams for providing the facilities and environment in which to conduct the research.

Many people have given their support through helpful technical discussions, assistance with laboratory equipment and analysis, and proof reading this document. While I cannot thank them all, I would like to acknowledge help from T. Banach, A. Boulares, P. Buckley, D. Brunelle, J. Carnahan, B. Crawford, D. LeGrand, P. Gundlach, S. Hobbs, P. Howson, G. Hutchens, J. Kelley, R. Kody, B. Miller, P. Rangaradjin, W. Richards, J. Serth-Guzzo, P. Sorrenson, T. Takekoshi, M. Takemori, M. Todt, K. Truby, S. Talibudden, L. Williams, and P. Wilson. You each know how you helped make this dream of mine a reality. Thanks.

ABSTRACT

MACROCYCLIC POLYMERS FROM CYCLIC OLIGOMERS
OF POLY(BUTYLENE TEREPHTHALATE)

MAY 1998

SAMUEL MILLER, B.S., Ch.E., OHIO UNIVERSITY

Ph.D., UNIVERSITY OF MASSSACHUSETTS

Directed by: Professor William J. MacKnight

This thesis describes the synthesis, polymerization, and characterization of poly(butylene terephthalate) (PBT) polymers as produced from cyclic oligomers of PBT using a stannoxane cyclic initiator. The properties of the resulting macrocyclic PBT polymer are compared to the properties of four commercial linear PBTs, covering the range of molecular weights for commercial polymers.

The macrocyclic polymers are found to have unique properties in both the melt and the solid state. In the melt, the macrocyclic polymers are found to have significantly lower viscosities vs. the linear resins at equivalent molecular weight. The results reported herein show viscosity differences from linear molecules that are much larger than the findings reported in the literature for macrocyclic and linear polystyrene systems. It is believed that the unique ring expansion polymerization of use in this research has resulted in producing simpler cyclic molecules, having no catenation or knotting, than have been reported elsewhere.

When crystallized, these cyclic molecules produce a semi-crystalline spherulitic structure. The spherulite formed is unique in that it is highly nucleated, rapidly

crystallized, and found to be the same spherulitic form only previously reported as being produced by slow cooling or solvent crystallization processes. The cyclic structure is believed to result in a lower intercrystalline tie chain density than found in melt cooled linear polymers.

This polymer, produced from cyclic oligomers, is proposed as being capable of being utilized as a thermoplastic composite resin, with sufficiently low viscosity in the oligomeric state, and sufficiently high polymerization and crystallization rates, that a melt process is feasible. While being very brittle, the fracture toughness of cyclic PBT is found to increase when the macrocyclic structure is degraded, increasing by three times within ten minutes of thermal degradation in the melt. A new initiator is proposed in the thesis, capable of producing linear PBT from cyclic oligomers, with the same reaction kinetics as the stannoxane initiator. Such a system is expected to be as tough as high molecular linear PBT, and have the chemical and heat resistant characteristics necessary for a new thermoplastic composite resin.

TABLE OF CONTENTS

## LIST OF TABLES

## LIST OF FIGURES

# CHAPTER 1

# INTRODUCTION

## 1.1 The Need for a New Class of Polymers

Traditionally, plastic applications requiring high modulus and heat resistance have been served by thermosetting resins such as epoxies and phenolics. Many of today's advanced composites utilize the processing advantages of low viscosity oligomeric thermosetting resins to infuse the glue that binds glass, carbon, and metallic fibers. The result is a new breed of materials that combines ease of formability with an exceptionally high stiffness to weight ratio. However, with today's focus on the environment, the use of thermoset products, because of their tightly crosslinked structural networks developed during processing, has been limited by the inability to recycle the at the end of their useful "lives" into any second generation usage[1,2]. Heat resistant thermoplastics, the so called "engineering resins", are competing for the higher temperature applications. However, these materials cannot be processed by traditional means into advanced composites because their high viscosities limit their capacity to wet and fill fiber mats or fiber bundles during processing

Tadmore has recently suggested[3] that a new frontier for polymer science is the development of processing methods capable of taking advantage of the theoretical ultimate performance characteristics of today's existing polymers. He suggests that it is the deep understanding of the polymer materials themselves at a molecular level combined with new design and manufacturing capabilities, which will provide the future for plastics applications.

There remains a void in the spectrum of materials for composite applications. There are no materials available on the market with the following three important characteristics: 1) the low viscosity necessary for making composite binders via melt infusion, 2) sufficient integrity to support the stresses of composite applications, and 3) being thermoplastic and thereby capable of being reground, remelted, and reprocessed into second generation structures. The ideal material to fill this need is one that is oligomeric and stable at room temperature, flows easily and wicks readily into composite weaves, mats or tows, and can be transformed readily during processing into a high molecular weight thermoplastic resin.

The current study is focused on an oligomeric polybutylene terephthalate that, in the presence of certain organometallic initiators possesses a combination of two unique characteristics. This material is 1) sufficiently fluid at processing temperature to be easily injected or pulltruded into glass fibers and 2) capable of rapid polymerization and crystallization at the processing temperature into a heat resistant and solvent resistant composite matrix, potentially suitable for use in a portion of the new generation of composite applications.

## 1.2 Overview of the Research

Polybutylene terephthalate (PBT) is a thermoplastic polyester produced commercially through the transesterification reaction of 1,4-butane diol and dimethyl terephthalate. The transesterified prepolymer can be post-reacted to any required molecular weight through a subsequent condensation reaction. In this process, the

stochiometry problems are minimized and the equilibrium reaction is driven by removal of the glycol by-product of the condensation.

PBT consists of both a flexible link (consisting of four methylene groups) and a rigid segment (a terephthalate group). The repeat unit for this polymer is:

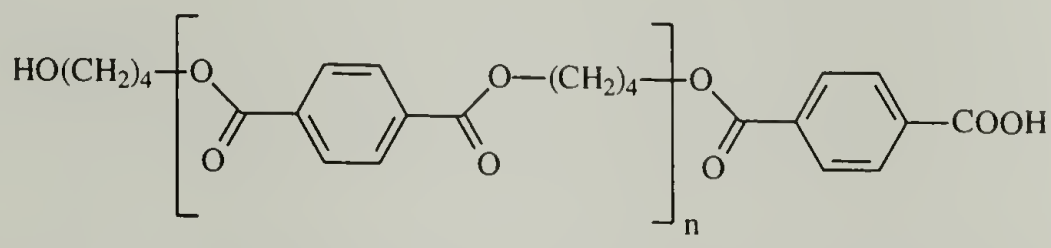


**Figure 1.1 Structure of conventional linear poly(butylene terephthalate)**

This polymer has been sold commercially since the late 1960's into niche markets which demand its unique combinations of performance characteristics. These characteristics result from its thermoplastic processing capabilities combined with its rapid crystallization kinetics and semicrystalline characteristics. The crystallinity of PBT allows that it is used in harsh environments which require resistance to a wide variety of chemicals, thermal and/or electrical insulating resistance, limited flexibility, and low friction and wear characteristics. Typical applications are found in automotive interior and exterior applications including under-hood connectors, household electrical appliances and connectors, and housings for tools. Blends and copolymers of PBT with amorphous resins which improve impact resistance of virgin PBT have opened a wide range of markets in exterior covers and housings from automotive bumpers to lawn equipment and sporting goods.

Although PBT has been successfully marketed for the past 29 years, its current role as a engineering thermoplastic has not changed significantly in the last 20 years[4]. Rather, recent product introductions have stressed the use of incremental processing

improvements and a recycling strategy which includes recovery of clean PBT parts for utilization in "green products" that are marketed for their recycle content. Future growth for PBT will be dependent on product proliferation strategies into areas based on incremental product improvements, or, as suggested through this study, radically new processing capabilities which allow for entry into entirely new application areas.

PBT is a semicrystalline polymer with crystallinity in the range of 35 to 45%. Through annealing, the crystalline content may be increased slightly, but the highest crystallinities reported in PBT are in the range of 55 - 60%[5]. The glass transition temperature for the non-crystalline fraction is 50° - 55° C, and the crystalline melting temperature is usually reported to be in the range of 225° - 232° C[6,7]. Wunderlich et.al.[8] has estimated the equilibrium melting temperature to be 245° C.

Although the molecule is polar, it does not exhibit hydrogen bonding, and is thus physically impervious to water. The stable crystalline nature of PBT leads to its continued expansion into a variety of applications which require high temperature stability and chemical resistance. And, being thermoplastic, PBT is a viable candidate for recovery and reuse, as the social drivers become stronger with today's increasing awareness of our environment and the need for ecologically friendly polymers increases.

It is the purpose of this study to examine the utility of oligomeric PBT to fit into the market currently enjoyed by low viscosity thermosetting resins in the production of polymeric binders for highly filled composites. These composites consist of glass fiber and carbon fiber bundles, either pulltruded directly into rods and shapes, or as woven mats which become rigid sheets when infused with a binding

polymer. The finished parts produced from these composites are strong, rigid, light weight, and highly energy absorbing on impact. The versatility of plastic processing leads to an expanding market for composite materials which is only limited by the use of thermosetting binders in an environment which is stressing the use of recyclable materials.

## 1.3 References for Introduction


1)Miller, S. "Cautions on the Use of Recycled Plastics," SPE Proceedings, New Orleans LA, **1993**.

2)Miller, S. "Quality, Cost, and Value in Recycled Plastic Materials," SPE Proceedings, Boston, MA, **1994**.

3)Tadmore, Z. *Plastics Engineering* **1994**, 35.

4)Kirsch, M.; Williams, D.*Chemtech*, April **1994**, 40-47.

5)Chang, E.; Kirsten, R.; Slagowski, E. *ACS Polymer Preprints* **1978**, *19*, 578.

6)Smith, J.; Kibler, C.; Sublett, B. *Journal of Polymer Science: Part A-1* **1966**, *4*, 1851-1859.

7)Farrow, G.; McIntosh, J.; Ward, I. *Makromol. Chem.* **1960**, *38*, 147.

8)Cheng, Z.; Pan, R.; Wunderlich, B.*Makromol. Chem.* **1988**, *189*, 2443-2458.

# CHAPTER 2

# CYCLIC POLYMERS

## 2.1 Cyclic Polymers Review

An excellent review of macrocyclic synthesis and subsequent ring opening polymerization has recently been published[1]. This chapter describes the fundamentals of cyclics formation and polymerization, with extensive discussion of cyclic carbonates, esters, ethers, ethersulfones, etherketones and etherimides.

Cyclic oligomeric structures are a known equilibrium by-product of most condensation polymer reactions. In melt polymerized linear PBT produced by the condensation of 1-4 butanediol with dimethyl terephthalate, the equilibrium ring content is found to be in the range of 1.5 - 2%[2]. The formation of cyclics in equilibrium with linear polymers was first postulated and reported by Carothers[3] for dilute solution polymerization reactions. Jacobsen and Stockmeyer[4] have theorized that a critical monomer concentration (CMC) must be present in an equilibrium polymerization to produce linear polymer. Below this concentration, the equilibrium will shift to primarily ring structures. While no CMC is reported for PBT in the literature, theory suggests that in dilute solutions the production of cyclic structures will be favored, leading to a method for producing cyclic oligomers for study and use.

Natural macrocyclic structures have long been known to exist. A ring structure of DNA was postulated by Fiers[5] in 1962. Electron micrographs of $\phi$X-RF DNA were published as early as 1963 by Kleinschmidt[6] and micrographs showing the circularity of DNA from bacteriophage $\phi$X-174 were published in 1964 by Freifelder[6]. In the 1980's,

synthetic polymers with macrocyclic structures were first reported for polystyrene[7-9] and also for polydimethyl siloxane[10]. Only recently have publications appeared[1,11,12] which report an macrocyclic structures in engineering thermoplastics (those with high melting temperatures). In this regard, the current research appears to be very timely.

Several publications deal with the existence of cyclic oligomeric structures being isolated and characterized from a variety of polymeric materials. The first literature reports on isolation of terephthalate polyester cyclics date back to 1954 when the cyclic trimer of polyethylene terephthalate was reported by Ross et al[13]. The cyclic dimer of PET was isolated and reported fifteen years later[14].

Zahn and coworkers[15,16] reported the reactive preparation of cyclic oligomers for polybutylene terephthalate using high dilution reactions of oligomeric diols and oligomeric diacid chlorides in conjunction with metal catalysts. Their conversion yields were typically low, with magnesium metal catalyst producing cyclic oligomers up to 40% yield. These preparations proved the capability of formation of cyclic polyester oligomers but lacked economic favorability for production methods. For further economic evaluation, a process was needed to produce higher yields utilizing less expensive and less toxic precursors.

Such a process has recently been reported[17-19]. In this study cyclic oligomers of polybutylene terephthalate were prepared through the pseudo-high dilution condensation of butanediol with terephthaloyl chloride using common catalyst technology (see Figure 2.1). This process, however, is not commercially economic due to the high cost of the acid chloride, the need to maintain rigorously dry conditions in the solvents and reactor, and other limiting process considerations.

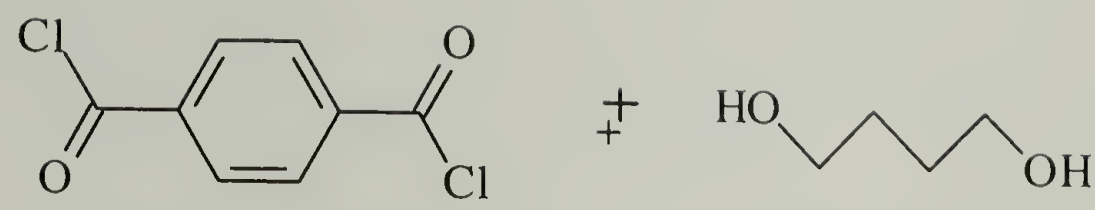


Terephthalyol Chloride + Butane Diol

Methylene Chloride
DABCO catalyst
25° C
High Dilution, Dropwise Addition, High Agitation

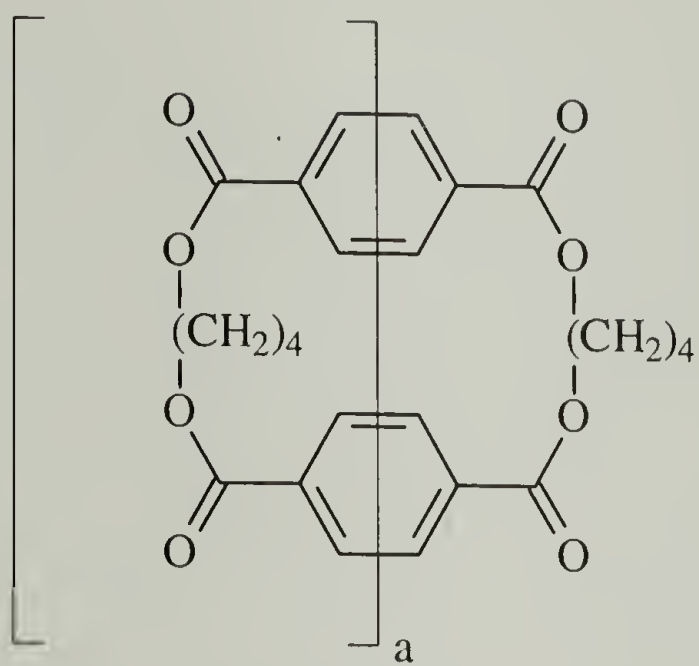


Cyclic PBT (a =1 - 6)

**Figure 2.1 Direct condensation reaction for preparation of cyclic oligomers of PBT.**

Another successful process has also been disclosed recently[20] wherein linear high molecular weight PBT has been depolymerized and converted to cyclic oligomers at 50 - 90% yield in dilute solutions using an organotin or an organotitanium catalyst. The schematic representation of this process is given in Figure 2.2, showing the conversion of linear PBT to cyclic structures with some linear low molecular weight polymer present as a removable, and recyclable, contamination.

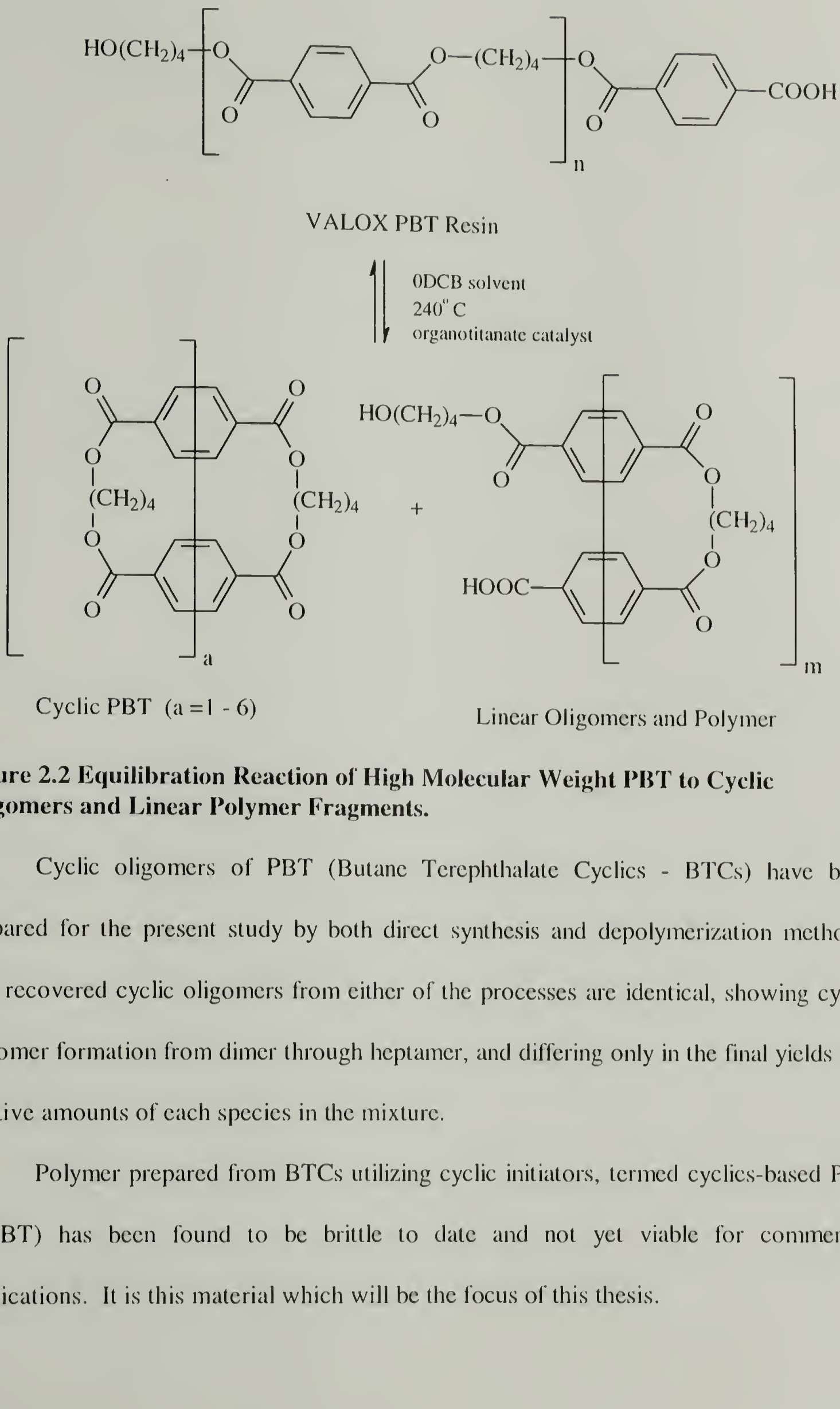


**Figure 2.2 Equilibration Reaction of High Molecular Weight PBT to Cyclic Oligomers and Linear Polymer Fragments.**

Cyclic oligomers of PBT (Butane Terephthalate Cyclics - BTCs) have been prepared for the present study by both direct synthesis and depolymerization methods. The recovered cyclic oligomers from either of the processes are identical, showing cyclic oligomer formation from dimer through heptamer, and differing only in the final yields and relative amounts of each species in the mixture.

Polymer prepared from BTCs utilizing cyclic initiators, termed cyclics-based PBT (c-PBT) has been found to be brittle to date and not yet viable for commercial applications. It is this material which will be the focus of this thesis.

## 2.2 Recent Work on Cyclic Polybutylene Terephthalate

The current research effort is a continuation of a study undertaken over the past three years by Kambour, et al.[21] to resolve questions related to the unusually high level of crystallinity of nascent c-PBT (n-c-PBT) (i.e. isothermally polymerized and crystallized from a melt of butylene terephthalate cyclic oligomers). Working with polymers produced using a cyclic initiator, he found that the n-c-PBT was capable of developing a degree of crystallinity significantly higher than previously reported for PBT. The excess crystallinity of n-c-PBT was assumed to be related to its macrocyclic topology which existed because a cyclic stannoxane catalyst was employed in the polymerization. This catalyst molecule has four active catalytic sites: each a tin-oxygen bond.

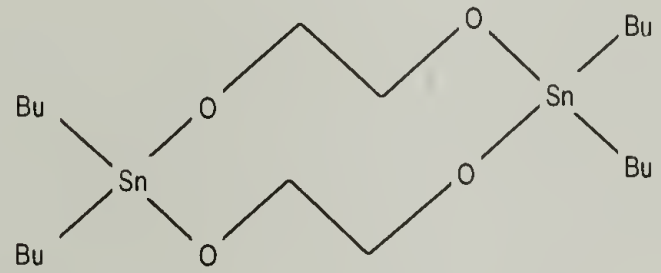


**Figure 2.3 Stannoxane cyclic initiator containing four Sn-O bonds, stabilized by four butyl ligands.**

A mechanism proposed by Takekoshi[22] for the polymerization of BTC using stannoxane initiator is shown in Figure 2.4. This form of polymerization, termed ring expansion polymerization because it preserves the cyclic nature of both the oligomer and initiator, allows for rapid growth of the ring as four active initiation sites may remain in the cyclic structure during polymerization.

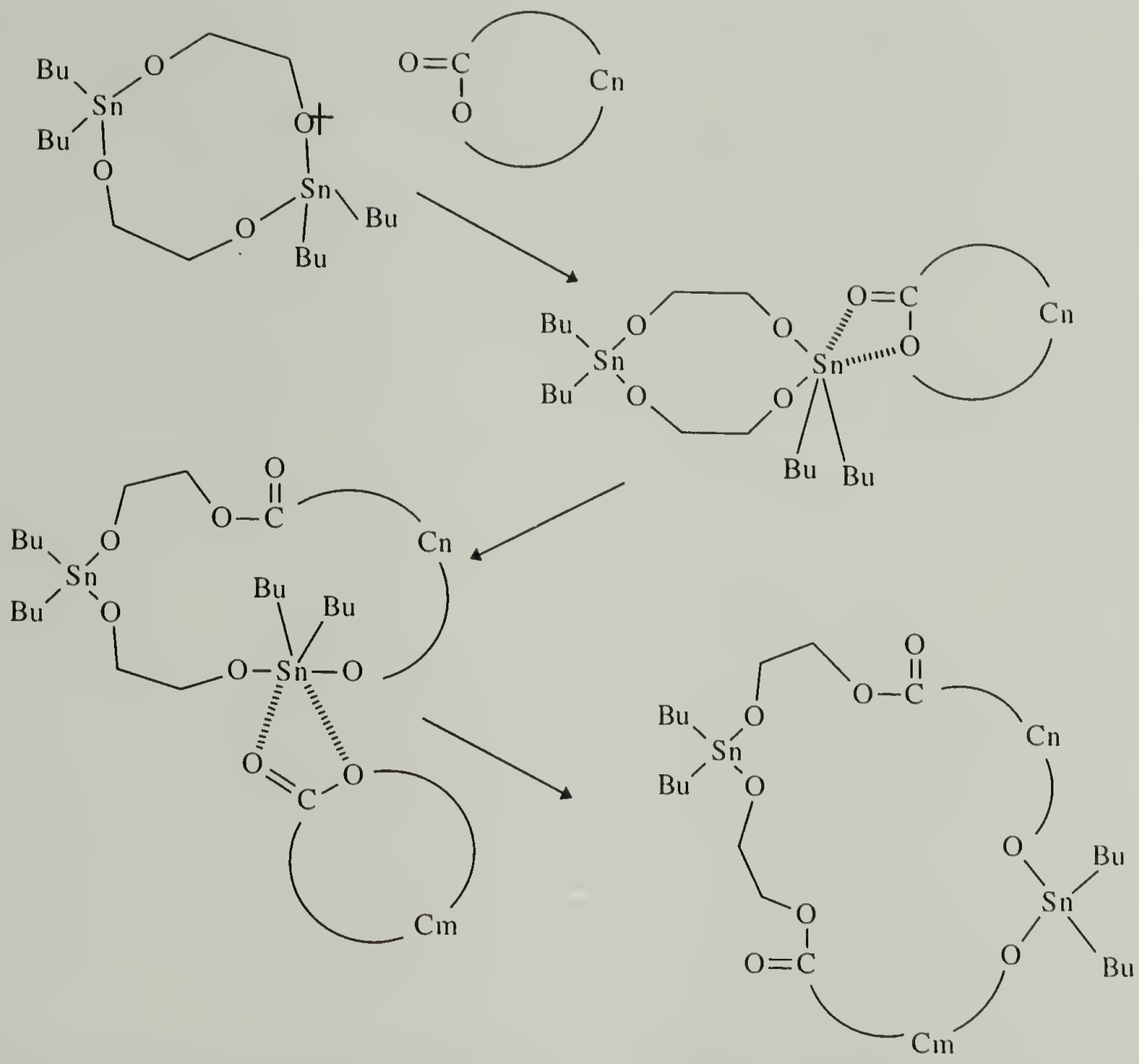


**Figure 2.4 Mechanism for ring expansion polymerization of BTC using stannoxane initiator. (Note that the polymerized c-PBT contains two separated fragments of the initiator molecule.)**

Mechanisms have been proposed that suggest a back-biting reaction that expels a large cyclic structure containing one or no initiator fragments. These reversible side reactions allow for a distribution of active and inactive macro-rings and a possible living system which reaches an equilibrium distribution of molecular weights. However, there is no mechanism proposed which results in linear polymer formation below the initiator degradation temperature. A degradation mechanism will be discussed in the Chapter 6 that can result in linear polymerfrom a macrocyclic structure.

As compared to a conventional linear PBT, the n-c-PBT was found to have a significantly higher heat of fusion, as measured by conventional DSC techniques, when polymerized and crystallized in the temperature range of 200° C. Subsequent melting and recrystallization of this (assumed) macrocyclic polymer yielded lower heats of fusion, the loss of crystallinity being proportional to the time spent in the melt prior to recrystallization. After extended time in the melt, the c-PBT was found to have a heat of fusion equal to that of conventional linear PBT. The loss of crystallizability was found to be irreversible.

The morphology of n-c-PBT was found to be spherulitic, but the spherulites were consistently smaller than spherulites formed on cooling conventional PBT from a completely melted sample. This may be due to the presence of heterogeneous nucleation sites in the c-PBT specimen. The possibility of dirt and dust causing excessive nucleation is more likely in PBTs produced from small batches of cyclic oligomers than in the commercial PBTs made in large-scale reactors.

The observable spherulitic morphology of PBT is more complex than expected from other conventional crystalline polymers (i.e. olefins, acetals, amides) in that the Maltese cross patterns observed in polarized light rarely consist of classical four arm patterns. Generally two armed crosses with broadly diffuse radial borders are observed in conventional PBT spherulites. The patterns observed by Kambour et al, in c-PBT were widely varied, from two and three-arm crosses, to highly complex radial patterns.

Crystallites in conventional PBT are characterized by a triclinic unit cell with parameters a = 5.96Å, b = 4.83Å, and c = 11.62Å, a = 115.2°, b = 99.9°, and g = 111.3° [23]. X-ray work done on n-c-PBT showed it to have the same unit cell as conventional

PBT. Therefore the chain microstructure of c-PBT and linear PBT are identical. However, low angle x-ray measurements show that the long periods in c-PBT is generally 20% below the long periods in conventional PBT for all temperatures of crystallization. As the temperature of crystallization increases, there is the expected increase in long spacing which is consistent with slower growth of fewer lamellae.

When degree of crystallinity is factored into the long spacing, the crystalline core thickness was found to be greater for n-c-PBT than for linear PBT. This implies that there is a much reduced interlamellaramorphous layer in the n-c-PBT.

A second result of crystallization from macrocyclic polymer structure may be a reduction in the number of tie chain molecules between adjacent lamellae. This should be the consequence of macro-rings having smaller radii of gyration than do linear chains with the same degree of polymerization[9,24-26]. Hadziioannou[27] reports a smaller radius of gyration for macrocyclic polydimethyl siloxane vs. its linear analog under theta conditions, with only a slight increase for a good solvent. He suggests that a thermodynamic barrier exists which limits the degree of entanglement of macro-rings based on their lack of chain ends, more compact single molecules, and fewer chain conformations available in the cyclic molecule.

Based only on their compactness, macrocyclic molecules in the melt should have a lower entanglement density vs. their linear counterparts. When crystallized, the resulting spherulitic structure from cyclic molecules should have fewer interlamellar tie chains. Tie chain development will be described in more detail in Section 6.2. Interlamellar tie chains are responsible for stress transfer between adjacent lamellae in a crystalline polymer. If the number of tie chains is significantly lower in c-PBT than in conventional linear PBT,

there should be an accompanying loss of stiffness at high strain, and a lower toughness in the bulk crystalline polymer. These effects will be examined and discussed in Sections 6.5 and 6.6.

## 2.3 Macrocyclic vs. Macrolinear Polymers

Cyclic polymers differ topologically from their linear counterparts, and consequently are expected to possess different characteristics. In the solid state, a high molecular weight glassy macrocyclic polymer should be similar in most respects to its linear counterpart. The properties of the bulk polymer are based on the segmental structural components of the chain, the molecular weight of the chain, and the intramolecular forces between adjacent chains. At high molecular weight, the chain ends have little effect in the solid state and the intramolecular forces are identical for both chain structures if the polymer has the same backbone structure.

In the melt, macrocyclic polymers are expected to diffuse more slowly than linears of equivalent molecular weight ($M_w$). Using model compounds, several researchers[28-30] have shown that linear chains exhibit higher self diffusion coefficients than macro-cyclic polymers. This is consistent with the assumptions of reptation theory, where chains are expected to diffuse based on higher entropy at the chain ends that create new space for diffusion, and allow the chain to move by random conformational changes in the backbone. By contrast, for a macrocyclic molecule to diffuse by reptation would require that a section of the backbone must act as a chain end, expanding into and occupying a different volume of the melt[31,32]. The probability of reptation in macrocyclic polymers is

equivalent to the probability of reptation causing sideways movement in a linear polymer chain.

At high molecular weight, where chain entanglements in the melt control the viscosity, the melt viscosities of linear and macrocyclic polymers (of the same molecular weight) are known to be different[24,25]. Below the critical entanglement molecular weight ($Mw_c$), the viscosity is directly proportional to molecular weight. Friction forces between adjacent molecules provide the only resistance to flow, and these forces increase linearly with molecular weight. Cyclic molecules, with smaller radii of gyration, have a lower entanglement density at all molecular weights. At low molecular weight, a cyclic molecule is expected to have a lower viscosity than the equivalent molecular weight linear. Semlyen et al[33] have reported that bulk viscosity of low molecular weight cyclic polydimethyl siloxane (PDMS) in the $M_w$ range of 4000 to 28000 is lower than the viscosity of linear PDMS at equivalent Mw at room temperature. This is just below the reported $Mw_c$ for entanglement coupling of PDMS ($24500 < Mw_c < 27000$)[34]. However, for very low $M_w$ PDMS (<4000) the room temperature viscosity is greater than that of equivalent oligomeric linears. The increased viscosity of the cyclic oligomers over linear oligomers is found to be most pronounced for molecules having less than 30 skeletal bonds. Stepto[34] suggests that whole molecules are involved in the frictional processes which control viscosity at low molecular weights. The restricted segmental mobility of the cyclic oligomer produces a resistance to shear stress which is responsible for an incremental increase in viscosity over that of equivalent oligomeric linear molecules.

The current study will investigate the rheological and mechanical differences in macrocyclic vs. macrolinear PBT. A wide range molecular weights will be considered

that will provide insight to the behavior of this polymer both below and above the $Mw_c$. However, no attempt will be made to characterize the properties of the oligomer (at very low $M_w$) as the intent of his study is to determine the utility of c-PBT as a matrix polymer for composite structures.

## 2.4 Questions about the Properties of c-PBTs

Earlier work[21,35] in stannoxane initiated c-PBT has left several unanswered questions concerning underlying factors that influence the toughness of the PBTs produced. Two major questions center on the degrees of crystallinity and the concentrations of intercrystalline links in these PBTs relative to such characteristics in conventional linear PBTs.

First, the degree of crystallinity in semicrystalline polymers can be a significant factor in their ultimate properties[36-39], the higher the crystallinity, the lower the ultimate strain at failure[40,41]. Thus, or cyclics-based PBTs may be less tough than the linear PBTs because the former are more crystalline than the latter.

However the concentration on intercrystalline links[42-45] in a semicrystalline polymer is also known to affect its ductility, the higher this concentration, the more ductile the material, all other things being equal. Because the radius of gyration, $R_g$, of a macrocyclic chain is smaller the $R_g$ of the corresponding linear chain[27], fewer intercrystalline links are likely to develop in the material comprised of linear chains during crystallization under conditions such that the rates of crystallization of the two materials are the same.

Thus the following question arises: did the brittleness in the macrocyclic PBTs stem from their relatively high level of crystallinity compared to that of conventional PBT,

or did this brittleness arise from the (suspected) lower level of intercrystalline links in the crystallized polymers? Subsidiary questions also arise. Do other initiators for the melt polymerization of these cyclics produce linear polymers that have properties more like those of conventional PBTs? Does the toughness of macrocyclic PBT, produced at 190°C and subsequently heat soaked to degrade the cyclic structure, also change to a toughness typical of VALOX PBT as the crystallinity drops? And, if so, can the toughness change be unambiguously tied to the drop in crystallinity alone?

## 2.5 References for Cyclic Polymers Review


1)Brunelle, D. *Macrocyclics for the Synthesis of High Molecular Weight Polymers, Chapter 6 in New Methods of Polymer Science*; Blackie Academic & Professional Press:, **1994**; Vol. 2.

2)East, G. C.; Girshab, A. M., *Polymer Communication* **1982**, *23*, 323-324.

3)Carothers, W.; Hill, J., *Journal of the American Chemical Society* **1933**, *55*, 5034.

4)Jacobsen, H.; Stockmeyer, W., *Journal of Chemical Physics* **1950**, *18*, 1600.

5)Fiers, W.; Sinsheimer, R., *Journal of Molecular Biology* **1962**, *5*, 424.

6)Freifelder, D.; Kleinschidt, A.; Sinsheimer, R., *Science* **1964**, *146*, 254.

7)Hild, G.; Strazielle, C.; Rempp, P., *Eur. Polym. J.* **1983**, *19*, 721-727.

8)Geiser, D.; Hocker, H., *Macromolecules* **1980**, *13*, 653-656.

9)Roovers, J., *Journal of Polymer Science: Polymer Physics Edition* **1985**, *23*, 1117-1126.

10)Edwards, C.; Stepto, R.; Semlyen, J., *Polymer* **1980**, *21*, 781.

11)Kricheldorf, H.; Lee, S.; Bush, S., *Macromolecules* **1996**, *29*, 1375-1381.

12)Kricheldorf, H.; Lee, S., *Macromolecules* **1995**, *28*, 6718-6725.

13)Ross, S.; Coburn, E.; Leach, W.; Robinson, W., *Journal of Polymer Science* **1954**, *13*, 405.

14)Repin, H.; Papanikolau, E., *European Polymer Science* **1969**, *A-17*, 3426.

15)Zahn, H.; Pepin, J., *Chem. Ber.* **1970**, *103*, 3041.

16)Meradkentis, E.; Zahn, H., *Chem. Ber.* **1970**, *103*, 3034.

17)Brunelle, D.; Bradt, J. "US Patent # 5,039,783," **1991**.

18)Brunelle, D.; Bradt, J. "US Patent # 5,214,158," **1993**.

19)Brunelle, D.; Brandt, J.; Serth-Guzzo, J.; Takekoshi, T.; Evans, T.; Pearce, E. "Semi-crystalline Polymers via Ring-opening Polymerization: Preparation and Polymerization of Alkylene Phthalate Cyclic Oligomers," American Chemical Society, Las Vegas, NV, V38, pp. 381-382, **1997**.

20)Brunelle, D.; Takekoshi, T. "Process for Preparation of Oligomeric Ester Cyclics via Depolymerization using Hydrolysis-resistant Titanates.," US Patent # 5,407,9841, **1995**.

21)Kambour, R.; Barnes, J.; Garbauskas, M.; Gundlach, P.; McCracken, L. "Microstructure, Morphology, and Crystallinity Level in Polybutylene Terephthalates Produced from Cyclic Oligomers: A Progress Report.," Manuscript in preparation, **1995**.

22)Takekoshi, T.; Brunelle, D. J. "Soluble titanium bisglycoxide catalysts useful for depolymerization of high molecular weight linear polyesters to produce macrocyclic oligoesters.," Patent Pending, **1995**.

23)Mencik, Z., *Journal of Polymer Science: Polymer Physics Edition* **1975**, *13*, 2173-2181.

24)McKenna, G. B.; Hadziioannou, G.; Lutz, P.; Hild, G.; Strazilelle, C.; Straupe, C.; Rempp, P.; Kovacs, A. J., *Macromolecules* **1987**, *20*, 498-512.

25)Roovers, J., *Macromolecules* **1985**, *18*, 1359-1361.

26)Roovers, J., *Macromolecules* **1987**, *21*, 1517-1521.

27)Hadziioannou, G.; Cotts, P. M.; tenBrinke, G., *Macromolecules* **1987**, *20*, 493-497.
28)Tead, S. F.; Kramer, E. J., *Macromolecules* **1988**, *21*, 1513-1517.
29)Mills, P. J.; Mayer, J. W.; Kramer, E. J.; Hadziioannou, G.; Lutz, P.; Strazielle, C.; Rempp, P.; Kovacs, A. J., *Macromolecules* **1987**, *20*, 513-518.
30)Tead, S. F.; Kramer, E. J.; Hadziioannou, G.; Antonietti, M.; Sillescu, H.; Lutz, P.; Strazielle, C., *Macromolecules* **1992**, *25*, 3942-3947.
31)Greasley, W. W., *Journal of Polymer Science, Polymer Physics Edition* **1980**, *18*, 27.
32)Klein, J., *Macromolecules* **1986**, *19*, 105.
33)Semlyen, J., *Pure and Applied Chemistry* **1981**, *53*, 1797-1804.
34)Stepto, R. F. T., *Eur. Polym. J.* **1993**, *29*, 415-418.
35)Kambour, R. P.; Banach, T. E.; Carnahan, J. C.; Garbauskas, M. F.; Gundlach, P. E.; McAlea, K. P.; McCracken, L. L.; Todt, M. L.; Takekoshi, T. "Macrocyclic Polybutylene Terephthalates: PBT Variants of Unusually High Crystallinities via the Ring Expansion Polymerization of Butylene Terephthalate Cyclic Oligomers Using a Cyclic Stannoxane Initiator," Manuscript in preparation,**1998**.
36)Ludwig, H. J.; Eyerer, P., *Polymer Engineering and Science* **1988**, *28*, 143-146.
37)Nielsen, L. E. *Mechanical Properties of Polymers and Composites*; Marcel Dekker, Inc: New York, NY, **1974**; Vol. 2.
38)Young, R. *Introduction to Polymers*; 2nd ed.; Chapman and Hall: New York, **1983**.
39)Chang, E. P.; Slagowski, E. L., *Journal of Applied Polymer Science* **1978**, *22*, 769-779.
40)Moginger, B.; Lutz, C.; Polsak, A.; Fritz, U., *Kunststoffe German Plastics* **1991**, *81*, 251-255.
41)Hobbs, S. Y.; Pratt, C. F., *Journal of Applied Polymer Science* **1975**, *19*, 1701-1722.
42)Keith, H. D.; Padden, F. J.; Vadimsky, R., *Journal of Polymer Science Part A-2* **1966**, *4*, 267-281.
43)Williamson, R. B.;Busse, W. F., *Journal of Applied Physics* **1961**, *38*, 4187-4196.
44)Keith, H.; Padden, F.; Vadimsky, R., *Journal of Applied Physics* **1971**, *42*, 4585-4592.
45)Frayer, P. D.; Tong, P. P.; Dreher, W. W., *Polymer Engineering and Science* **1977**, *17*, 27-31.

# CHAPTER 3
# STATEMENT OF RESEARCH

It is the intention of this research that we investigate the rheological and solid state properties of polymers produced from cyclic oligomers of PBT. Of primary interest is the characterization of polymers produced using the cyclic initiator, stannoxane. This work will continue the studies covered in the former chapter on cyclic polymers. Primary questions to be addressed by this work were proposed at the end of that chapter.

By taking on this research, we hope to elucidate convincing evidence that the polymers produced by the stannoxane initiation of butane terephthalate cyclic oligomers are in fact macrocyclic polymers. The evidence will come from correlation of the results of a broad series of characterization. The crystalline nature of the PBT polymers will impose barriers that will make the solution characterization of these molecules difficult. However, working within this limitation, the thermal transitions, polymerization rates, crystallization rates, molecular weights, thermal degradation characteristics, response to mechanical stresses, and fracture behavior of the resins will be determined. These characteristics will be compared to the literature reports, the characteristics of linear commercial PBT resins, and to linear polymers produced from cyclic oligomers of PBT.

The results of this research will lay new groundwork for continuing research into the nature of cyclic macromolecules. Differences between the results of this work and published literature on similar structures will provide new insight into molecular mechanisms which control the performance of structural materials. While this research will not result in preparation of thermoplastic composite structures, it will provide valuable insight into how these composites may be more readily produced.

# CHAPTER 4

# SYNTHESIS OF BUTYLENE TEREPHTHALATE CYCLIC OLIGOMERS

The butane terephthalate cyclic (BTC) oligomers were synthesized following the methods of Brunelle[1]. Based on Brunelle's recommendations, a direct synthesis condensation reaction was scaled from his 3 liter bench reaction to a 12 liter reactor. This was done as an intermediate trial prior to preparing a large-scale pilot plant run. Three 12-liter reactions were attempted in the 12-liter reactor, with the last two being successful and producing greater than 30% yield of high purity BTC oligomers.

The 12 liter reaction was then scaled-up to a 50 gallon reactor to produce a single batch of BTCs which could be used throughout this study. This reaction involved considerable effort on behalf of many people who's willing contributions are greatly appreciated and are recognized in the acknowledgments section of this thesis.

One attempt was made to prepare BTC oligomers through a depolymerization of commercial high molecular weight linear PBT. This process has also been described by Brunelle[2,3]. While successful in producing cyclics, equipment was not available to scale this process to a size necessary obtain sufficient quantities of BTC oligomers needed for this research.

Each of these three processes are described in sufficient detail that a similar preparation should result in the same quality of BTCs, should this work be continued.

## 4.1 Bench Scale Preparation Method for BTCs

Butane terephthalate cyclic oligomers were prepared in a high agitation, dilute solution reaction of terephthaloyl chloride (TPC) and 1,4 butane diol (BD). The

reaction was run in excess methylene chloride ($MeCl_2$) solvent and was catalyzed using diazobicyclo[2,2,2]octane (DABCO). The reaction was presented earlier in Figure 2.1.

TPC (1.928 mol, 391.3 g) was dissolved in dry methylene chloride (7.17 L, 948.6 g) to produce a clear solution. BD (1.928 mol, 173.7 g or 170.8 ml) was mixed with tetrahydrofuran (THF) (<50 ppm $H_2O$) to lower the BD's viscosity and thus allow constant flow rate pumping throughout the reaction. Eight liters of methylene chloride, the solvent for the reaction, were dried to less than 10 ppm water using 4x molecular sieve. The DABCO catalyst was pre-dissolved in dry triethylamine (TEA). Prior to the reaction, all glassware was assembled and purged with dry nitrogen for at least 12 hours.

The reactor consisted of a 12-liter three-neck round bottom flask fitted with an impeller stirrer, nitrogen purge, temperature monitoring thermocouple, and two pump inlets for the reactants. To control the temperature of the exothermic reaction, the reactor was immersed in a bath to which ice could be added. The reactor was first charged with the dried solvent and the DABCO/TEA catalyst solution was added with maximum agitation. The co-reactants were metered stochiometrically into the reactor, keeping the stochiometric ratio within 1% to maximize cyclic yield. The addition of reactants was drop-wise from a cannula placed below the solvent level, and the total reaction took 1 to 2 hours. Temperature was maintained between 22° and 28° C. When the reactant addition was complete, the reactor was allowed to stir for 10 minutes, after which time a sample was taken, quenched with water, and analyzed using High Pressure Liquid Chromatography (HPLC). If the analysis showed the

presence of OH capped linears, a sufficient amount of the TPC/TEA solution was added to complete the reaction. After an additional 15 minutes of reaction, another sampled was removed and analyzed by HPLC. When OH linears were not detected by HPLC, the reaction was quenched using 120 ml of de-ionized water and stirred for 15 minutes to render the catalyst unreactive.

Linear anhydrides were washed from the cyclic mixture by the addition of 120 ml $NH_4OH$, followed by 10 minutes of agitation and subsequent separation of the aqueous layer using a separatory funnel. The aqueous phase contained a rag-layer of linear acids and anhydrides. Careful re-washing and separation at the liquid-liquid interface cleanly separated these molecular species and resulted in a maximum yield of cyclics.

Recovery of the oligomers from the methylene chloride solvent was accomplished by first adding 100 g each of $MgSO_4$ and Celite (powdered clay) and stirring to absorb any residual water. Vacuum filtration of this solution through a 1 inch layer of Celite produced a clear organic solution of cyclic oligomers in methylene chloride. Rotovapping the excess solvent from this liquor produced a solution of creamy consistency. This solution was then added to an excess of the antisolvent hexane and the cyclic oligomers were crystallized out of solution. The hexane was removed by a separatory filtration and the powder was further dried under vacuum overnight at 50° C. This process yielded about 30% recovered oligomers, with another 5% oligomers potentially recoverable when washed from the Celite clay filter.

A typical (HPLC) trace of the recovered BTCs is shown in Figure 4.1. The elution order is dimer through septomer, with dimer being about 45 - 50 % of the

recovered cyclics. A small peak attributed to linears, if present, will be seen between $C_2$ and $C_3$, near the leading shoulder of $C_3$.

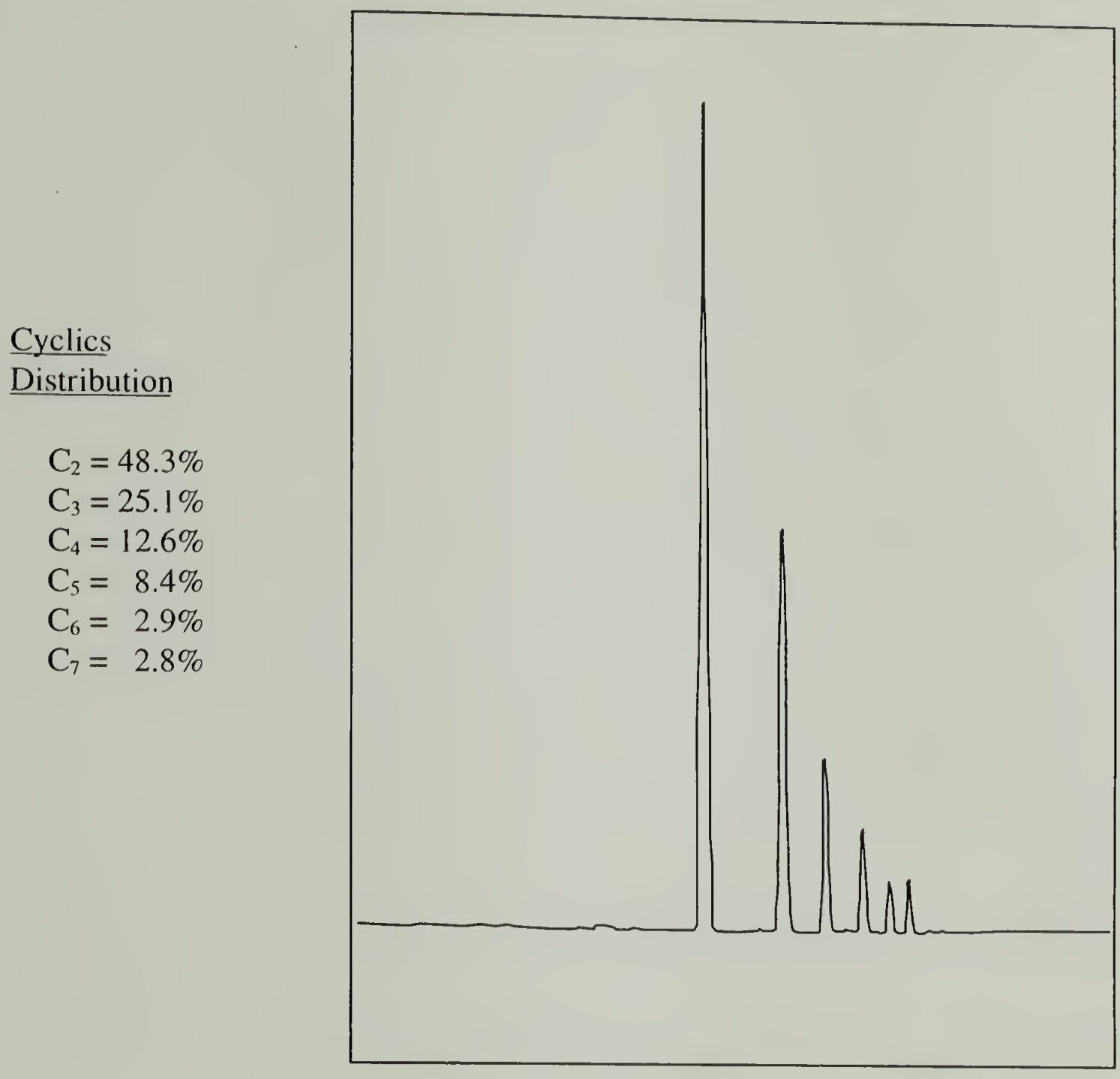


**Figure 4.1 HPLC trace of oligomer distribution in synthesized butylene terephthalate cyclics.**

## 4.2 Pilot Plant Scale Synthesis of BTCs in a 50 Gallon Reactor

A scale-up of the bench synthesis was carried out to provide a single batch of consistent BTC for continued evaluation. The reactor used was a 50 gallon, glass lined, continuous stirred tank reactor, fitted with heating and cooling lines. The

reaction, scaled-up about 12 times from the bench scale reaction, was modified to adapt to the available equipment and make use of additional clean-up processes deemed necessary for improving the quality of the resulting BTC oligomers. The process, as reported below, produced about 2.9 Kg of pure BTC oligomers.

DABCO catalyst and triethyl amine (TEA) were ordered from Fisher Scientific and used as received. Methylene chloride was used from unopened 4-liter bottles after treating with phosphorus pentoxide to react any residual water followed by acid neutralization using TEA. The reaction required the following amounts of raw materials:

| | |
|---|---|
| TPC | 7.1 Kg |
| BD | 3.1 L |
| THF | 3.1 L |
| $MeCl_2$ | 158 L |
| DABCO | 200 g |
| TEA | 10 L |

Three solutions are prepared prior to starting the synthesis:

*TPC / $CH_2Cl_2$ Solution*

- Terephthaloyl chloride (35.0 mol, 7.106 Kg)
- Dry methylene chloride (130 L., 17.225 Kg)
  In a 10 gallon mixing container, dissolve TPC in $MeCl_2$ with constant stirring to produce a clear solution.

*BD / THF Solution (1:1 by volume to lower the viscosity of the BD)*

- 1,4-butane diol (35.0 mol, 3.101L, 3.154 Kg)
- Tetrahydrofuran (3.101L)
  Mix BD into THF to form a uniform solution, maintain continuous stirring during addition to the reactor.

*Catalyst Solution : DABCO / TEA*

- 1,4-diazobicyclo[2,2,2]octane (1.748 mol, 106.1g)
- Triethylamine, solvent for catalyst and acid neutralizer (69 mol, 9.591L, 6.928 Kg)
  Dissolve DABCO in TEA to form a clear solution.

Prior to the synthesis, all equipment was rigorously cleaned. The pumps used for addition of the reactants were calibrated using trial solutions prepared from the same reactants.

192 Kg (145L) of dry methylene chloride was first charged into the 50 gallon reactor which was equipped with a nitrogen purge, condenser, impeller, baffles, two inlet tubes, and oil cooling. The DABCO / TEA solution was added to the reactor and the stirring was increased to the maximum speed to obtain the highest possible shear mixing during thereaction.

The TPC / $CH_2Cl_2$ solution and BD / THF solution were stochiometrically added to the reactor using pre-calibrated pumps. Inlet for the two solutions was below the solvent level in the reactor. Addition of the reactants took approximately one hour. As the reaction is exothermic, the temperature was controlled and maintained inthe range of 22 - 28° C during addition of the reactants.

After complete addition of the reactants the reactor was allowed to stir for an additional 10 minutes. A sample was removed from the reactor, quenched with de-ionized water, and analyzed using HPLC. If OH end-capped linear oligomers were detected, addition of the appropriate amount of TPC / TEA was used to complete the reaction while stirring. After an additional 15 minutes, another sample was removed and the HPLC analysis repeated. When no OH end-capped linear oligomers were detected by HPLC, the reaction was quenched by adding 2 L of de-ionized water. The reactor was stirred for an additional 15 minutes to completely quench the reaction. Two liters of $NH_4OH$ were then added precipitate any anhydrides and the reactor stirred for another 15 minutes.

To clean the reaction mass, it was first filtered through a 40 inch Tolhurst centrifugal basket filter lined with a 3-8μ polypropylene filter bag until the solution was clear. The reaction mixture was then acidified by pumping it back into the reactor and stirring it with 50 L of 1.5M HCl for 15 minutes at low speed. This step was done to convert the end groups of any linears to acid end-caps which could subsequently reacted and removed.

The organic layer was then separated from the aqueous layer and subsequently washed with 50 L of 0.15M HCl for 15 minutes at low speed. The organic layer was then stirred vigorously overnight at room temperature with 17 gallons of 2M NaOH solution. Two pounds of basic alumna (80-200 mesh) was added at this step to remove any acid-capped linear oligomers and keep the solution basic. The mixture was stirred one hour by hand then left to settle overnight. The organic layer was separated from the aqueous layer and re-washed with de-ionized water until the pH was determined to be neutral.

The organic phase was then filtered through a 10 μ cartridge filter to remove any residual alumna. The organic layer was finally separated by steam crumbing. This was accomplished by heating 35 gallons of water to 90° C in the reactor and pumping the organic solution to the top of the reactor and sparging it slowly into the hot water. The solvent was flashed away from the BTCs, leaving the powdered oligomers in a water suspension. The water was filtered off in a spin dryer for 2 minutes at 700 rpm and final drying was done at 50° C overnight under vacuum.

The yield from this run was found to be 28 % pure BTC oligomers.

## 4.3 Depolymerization of PBT under Conditions of High Dilution

The depolymerization of solvated PBT in high dilution is reported[2] to produce a similar distribution of cyclic oligomers to what is reported above. The depolymerization reaction is shown in Figure 2.2. Two attempts were made to produce oligomers through this process, with success on the second try. The process is outlined below, but the process was abandoned in this work because only small batches of oligomers could be prepared due to limited size of the available reaction vessel.

An 8-liter continuous stirred tank pressure reactor was first charged with 5.5 L of orthodichloro benzene (ODCB) and heated to 85° C under a nitrogen purge to dry the solvent. After one hour the residual moisture was measured and found to be 8.3 ppm. 60.5 g of high molecular weight linear PBT (VALOX 315 PBT) were added, the pressure fittings tightened, and the stirring rate increased to 400 rpm. The temperature was increased to 240° C over 20 minutes. When the reaction temperature was reached, 11.0 ml of a bi-cyclic catalyst (titanium butanediol / diethylene glycol) was added through a pressure port on the reactor and the reaction was monitored for 30 minutes within a + 2° / -4° C temperature range.

After 30 minutes, the temperature was set to 100° C. The reactor required 60 minutes to cool to this temperature, after which time 3 ml of de-ionized water were added to quench the catalyst. The solution was then filtered through a wound fiberglass cartridge filter to remove the linear resins which had come out of solution on cooling.

The ODCB/oligomer solution was then concentrated using a Rotovap evaporator until a creamy solution remained. The oligomers were separated by pouring the solution into a flask containing hexane antisolvent under high agitation. The crystallized BTC powder was separated in a vacuum filter and dried for two days at 50° C.

This process produced a 54.3 % yield of pure BTC oligomers.

## 4.4 References for Synthesis of BTC Oligomers


1)Brunelle, D.; Brandt, J.; Serth-Guzzo, J.; Takekoshi, T.; Evans, T.; Pearce, E. "Semi-crystalline Polymers via Ring-opening Polymerization: Preparation and Polymerization of Alkylene Phthalate Cyclic Oligomers," American Chemical Society, Las Vegas, NV, V38, pp. 381-382,**1997**.

2)Brunelle, D. J.; Serth-Guzzo, J.; Kailasam, G.; Wilson, P.; Takekoshi, T.; Webb, J.; Littlejohn, M., *In Publication* **1997**.

3)Brunelle, D.; Takekoshi, T. "Process for Preparation of Oligomeric Ester Cyclics via Depolymerization using Hydrolysis-resistant Titanates.," US Patent # 5,407,984, **1995**.

# CHAPTER 5

# INITIATOR SYSTEMS AND POLYMERIZATION OF BTCs

During the course of this research, two initiator systems were used to polymerize the BTC oligomers. These two initiators are chemically similar but different in structure. The difference results in different topologies of the polymer which is produced. A cyclic stannoxane initiator was used to produce macrocyclic polymers, while tributyltin ethoxide (TBTE) initiator was used to produce linear polymer. Each will be introduced independently in this section.

## 5.1 Stannoxane

Tin compounds with a wide variety of structures have been shown to be effective in the polymerization of lactones and cyclocarbonates[1-3]. These initiators have in common one or two active bonds, with the active polymerization site being the Sn-O bond. The tin is generally stabilized by two or three short alkane structures, typically butyl groups. Kricheldorf has reported on the successful polymerization of polylactones[2] using the following three cyclic variations of butyltin alkoxides:

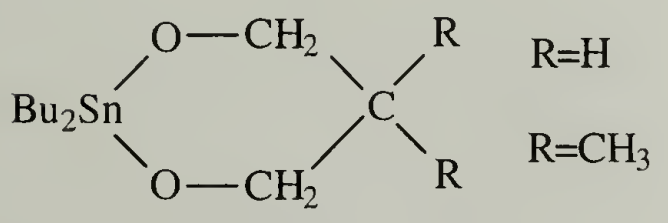


I.

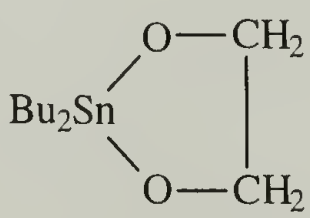


II.

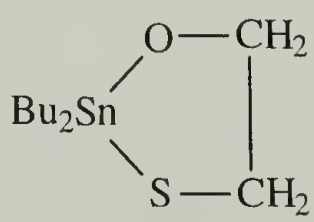


III.

Using these cyclic initiators, he has shown that the reactivity of the initiators for insertion polymerization is based on the number of Sn-O bonds in the initiator. He also concluded

that initiator II does not normally exist as a monomer, rather as the dimer IV is more stable:

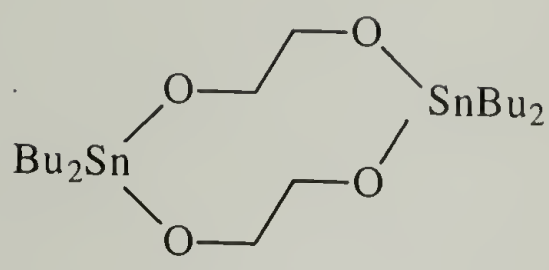


IV.

The dimer of dibutyl tin dioxide (IV) was first reported by Ramesden[4]. This is the initiator used in the early polymerization of cyclic oligomers of PBT[5]. The initiator is technically 1,1,6,6-tetra-n-butyl-1,6-distanna-2,4,6,10-tetraoxyacyclodecane which for convenience in naming will hereafter be shortened to stannoxane. While not a true stannoxane molecule (which be definition contains a Sn-O-Sn linkage) initiator IV (stannoxane) has four Sn-O linkages, each capable of insertion polymerization of lactones or other esters.

Other forms of cyclic dibutyl tin initiators have been reported for polymerization of lactones and lactams[1-3];

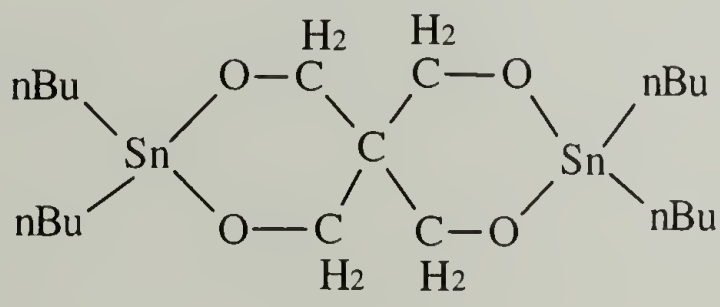


V.

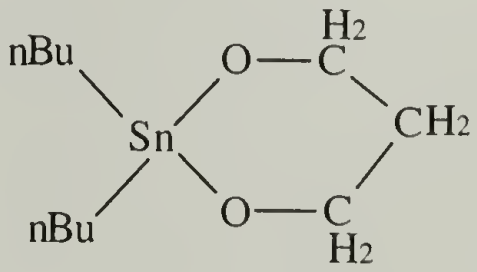


VI.

Variations of these initiators may contain one or more Sn-S linkages in place of the Sn-O linkages but the stannomercaptyl linkages are not efficient in polymerization of lactones.

Brunelle has reported the ring expansion polymerization of cyclic BPT oligomers through the mechanism shown in Figure 5.1. The frontier orbitals on the tin atom are coordinated to the carbonyl in the ester and a bond exchange takes place that results in breaking and reforming one Sn-O and one C-O bond. Because there is little ring strain in the cyclic oligomers, and none in higher molecular weight cyclics, the expansion is athermal. It is important to note that the tin environment has not changed through the nearest three atomic links on either side of the tin. The reactivity of the Sn-O link is not altered by the expansion reaction, which remains unbroken throughout the entire polymerization process. Note also that this polymerization has no by-products and thus may readily proceed to high molecular weight as compared with normal step polymerization reactions.

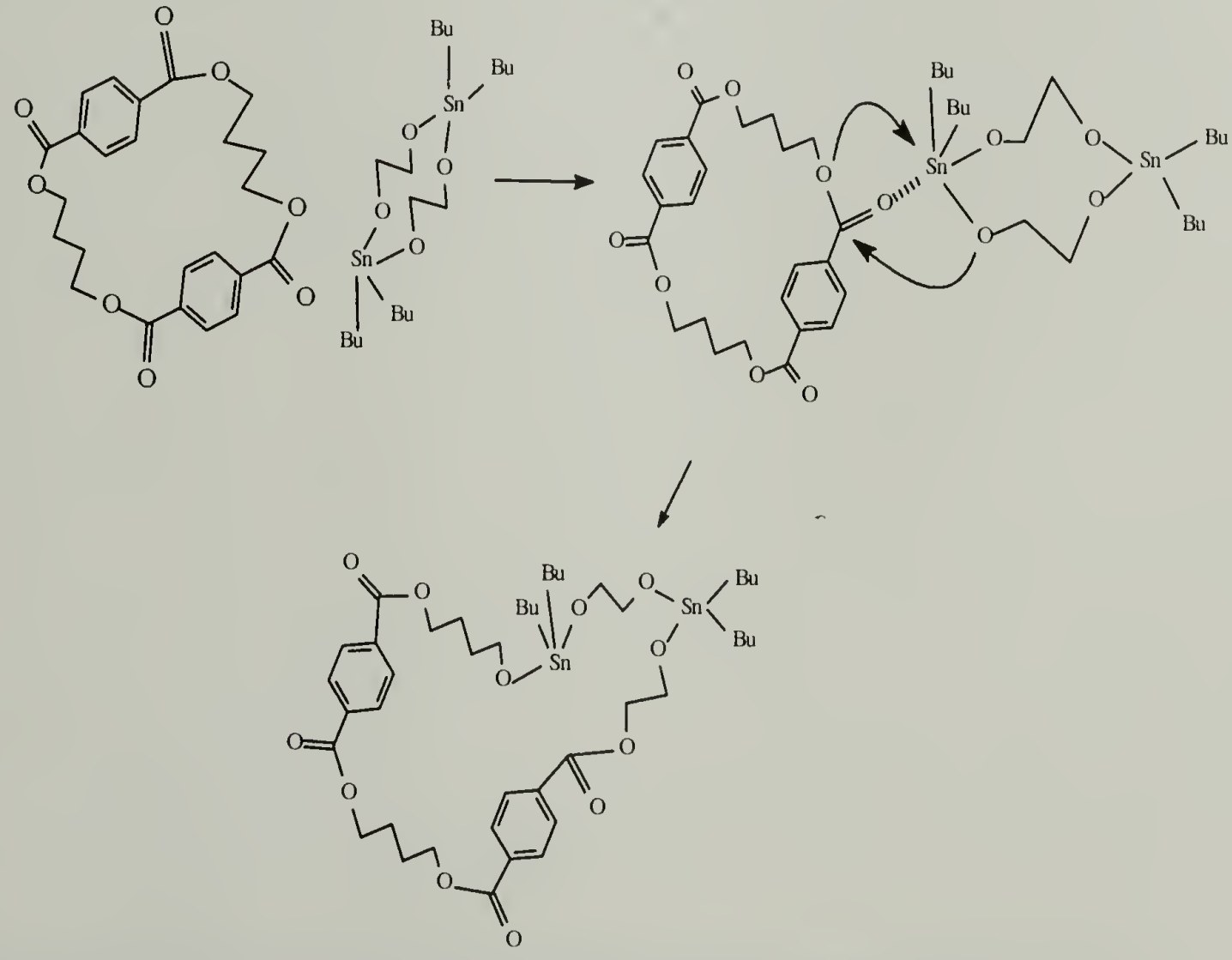


**Figure 5.1 Ring Expansion of a cyclic dimer of PBT using stannoxane initiator.**

This mechanism can easily be generalized to any size of cyclic PBT being expanded by a stannoxane molecule. Once the first ring has been opened, the active bonds will continue to add oligomers, or other stannoxane-containing rings and the molecular weight will continue to increase as the ring expands. The molecular weight of the resulting polymer is controlled by the molar ratio of monomer to initiator (the M/I ratio).

Ring separation or a ring-shrinking reaction is also believed to occur[6] whereby a backbiting reaction within an existing macrocyclic structure can expel a smaller ring. The expelled ring may or may not contain active polymerization sites. The general form on this reaction is shown in Figure 5.2.

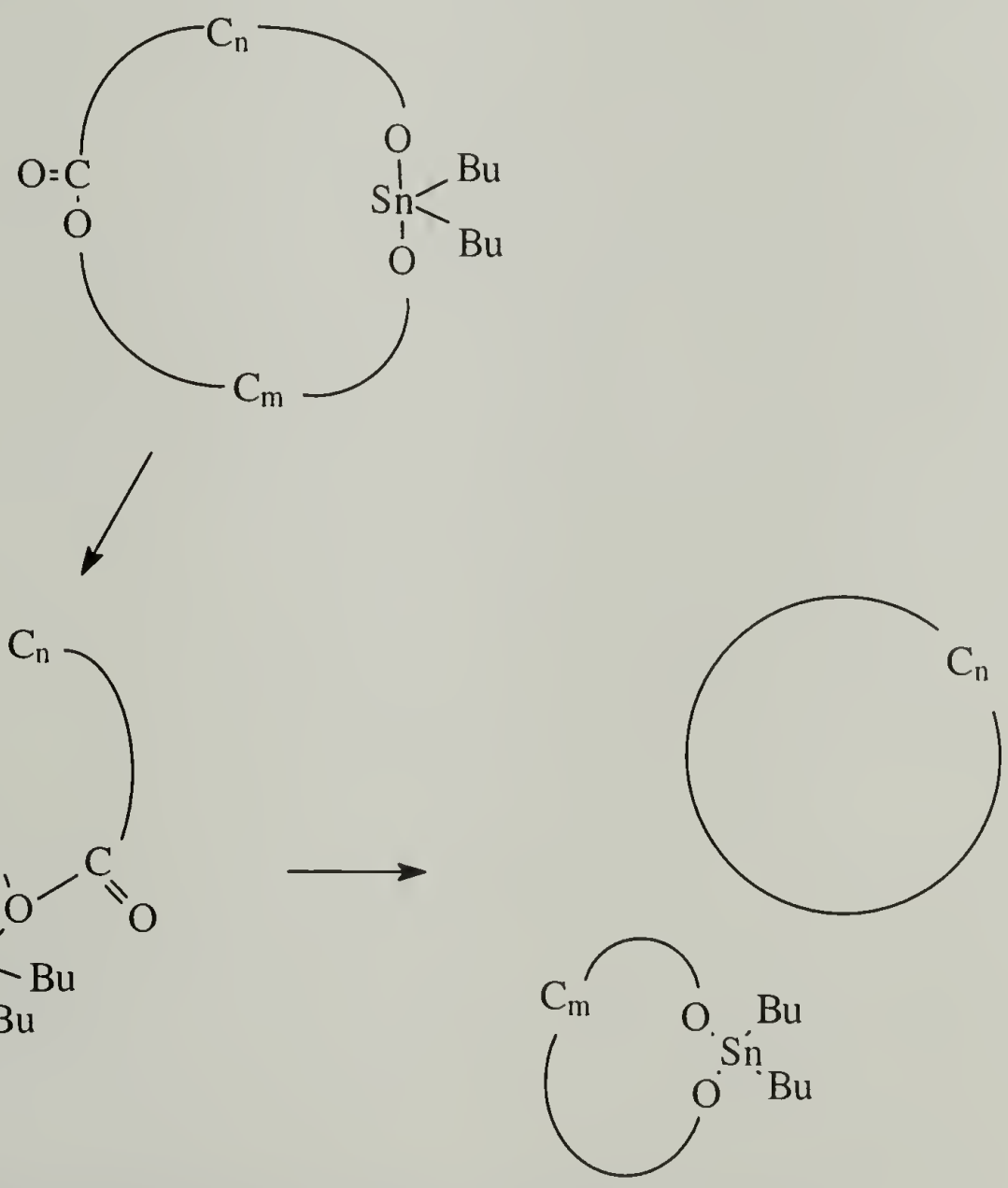


**Figure 5.2 Ring exchange reaction showing a reduction of ring size.**

In the exchange reaction shown above, an active ring of size ($C_m + C_n$) is reduced by a backbiting reaction. Fragment $C_n$ is expelled as a large inactive ring, while the active ring fragment $C_m$ is available for continuing polymerization. As long as the stannoxane fragment is active, these re-equilibration reactions can continue. The final molecular weight of a system of polymerizing oligomers is primarily dependent on the M/I ratio as shown in Figure 5.3. (Because these molecular weights were determined using the GPC, Mw values for cyclics presented in this section have been "corrected" to linear equivalent Mw as described in detail in Section 6.2) The reaction rates for ring expansion and ring reduction will control the final distribution of molecular weights in the cyclic polymer.

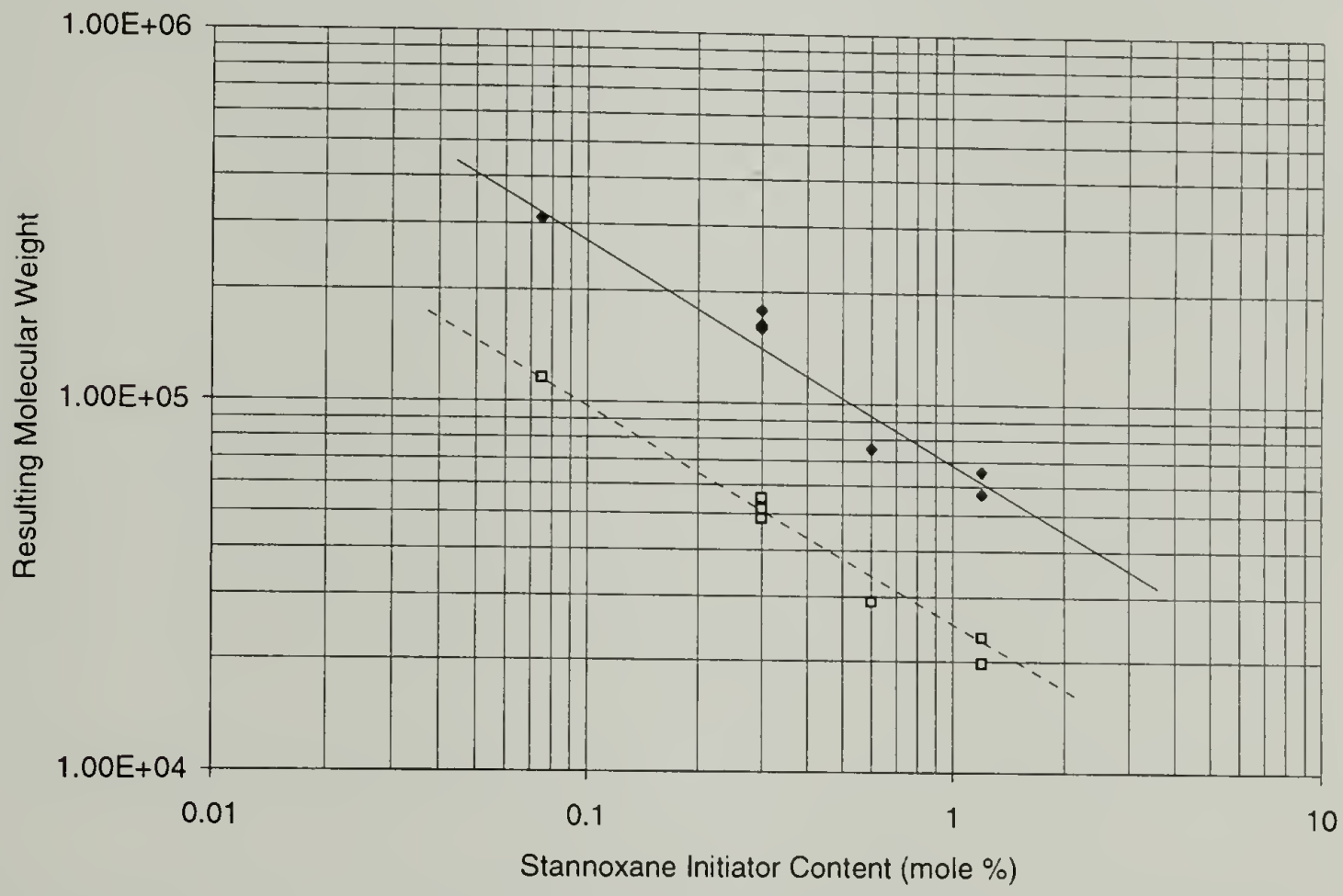


**Figure 5.3 "Corrected" apparent molecular weight of polymer as a function of stannoxane initiator content at 220° C. Solid line is $<M_w>$, dotted line is $<M_n>$.**

Two degradation processes are known which open the macrocyclic polymer chain and result in linear polymers. Thermal stability of the stannoxane appears to limit the upper temperature where macrocyclic structures may be stable. A thermogravametric

analysis (TGA) of the stannoxane initiator shows a loss of weight in the initiator at 220° C as shown in Figures 5.4 and 5.5.

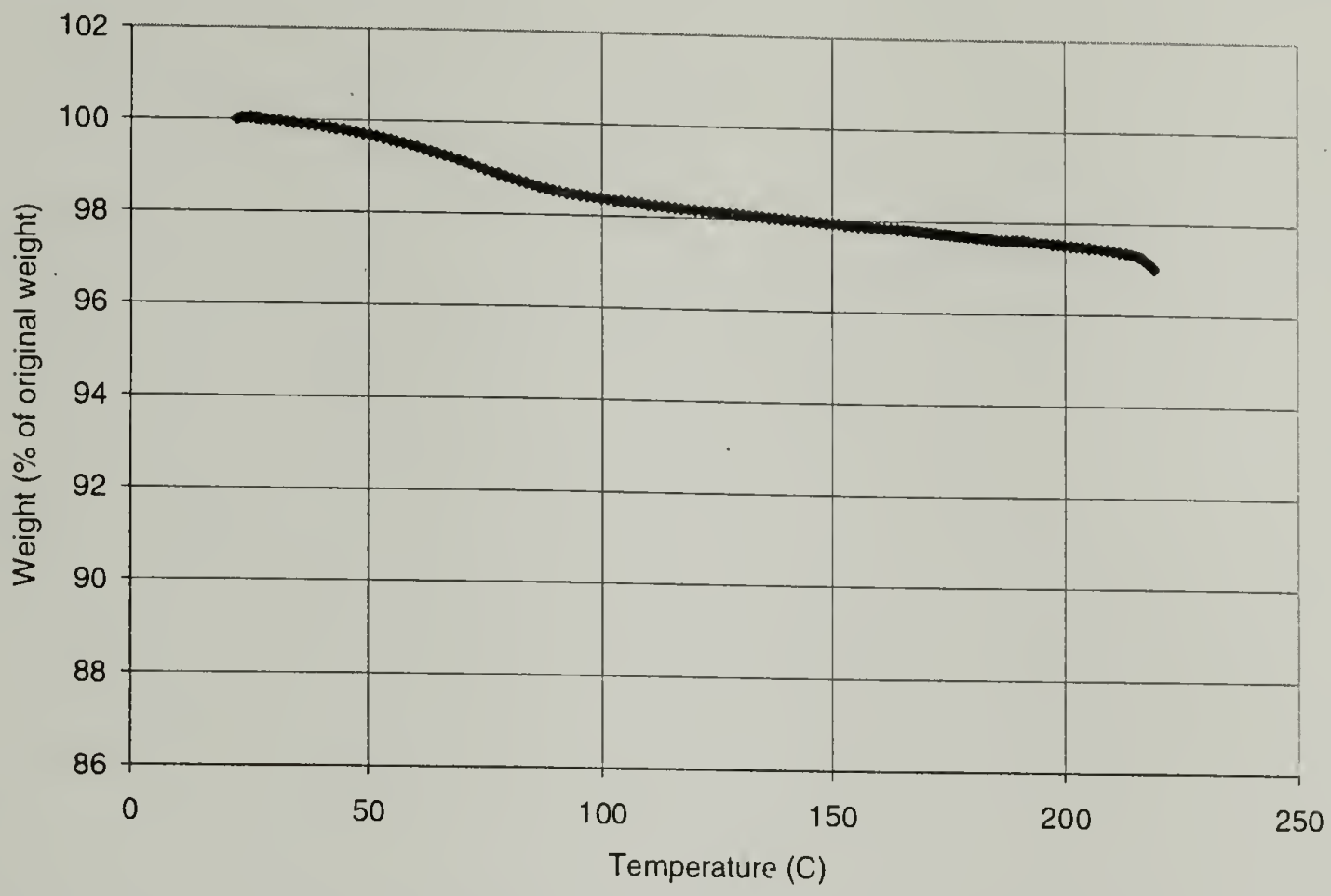


**Figure 5.4 Thermogravametric analysis of stannoxane initiator on heating.**

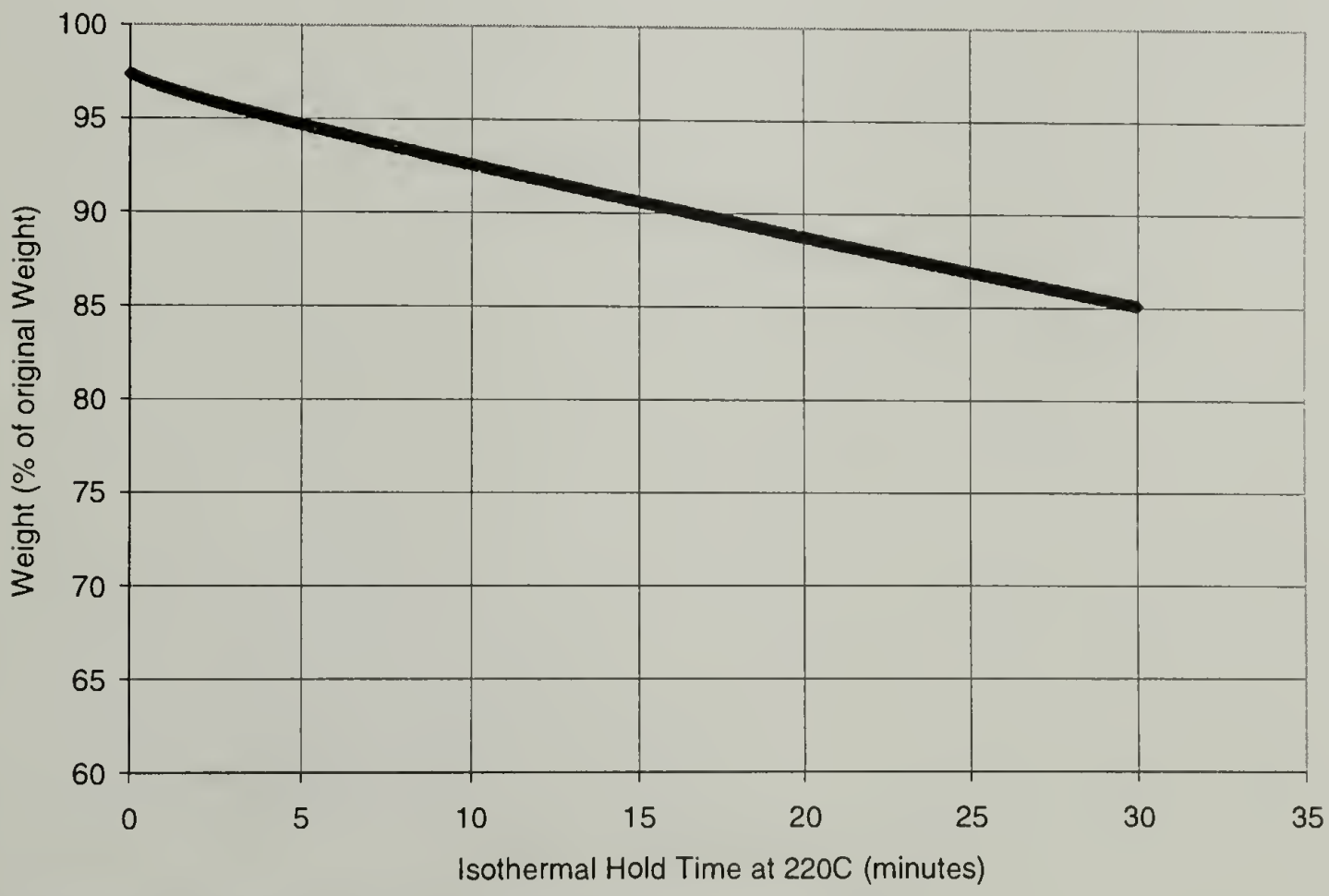


**Figure 5.5 Isothermal TGA of stannoxane at 220° C.**

Stannoxane is seen to lose about 12 % of its weight within 30 minutes when held isothermally at 220° C. The weight loss between 50° and 100° C on heating is probably residual moisture. Problems with thermal stability of the stannoxane link are suspected when polymer produced from this initiator is heated above the melting point (ca. 225° C). The PBT chain is known to degrade when held above 250° C for extended times. The kinetics for the two degradation processes are much different, with the stannoxane initiator degrading much faster than the PBT segments.

Another type of stannoxane degradation may come from having water present under high temperature conditions. While moisture was not observed as a problem during storage of the BTC or the stannoxane powder, the powders were always dried prior to high temperature uses, i.e. compression molding, oven polymerization, and rheology studies. Moisture possibly caused degradation during a solution NMR study (reported in Section 6.4.3.2) where end group analysis was performed to determine the extent of linear resin in a supposed macrocyclic specimen. The proposed mechanism for water degradation is shown in Figure 5.6. Only hydroxyl end groups are produced when this mechanism is responsible for degradation.

The stannoxane initiator is produced by the condensation reaction of dibutyltin oxide and ethylene glycol with the liberation of water:

$$2Bu_2SnO + 2HO(CH_2)_2OH \rightarrow Bu_2SnO_2(CH_2)_2O_2SnBu_2 + 2H_2O.$$

The reaction is carried out in a closed flask equipped with a heater, stirrer, and thermometer, and fitted with a modified Dean Stark trap and condenser for removing and collecting the water. Stochiometric quantities of the reactants are added with sufficient

toluene to dissolve the solids. The reaction is slowly heated to 114° C, while monitoring the collection of by-products. The modified collection trap allows light solvent to be returned to the reaction flask while retaining the (heavier) water in the trap. When the water level is constant in the trap, the reaction is finished. The product is collected and dried at 50° C then ground and stored in a dessicator until needed.

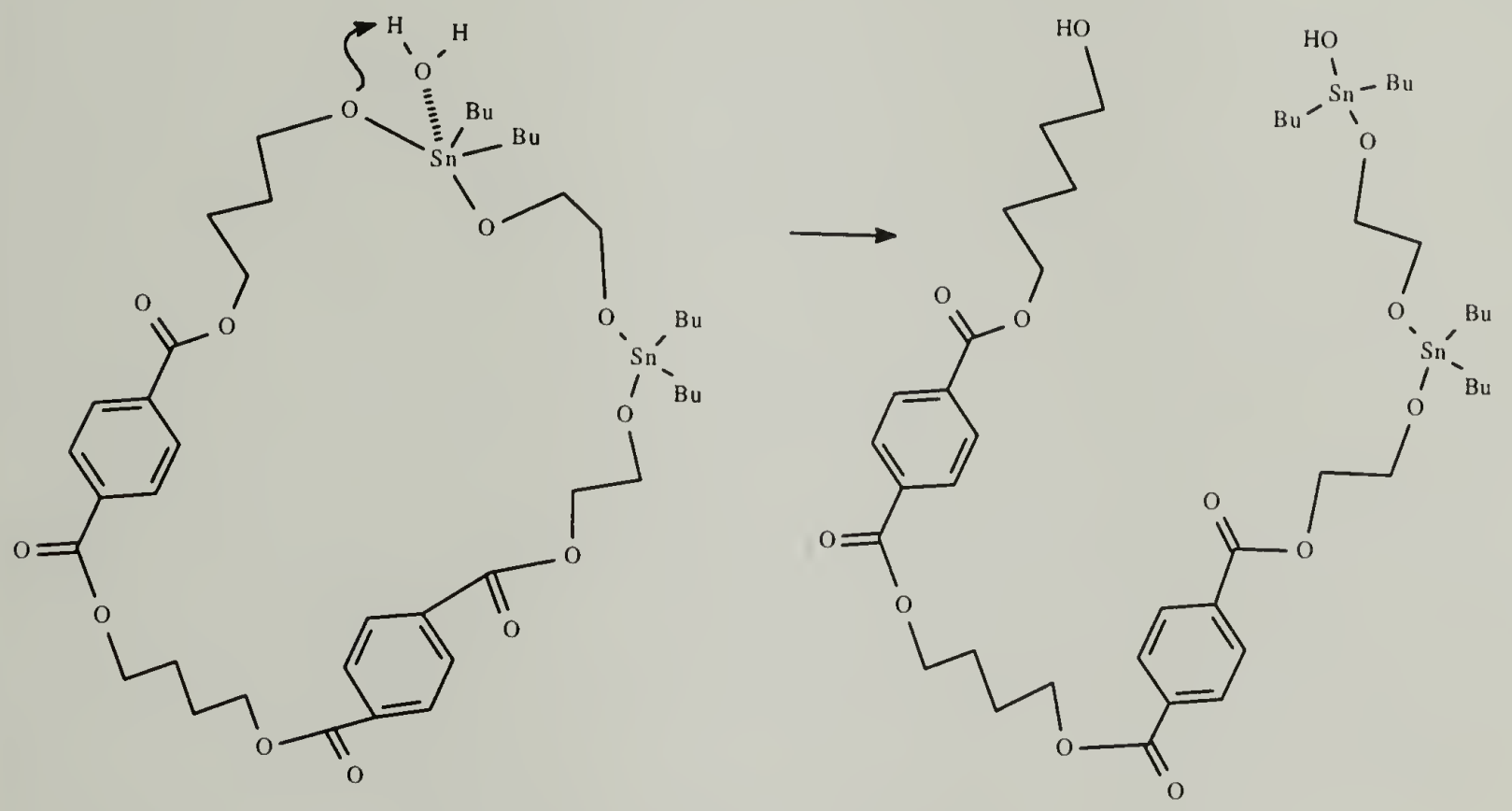


**Figure 5.6 Mechanism for water degradation of a cyclic chain resulting in only hydroxyl endgroups.**

The quality of the stannoxane product was determined by DSC melting points as well as its ability to polymerize BTCs to high molecular weight and high crystallinity. The DSC trace for stannoxane of high purity is shown in Figure 5.7.

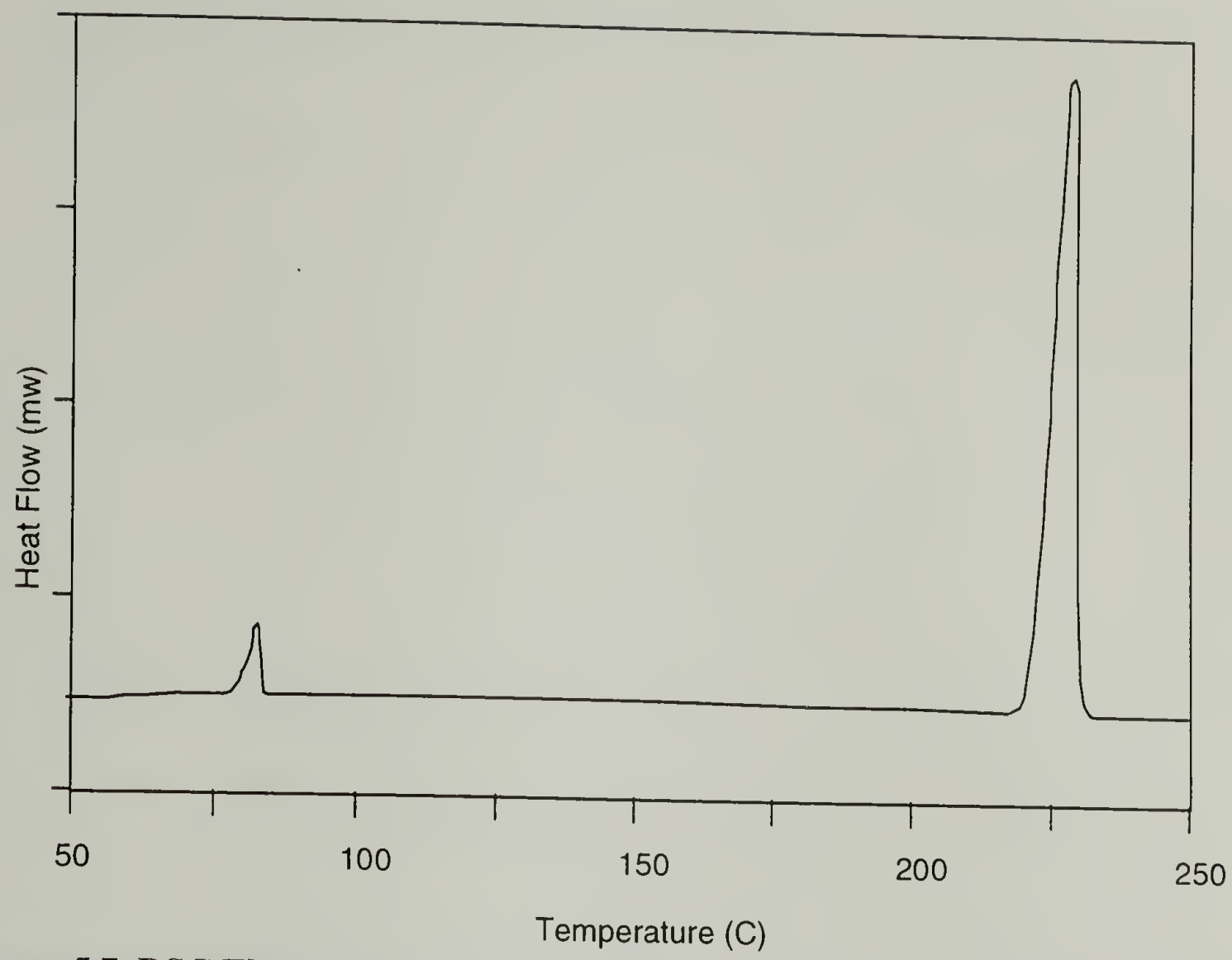


**Figure 5.7 DSC Thermogram of a batch of stannoxane initiator synthesized in this work.**

The primary melting point of the stannoxane product is 230° C. The initiator is soluble in methylene chloride and dispersions of both initiator and cyclic oligomers were prepared through solution blending, followed by slow drying to evaporate the solvent. Once dispersed, the initiator is active at temperatures as low as 160° C[7]. This low temperature activity is believed to be through solvation in the BTC oligomer melt.

The source of the low temperature endotherm is not known. It may be moisture, as seen in the TGA trace at the same temperature (see Figure 5.4), but it is present in both a first and second heating trace using a crimped DSC pan. Another possibility is that this is the monomer, $Bu_2Sn(O(CH_2)_2O)$, which was not isolated but is suspected to be present

at equilibrium in low quantities. However, the presence of this monomer would not account for the low temperature TGA weight loss.

## 5.2 Tributyltin Ethoxide

Tributyltin ethoxide, hereafter referred to by the acronym TBTE, is structurally similar to stannoxane, but is incapable of producing a cyclic macromolecule. (It is conceivable that a backbiting reaction analogous to the ring reduction reaction of Figure 5.2 could produce a small number of macrocyclic molecules.)

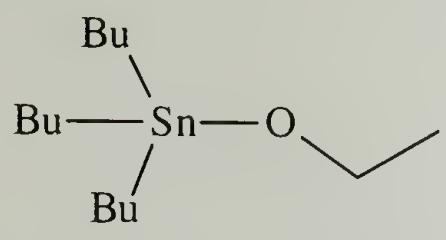


TBTE has nearly the same bond environment surrounding the active Sn-O bond, but the tin has less electropositive character than the stannoxane tin. Stannoxane has two electron-withdrawing oxygen atoms and two electron-donating butyl groups, whereas TBTE has only one electron-withdrawing oxygen and three electron-donating butyl groups. The resulting lesser charge on the TBTE tin leads to a lower coordination potential vs. the stannoxane tin.

TBTE will be shown in Section 6.2.4.1 to be a slower initiator than stannoxane for polymerization. There are two reasons for the lower reactivity. First, TBTE has only a single reactive site whereas stannoxane molecule contains four potential reactive sites. On a molar basis, each initiator produces the same molecular weight, but the stannoxane initiator should be four times faster, based only on the higher reaction site density in this system. Second, in studies where four times the molar level of TBTE was used, this initiator was found to be slower than stannoxane in polymerizing BTCs. The greater

nucleophylic character of the stannoxane tins is believed to cause an additional increase in polymerization rate.

The TBTE used in this study was purchased from Aldrich Chemical Company and was used without further purification. As a purity check, a sample was scanned in a Fourier Transform Infrared Spectrometer (FTIR) using hermetic cells of two different thickness. The thinner cell (0.025 mm) was used to see details of the aliphatic structure and the thicker cell (0.50mm) was used to see fine structure not evident in the spectrum obtained using the thinner cell. In each case 64 scans were recorded. Table 5.1 gives the results. From this table it can be concluded that TBTE is present in large quantities and there is no tributyltin hydride or hydroxide present.

**Table 5.1 FTIR results on TBTE from Aldrich Chemical Company.**

| Bond | Wavenumber | Intensity |
|---|---|---|
| *Peaks Identified* | | |
| Sn-C | 570-450 $cm^{-1}$ | Medium / Strong |
| Sn-O | 780-580 $cm^{-1}$ | Strong |
| C-O stretch | 1450-900 $cm^{-1}$ | Strong |
| C-C stretch | 1250-800 $cm^{-1}$ | Strong |
| C-H (alkane) | 3100-2800 $cm^{-1}$ | Strong |
| C-H rocking | 900-660 $cm^{-1}$ | Strong |
| *Peaks not found* | | |
| Sn-H | 1800-1855 $cm^{-1}$ | |
| O-H | 1200-1450 $cm^{-1}$ | |
| | 3800-3300 $cm^{-1}$ | |

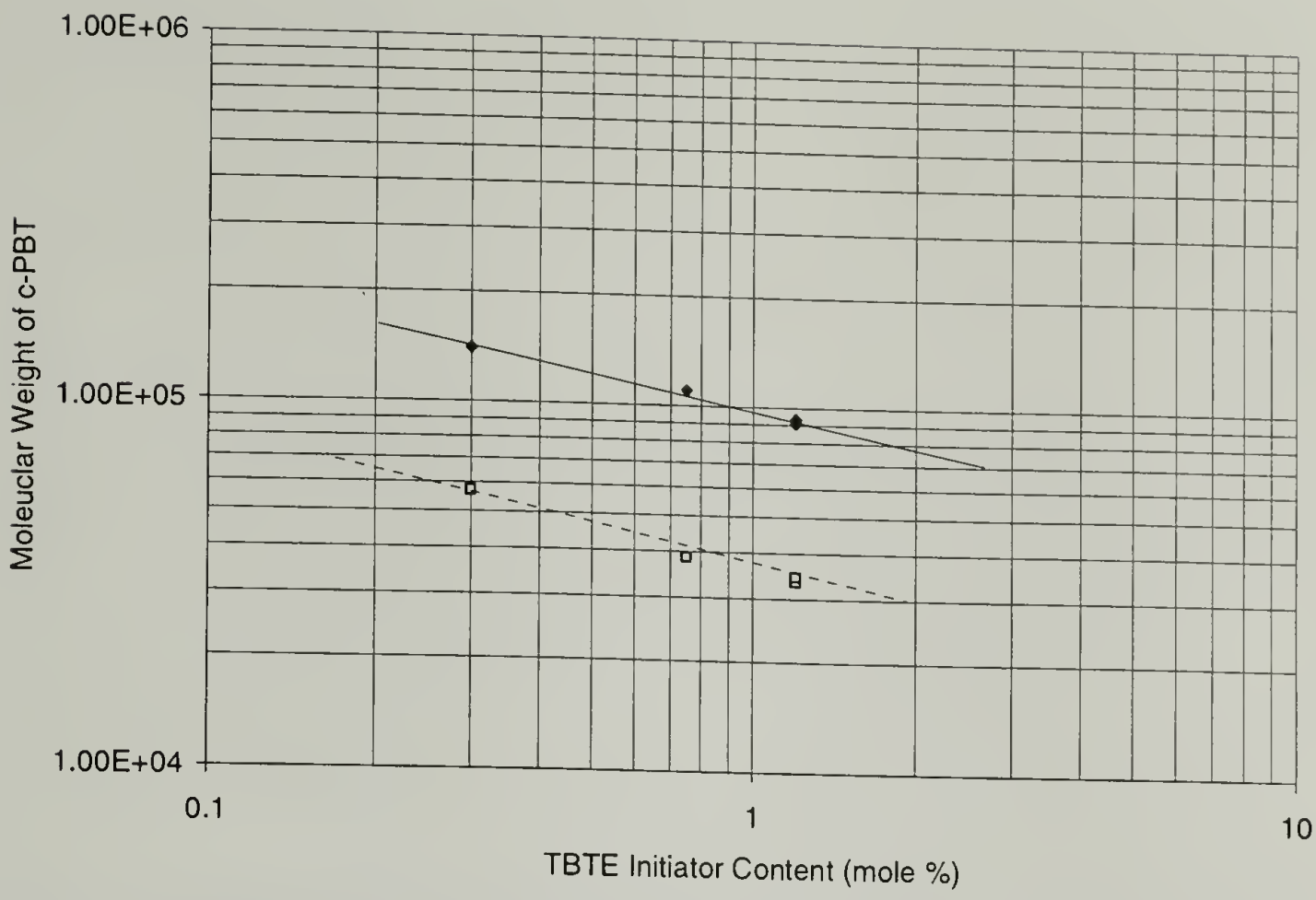


**Figure 5.8 Apparent molecular weight of linear c-PBT, produced using TBTE initiator at 215° C, as a function of initiator content. Solid line is $<M_w>$, dotted line is $<M_n>$.**

Polymerization with TBTE is also an insertion polymerization, common for a ring opening polymerization initiator. The ring opening is nearly athermal, and the entropy of the chain decreases slightly with each insertion. There is no by-product of polymerization and the polymer proceeds easily to high molecular weight. As for stannoxane polymerizations the molecular weight is determined by the M/I ratio, shown in Figure 5.8.

At equivalent initiator contents that are the same on a molar basis, TBTE produces much higher molecular weight polymer when compared to stannoxane as shown in Figure 5.3 (notice that there is also a 5° C temperature difference in the two figures). As the initiator content is decreased, and polymers of higher molecular weight are produced, the difference between the two initiators is diminished. The following two figures highlight this difference between initiator systems. At low initiator content, the two systems appear

low Mw produced by high levels of stannoxane initiator may result from a more rapid equilibration of the ring sizes as proposed in Figure 5.2.

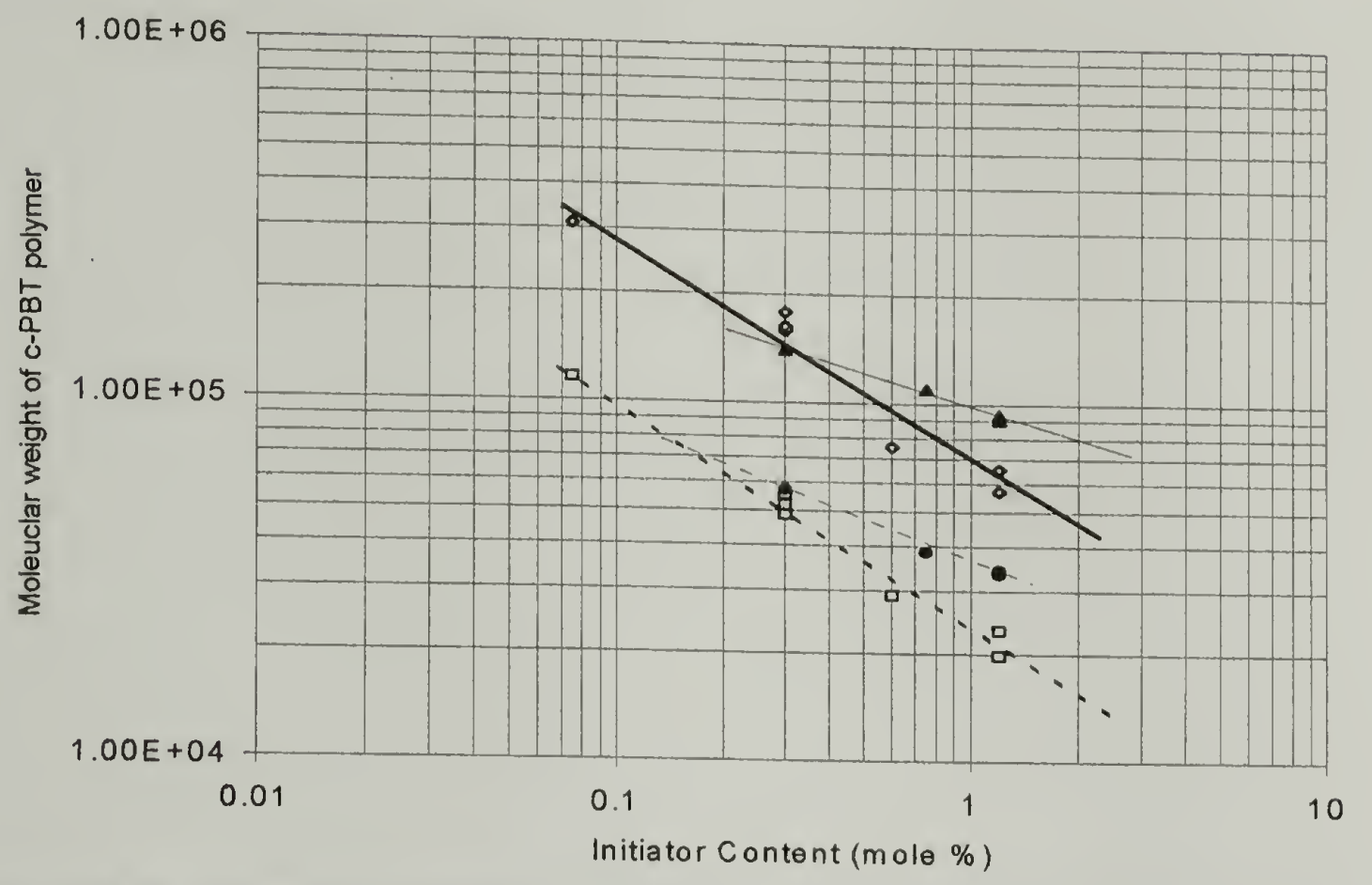


**Figure 5.9 Equivalence of the two initiator systems used in polymerization of c-PBT. Solid lines are <$M_w$>, dotted lines are <$M_n$>. Dark lines are stannoxane initiator, light lines are TBTE initiator.**

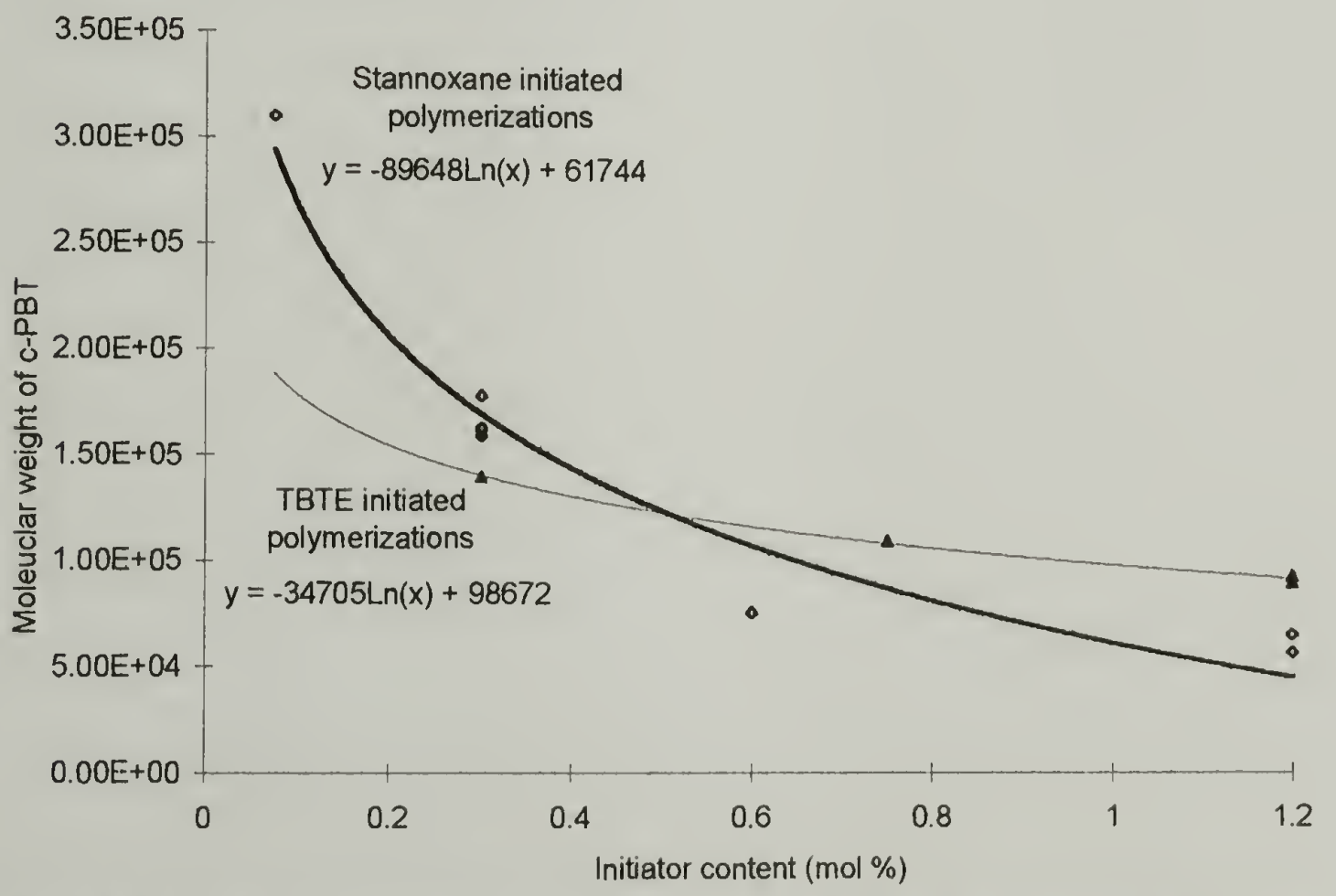


**Figure 5.10 Linear presentation of the data in 5.9 with logarithmic fit curves.**

The concept of molecular weight being a function of ring equilibration rate is also supported by the temperature dependence of the molecular weight for stannoxane initiated polymerizations. As shown in Figure 5.11, higher polymerization temperatures produce polymers of lower molecular weight. These data were taken after times ranging from 10 to 60 minutes in the melt following polymerization. The only correlation to time is seen in the 220° C specimens which were cooled after only 10 minutes in the melt. These specimens have slightly higher than predicted $M_w$ and $M_n$ vs. specimens which spent longer times in the melt. The lower molecular weight at higher temperatures must be the result of more activity (redistribution) in the hotter melts. The divergence in the lines representing $M_w$ and $M_n$ shows that the polydispersity index (PDI) also increases as the polymerization temperature increases. The increase in PDI is a direct measure of the molecular weight distribution. Higher PDI is found at higher temperature because the cyclic melt has sufficient living character that a redistribution in molecular weight continues after the oligomers have been fully polymerized.

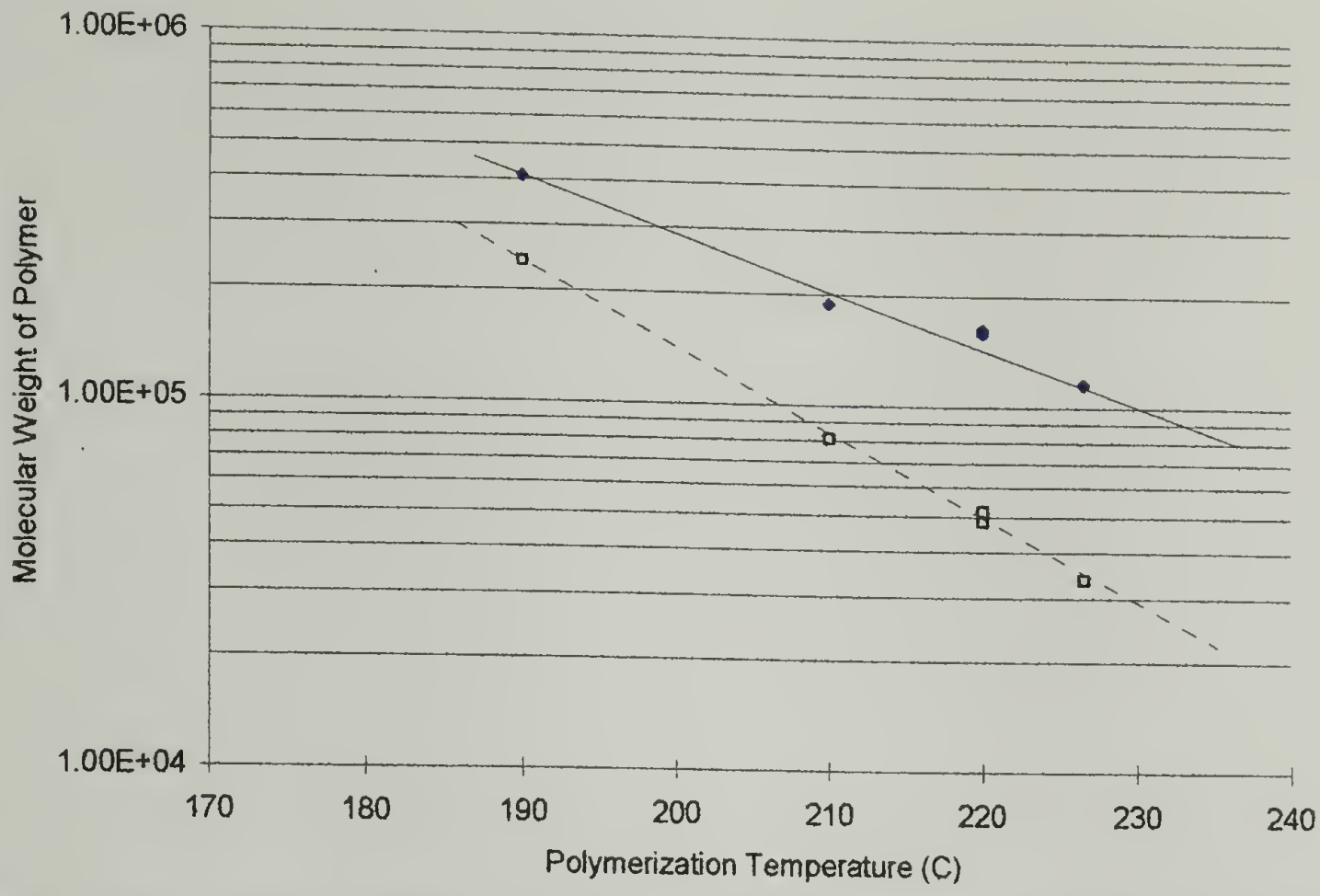


**Figure 5.11 "Corrected" molecular weights for stannoxane initiated polymerizations at different temperatures. Solid line is $<M_w>$, dotted line is $<M_n>$.**

## 5.3 Proposed New Initiator: Dibutyltin Diethoxide

Degradation of the Sn-O links in a TBTE initiated c-PBT chain has minimal effect on the molecular weight of the polymer. Addition of two linear chains during polymerization with TBTE initiator only produces two chains with none, one, or two tributyl tin endgroups. Degradation of the Sn-O link therefore only removes the endgroup from the linear chain. Degradation of the same Sn-O links in a stannoxane initiated c-PBT has a more dramatic effect as each chain appears to contain an average of 3 - 4 tin residues (based on Mw determination of specimens degraded during rheology studies reported in Section 6.3). The polymerization rate and hydrolytic stability of the stannoxane molecule make it the more attractive initiator of the two for further investigation aimed at developing a commercial product. A still more ideal initiator may be an as-yet untested agent such as dibutyltin diethoxide (DBDE):

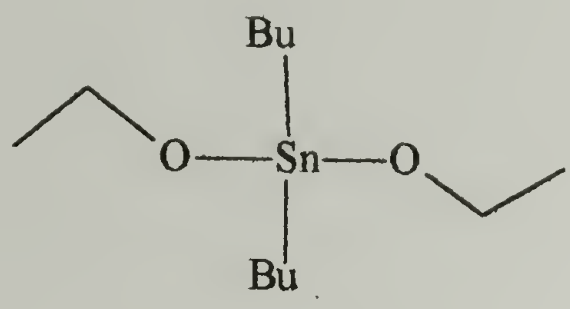


The Sn-O bonds in this molecule are just as polar as those in the stannoxane used in this research and should therefore give rise to the same polymerization kinetics. This bifunctional initiator would only produce linear molecules through ring opening, insertion polymerization. PBT polymer from this initiator can be expected to have characteristics similar to those of commercial linear PBT. After producing high molecular weight polymer, thermal degradation would result in a bisection of the chain. Quenching the reaction by the addition of water should result in hydroxy endcapping one end of the chain and leaving an ethoxy endcap at the other end.

If the brittleness in the current c-PBT arises from the high crystallinity and / or low level of intercrystalline links, and if these characteristics stem from the suspected macrocyclic topology of stannoxane initiated c-PBT, then using the DBDE initiator should result in polymers with toughness equivalent to that of the commercial PBTs. This initiator, which is easily prepared from readily purchased reactants, remains to be investigated. This is one of the primary recommendations for further research which results from the current investigation.

## 5.4 References for Initiator Systems and Polymerization


1)Kricheldorf, H.; Lee, S. *Macromolecules* **1995**, *28*, 6718-6725.

2)Kricheldorf, H.; Lee, S.; Bush, S. *Macromolecules* **1996**, *29*, 1375-1381.

3)Kricheldorf, H. R.; Lee, S. *Macromolecules* **1996**, *29*, 8689-8695.

4)Ramesden, H. E.; Banks, D. R. *US Patent # 2,789,994*; Ramesden, H. E.; Banks, D. R., Ed., **1957**.

5)Brunelle, D.; Brandt, J.; Serth-Guzzo, J.; Takekoshi, T.; Evans, T.; Pearce, E. "Semi-crystalline Polymers via Ring-opening Polymerization: Preparation and Polymerization of Alkylene Phthalate Cyclic Oligomers," American Chemical Society, Las Vegas, NV, V38, pp. 381-382, **1997**.

6)Takekoshi, T.; Brunelle, D. J. "Soluble titanium bisglycoxide catalysts useful for depolymerization of high molecular weight linear polyesters to produce macrocyclic oligoesters.," Patent Pending, **1995**.

7)McAlea, K.; Todt, M., Unpublished results.

# CHAPTER 6

# CHARACTERIZATION OF c-PBT

The following chapter presents the characterization which was done to understand the response of c-PBT under a wide variety of conditions. Thermal, rheological, mechanical, and analytical techniques have been used to determine how this polymer is different from the commercial linear PBTs which are well characterized. The results of this broad analysis support the hypothesis that the c-PBT produced using stannoxane cyclic initiator is indeed a cyclic macromolecule with many unique properties.

Four commercial linear PBT resins are also characterized in this section. These resins were supplied by the GE Plastics Co. The are designated by the commercial trade name VALOX® PBT resins. The four resins are: VALOX® 315 PBT, VALOX® 310 PBT, VALOX 295® PBT, and VALOX 195® PBT, in order of decreasing molecular weight. It should be noted that VALOX 195® PBT resin is no longer a commercial product. It is also noted that the results of all characterization methods reported herein do not reflect the typical properties for these PBT resins and should not be interpreted as representative of the products sold by GE Plastics.

## 6.1 Molding and Characterization Techniques

This section will give an overview of the characterization techniques selected for evaluating the polymers produced in this study. The characterization of solid c-PBT requires that the polymer be produced as well consolidated, uniform specimens. Standard molding practices are not designed for polymerization during melt processing. Thus some

---

® VALOX is a registered trademark of GE Plastics Co.

modification of existing processes was required to accommodate for the low viscosity of the oligomers. Before discussing the characterization techniques, the following section describes these modified processes and gives the details for producing acceptable test parts of c-PBT.

### 6.1.1 Molding Techniques for c-PBT

Prior to molding the cyclic oligomers it was necessary disperse the initiator at a molecular level. This was accomplished for each batch of cyclic oligomers described in the following sections by co-dissolving predetermined amounts of both the cyclics powder and the initiator powder in dry methylene chloride, stirring the mixture until a consistent solution was obtained, and then slowly drying the solvent until a thick paste remained. Final drying of the solvent was done using a labcratory vacuum oven at about 50° C and about 10 psig of vacuum. A dry nitrogen sweep-stream was regulated into the oven during the drying to carry off the residual solvent and maintain a low vacuum during drying. After drying overnight, the mixture was ground to a fine powder using a mortar and pestle and stored until needed in glass jars with metal lids to prevent exposure to ambient humidity. Prior to molding, the powders were redried for four hours at 110° C.

Polybutylene terephthalate cyclic oligomers are distinguished from polymeric PBT by their unique processing characteristics that make is possible to infuse the low viscosity melt into very thin openings such as are typically found in composite preforms. Composite structures are a class of materials which make use of multiple materials, each selected for its individual characteristics. Continuous glass fiber composites for example, take advantage of the modulus of the fibers for their high stiffness. However, without an

effective adhesive to bond the fibers together, the composite would only be useful in uniaxial tension, having no resistance to shear or to forces acting transverse to the fiber axis under bending. Polymer "glues" are therefore used to bind together the adjacent fibers, and form a rigid bundle of fibers which acts as a continuum and have resistance to shear loading as well as tension. A polymer can only be useful as a composite adhesive when it can penetrate all interstices and wet all surfaces of the composite filler. Thermosetting resins have traditionally filled this need because of the low viscosity of the monomers which allows easy flow into glass mats and tows. After infusion they can be crosslinked into high molecular weight polymers.

Neat molten cyclic oligomers of PBT have a very low viscosities, about 3500 poise at 190° C and less than 20 poise at 215° C. For the experiments in this study, the actual viscosity of the oligomers was not important, since the initiator would begin polymerization as soon as the oligomers were melted. A study of the polymerization rate and crystallization rate at a series of temperature above the oligomer melt temperature is the subject of a later section.

Due to the limited supply of butane terephthalate cyclic oligomers (BTCs) available for this study, compression molding was selected for specimen preparation since this was determined to be the processing technology readily available that was the most conservative in terms of material usage. In order to prepare usable specimens for mechanical evaluations, it was first necessary to find a way to overcome the problems created by compression molding a low viscosity melt.

Compression tools which form defined shapes fall into two general types: frame tools and closed molds. Frame tools are the simpler tools to build and use as they consist

of a plate into which the desired shape has been cut out as shown in Figure 6.1. The frame is placed on a support surface, generally a flat plate, the molding resin is loaded into the frame, and a second plate is used to cover the tool and compress the melt. The thickness of the final part is determined by the thickness of the frame used in molding. This type of tool is successfully used for compressing high viscosity polymer melts which take the shape of the frame, but are restricted from flowing through the vents created by the frame and its cover plates. Low viscosity melts have a tendency to flow out of these vents unless precautions are taken to machine the frame and plate to matching fine tolerances. This is rarely done for compression molding; instead closed molds are used.

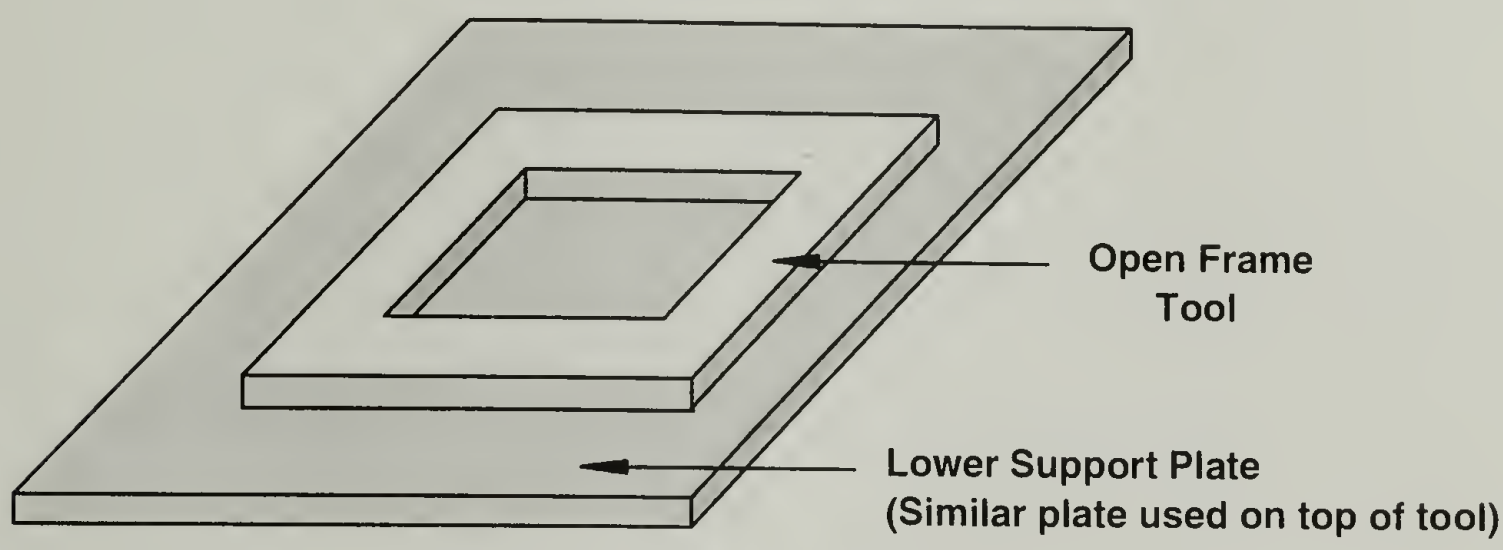


**Figure 6.1 Open Frame Tool for Compression Molding**

Closed molds for compression are more complex and can be used to make parts of different thickness. As shown in Figure 6.2, these molds consist of a heavy outer frame and four internal parts: two surface plates and two beveled shims which serve to tighten the tool upon compression. The closed mold is better for retaining a low viscosity melt, but suffers from the direct application of the compression load on the melt - which in turn squeezes the low viscosity melt out through the tool vents.

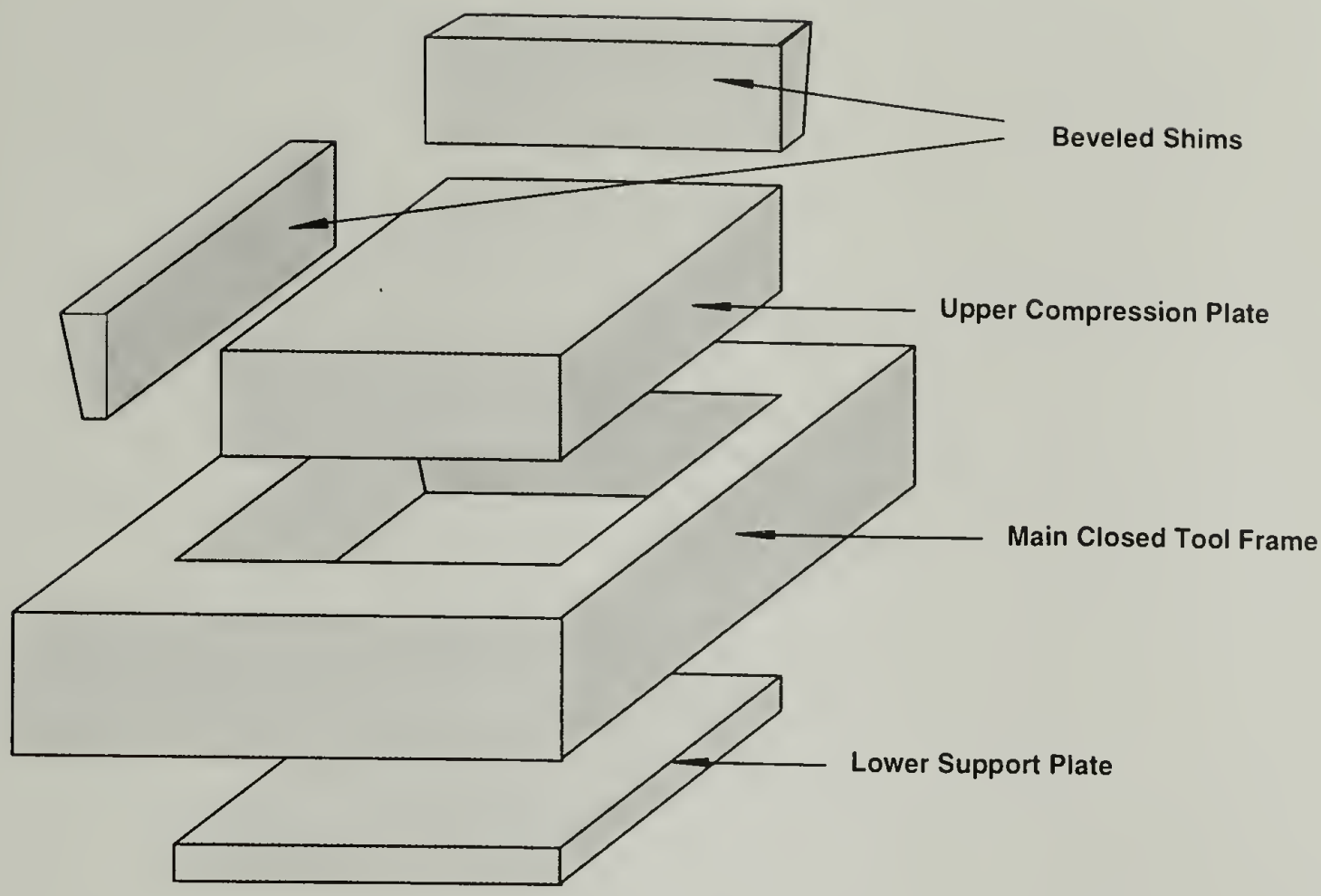


**Figure 6.2 Exploded View of a Closed Mold for Compression Molding**

Each type of compression tool was successfully used to mold the c-PBT resins, with modifications to accommodate for the resin viscosity. Thin plaques of c-PBT were successfully molded in a 4 x 5 x 0.1 inch frame mold by first lining the frame with a layer of aluminum foil. Once the frame was placed on the support plate, the foil liner was made to conform to the walls of the frame and smoothed to minimize replication of creases in the final polymer part. This foil liner could contain the oligomer melt during polymerization However, the molded part tended to adhere to the foil liner. The use of mold release was found to be rather ineffective The best solution found to remove the foil from the polymer surfaces was an overnight soak in nitric acid. The finished parts from frame molding would generally have some voids caused by excessive shrinkage of the PBT, as the part was not under direct pressure during cooling.

A closed mold technique was found to be easier to use in producing well consolidated specimens. Two such tools were used to produce most of the mechanical specimens tested in this study. Even though this type of tooling has thinner vents, it was nevertheless found that the melt could be forced out of the vents when subjected to high pressures. To overcome most of this problem, the oligomers were first polymerized in a laboratory oven. The dried powdered oligomer, with dispersed initiator, was placed in a Teflon® coated heavy aluminum foil boat having the same internal dimensions as the mold. Polymerization was generally carried out at 190° C for 30 - 45 minutes with nitrogen flowing through the oven. The polymer was then placed in the closed tool and allowed to melt under the pressure of the upper tool plate. Once melted, the tool was moved to the cold side of the compression press, where pressure was applied during crystallization and cooling. A surface thermocouple was placed on the tool surface and the cooling rate was determined to be 11° C/minute. When the temperature of the tool surface reached 110° C, and the polymer had crystallized, but was still above Tg, the pressure was released. The tool was removed and disassembled by pressing the part from the tool using a small Carver press.

Release from the tool was facilitated by first adhering a sheet of self adhesive Teflon coated aluminum to the upper and lower tool plates. When tool sticking became a problem, the sides and shims were coated with a fine misting of Slide Hi Temp 1000® high temperature mold release.

---

® Teflon is a registered trademark of the E.I. DuPont Co.

® Slide Hi Temp 1000 is a registered trademark of Percy Harms Corp.

A third compression tool was used in the preparation of the SENB fracture specimens discussed in Section 6.6. This tool was a closed tool with inner dimensions of 5.0 inches by 0.50 inches. This closed tool differed from the plaque tool shown above in that it had no beveled shims. This tool was hardened steel with tight tolerance machining to keep the vents small, but it could only be used to mold polymerized c-PBT as the oligomer would easily flash out of the cavity upon first melting.

Other processes could be developed for producing parts from PBT cyclics. While this study was concerned with the characteristics of the neat polymer, composite structures could be produced by similar compression processes, where the fiber was placed in the tool and the oligomer dispersed into the fibers during processing, or through a continuous fiber wetting processes. In continuous processing, a bundle of fibers are pulltruded through a low viscosity melt pool which infuses and binds the fibers. The shape of the finished part is produced through drawing this hot glass / polymer bundle through a cooling mandrel for thermoplastics or a hot curing mandrel for thermosets. To make this process work for thermoplastic cyclics, the initiator would need to be part of the fiber coating, as the oligomeric melt pool would need to be kept from polymerizing until it had been dispersed into the fiber bundles. This continuous process needs further exploration as it offers promise in the production of high volume, thermoplastic composite structures.

Technology has been developed for epoxies, alkyds, and other thermosetting resins that have low viscosity monomers which allow for the resins to be "B-staged" into a partially cross linked state which is subsequently cured more fully when formed into a final shape. This B-stage technology allows for more easily handling the otherwise difficult

powders or liquids during processing. There is no known correlation to B-staging in the polymerization of cyclic oligomers as described in this research.

### 6.1.2 Characterization Techniques Useful in Understanding c-PBT

A complete understanding of any material involves characterization through a series of techniques, each used to probe a different aspect of the material's character. Through repeated and precise studies of the responses that a material gives to a systematic series of probing tests, it is possible to build a consistent picture of the structure of the material from its atomic composition and architecture, through its molecular superstructure (such as the crystal structure for crystallizable materials), and even its interactions with other phases dispersed throughout the material's continuum.

The object of this study was to determine the structural differences between cyclics based PBT and conventional PBTs. Thus the characterization techniques used were selected to accentuate the suspected differences in the polymer which could be related to the basic structural makeup of the polymer chain. The fundamental differences between PBT produced from direct condensation synthesis to linear chains vs. expansion of cyclic oligomers into macrocyclic rings could simply be the result of the use of different polymerization catalysts. To allay this concern, TBTE initiator was used in many parallel experiments where stannoxane initiated c-PBT was being studied as a unique material.

Documented differences in the crystallizability from earlier studies[1] of the two types of PBT were the initial focus of the study. Using the DSC as a thermal probe, it was possible to expand the study of crystallization rates at different isothermal polymerization temperatures. A richer understanding of the initiator has been established through varying

the level of initiator, as well as comparing the two types of initiators under identical polymerization and crystallization conditions.

The DSC was not capable of determining the rates of polymerization. Because this ring expansion polymerization involves the breaking and reforming of two sigma bonds per monomer addition, the polymerization reaction is athermal. Polymerization rates were therefore determined through isothermal rheology studies. The polymerization reaction using stannoxane initiator was found to be so fast that it was finished before the temperature could become stabilized in the rheometer. For TBTE, it was possible to determine polymerization as well as crystallization rates as a function of polymerization temperature. Isothermal rheology studies were also used to determine the low shear viscosity of both the c-PBT resins and the linear resins. This characterization is critical to understanding the chain structure, as the low shear (zero shear) viscosity is highly dependent on the degree of entanglement of the polymer chains. With macrocyclic polymers, it is hypothesized that there would be less entanglement for a given molecular weight and thus the low shear viscosity should be lower for c-PBT at an equivalent molecular weight.

Molecular weight determinations were done using either a Hewlett Packard Gel Permeation Chromatograph (GPC) fitted with 10x4, 10x5, 500 Å columns or a Polymer Labs Mixed C5μ column eluting at 0.75 ml/min with 3% isopropanol $CHCl_3$. Narrow molecular weight linear polystyrene standards were used in calibration as no narrow molecular weight PBT standards are readily available. The molecular weights reported herein are consistent with reported values from earlier work on linear and cyclic PBTs[1,2].

Macrocyclic PBT may not be accurately represented by <Mw> obtained from GPC as described in Section 6.4.1.

Intrinsic Viscosity (IV) was also hypothesized to have a dependence on chain architecture. If macrocyclic molecules have a smaller hydrodynamic radius than linear chains of equal molecular weight[3], then a solution of these molecules should have a lower resistance to flow in a shear field. This would result in a lower intrinsic viscosity for cyclic resins vs. their linear counterparts at a given molecular weight. IVs for the linear resins are determined by dissolving the resins in strong solvents, i.e. hexafluoro isopropanol or a mixture of phenol and tetrachloro ethane[4]. The free alcohol groups in these solvents is known to open the stannoxane link[5], rendering the cyclic molecules linear, thus obfuscating the measurements. The ability to determine accurate IVs for the cyclic resins has been hindered by the lack of a good solvent for these molecules and no IV data is included in the results . A more complete discussion of the use of this technique for differentiating cyclic and linear resins is found in Section 6.4.2.

Static light scattering is a powerful technique for determining fundamental parameters of molecular structure. This technique allows one to measure molecular dimensions in a solvent; thus obtaining from the same solvated specimen both $<M_w>$ and radius of gyration (the mean square radius of gyration, $R_g^2$, also denoted as $<s^2>^{1/2}$). In addition, the degree of solvation may be determined by a calculation of $A_2$ for the polymer / solvent combination. By comparing the ratio of $<M_w>/ R_g^2$ it is possible to differentiate a system of linear molecules from a system of cyclic molecules which would have different average $R_g^2$ for the same average $M_w$. The problem of finding a good solvent for cyclic PBT again prevented meaningful measurement the of $R_g^2$ using static

light scattering techniques. While it is possible to determine a molecular weight $R_g^2$ for conventional PBT resins using light scattering, the measurements on c-PBT have not been successful.

Mechanical testing has proven to be fruitful in elucidating differences between the macrocyclic and linear PBTs. Tensile and compressive characterization have shown the crystallinity to be the main determinant of modulus. This is also reflected in dynamic mechanical measurements made on solid specimens of both linear and cyclic PBT. Fracture toughness measurements have shown a surprising result in this research. While the cyclics-based PBT is known to be brittle, degradation of the cyclic structure can result in a linear molecular structure of high molecular weight. This "linearized" resin can have a higher toughness than the original, higher molecular weight cyclic resin. This finding is explored through extensive toughness measurements of the linear resins and cyclic resins using four different fracture specimen geometries. A series of controlled degradation experiments are employed to document the toughness enhancement of the c-PBT.

Microscopy studies have been done to evidence the nature of the fracture path through the spherulitic structure of PBT. Some etching of the polymer surfaces has been attempted to determine differences in the nature of the spherulites obtained from the linear and cyclic molecules.

### 6.1.3 References for Molding and Characterization Techniques


1)Kambour, R.; Barnes, J.; Garbauskas, M.; Gundlach, P.; McCracken, L. "Microstructure, Morphology, and Crystallinity Level in Polybutylene Terephthalates Produced from Cyclic Oligomers: A Progress Report.," Manuscript in preparation, **1995**.

2)Brunelle, D.; Brandt, J.; Serth-Guzzo, J.; Takekoshi, T.; Evans, T.; Pearce, E. "Semi-crystalline Polymers via Ring-opening Polymerization: Preparation and Polymerization of Alkylene Phthalate Cyclic Oligomers," American Chemical Society, Las Vegas, NV, V38, pp. 381-382, **1997**.

3)Hadziioannou, G.; Cotts, P. M.; tenBrinke, G., *Macromolecules* **1987**, *20*, 493-497.

4)Borman, W. F. H., *Journal of Applied Polymer Science* **1978**, *22*, 2119-2126.

5)Brunelle, D. J., Personal Communication.

## 6.2 Crystallization

Poly(butylene terephthalate) is among the easiest of the synthetic polymers to crystallize. Its rapid crystallization kinetics make it difficult to produce amorphous PBT unless specimens are very thin and quenching is very rapid. Because of this propensity for crystallizing, an understanding of the properties of PBT must be based in an understanding of the morphology. PBT polymerized from cyclic oligomers using stannoxane initiator is unusual in the speed of its crystallization and the resulting high degree of its crystallinity. A detailed study of the crystallization of cyclic and linear PBT has been undertaken to help elucidate the fundamental characteristics which result in the unusual crystallizability of this material. Before discussing the results of the present study, a review of the crystalline morphology of PBT is presented.

### 6.2.1 Review of the Crystalline Morphology of PBT

When polymerized and crystallized at 190° C, PBT from cyclic oligomers has a 50% crystalline structure, consisting of lamellae which exhibit a single melting peak at 225° C. Upon melting and recrystallization, the degree of crystallinity decreases, as well as the peak melting temperature. By monitoring the shape and temperature of this melt peak (after melting and recrystallization) as a function of heat soak time in the melt, it is found that a the single high temperature melt peak splits into two distinct peaks, the upper peak remaining at 225° C, while a second peak, of diminishing size, moves to lower temperatures with increased heat soak time. These two peaks correlate well with the two types of spherulites[1] known to exist in PBT: usual and unusual spherulites, differentiated by their light scattering patterns as well as their thermal and mechanical properties.

Stein and Misra[1] originally identified the two spherulitic types through a set of experiments in which 1 mil-thick specimens of PBT were melted between glass slides in a 245° C oil bath, and then isothermally crystallized by quenching into another oil bath at a series of lower temperatures. Their results demonstrate that isothermal crystallization above 180° C (where the degree of under-cooling is small and the rate of crystallization is lower) produces an "usual" spherulite; one where the optical pattern from crossed polarized light produces a Maltese cross with the dark arms positioned at 0° and 90° to the optical axes of polarization (see Figure 6.3 a). The usual spherulite produces a $H_v$ SALS pattern with intensity lobes at 45° to the polarized light (see Figure 6.3 b).

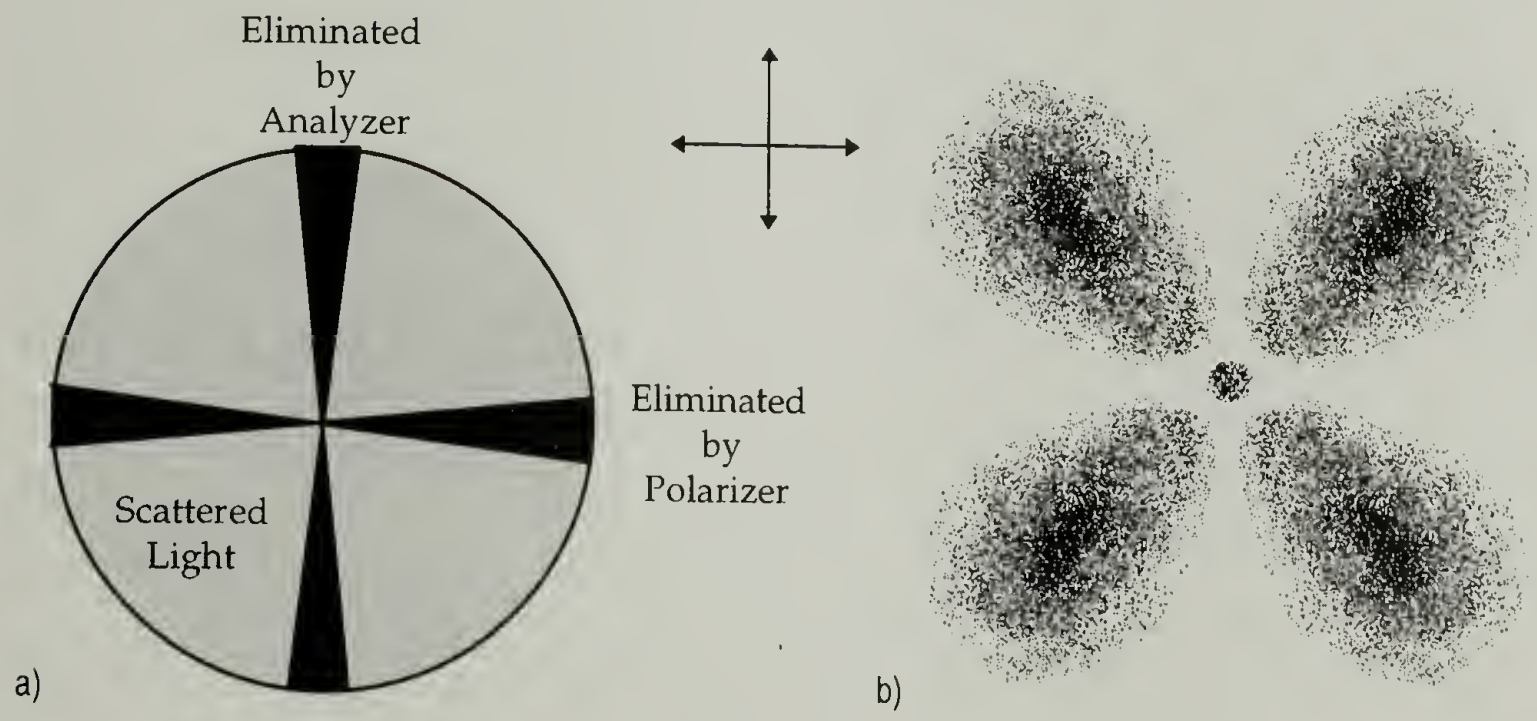


**Figure 6.3 a) Illustration of the Maltese Cross observed in polarized optical microscopy of usual spherulites in PBT. b) Illustration of the clover-leaf pattern observed in SALS of usual spherulites in PBT. Direction of polarization axes are shown by the accompanying arrows.**

When PBT is isothermally crystallized at higher crystallization rates (where crystallization takes place at temperatures below 180° C), a different type of spherulite results. This "unusual" spherulite is identified by a 45° rotation of the Maltese cross

pattern observed in polarized optical microscopy. Consistent with the shift in polarized light is a rotation of the $H_v$ pattern (relative to the crossed polarized source light) produced from small angle light scattering (SALS) from the solid films. The unusual spherulite produces a SALS pattern with intensity lobes at 0° and 90 ° to the polarization planes. This unusual spherulite is also known to exist in synthetic polymers such as poly(tetrafluoro ethylene)[2] and natural polymers such as collagen[3]. The usual spherulites are common to most synthetic polymers and have been reported for PET[4] and polyethylene[5].

Melt cooled linear PBT is interesting in that it produces both types of spherulites, dependent on the temperature and rate of crystallization. Nucleation density also depends on the temperature where crystallization begins. A larger degree of undercooling, defined as the difference between the melt temperature and the crystallization temperature ($T_m$ - $T_c$), produce a higher nucleation density and result in smaller spherulites. The literature values for spherulites sizes in isothermally quenched and crystallized PBT[1] range from 15 μm diameter for crystallization at temperatures between 180° and 190° C, to 6 - 8 μm for crystallization at temperature between 30° and 50° C.

When injection molded, PBT specimens show a range of spherulite sizes which increase with depth away from the quenched amorphous surface[6]. The first signs of crystallinity appear below the amorphous molded surface as a transition zone of high nucleation density (and small spherulites) below which exists a core with larger spherulites. The cooling rate, as a function of distance from the surface, determines the nucleation density and the crystallization rate. Injection molded PBT is reported as having

(unusual-type) spherulites ranging in size from 20 μm diameter[7] to 10 μm diameter[6] with the differences depending on the melt and mold temperatures used in injection molding. At this point it is important to understand that the type of spherulite found in PBT cooled from a melt depends on the kinetics of crystallization, and faster crystallization produces small, unusual spherulites.

By contrast, c-PBT produced by isothermal polymerization and crystallization at 190° C is composed on only usual spherulites. These spherulites are very small, on the order of 2 - 3 μ as determined by SALS, but are produced by very fast crystallization. This finding appears to be unique in that the best literature reports of the usual spherulites in PBT are from slow cooling or high temperature isothermal crystallization, each resulting in large usual spherulites. The usual spherulites in nascent c-PBT are evidence that macrocyclic PBT crystallizes easily into well defined lamellae without the energetic barriers associated with linear PBT. The SALS pattern of thermally degraded c-PBT shows a mixture of usual and unusual spherulites.

The following literature survey of the two spherulitic forms in PBT is included to help elucidate the differences in the crystallization process which results in each type of spherulite. Ludwig and Eyerer[8] characterized PBTs consisting of the two types of spherulites and found these specimens also show mechanical and thermal differences. PBT specimens formed by injection molding into cold tooling produced a predominance of unusual spherulites. Specimens injection molded into hotter tooling were primarily of the usual type spherulites. Differences were found in hardness, yield stress, and heat of fusion for the two types of spherulitic material. A summary of their results is shown in the following table.

**Table 6.1 Comparison of the properties of usual and unusual PBT spherulites. Data from Ludwig and Eyerer[8].**

| | Unusual Spherulites | Usual Spherulites |
|---|---|---|
| **Preparation Conditions:** | | |
| Mold Temperature (° C) | 60 | 118 |
| Cooling Rate | Fast | Slow |
| Specimen Thickness (mm) | 3 | 5 |
| **Observed Results:** | | |
| $\Delta H_f$ (J/g) | 48 | 60 |
| Yield Stress (MPa) | 50 | 55 |
| Fibril Arrangement | sickle-shaped | radial pattern |
| Hardness (MPa) | 138 | 148 |
| Reported Tm (° C) | 225 | 220 |
| Shear Modulus @ 0° C (GPa) | 1 | 1.2 |

What is shown is that slower cooling produces a) higher crystallinity, b) usual type spherulites, and c) greater rigidity in the polymer. At least some of the increased rigidity can be attributed to the increased crystallinity. The correlation of the increase in rigidity with the type of spherulite formed remains to be proven. Micrographs of the fibril patterns within the two types of spherulites give evidence for differences in the off-axis light scattering. The usual spherulite has radial fibrils and produces a $H_v$ pattern similar to polyethylene, with its regular chain-folding crystal morphology, while the unusual spherulite has sickle-shaped fibrils containing lamellae that produce a strong off-axis component to the $H_v$ pattern. Ludwig and Eyerer show a series of DSC heating thermograms from injection molded specimens as well as specimens cooled in the DSC at rates from 0.1° C/min to 30° C/min. (While they do not report the heating rates for these thermal studies, it is concluded from the curve shapes and reported temperatures that the heating rate for each specimen was no more than 20° C/minute.) From these DSC results,

they conclude that the usual spherulite has a melting point of 220° C while the unusual spherulite is correlated with a melting peak of 225° C. (This conclusion is opposite to the conclusion of Stein who used a hot stage polarizing microscope to observe unusual spherulites transforming into usual spherulites on heating. Stein concludes that the early melting of unusual spherulites can allow a perfecting to the usual type spherulite, which then melts at a higher temperature.).

Yeh and Runt[9] document the effects of heating rate on the size and position of multiple melting points in PBT following a series of annealing studies. Their specimen preparation consisted of compression molding PBT of relatively low molecular weight (Celanex® 2000) at 250° C followed by quenching into ice water. Analysis of these films showed that they were already 30% crystalline, consisting primarily of usual type spherulites. Their explanation for this type of crystalline structure is that the specimens were air cooled for 15 seconds during removal from the hot press prior to quenching - sufficient time at temperature to nucleate and partially crystallize the specimens. On heating in the DSC, two melt peaks were found for specimens annealed at temperatures between 90° C and 198° C. In all cases, the higher (and larger) melting peak (peak 2) was centered at 220° C with the lower melt peak (peak 1) located just above the annealing temperature. As the annealing temperature was increased, the upper peak began to show a strong melt shoulder at 225° C. Annealing at 198° C resulted in an unique dual melt endotherm where peaks 1 and 2 were nearly identical in area. Annealing at temperatures

---

® Celanex is a registered trademark of Hoechst Celanese Co.

from 205° C to 218° C produced only a single melt peak, which increased in peak temperature as the annealing temperature was increased.

Annealing at 198° C produced two peaks when the specimen was subsequently heated at 20° C/minute. When the rate of heating in the DSC was increased, the relative sizes of the two melt peaks began to change. At 2.5° C/minute, the peak 1 was diminished and peak 2 was large. At 40° C/minute, peak 1 was large, and peak 2 was suppressed. This change is consistent with a remelting and recrystallization model in which the rate of recrystallization is the limitation in producing a large peak 2. Again, these researchers concluded (erroneously?) that both peak 1 and peak 2 are associated with the melting of usual spherulites.

Moginger[7] et al. have reported on a similar relationship between the properties of PBT and the resin's morphology. They also present a series of DSC traces from injection molding specimens produced from melts having temperatures between 230° C and 255° C, all using a constant mold temperature of 60° C. On heating in the DSC at 10° C/minute, all specimens were found to have virtually identical melting behavior. This is the result of latent crystallization, which continues above 190° C on heating in the DSC at a low rate, and tends to produce identical crystallinity in all specimens. When the DSC heating rate was increased to 100° C/minute, it was found that the specimens produced from melts having higher melt temperature exhibit a higher heats of fusion. A distinct shoulder appears on the upper edge of the melt endotherm for specimens produced at the highest melt temperatures. These researchers speculate that this shoulder is due to the presence of the usual-crystal form in the more slowly cooled specimens. Consistent with this

crystalline form was a loss of tensile elongation (from 30% in specimens molded using a low melt temperature to 3% in specimens molded using a high melt temperature) and a lowering of the creep compliance. The difference in melting behavior of specimens all quenched into a tool the same temperature using different melt temperatures is believed to be related to the longer time the melt spends in the temperature range for crystallization (210° - 185°C) during rapid cooling in injection molding. Based on a model of the cooling process, the specimens molded from a 255° C melt spend 5 seconds in this temperature range, whereas the specimens molded from a 230° C melt spend only 2.5 seconds in the crystallization temperature range. With a fast reported crystallization half time for PBT of only 30 seconds[10], it appears that the spherulitic superstructure developed within the first five seconds of crystallization determines the type of spherulite that dominates the morphology.

Kim and Robertson[11] discuss the multiple melting peaks of PBT in terms of the thermodynamics of lowering the upper melt peak temperature (originally at 225° C) by annealing at lower temperatures (between 180° and 210° C). This treatment results in a double peak where the more stable original (usual type) crystals now have a lower melt temperature. They give a thermodynamically acceptable justification for the observed phenomena by allowing that amorphous interlamellar chains can crystallize during annealing. If the annealing temperature is below 180° C, independent (unconnected) new crystals form in the interlamellar regions, giving rise to a higher degree of crystallinity in the annealed material, without changing the melt temperature of the original stable crystals. However, when annealing is carried out near the melt temperature, an additional

crystallization takes place, in which amorphous material near the surface of existing crystals begins to crystallize on and couple to the existing crystal surfaces, increasing the thickness of the original lamellae, while creating defects in these crystals. The effect is to lower the melt temperature of the original crystals, while increasing the crystallinity of the material, through both coupled and unconnected crystal development.

### 6.2.2 Usual Spherulites in Macrocyclic PBT

PBT produced from cyclic oligomers, using the stannoxane initiator, contains only one type of crystal as evidenced by a single peak on the DSC thermogram. This peak is symmetric, is centered at 225° C, and is typical of the "usual" spherulitic structure defined by Stein[1]. SALS $H_v$ patterns from 15 μm-thick sections of this polymer have confirmed the spherulites found in c-PBT polymerized with stannoxane and crystallized at 190° C are the usual-type spherulites. As shown in Figure 6.4, when this material is melted, held in the melt at 250° C for increasing periods of time, and then recrystallized at 190° C, the character of the spherulite produced changes. This change seen first is a lowering the melt temperature (at melt soak times from 1 minute to 10 minutes). Subsequently, the endotherm peak splits into two independent peaks (with melt soak times from 15 minutes to 60 minutes)

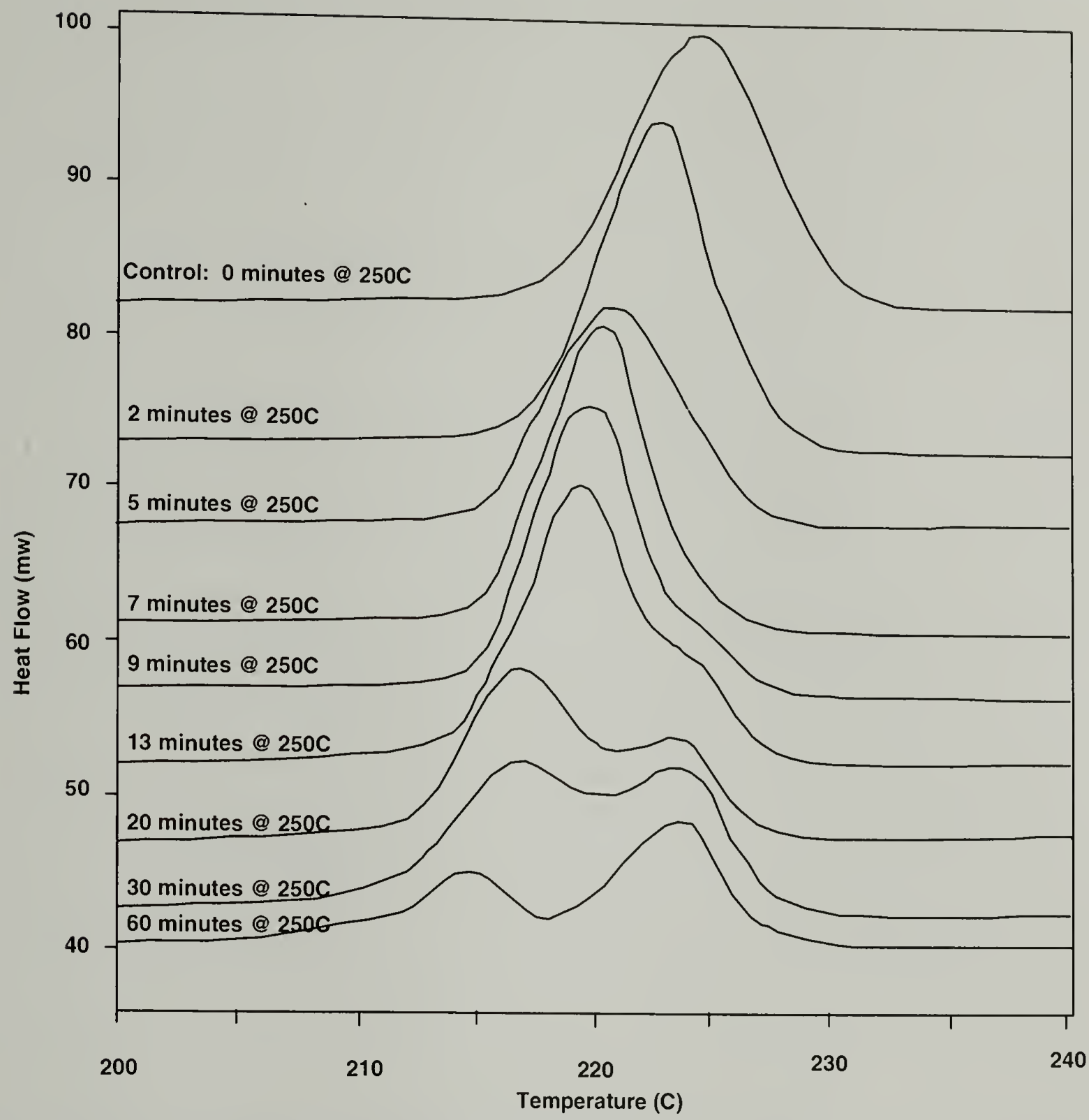


**Figure 6.4 Crystallization endotherms resulting from c-PBT which had been held in the melt for times indicated, then recrystallized at 190° C. Traces show the endotherm shape on heating at 20° C /minute following recrystallization.**

The temperature of the upper peaks corresponds to the $T_m$ of the usual-type spherulites. The peak of the lower endotherm at short melt soak times corresponds to the unusual spherulite, which lowers with increased melt soak time. Accompanying the lowering of the endotherm temperature is an irreversible loss of crystallizability as determined by a lowering of the heat of fusion with increased heat soak times in the melt. Thus the heat soak process reduces the crystallizability of the c-PBT, while also changing

the type of spherulite produced on recrystallization. SALS patterns from heat soaked c-PBT show a mixture of usual and unusual spherulites.

Small angle light scattering (SALS) patterns of a high molecular weight c-PBT produced by the isothermal polymerization and crystallization using 0.12 mol % stannoxane initiator at 190°C, clearly shows a predominance of very small spherulites of the usual type. Spherulites of this type are known to by produced in linear PBT only by slow crystallization processes e.g., by isothermal crystallization at small undercooling, by slow cooling from the melt, or by slow evaporation of a polymer solution. Usual spherulites, with their high melting temperatures and high heats of fusion, are the result of slowly crystallizing linear polymers, allowing time for crystal perfection and allowing for incorporation of more crystallizable material during primary crystallization.

The occurrence of usual spherulites in a rapidly crystallized macrocyclic c-PBT at 190° C is thereby unexpected. However, following compression molding to produce the SALS specimen, this material exhibited an onset of melting at 223° C and a peak melt temperature of 233° C, and a heat of fusion of 70 J/g. Using a different specimen to study polymerization in the DSC, crystallization at 190° C was initiated in 1.5 minutes, peak crystallization rate was at 4 minutes, and the crystallization exotherm ended at 8 minutes. (These times included both polymerization and crystallization.) The symmetry of the crystallization peak and size of the subsequent melt endotherm suggest that the polymerization was complete within the observed crystallization time at this temperature.

These studies lead to the conclusion that cyclic PBT, isothermally polymerized and crystallized at temperatures as low as 190° C, produces spherulites which are produced

only in melt cooled linear PBT under crystallization conditions which allow for slow development of more perfect crystal structure[1,7,12]. At very high crystallization rates, the cyclic PBT structure allows for the development a crystal perfection not achievable from a linear PBT structure. This observation will be used later in discussions of molecular dimensions as they relate to crystal perfection.

### 6.2.3 Effect of Thermal Soak on the Crystallizability of c-PBT

Work by Kambour on the crystallinity of c-PBT[13] showed that the high crystallinity of macrocyclic PBT, produced by isothermal polymerization and crystallization at 190° C, was lost on thermal soaking above the melt temperature. As described in Section 2.2, the heat of fusion on first melting was over 70 Joules/gram, but decreased over 1 hour of heat soak at 250° C to a value of about 50 Joules/gram. The loss of crystallizability was found to be irreversible. Figure 6.5 shows the combined data from Kambour's earlier work and data obtained in the present study (using different batches of cyclic oligomers and initiator). Also shown are the heats of fusion for two different commercial PBTs cooled from the melt and crystallized under the same conditions.

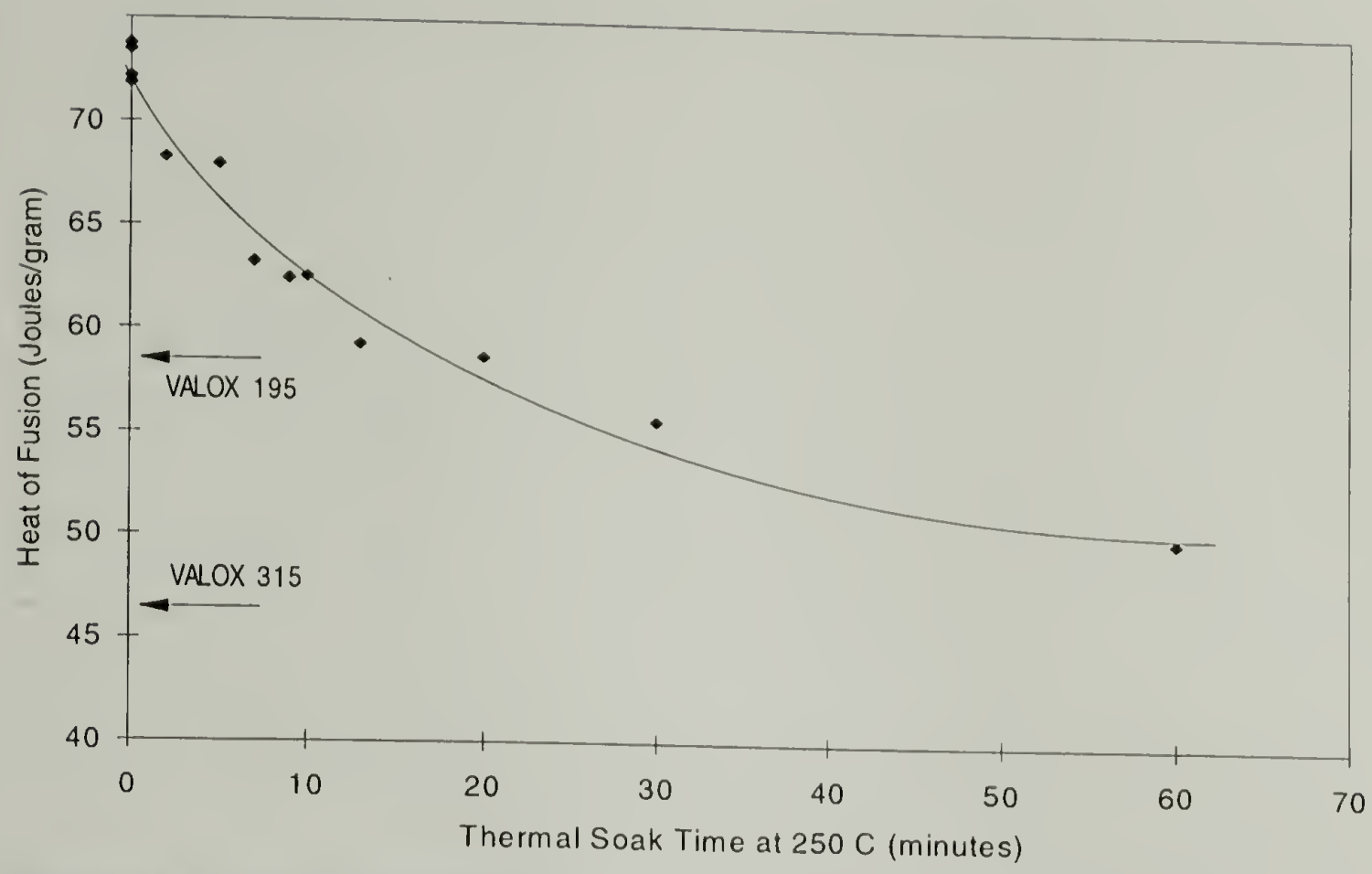


**Figure 6.5 Loss of Crystallizability of c-PBT following heat soak at 250°C.**

Consistent with the loss of crystallizability is a loss of crystal perfection, evidenced by a decrease in the melting point of the polymer following thermal soaking in the melt. Figure 6.4 shows the shape of the subsequent melting endotherms following heat soaking at 250° C, cooling to 190° C, re-crystallizing for 15 minutes, and reheating through the melting temperature. The peak melting temperature decreases with thermal soak time. After 9 minutes, the endotherm begins to develop a high temperature shoulder and the single endotherm is seen to split into a double melting peak after 20 minutes of heat soaking. The control shows a melt peak temperature of 225° C. The double melt endotherms have peak temperatures of 215° C and 225° C.

Examination of the spherulites formed on first crystallization (representative of the control curve in Figure 6.4) shows that they are the usual type spherulites, and the melting temperature and high crystallinity confirm this finding. On melting and holding for short

times at 25° C, the stannoxane links in these macrocyclic chains begin to open, resulting in some linear chains with increased radius of gyration. On recrystallization, the cyclic polymer nucleates rapidly, but the presence of some linear polymer prevents the development of high crystallinity. With increased time in the melt, cyclic degradation continues, and the resulting linear polymers begin to predominate the melt. On cooling and crystallizing after extended melt soak times, more mixed type spherulites are formed, which show a lower initial melting point. The lower melting point is the result of less perfect crystals and/or the presence of lower molecular weight linear polymer. As this polymer melts on reheating at 20°C / minute, it may partially recrystallize on heating to the more stable, usual spherulitic form. This latent-formed usual-type spherulite then melts at a higher temperature, resulting in a distinct double melting endotherm.

The crystallization exotherms following heat soaking show faster nucleation and crystallization than were found during original polymerization and crystallization. However, this may be explained by the fact that nucleation begins on cooling, before the melt reaches the isothermal recrystallization temperature of 190° C. By the time the DSC is stabilized at the recrystallization temperature, much of the crystallization is finished and no direct comparison of recrystallization rates with original crystallization rate can be made.

The loss of crystallizability is irreversible. Only the nascent macrocyclic molecules can nucleate rapidly and densely at low temperatures, and crystallize into very small usual spherulites, with high crystallinity and a high degree of crystal perfection.

In order to better understand the polymers being characterized, it was necessary to first understand the conditions which affect the morphology of the polymer. To this

end is was necessary to produce and characterize polymer using both the stannoxane initiator and the chemically similar but topologically dissimilar TBTE initiators and to compare the characteristics of the polymer products.. By studying the polymerization over a range of temperatures, it was also possible to determine the relative crystallization rates of the different c-PBT structures produced from the two initiator systems.

### 6.2.4 Crystallization Rate Studies on c-PBT

Polymerization and crystallization studies were carried out in a Perkin-Elmer Series 7 Differential Scanning Calorimeter (DSC) under isothermal conditions. The isothermal polymerization temperatures were selected to cover the range from just above the melting range of the oligomers to the experimentally determined temperature where the crystallization rate was too slow to monitor by using the DSC. Figure 6.6 shows a thermal fingerprint for the slow heating of cyclic oligomers containing 0.3 mol % stannoxane initiator from room temperature through the melt temperature of the polymer. The lowest temperature selected for polymerization rate studies was 170° C.

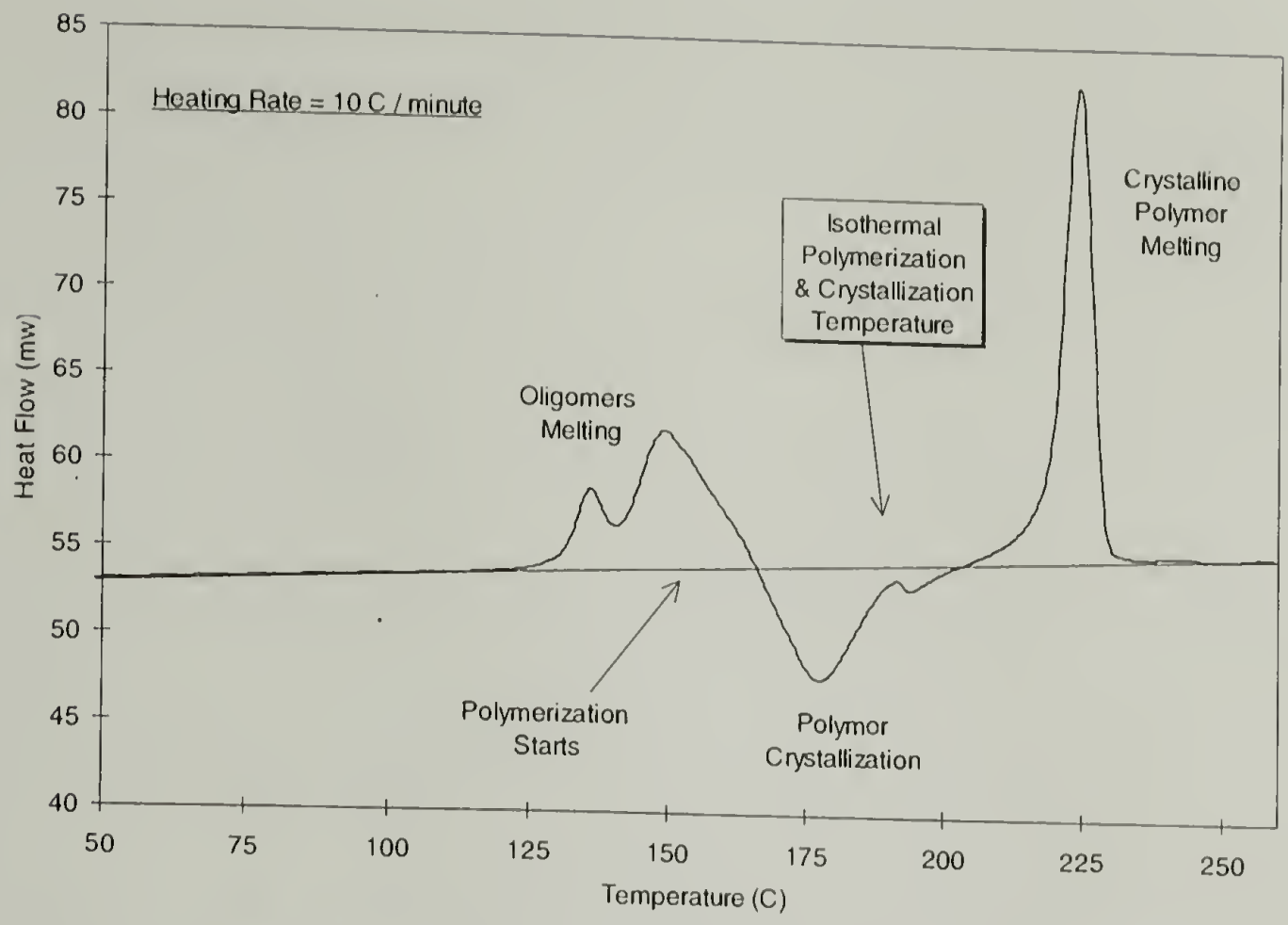


**Figure 6.6 DSC heating trace of cyclic oligomers of PBT containing 0.3 mol % stannoxane initiator. Heating rate = 10° C / min.**

A quantity of BTC oligomers, containing a predetermined amount of initiator (prepared by co-dissolution as described in Section 6.1), was rapidly heated to a temperature above the melting point of the oligomers. The system was then held at a constant temperature while monitoring development of the crystallization exotherm. These studies were performed over a temperatures from 170° C, where the oligomers are just fully melted, to 212° C, where the crystallization was so slow that the end of the exotherm and return to baseline was difficult to determine.

Following crystallization, each specimen was heated to 260° C at 20° C per minute and the melting endotherm was recorded for analysis. The critical data for comparison and analysis were found to be 1) the nucleation time for crystallization, 2) the crystallization half times (determined as the difference between crystallization onset time

and peak crystallization time), 3) onset temperature for melting, 4) peak temperature(s) for melting, 5) size of the melt endotherm (heat of fusion on melting), and 6) shape of the melt endotherm.

TBTE initiated specimens were prepared at initiator levels from 0.30 mole % to 1.17 mole %. The TBTE initiator is known to be extremely hygroscopic, with hydrolysis rendering the initiator inactive. Working in a dry box, dried BTC oligomers were first dissolved in an excess of dried methylene chloride. The liquid initiator was then added volumetrically to the BTCs using a dried micro-syringe. With continuous stirring, the solvent was slowly evaporated into a dry nitrogen stream, followed by vacuum drying and grinding, always under dry nitrogen conditions.

Mixtures of BTCs and the stannoxane initiator were prepared by co-dissolution in a similar manner, without the need for the anhydrous atmosphere. These mixtures were produced in a range of 0.035 to 1.14 mol % initiator to determine the optimum content for high crystallinity. At 0.30 mol % and above, the crystallinity of c-PBT was constant at just over 70 J/g as shown in Figure 6.7. This level of initiator had been used in earlier work and was selected for much of the work in the present research. For this study, initiation with a single stannoxane level only of 0.3 mole % was selected for comparison to TBTE. The experimental design for this study is shown in Table 6.2.

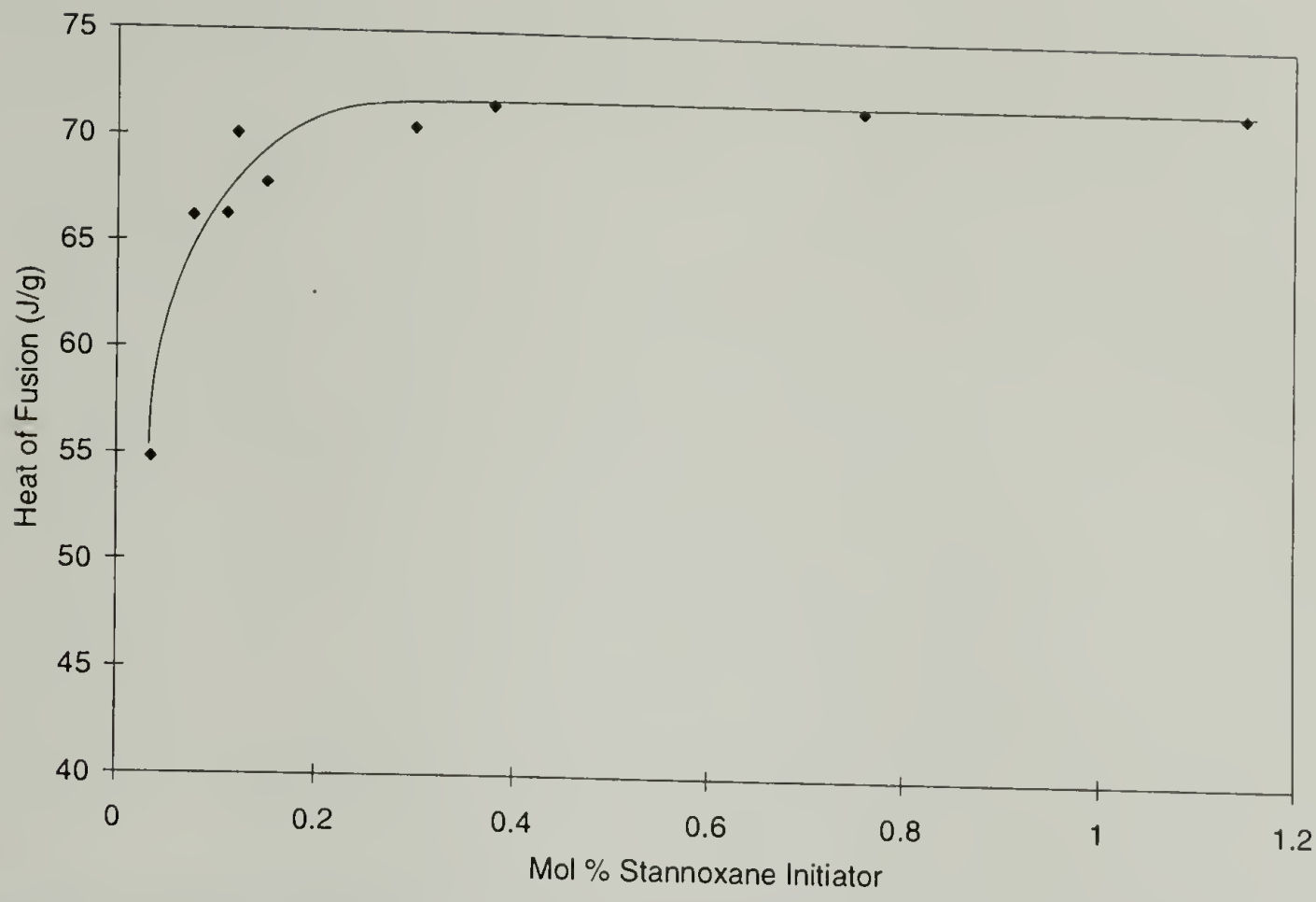


**Figure 6.7 Heats of fusion for c-PBTs with different levels of stannoxane initiator following isothermal polymerization at 190° C.**

**Table 6.2 Experimental Design for Isothermal Polymerization and Crystallization.**

| | 170°C | 180°C | 190°C | 197.5°C | 200°C | 205°C | 212.5°C |
|---|---|---|---|---|---|---|---|
| 0.30 % TBTE | x | | x | | | x | |
| 0.43 % TBTE | | | x | | | | |
| 0.59 % TBTE | x | x | x | | x | x | x |
| 0.73 % TBTE | | | x | | | | |
| 0.93 % TBTE | x | | x | | | | |
| 1.17 % TBTE | x | x | x | x | | x | x |
| 0.30% Stannoxane | x | x | x | x | | x | x |

### 6.2.4.1 Discussion of Crystallization Rates

Polymerization is a thermally activated process which increases in rate with increased temperature. The ring expansion polymerization of cyclic oligomers using a cyclic initiator proceeds with mechanisms similar to addition polymerization in which the active initiator site (the tin - oxygen bond) acts like an active radical site. Rather than

radical transfer down a growing linear chain, the active site remains stationary and the new oligomer material is inserted adjacent to the active site. Thus polymerization proceeds by expanding a ring containing at least one tin residue (each tin having two active polymerization sites). As the temperature is increased, the polymerization rate increases until all available oligomer is incorporated into existing polymer, and only transfer reactions continue which tend to re-equilibrate the molecular weight (See Figure 5.2). This re-equilibration process may involve back-biting reactions which expel smaller rings and even dead rings (those which contain no active tin - oxygen sites), that may become incorporated into another molecule at a later time. The re-equilibration process is able to continue until the polymer is quenched into a glassy state, or until nucleation and crystallization limits the mobility, and thus the reactivity, of the active chains.

Nucleation times and crystallization rates are controlled by the degrees of undercooling of the melt, with lower temperatures favoring faster crystallization. The greater the difference between melt temperature and crystallization temperature, the faster the crystallization will proceed. Crystal perfection and lamellar thickness are also related to the degree of undercooling, For linear polymers, the slower the crystallization, the higher the probability of forming less defective crystals. Also for linear polymers crystallized from the melt, the lamellar thickness is inversely proportional to the difference between the melt temperature and the crystallization temperature.

Both the ring expansion polymerization using stannoxane cyclic initiator, and the ring opening polymerization using TBTE initiator proceed by the kinetic rules of polymerization. As the temperatures of isothermal polymerization and crystallization increase, the rates of polymerization increase, and the rates of crystallization decrease.

Polymerization using either initiator is an athermal process, involving the breaking and formation of the same bonds to increase molecular weight. Therefore, only the times and rates associated with the crystallization (but not polymerization times or rates) could be determined using a DSC. Figures 6.8 through 6.10 show the onset, peak, and end of the crystallization exotherm using stannoxane and two levels of TBTE as functions of temperature. Figure 6.11 compares the initiation times for crystallization from these plots and Figure 6.12 shows the crystallization half times from each experiment, calculated as the difference in time between the onset and peak rate of crystallization.

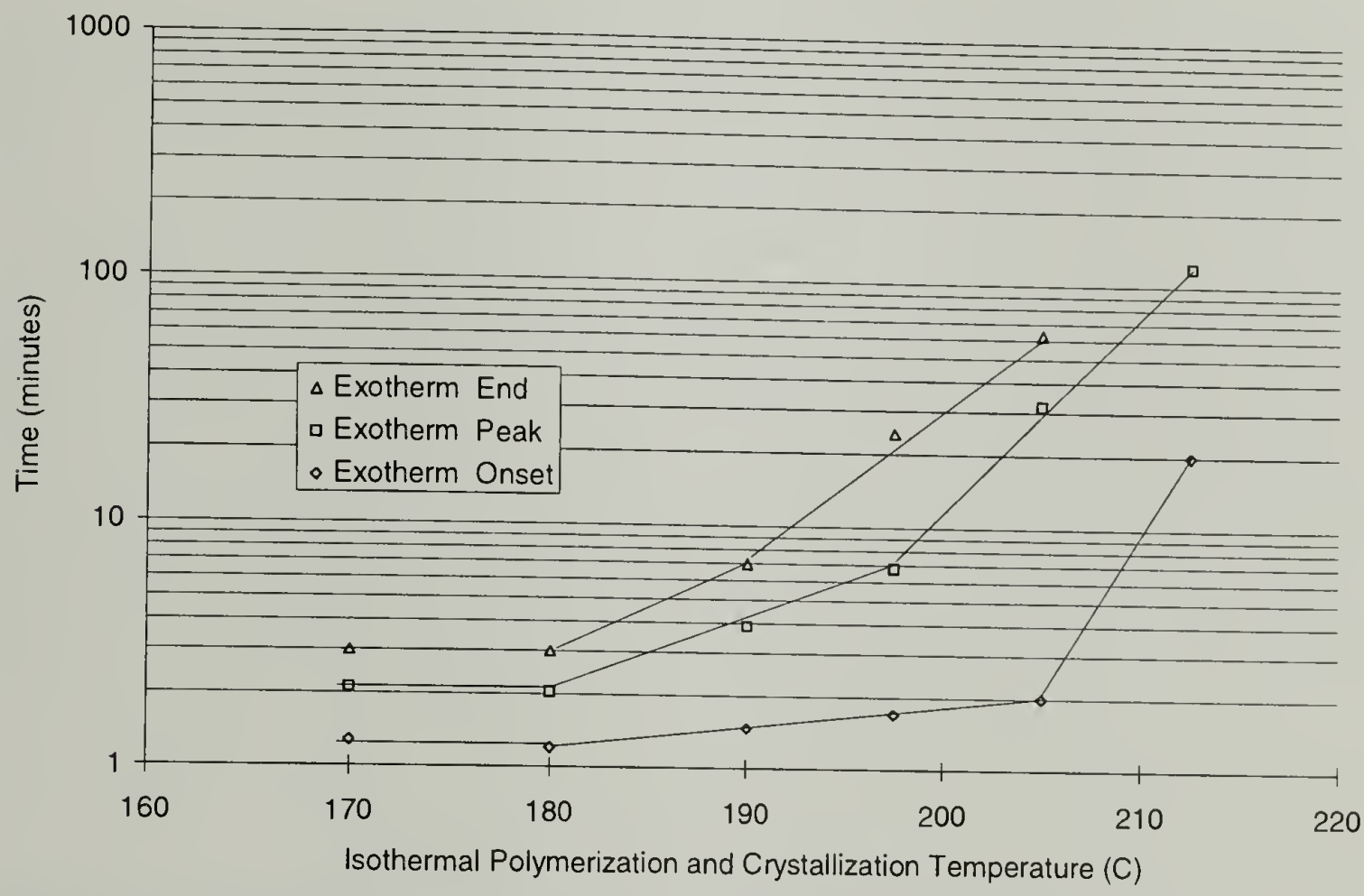


**Figure 6.8 Crystallization exotherms for c-PBT initiated with 0.3 mol % stannoxane.**

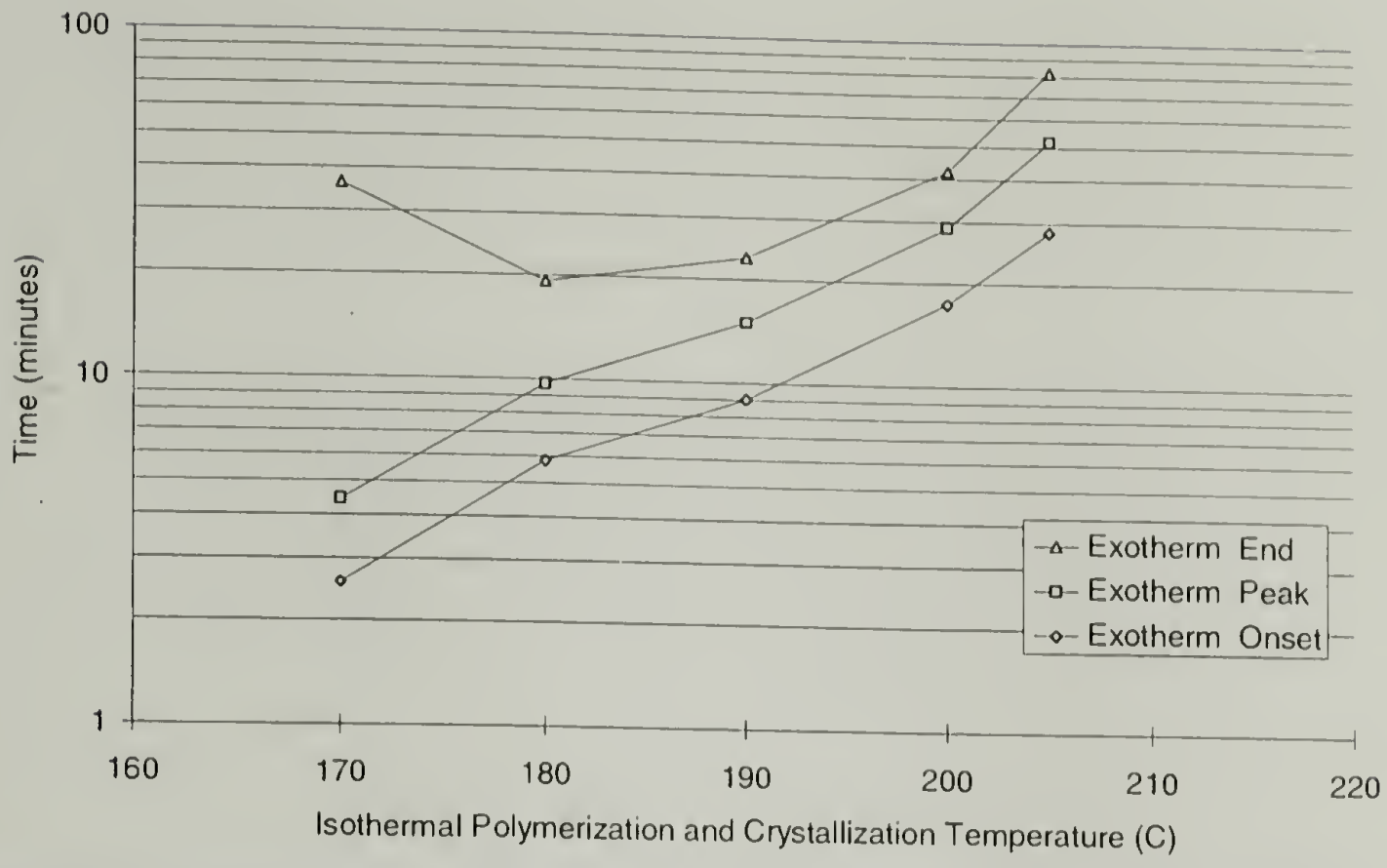


**Figure 6.9 Crystallization exotherms for c-PBT initiated with 0.6 mol % TBTE.**

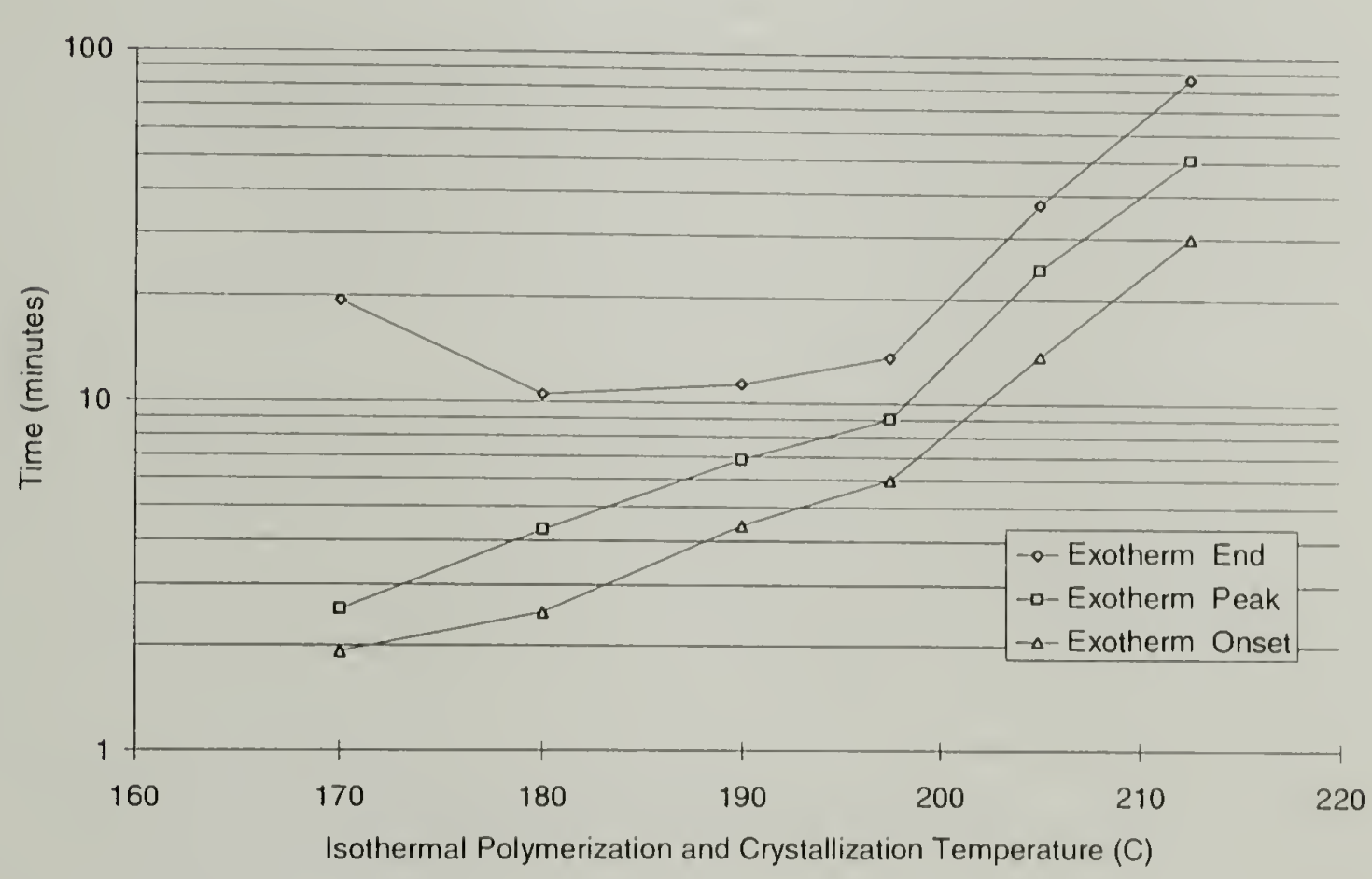


**Figure 6.10 Crystallization exotherms for c-PBT initiated with 1.2 mol % TBTE.**

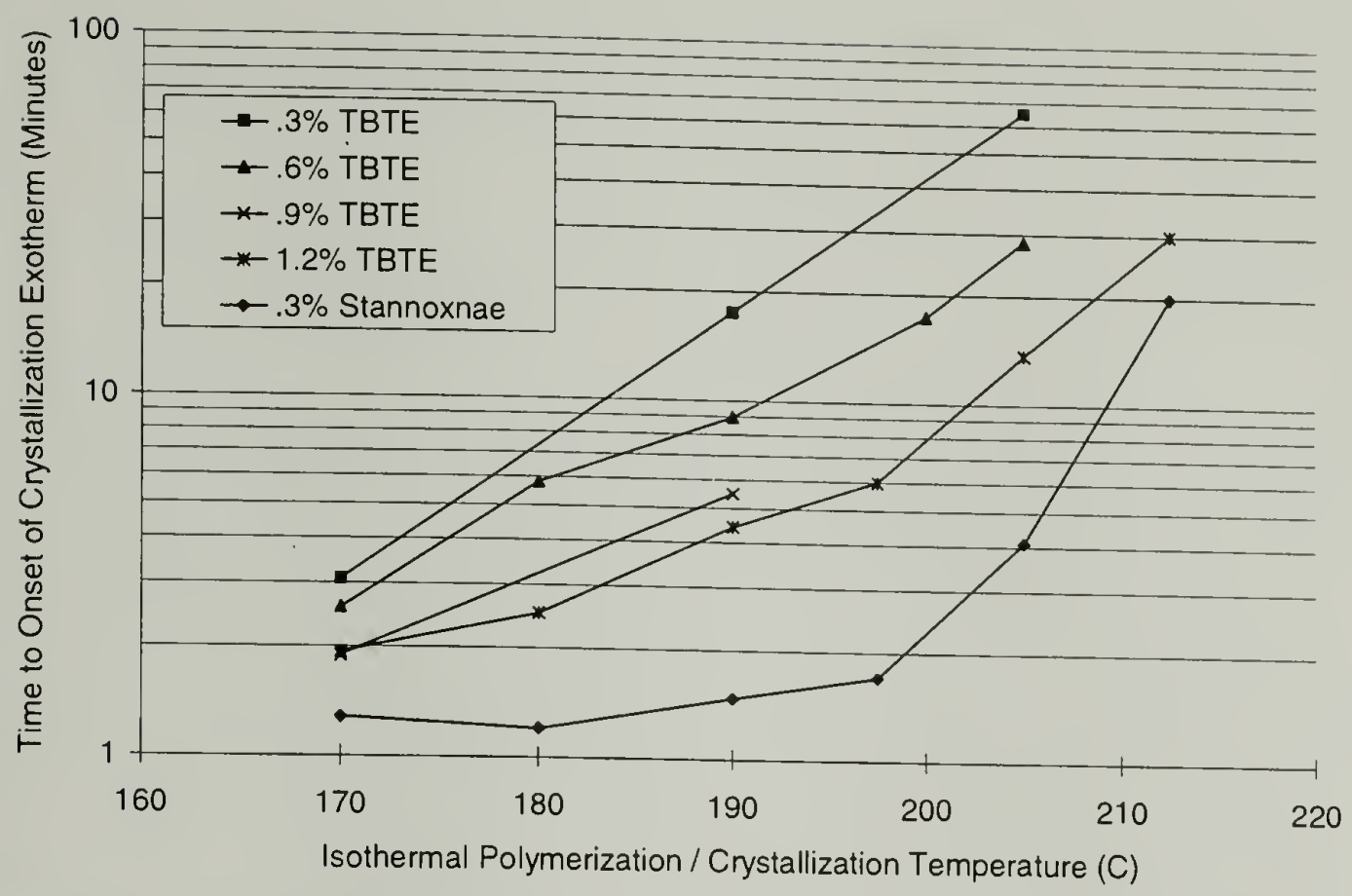


**Figure 6.11 Onset of crystallization exotherm as a function of temperature for c-PBTs.**

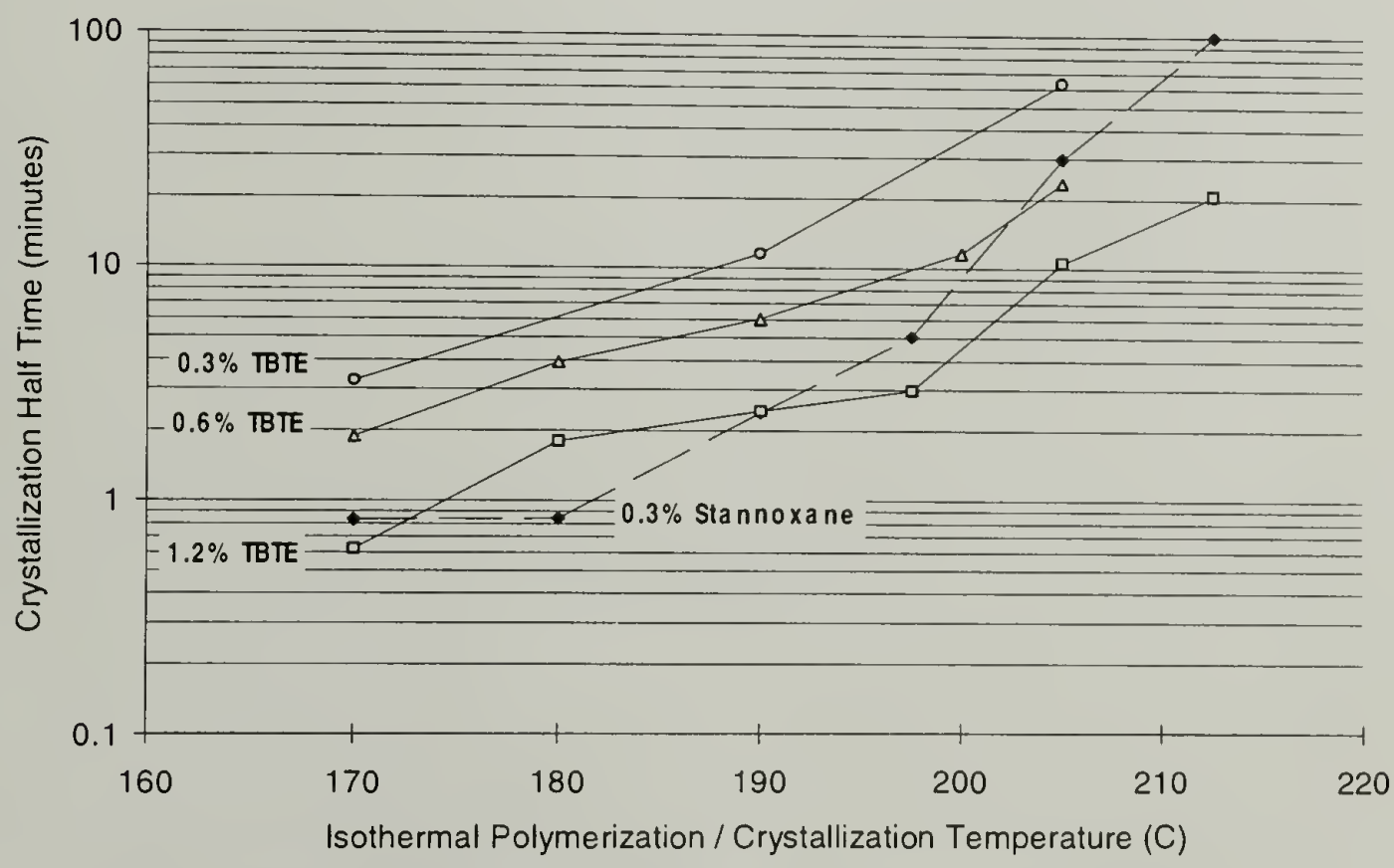


**Figure 6.12 Crystallization half times as functions of temperature for c-PBTs.**

Stannoxane initiator was found to produce a symmetric crystallization exotherm at temperatures of crystallization below 190° C (Figure 6.8), while TBTE produces a symmetric crystallization exotherm only at temperatures above 190° C (Figures 6.9 and 6.10). Stannoxane also produces c-PBT having a shorter initiation time for crystallization at all temperatures (Figure 6.11), and a faster half time for crystallization at low temperatures (Figure 6.12).

As the molecular weight of the PBT polymer increases, its crystalline melting point increases. Cyclic oligomers of PBT melt over a range of temperature from 125° to 160° C. PBT polymer is known to have a crystalline melting point in the range of 220° - 225° C (which can be increased through careful annealing). Crystallization will not begin at the temperatures investigated in this study until polymerization has proceeded sufficiently to produce some high polymer. Therefore, based on the onset time for crystallization, it can be concluded that a the polymerization of PBT using stannoxane as the initiator is faster than polymerization of PBT using the TBTE initiator. (In Section 6.3.2.2, where the rates of polymerization are determined through rheological studies, an explanation is given for the rate differences which involves the electronegativity differences between the two initiators.)

For TBTE initiated polymerization, the higher levels of TBTE are found to produce faster crystallization vs. the lower levels. This is the direct result of more high polymer chains being produced within a given time than are produced within the same time using a lower initiator level.

Once crystallization has initiated, the process continues as long as sufficient polymer remains which can be attached to a growing crystal face. In the case of stannoxane initiated c-PBT, this process is symmetric with time, first increasing in rate, reaching a maximum rate of crystallization, and then decreasing rapidly as crystallization ends. At the end of crystallization, all available crystallizable material has been added into the existing lamellar structures, allowing only interlamellar material to remain as amorphous polymer. While being at least 140° C over the Tg of amorphous PBT, this energetic amorphous intercrystalline material is inhibited from addition to existing crystals through a combination of restrictive mechanisms that may include 1) intercrystalline tie chains linking adjacent lamellae, 2) defective or random placement of adjacent lamellae, 3) entanglements consisting of non-adjacent re-entry loops or loose loops of polymer chains at the surface of a lamella, or 4) other types of loose chain knots or entanglements which limit the mobility of chain segments to crystallize.

By contrast, TBTE initiator is slower to polymerize cyclic oligomers of PBT. The time to initiate crystallization is delayed at all temperatures of crystallization, implying a longer time to develop the molecular weight necessary for crystal nucleation. At the lowest temperature of polymerization, the crystallization exotherm takes on a unique shape as evidenced by a delay in the time to end of crystallization. The TBTE initiated crystallization exotherm at low temperature exhibits two distinct rates of crystallization as shown in Figure 6.13.

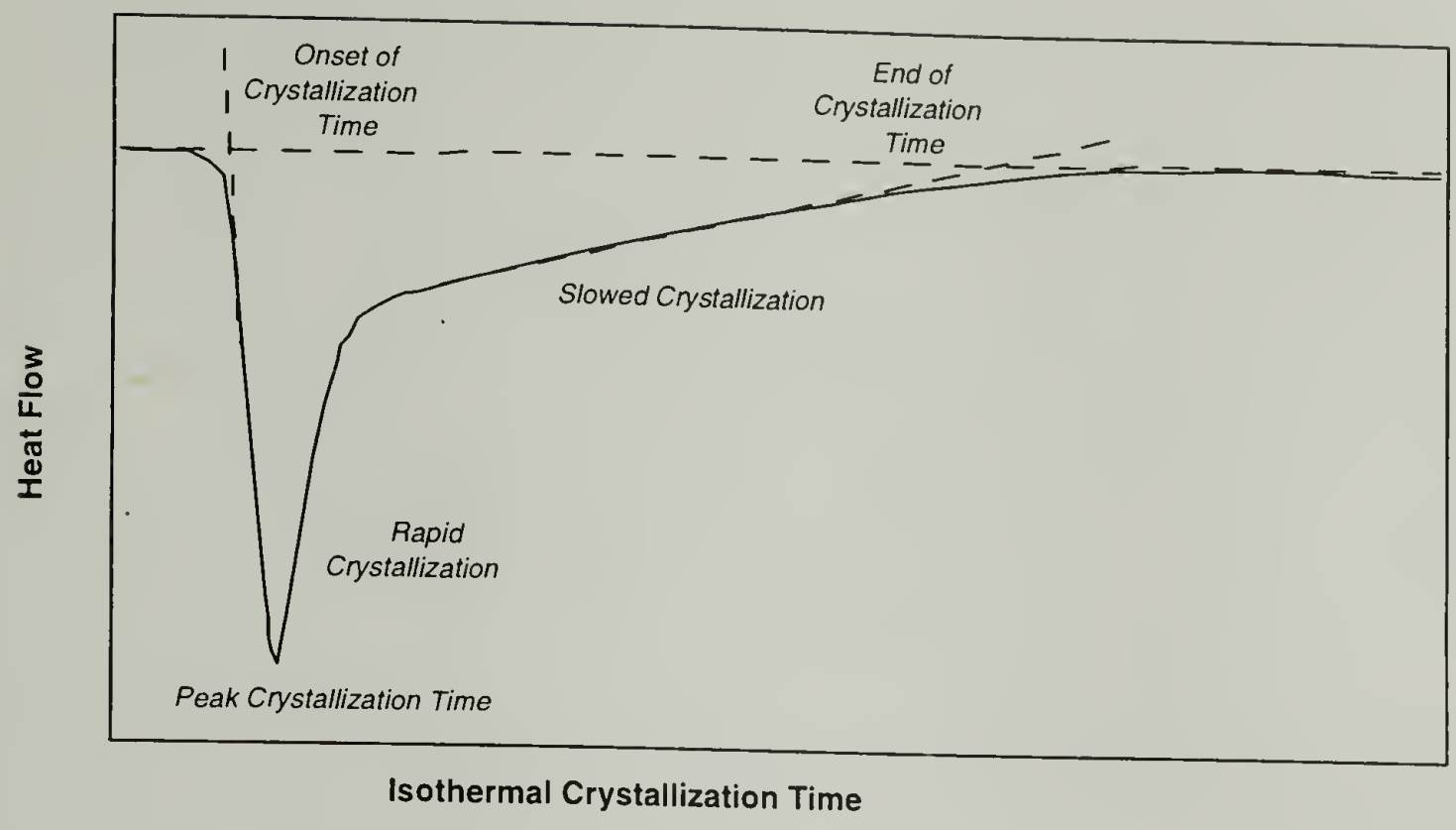


**Figure 6.13 Asymmetric crystallization exotherm resulting from TBTE-initiated polymerization of BTCs at 170° C.**

The change in crystallization rate suggests that there is a mechanism which becomes operative late in crystal development whereby crystallization is inhibited, but still possible. Knowing that the polymerization rate is slower for the TBTE initiated system (compared to the stannoxane initiated system which results in a symmetric crystallization exotherm at these temperatures), it may be speculated that the crystallization has begun well before polymerization was complete. Once polymerized, crystallization rates for the two systems should be the same, as both systems produce the same high polymer. However, the change in crystallization kinetics for the TBTE initiated system suggests that the polymerization is rate limiting at this temperature. Polymerization proceeds by an insertion mechanism, which consumes oligomer in the vicinity of the active chain end (the TBTE residue remains on the growing chain end during insertion polymerization), and nucleation can occur only after the polymer reaches a sufficiently high molecular weight. This model suggests that a single chain may have one end attached to a developing

crystallite, while the free end is still involved in polymerization. As the macromolecule grows at the active chain end, it is reeled toward the growth surface and added to the developing lamella. The spherulitic skeleton which develops during rapid primary crystallization would become space filling before polymerization is complete. If this condition occurs, diffusion of the remaining oligomer may be slowed, thereby slowing the rate of polymerization, and consequently slowing the rate of crystallization. Neither polymerization or crystallization are stopped by this process, but continue at a slower rate until all oligomer is depleted. The resulting polymer formed at this temperature is found to be very highly crystalline as evidenced by its subsequent melting endotherm being greater than 70 J/gram.

From Figure 6.12, the crystallization half times are seen to increase with crystallization temperature for polymers made with both initiators. This results from a reduction in the degree of undercooling with increasing temperature. However, the cyclic polymers produced by stannoxane initiator have a different dependence of crystallization half-time on temperature than do the linear polymers produced by the TBTE initiator. With less undercooling, nucleation density is also decreased. While the nucleation time, as determined by the onset of crystallization (see Figure 6.11), is shorter for the stannoxane initiated polymers at all temperatures, the increasing half-times of crystallization must result from less favorable crystallization conditions for the macrocyclic molecules. This may be the result of relatively slower diffusion[14,15] for the macrorings vs. linear chains. This limit in the rate of crystallization for macrocyclic molecules vs. linear molecules is not well understood.

A lower limit of the polymerization rate for stannoxane initiated polymerization may be determined from Figure 6.8. At both 170° and 180° C, the crystallization endotherm ends within three minutes of reaching thermal equilibrium, and the crystallization exotherms are symmetric. If the asymmetric endotherm found in the slower TBTE initiated system (at the same temperatures) results from continued polymerization during crystallization, we may assume that the polymerization with stannoxane is complete within the time frame of the crystallization. (In the following discussion of melting endotherms, the polymer from this low temperature polymerization is found to be highly crystalline, and thereby fully polymerized. If significant amounts of oligomer had remained in the system, the melt endotherms would have been reduced.) If the polymerization is complete within three minutes at 170° C, it must be even faster at higher temperatures. In Section 6.3.2.2, an attempt to measure polymerization rate using a parallel plate rheometer is described. For studies in which stannoxane is used as the initiator, polymerization is found to be complete in the five minutes required for the rheometer's temperature to recover (following specimen insertion) at temperatures as low as 110° C. While the TBTE-based polymerization rates may be measured in the rheometer, stannoxane-based polymerizations are too fast to be determined by either of these two techniques.

From Figure 6.11, the nucleation time for crystallization of stannoxane initiated c-PBT is seen to increase dramatically above 200° C. While nucleation times for crystallization of the linear polymers increase uniformly with temperature, the macrocyclic polymer appears to be inhibited from nucleation as the temperature is increased. Also, a

large difference is seen in the times for nucleation between the linear and macrocyclic structures, although all samples were prepared form the same batch of BTC oligomers. This slower nucleation from the linear molecules, all of which are fully polymerized prior to crystallization at the higher temperatures, is evidence that heterogeneous nucleation from minute dust or dirt particles is not the only mechanism for nucleation, If heterogeneous nucleation were the only mechanism, each polymer would exhibit the same rate of nucleation with temperature as the polymer chains are not differentiated from nucleation by a foreign particle. The delayed nucleation in the macrocyclic structure at increased temperatures appears to be related to the uniform expansion of the molecule. As the temperature increases, the expanding cyclic molecules approach the nucleation times of the linear molecules. This implies that at lower temperatures, the higher concentration of slowly diffusing chain segments, characteristic of the macrocyclic polymer, is more energetically favored to nucleate crystallization vs. the linear chains which have higher entropy and higher diffusion rates. No studies were attempted where nucleation agents were intentionally added to bias the system toward heterogeneous nucleation.

#### 6.2.4.2 Discussion of Melting Endotherms

Stannoxane initiator produced high polymer which has a single sharp melting endotherm. The temperatures for onset, peak and end of the endotherm are shown in Figure 6.14. Peak temperature is simply determined as the temperature where the endotherm is centered. Onset and end temperatures are determined by extrapolation of the steepest portion of the leading and trailing edge of the peak to the baseline. The

reported values are therefore idealized and cannot accurately represent any broadening of the peak from the presence of less perfect crystals.

For macrocyclic PBT the shape of the endotherm is symmetric regardless of crystallization temperature. However, the melt peak increases uniformly in temperature as the crystallization temperature increases. This increase in peak melt temperature is also seen when conventional PBT is annealed above its glass transition temperature. The annealed polymer exhibits both an increase in crystallinity and, if the annealing temperature is high enough, an increase in melting temperature.

As discussed in Section 6.2.1, PBT is known to exist in two unique stable spherulitic forms as first documented by Stein and Misra[1]. These two forms, referred to as the "usual" and "unusual" spherulites, are differentiated by their melt temperature with the unusual type spherulite melting at 220° C and the usual type spherulite melting at 225° C. As described earlier, Ludwig and Eyerer[8] have studied the effect of processing conditions on the morphology of PBT and documented several other differences between the two spherulitic types.

The melting peaks c-PBT are well above the values published by Cheng and Wunderlich for isothermally crystallized linear PBT[16]. They show an upper melting peak at 222° C for melt crystallized polymer at crystallization temperatures as high as 217° C (where the crystallization took 10 hours). Crystallization times for Wunderlich's linear polymers are in the same range of times as those in the present study. By contrast, stannoxane initiated c-PBTs produced at all melt temperatures yield only a single melting peak, and the melting temperatures are as much as 15° C higher than those of the melt crystallized linear polymer. In all cases shown in Figure 6.15, the polymer produced by

isothermal polymerization and erystallization of BTC oligomers forms more perfeet PBT erystals, as judged by melting temperatures, than are formed by cooling a conventional linear polymer from the melt. This is not an effect of annealing as crystallization times are similar. The two studies used different DSC heating rates; 10° C/minute in Wunderlieh's study vs. 20° C/minute in the present study. The differenee in heating rates should only result in a consistent shift in observed temperatures between the studies. Heating rate alone cannot explain the large differences in melting points. Rather, the e-PBT appears to erystallize more eompletely, and with fewer defeets than does commereial linear PBT.

Heats of fusion for stannoxane-initiated c-PBTs are found to be nearly independent of crystallization temperature, implying that the degree of erystal perfeetion has not been altered by ehanging the speed of crystallization for maeroeyelie PBTs. Figure 6.16 shows a slight increase in heat of fusion with erystallization temperature, but the slope of the line formed by a least squares fit of the data is so elose to zero that little or no significance can be to this apparent slight increase. The important finding is that at all polymerization temperatures, the heat of fusion is above 70 Joules/gram.

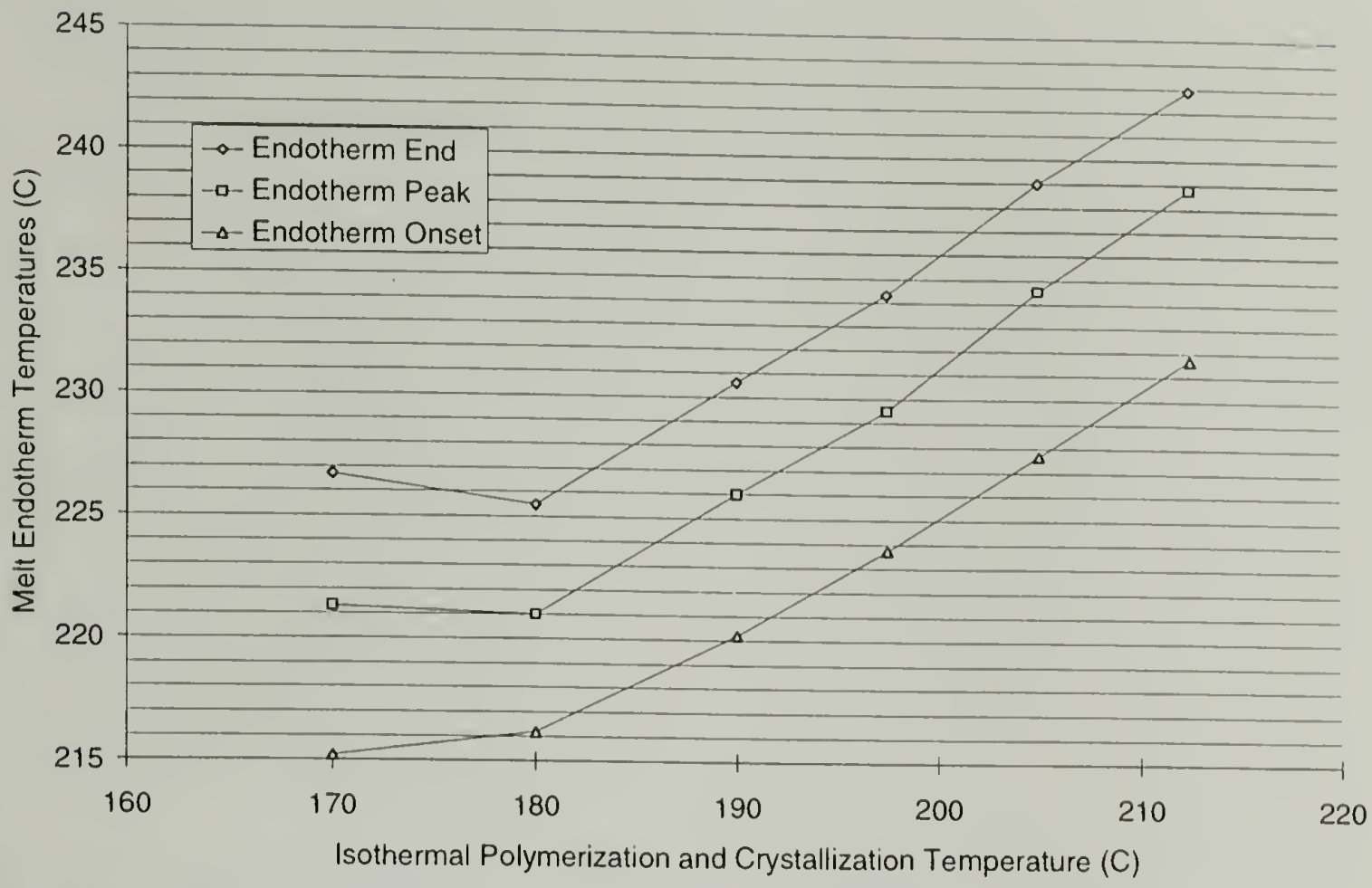


**Figure 6.14 Melt Endotherm temperatures for c-PBT initiated with 0.3 mol % stannoxane.**

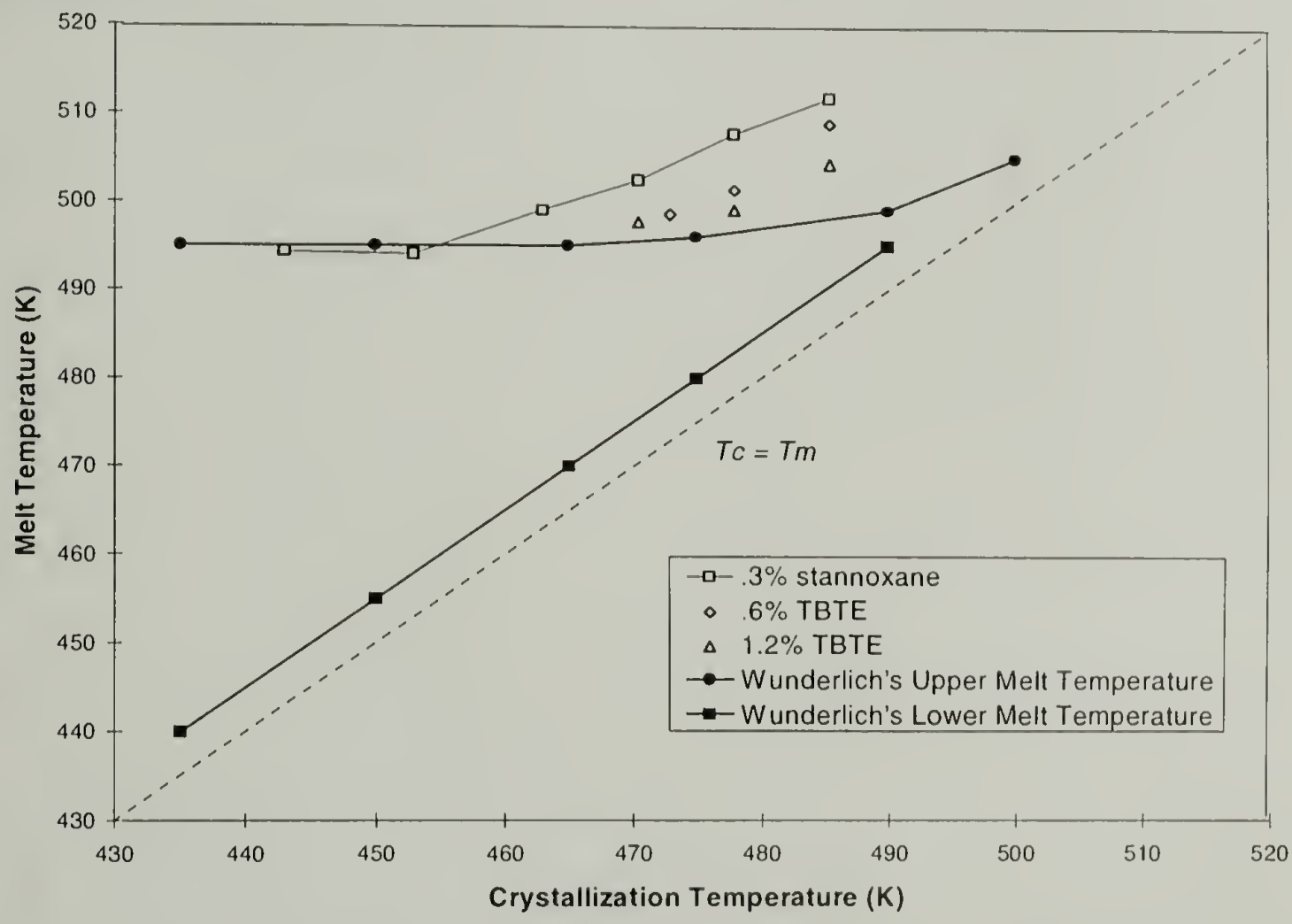


**Figure 6.15 Detail of Wunderlich's relationship[16] between melting temperature, Tm, and crystallization temperature, Tc, of PBT. Data included for c-PBT from both initiators used in this work.**

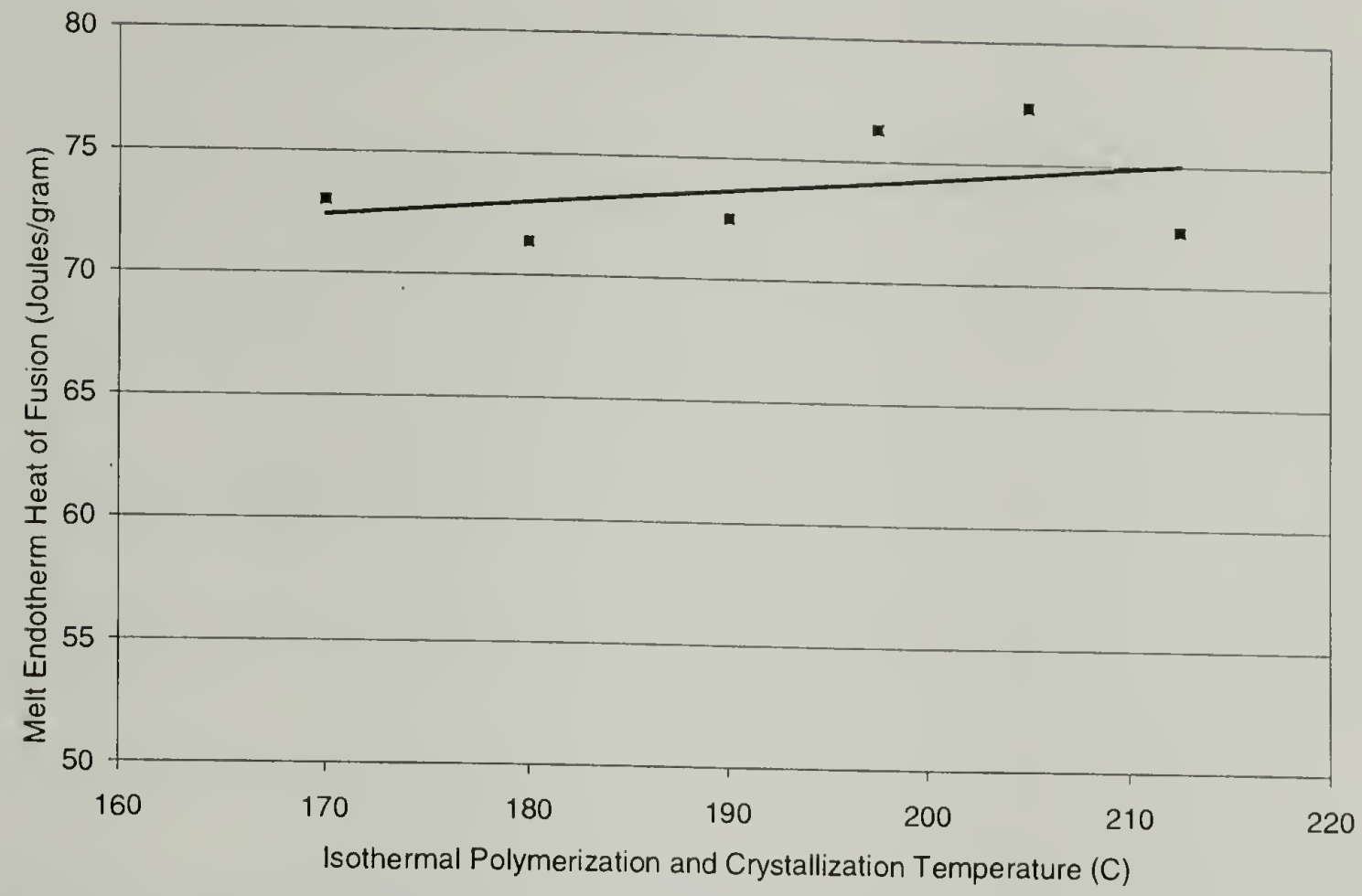


**Figure 6.16 Melt endotherm heat of fusion for c-PBT initiated with 0.3 mol % stannoxane.**

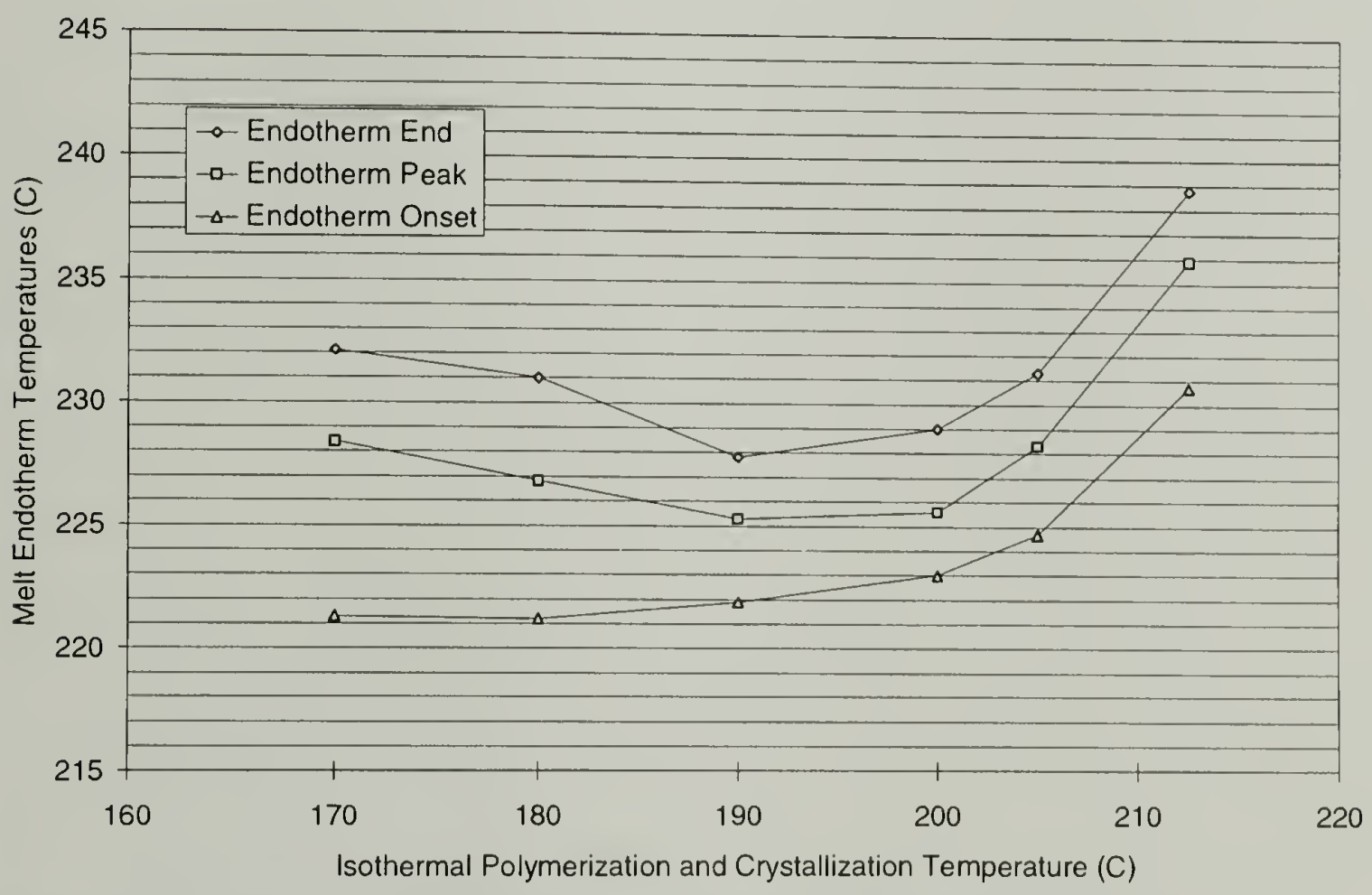


**Figure 6.17 Melt endotherm temperatures for c-PBT initiated with 0.6 mol % TBTE.**

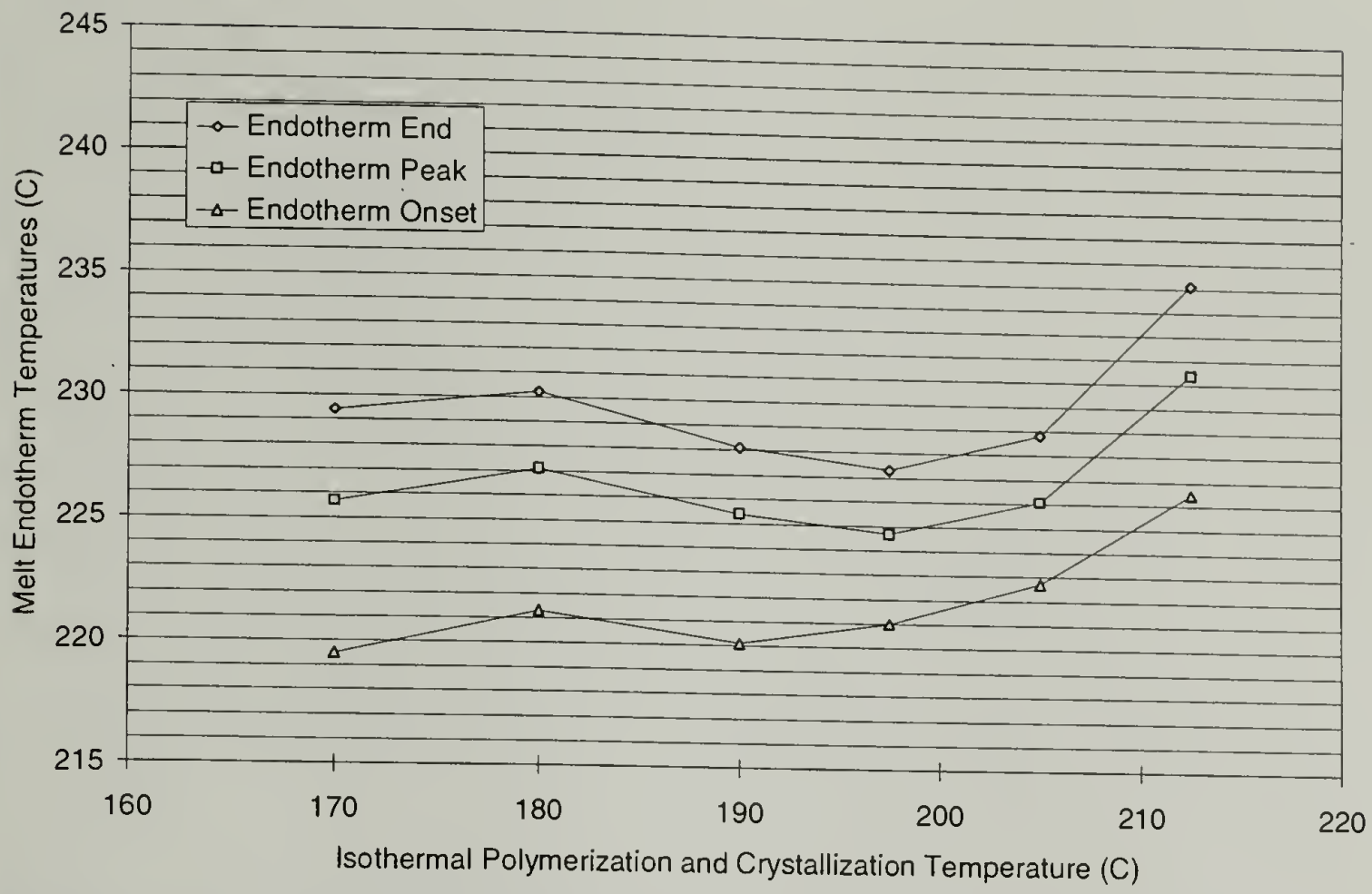


**Figure 6.18 Melt endotherm temperatures for c-PBT initiated with 1.2 mol % TBTE .**

Figures 6.17 and 6.18 show the temperatures of the melt endotherm for c-PBTs polymerized using two levels of TBTE initiator. The breadth of the peak is misleading in these figures, as the melt endotherm was very broad at low polymerization temperatures. At the lowest temperature, 170° C, a broad double peak was evident as shown in Figure 6.19. The lower temperature (smaller) peak is centered at 193° C, independent of the TBTE initiator content. As the polymerization temperature is increased, the first peak disappears, but is replaced by a long leading edge of the melt endotherm starting about 20° C over the polymerization temperature.

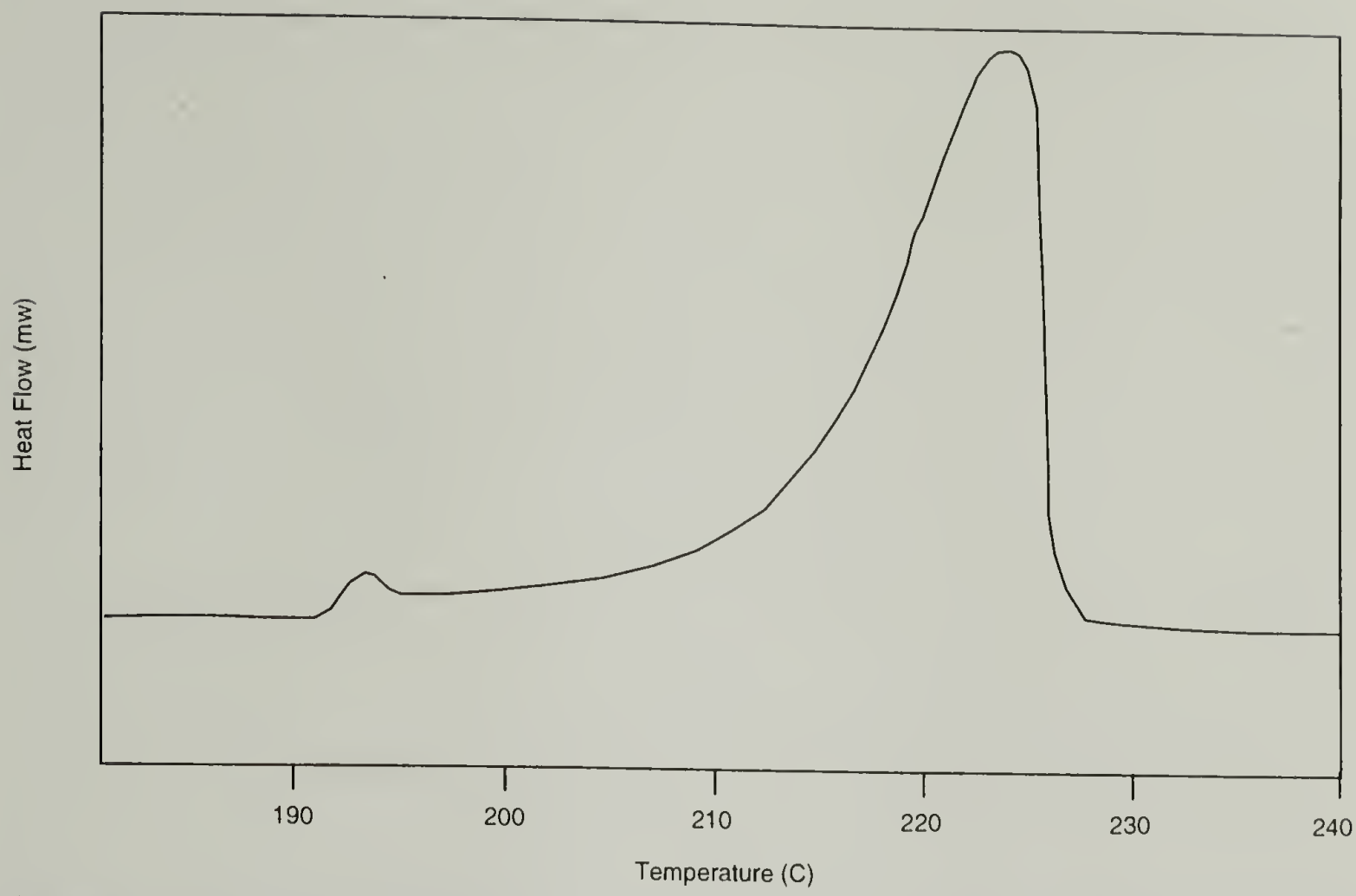


**Figure 6.19 Broad double melt endotherm for TBTE-initiated c-PBT produced at 170° C.**

By contrast to the result presented in Figure 6.16, the heat of fusion for linear c-PBT, produced using TBTE initiator, is a strong function of temperature as shown in Figure 6.20. As polymerization temperature is increased, the crystallizability of TBTE initiated c-PBT is lost. At low initiator content, there is a rapid rate of loss of crystallizability with increasing temperature. As the initiator content is increased, and more chains are produced, the rate of loss of crystallizability is slowed. The only difference between the resulting polymers is their molecular weight, based on the M/I ratio demonstrated in Figure 5.8. To understand the crystallizability differences between the different molecular weight polymers, one must understand the crystallization process which is operating.

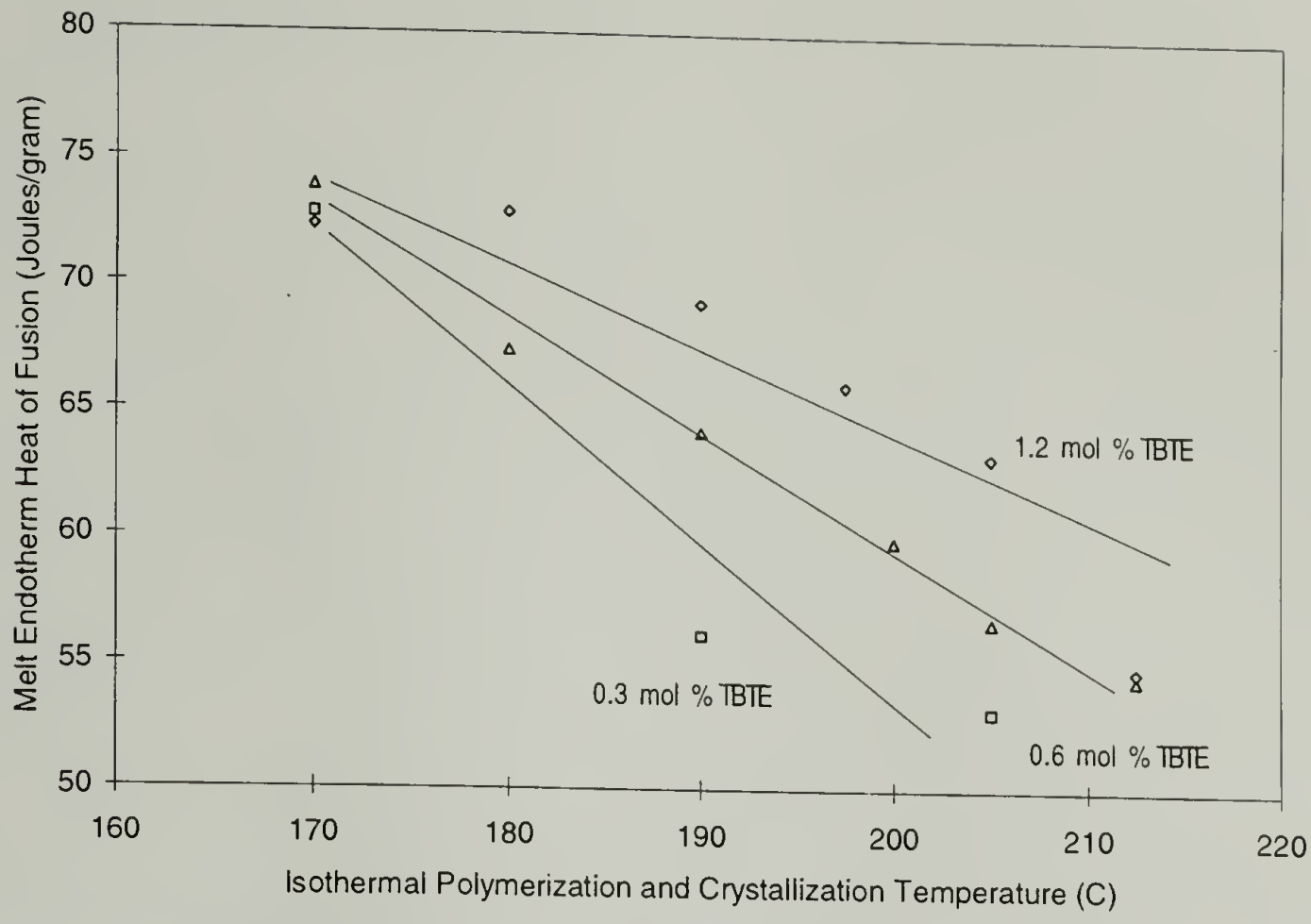


**Figure 6.20 Melt endotherm heats of fusion for TBTE-initiated c-PBTs.**

### 6.2.5 Model of Crystallization in Semi-crystalline Polymers

Many excellent references cover the basic model of polymer crystallization of which a few are given as general reference[17-19]. Crystallization into spherulitic morphology begins with nucleation, where the first collapsed chains become energetically stable and a crystal embryo is formed. Rapid crystallization from the nucleus continues via lamellar growth as available molecular chains are first attached to the growth front, and then continue to add to the lamellae as they are reeled form the melt to the growing crystal. As a molecule is incorporated into the crystal, it is energetically favorable for it to fold and continue adding to a single lamella. This growth continues as new lamellae form, to fill the space around the nucleus, growing radially until they impinge on growth radiating from neighboring nuclei. When this happens, the spherulitic skeleton is established and no further radial growth is possible. This marks the end of primary crystallization. Further

crystallization takes place to fill the volume between the skeletal lamellae by secondary addition of crystals in a more random pattern. Secondary crystallization, being more random than primary crystallization, may result in a less perfect crystal structure. The molecules which are crystallized during secondary crystallization may already be part of a primary crystal, or may even extend between several crystals as tie chain molecules. Secondary crystallization, while adding significantly to the overall crystallinity of the polymer, results in less perfect crystals which exhibit a distribution of melting points below that of the primary crystallites.

In TBTE-initiated c-PBT, crystallized at 170° C, the large degree of undercooling drives rapid primary crystallization. The delay in nucleation time vs. stannoxane-initiated c-PBT (Figure 6.11) is evidence of less dense nucleation, resulting ultimately in a distribution of larger spherulites. Once primary crystallization is finished and the spherulitic skeleton is established, there exists a solid framework of crystal structure. Filling the intercrystalline regions are a "solution" of unreacted cyclic oligomers.. As only polymer can become part of the growing crystal structure, and there are a finite number of reactive polymerization sites available to continue the polymerization, the cyclic oligomers must diffuse to a reaction site. As more of the oligomer is converted to polymer and the crystalline content increases, diffusion of the oligomer slows and the probability of being near a reactive site become lower. These two factors may be responsible for the delay crystallization rate at 170° C. As new polymer is formed during secondary crystallization, it does not form highly perfect crystals, but crystallization takes place to fill available space within the spherulitic skeleton. The nascent polymer is not restricted from crystallization,

as it is added to a crystal growth front as soon as the oligomer is inserted at a polymerization site.

As the polymerization temperature is increased, the nucleation density is lowered. Crystallization from fewer nuclei form larger spherulites during primary crystallization. These spherulites have longer radial skeletal arms that diverge from the nucleus leaving more amorphous volume to be filled during secondary crystallization. The broad melting peaks found in the low temperature polymerized TBTE specimens are the result of a large degree of secondary crystallization which results in less stable crystals.

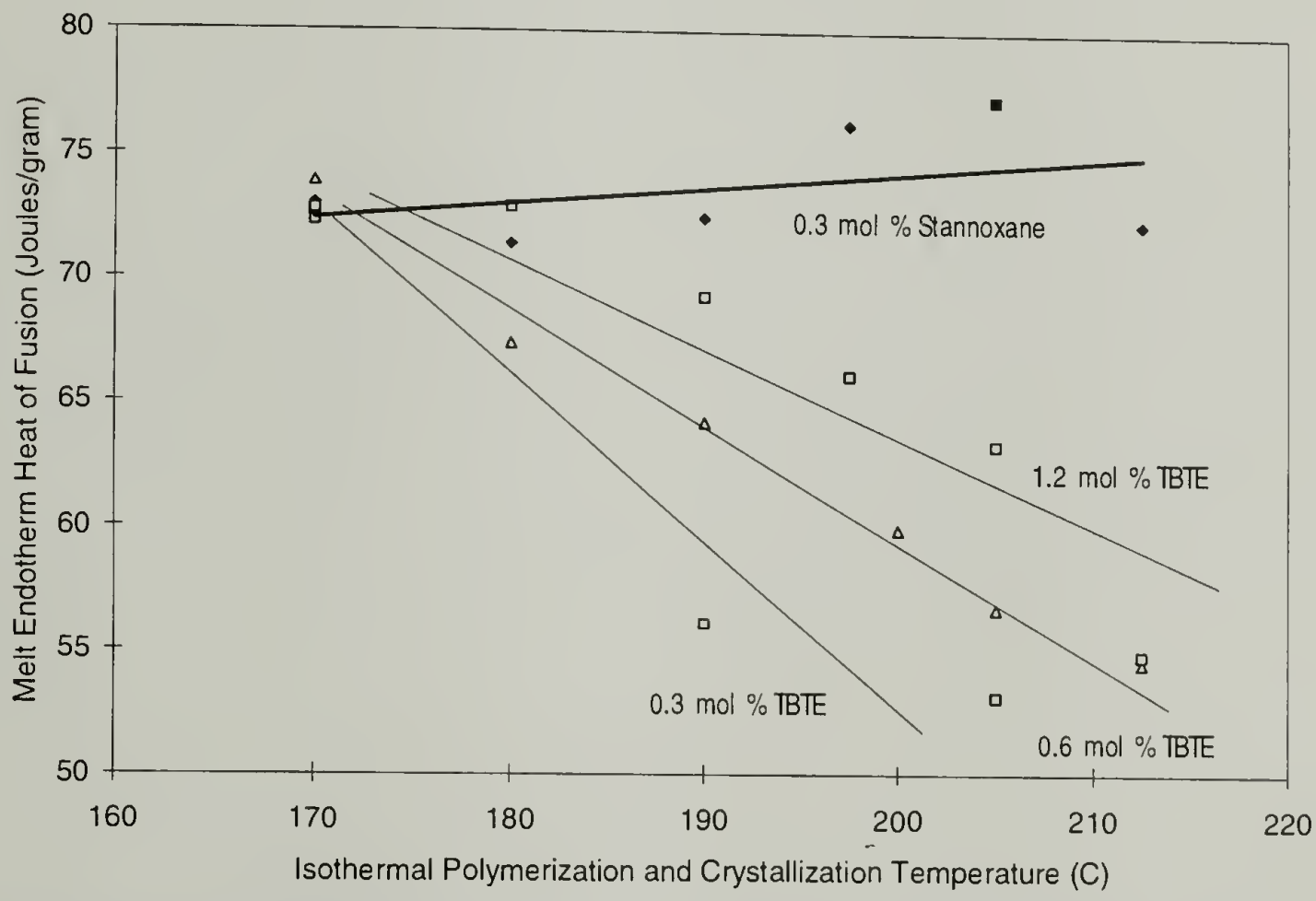


**Figure 6.21 Heats of fusion for all c-PBT as a function of polymerization and crystallization temperature.**

The effect of the molecular weight differences seen in Figure 6.21 is twofold. Higher initiator content produces more growing chains. The polymerization rate is slow for TBTE at low polymerization temperatures and several chains of critical molecular weight must in proximity for nucleation to begin. With more polymerization sites active,

the higher initiator content results in a faster nucleation (Figure 6.11). Not only is the time for nucleation shorter, but also the crystallization half-time is faster with more independent chains growing from the oligomer pool (Figure 6.12). The higher nucleation density produces smaller spherulites, which result in less secondary crystallization. More important, much of the crystallization which takes place at low temperatures is from oligomer being added to the polymer chains which have already began to crystallize. This produces only short amorphous segments attached to crystal growth fronts, which have a low probability of becoming part of more than one lamellae. Thus, the resulting polymer has less un-crystallizable material resulting from loose loops, non adjacent reentry chains, and intercrystalline tie chains.

The differences in ability to crystallize between cyclic and linear polymer produced form BTC, is not based on the time required for crystallization. Although cyclic molecules initiate crystallization faster than linear molecules, when the resulting crystallinity is normalized by the time for crystal nucleation, the crystallinity differences become apparent as shown in Figure 6.22. Using this criteria, all of the linear polymers collapse into a single distribution, not differentiated by molecular weight. The trend is toward lower crystallinity with longer time for nucleation. The fully polymerized linear c-PBT is inhibited from further crystallization by the same mechanisms which limit the crystallinity of commercial linear PBT. Figure 6.23 shows the same trend when heat of fusion is plotted vs. time to peak crystallization, suggesting that linear molecules cannot produce as high of crystallinity as cyclic molecules in the same time frame for crystallization. At the highest temperatures of isothermal polymerization, the melt temperature of the linear polymer increases while the heat of fusion decreases. This suggests that linear molecules,

under slow crystallization conditions, can form relatively defect free crystallites, but even under these conditions the linear chains cannot crystallize as completely as macrocyclic molecules. With both systems fully polymerized prior to crystallization, the differences in crystallizability must be the result of linear chains having a greater radius of gyration, which results in a greater number of intercrystalline tie chains in the fully crystallized material. This hypothesis will be supported by mechanical testing results shown in Section 6.5 where the macrocyclic PBT polymers have lower (compressive) yield stresses than linear PBT polymers, when compared at the same degree of crystallinity.

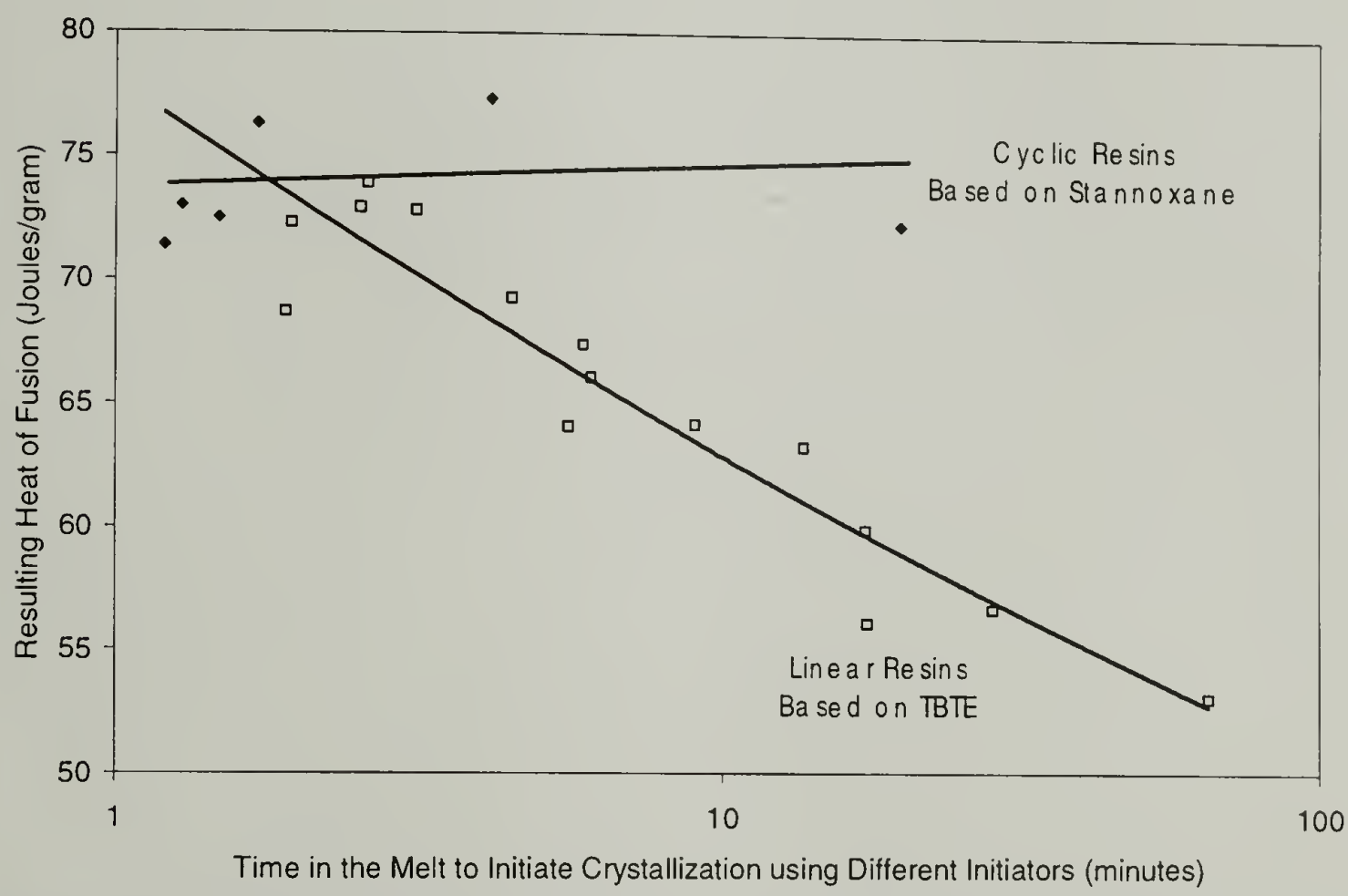


**Figure 6.22 Heat of Fusion as a function of time to initiate crystallization at all temperatures.**

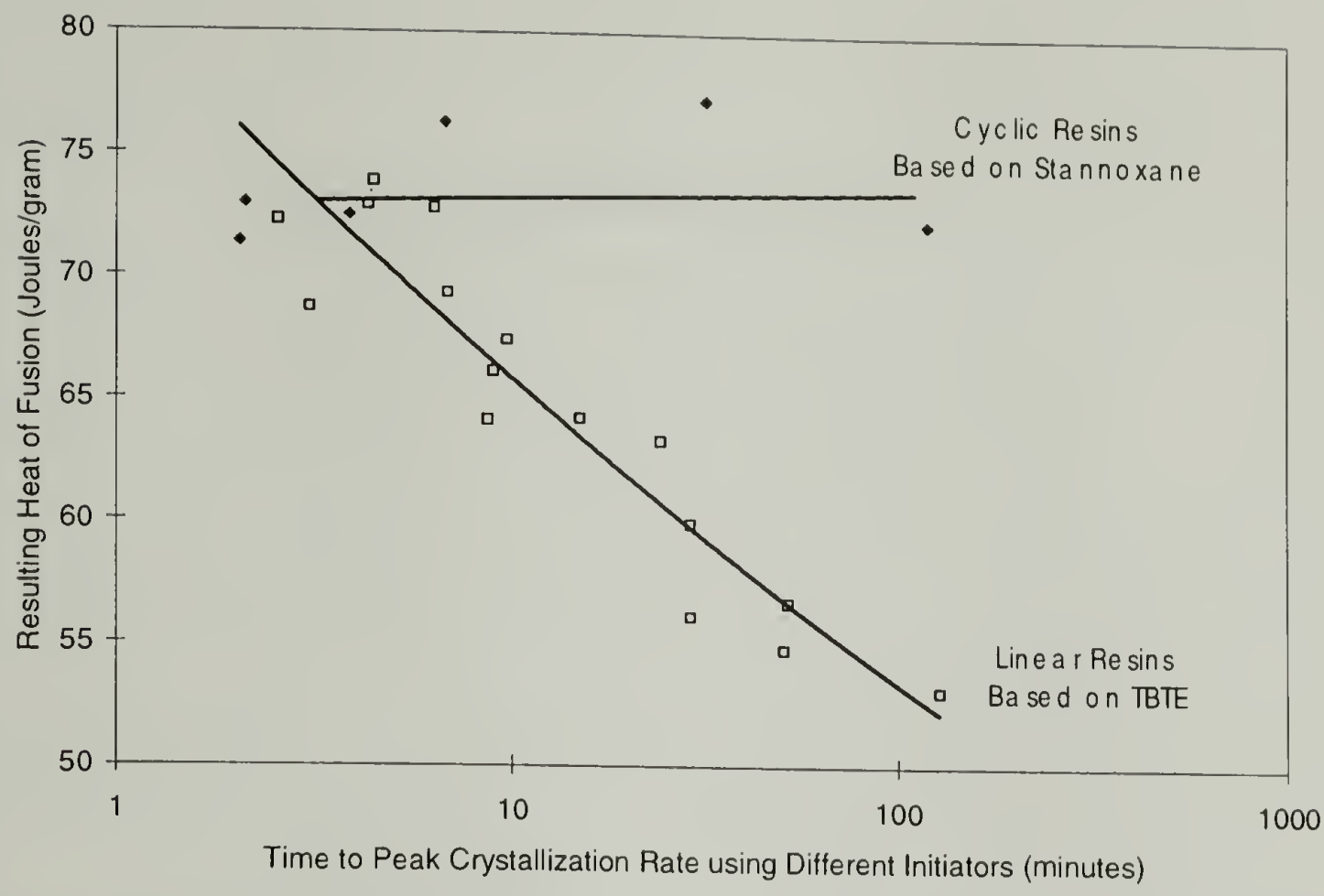


**Figure 6.23 Heat of Fusion as a function of time to peak crystallization rate for all temperatures.**

### 6.2.6 References for Crystallization


1)Stein, R. S.; Misra, A., *Journal of Polymer Science: Polymer Physics Edition* **1980**, *18*, 327-342.
2)Stein, T. S.; Rhodes, M. B., *Journal of Applied Polymer Science* **1960**, *31*, 1873.
3)Chien, J. C. W.; Chang, E. P., *Macromolecules* **1972**, *5*.
4)Misra, A.; Stein, R. S., *Journal of Polymer Science, Part B* **1972**, *10*, 473.
5)Stein, R. S.; Rhodes, M. B., *Journal of Applied Physics* **1960**, *31*, 1873.
6)Hobbs, S. Y.; Pratt, C. F., *Journal of Applied Polymer Science* **1975**, *19*, 1701-1722.
7)Moginger, B.; Lutz, C.; Polsak, A.; Fritz, U., *Kunststoffe German Plastics* **1991**, *81*, 251-255.
8)Ludwig, H. J.; Eyerer, P., *Polymer Engineering and Science* **1988**, *28*, 143-146.
9)Yeh, J. T.; Runt, J., *Journal of Polymer Science: Polymer Physics Edition* **1989**, *27*, 1543-1550.
10)Hobbs, S.; Pratt, C., *J. Applied Polymer Science* **1975**, *19*, 1701-1705.
11)Kim, J.; Nichols, M. E.; Robertson, R. E., *Journal of Polymer Science: Part B: Polymer Physics* **1994**, *32*, 887-899.
12)Keller, A., *Plastics and Polymers* **1975**, 15 - 29.
13)Kambour, R.; Barnes, J.; Garbauskas, M.; Gundlach, P.; McCracken, L. "Microstructure, Morphology, and Crystallinity Level in Polybutylene Terephthalates Produced from Cyclic Oligomers: A Progress Report.," Manuscript in preparation, **1995**.
14)Mills, P. J.; Mayer, J. W.; Kramer, E. J.; Hadziioannou, G.; Lutz, P.; Strazielle, C.; Rempp, P.; Kovacs, A. J., *Macromolecules* **1987**, *20*, 513-518.
15)Tead, S. F.; Kramer, E. J.; Hadziioannou, G.; Antonietti, M.; Sillescu, H.; Lutz, P.; Strazielle, C., *Macromolecules* **1992**, *25*, 3942-3947.
16)Cheng, Z.; Pan, R.; Wunderlich, B., *Makromol. Chem.* **1988**, *189*, 2443-2458.
17)Woodward, A. E. *Understanding Polymer Morphology*; Hanser: Cincinnati, **1995**.
18)Rodriguez, F. *Principals of Polymer Systems*; McGraw Hill: New York, **1970**.
19)Young, R. *Introduction to Polymers*; 2nd ed.; Chapman and Hall: New York, **1983**.

## 6.3 Rheology Studies

When a polymer melt is sheared, it resists this shear with a stress which rises with the rate of shearing. This proportionality is called the viscosity of the melt, i.e.

Viscosity = Shear Stress / Shear Rate.

The response of a polymer melt or a concentrated solution to shear is different from that of a dilute solution. The effect of shear on a dilute solution of molecules is to deform and align the molecules, resulting in a linear relationship between molecular weight and viscosity. However, in concentrated solutions and polymer melts, where the molecules are concentrated enough and large enough to become entangled, the principal effect of shearing is to disrupt the entanglements[1]. Polymers in dilute solutions may not be entangled unless they have very high molecular weights, usually over 400,000 and sometimes only over one million, whereas polymer melts are known to be entangled at molecular weights in the range of 3,000 to 50,000[1]. The melt viscosity of low molecular weight (oligomeric) polymer is found to be independent of shear over a wide range of shear rates; however, as the molecular weight of the polymer increases, an abrupt increase in shear sensitivity is found at a critical molecular weight. Below this critical molecular weight, viscosity is found to increase as $M_w^1$, whereas above this molecular weight, viscosity increases as $M_w^{3.4}$ for a broad range of polymers.

Working with both cyclic and linear PBTs in the present study, gave the opportunity to determine the effect of chain topology on the melt viscosity. An earlier study on the melt viscosity of low molecular weight poly(dimethyl siloxane)s by Dodgson[2] gave the result that for unentangled systems, cyclic molecules have about one half the viscosities of linear resins of the same molecular weight. This is in agreement with a

theoretical prediction by Bloomfield and Zimm[3] for dilute solutions of linear and cyclic molecules. Roovers[4] published data comparing the viscosities of cyclic and linear polystyrenes of similar, narrow molecular weight distributions. Working over a wide range of molecular weights, he showed that above about 20,000 Daltons, each cyclic polystyrene exhibited a lower viscosity vs. its linear analog. The same study also demonstrated that the critical entanglement molecular weight, $Mw_c$, for cyclics is slightly higher than that of linears. (Unfortunately, there appear to be no published studies of the molecular weight dependence of linear PBT's melt viscosity over a range of molecular weights wide enough to allow determination of a value of $Mw_c$ with which our value could be compared.).

In this work, two different sets of rheology studies were completed for the macrocyclic and the commercial linear PBTs. A thermal stability study was done to determine the shear sensitivity of the resins and changes in shear sensitivity with time as the macrocyclic structure was thermally degraded to linear resin. In a second rheology study, the rates of polymerization were investigated by polymerizing PBT cyclic oligomers while monitoring the change in viscosity over a range of temperatures.

### 6.3.1 Thermal Stability Study of PBT Resins

The first rheology study was done to determine both the shear sensitivity and thermal stability of the resins and was carried out at temperatures well above the melting range of linear resins. This study involved pre-polymerizing specimens of c-PBT and monitoring their viscosity and shear moduli for up to one hour at temperatures of 230°, 240°, and 250° C over a shear range of 0.1 to 500 radians/second. Similar data were then

obtained using four commercial grades of VALOX PBT resin at 250° C. The c-PBTs in this study were initially high molecular weight polymers produced from polymerization of BTC's using either 0.12 mol % or 0.3 mol % stannoxane. The GPC apparent weight average molecular weights of the cyclic polymers were determined to be 290,000 and 134,000 respectively prior to the melt study.

To determine the shear sensitivity of the resins, consecutive shear rate sweeps were conducted at five minute intervals for one hour. The thermal stability was determined by correlating the data collected in each sweep,.

The results of this characterization are presented as plots of storage modulus (G'), loss modulus (G"), and viscosity ($\eta$) vs. time for each temperature and resin over the range of frequencies. For clarity, a three dimensional contour plot of each data set is also included. This plot maps the response surface of each dependent variable across the field of shear rate and time. Comparison plots of the resins at a constant temperature, or multiple temperatures for a single resin have been included where they show informative results.

An apparent molecular weight was determined by GPC for each resin prior to testing. Following each rheology study, the test specimens were collected from the rheometer and the molecular weight was again determined to provide evidence of degradation during the test as well as a second data point for plotting viscosity vs. molecular weight.

#### 6.3.1.1 Specimen Preparation

Cyclic resins were pre-polymerized into 3 gram billets which were re-melted in the rheometer prior to testing. The powdered BTCs, containing a solution-dispersed quantity of initiator, was first dried between 110° and 120° C for 2 to 3 hours, then compressed by quantities of 3 grams into preforms of 0.9 inch diameter using a circular compression tool. The pressure was slowly increased to 5000 pounds on the tool (ca. 5500 psi on the powder) while allowing time for relaxation and sintering. After one minute, the tool was opened and the sintered disk placed in a heavy foil "boat", which was pre-shaped to maintain shape of the billet during polymerization. The sintered specimens were then placed in a 190° C oven and allowed to polymerize and crystallize for 20 minutes after temperature recovery to 190° C. Temperature was monitored by using a thermocouple which was placed under one of the specimen "boats". Following polymerization, the specimens were removed to a dry container and kept dry until placed in the rheometer.

All rheology specimens of linear PBT were prepared from 6" by 8" injection molded plaques. VALOX 195, 295, and 315 grades of PBT were injection molded at 0.25 inch thickness, while VALOX 310 PBT was injection molded at 0.125 inch thickness.

The molded plaques were first thinned to a nominal 0.1 inch thickness by compression molding. The thinning process involved using a 6" by 6" frame mold of 0.10" thickness and placing properly sized solid plaques in a preheated compression press at 250° C. After allowing sufficient time for crystal melting (1.5 to 2 minutes), the press was closed slowly to a pressure of 1500 pounds. After one minute, the specimens were transferred to a cold press and allowed to cool under 1500 pounds pressure for two

minutes. The specimens were immediately removed from the compression tooling and cooled to room temperature without fixturing (i.e. without constraints). If the cooling plaques are left in the press too long, tensile stresses, resulting from excessive shrinkage of the crystalline phase, cause residual stresses in the plaques. (This stress is sufficient to fracture a cooling plaque of low molecular weight if it is not released from the surface constraints.) After cooling to below $T_g$, the thinned plaques were cut to the proper diameter using an arbor press and punch tooling. Specimens of the same thickness were prepared in three diameters to determine the proper specimen volume for optimal filling of the rheometer gap. Using a standard gap of 2.0 mm between the shearing fixtures, specimens of each diameter were melted and evaluated for thermal stability in a parallel plate test mode using a Rheometrics Model RDS rheometer.

#### 6.3.1.2 Results of the Thermal Stability Study

For Newtonian polymers, the viscosity is known to be independent of the shear rate. Polymer molecules above their critical molecular weight have entanglements with an appreciable lifetime. At low rates of shear, these entanglements have time to relax and reform in the melt before shear stresses develop which would orient the molecules. Many polymers exhibit a Newtonian viscosity plateau over a range of low shear rates where the relaxation times of the molecules are shorter than the shearing times. In this low shear region, high molecular weight polymers maintain their natural unhindered conformations and the viscosity of the polymer is constant, as the shear rate is directly proportional to the shear stress or flow resistance in the system. Low frequency (low shear rate) studies can therefore be used to determine the approximate zero shear viscosity of a polymer resin.

At higher shear rates, the applied motion becomes faster than the relaxation time for the system, and the entangled molecules extend or elongate in the shear field before the entanglements can relax, thus decreasing the entropy in the melt[5]. The reduction in melt entanglements decreases both the melt elasticity and the melt viscosity, as the less entangled molecules have less resistance to motion. This effect is reversed when the applied shear motion ceases and the molecules have time to relax back to their natural coil dimensions. The frequency response and thermal stability of the PBT resins could be investigated by repeatedly scanning a wide range of frequencies while holding each resin in the melt for an extended time.

Using a Rheometrics parallel plate rheometer at constant temperature, a single melt specimen was scanned through three and a half decades of frequency while the melt storage modulus and melt loss modulus were recorded. Melt viscosity was determined using the frequency normalized moduli as:

$$\eta = \sqrt{\frac{G'^2}{\omega} + \frac{G''^2}{\omega}} \ .$$

Twelve consecutive frequency sweeps were run at five minute intervals and the data were then used to determine a) the lowest frequency for consistent data and b) the thermal stability (rate of viscosity loss) for the resins. A typical set of viscosity response curves for a linear resin (VALOX 315 PBT) is shown in Figure 6.24. (While the shear rate dependence of viscosity is normally shown on a double log plot, the viscosities are plotted here on a linear scale to magnify small changes in viscosity.)

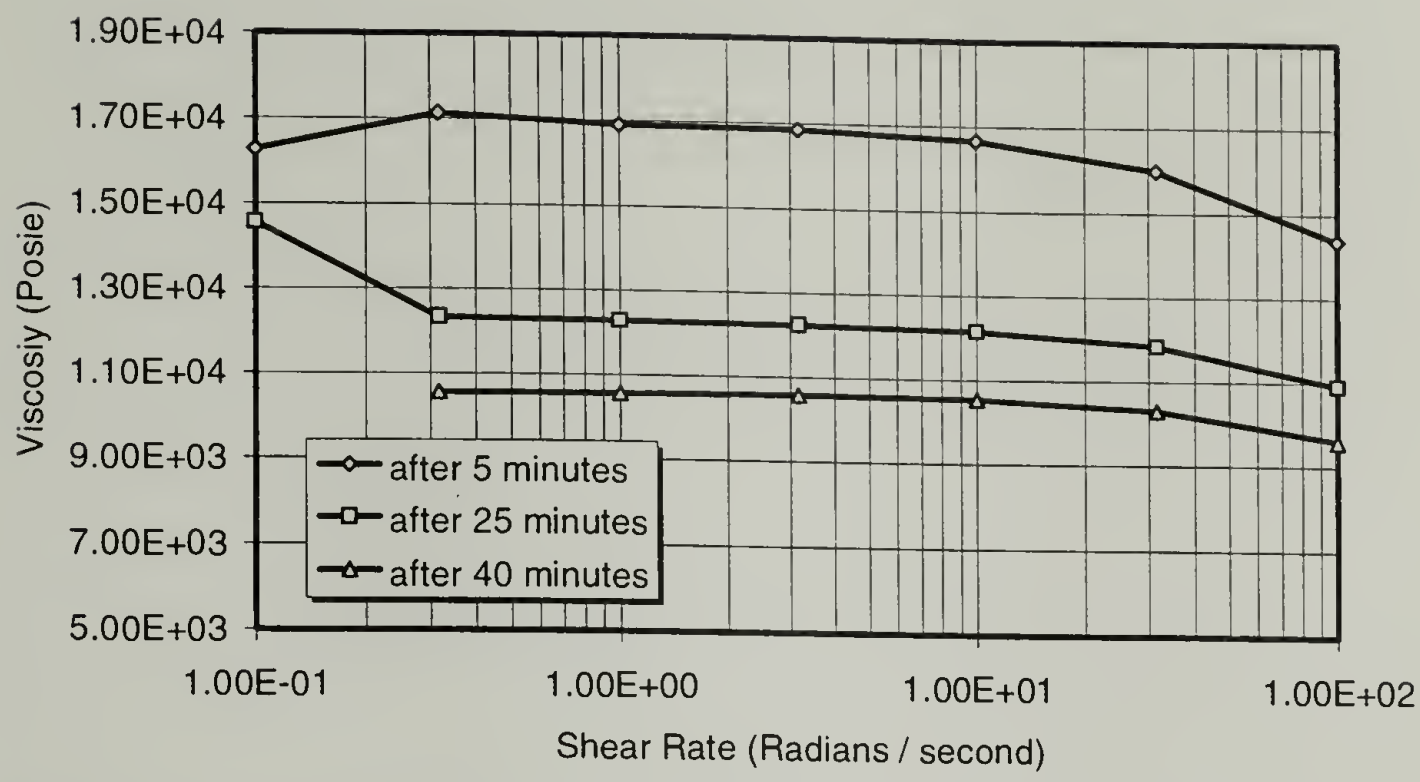


**Figure 6.24 Shear Sensitivity of VALOX 315 PBT at increasing times in the melt at 250° C. Legend shows time spent in the melt.**

Frequency sweeps at only three times are shown for the sake of clarity. The end of the Newtonian plateau is seen to occur at about 10 to 30 radians/second. The five minute curve shows a break in the viscosity at lower shear rate that is not seen in the curves taken at later times. This is believed due to the high molecular weight resin (at short times) having a longer relaxation time in its relaxation spectrum than is the case for the resin that has been slightly degraded. It is apparent that below 1.0 radian/second, the data becomes unstable. This instability is found in all of the resins studied and is the result of insufficient torque being generated in the melt at low frequencies. This is not a material limitation but is related to the sensitivity of the transducer used for determining shear stress. Consequently, a frequency of 1.0 radian/second was selected as the best approximation of zero shear viscosity.

The elastic and loss components of the melt modulus of VALOX 315 PBT at 250° C are shown in Figures 6.25 and 6.26. The data in these two figures are plotted with modulus as a function of time, and the different frequencies of the test are shown as cross

plot lines. Both moduli are found to decrease linearly with time, indicating thermal degradation in the linear PBT chains at 250° C. Loss modulus (G") dominates the elastic modulus (G') which indicates that the material is fully melted and is not crystallizing during the experiment. At low frequencies, the melt fully dissipates the applied energy, and G' is below the measurement threshold for this instrument.

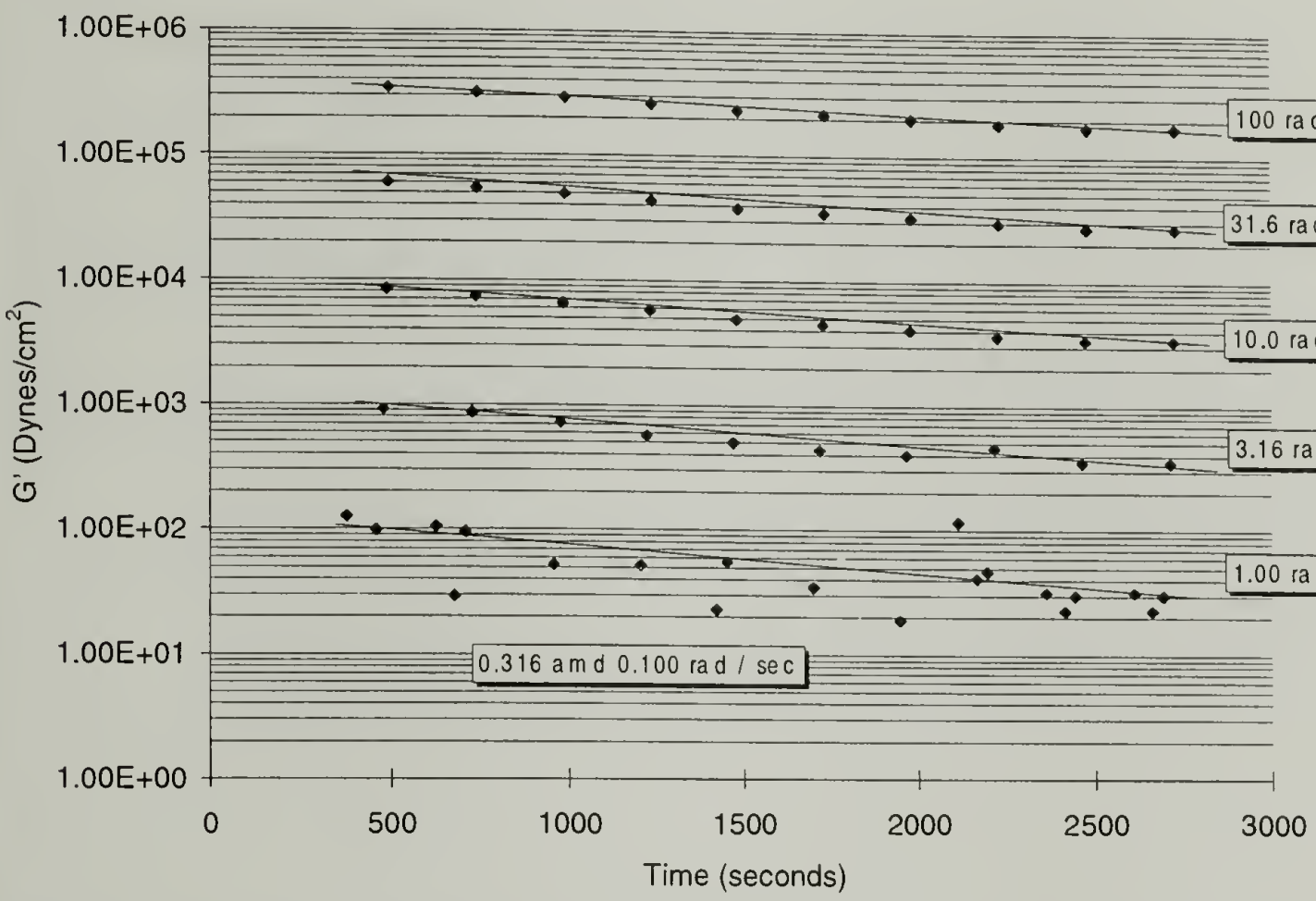


**Figure 6.25 Elastic Modulus of VALOX 315 PBT as a function of time and frequency at 250° C. Shear rates are shown for each curve.**

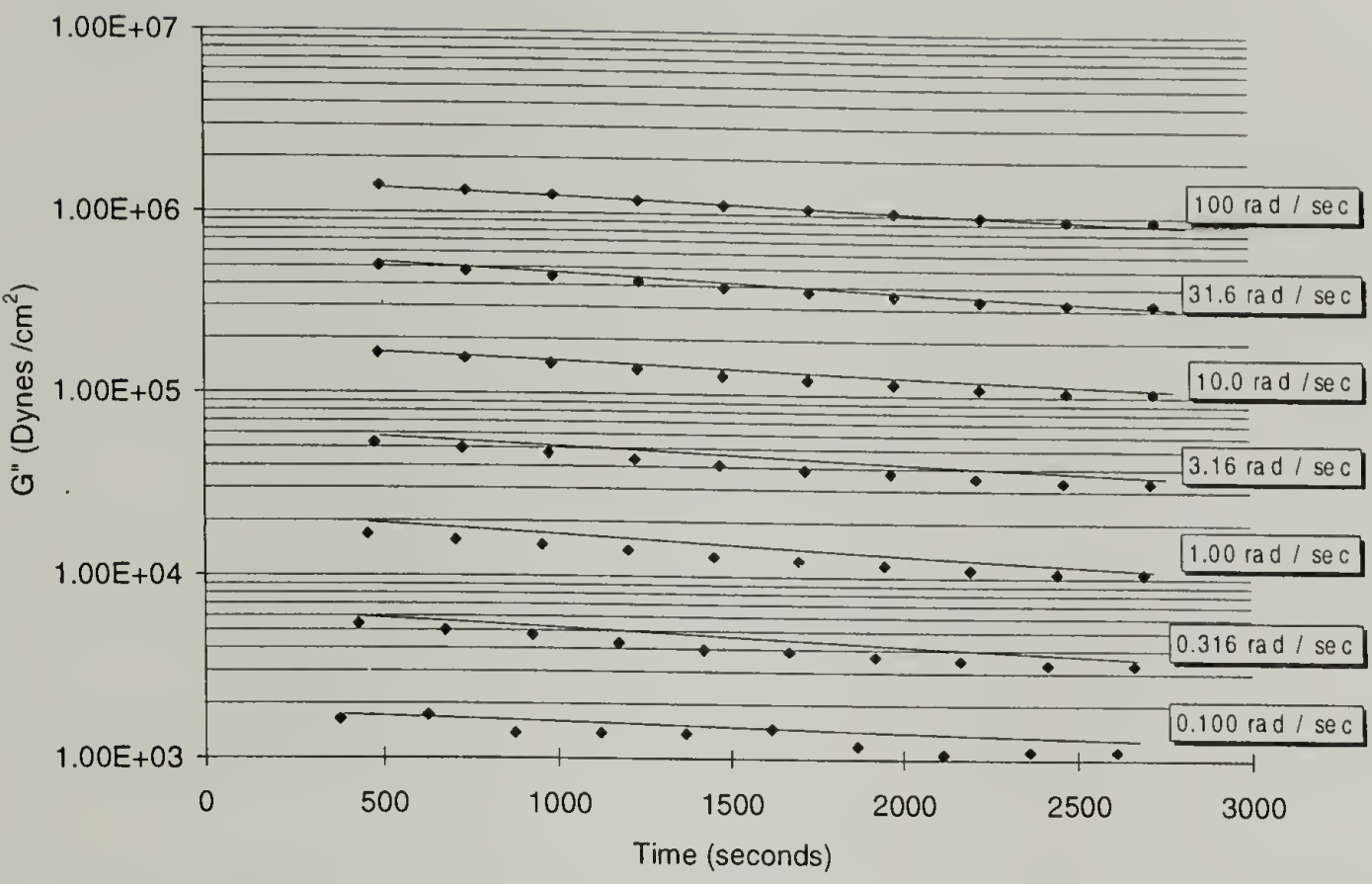


**Figure 6.26. Loss Modulus of VALOX 315 PBT as a function of time and frequency at 250° C. Shear rates are shown for each curve.**

Based on the data in the above two plots, a plot of viscosity for VALOX 315 PBT was prepared and is shown in Figure 6.27. Here it is seen that there is very little shear sensitivity in this resin over the range of frequencies shown. Thermal stability is determined as the change in viscosity with time.

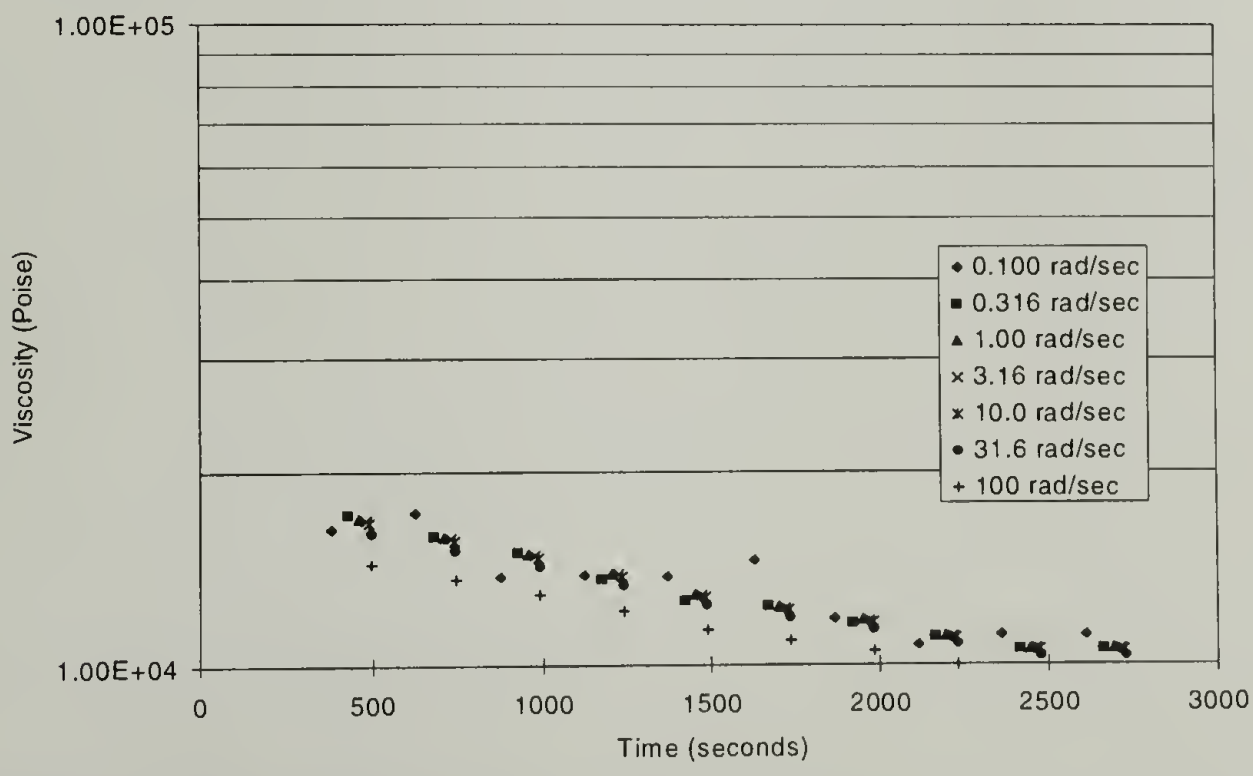


**Figure 6.27 Thermal Stability of VALOX 315 PBT at 250° C. Legend shows shear rates.**

VALOX 315 PBT shows a non-linear loss of viscosity with time, decreasing by a factor of about 2 during the 50 minutes of melt exposure at 250° C. Based on the theoretical considerations discussed in Section 6.3.1.6, a non-linear viscosity drop could be expected from a constant rate of degradation, or constant rate of change in molecular weight. The rheological behavior of this high molecular weight PBT shows some thermal instability, not found in the linear PBTs of lower molecular weight as shown below.

A better visual presentation of the elements in each of the above three graphs is shown as a three dimensional contour plot of the dependent variables as functions of both time and shear rate. Figures 6.28 through 6.30 show the contour plots for G', G", and viscosity of VALOX 315 PBT.

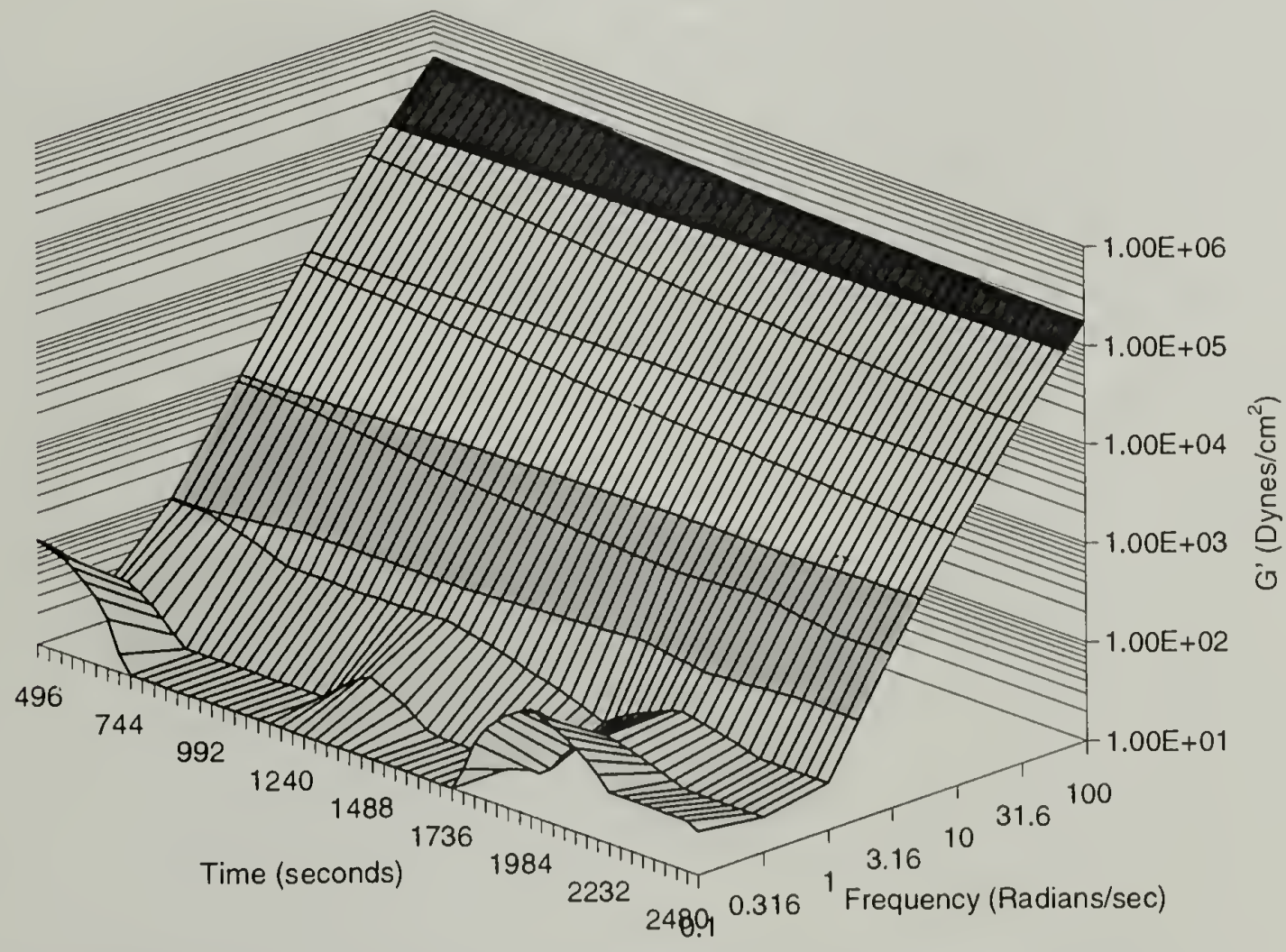


**Figure 6.28 Contour plot of Storage Modulus for VALOX 315 PBT at 250° C.**

Some explanation is needed here for interpretation of the contour plots. These surfaces represent smooth contours of the individual data points collected during rheology testing. The plots cannot easily show the slopes in multiple directions. Therefore, different shading is used to show where the contour crosses a decade line in modulus or viscosity. Overlaid with the decade separation lines are lines of constant time and constant frequency. These lines are not necessarily parallel or orthogonal to the decade lines, but are used to trace isochrones on the plot.

Some study of these contour plots may be necessary to fully appreciate the significance of this type of data presentation. A three-dimensional plot of the rheology data allows the reader to easily determine the relative significance of frequency and time dependence of the viscosity. When the contour is relatively flat (as found in Figure 6.42 above 1.0 radian/sec.), the polymer is thermally stable and insensitive to frequency. When the contour shows a complex curve (as found in Figure 6.59) the relative importance of the changing responses to both frequency and exposure time are readily observed. The same information can be obtained from the two dimensional plots of the data by studying the relative positions of the isochrones in the viscosity vs. shear rate plots.

Similar characterization was completed for each of the three other linear PBT resins. Their two dimensional plots and contour plots are shown in the following set of figures. A discussion and comparison of the data follows the last contour plot of the linear resins.

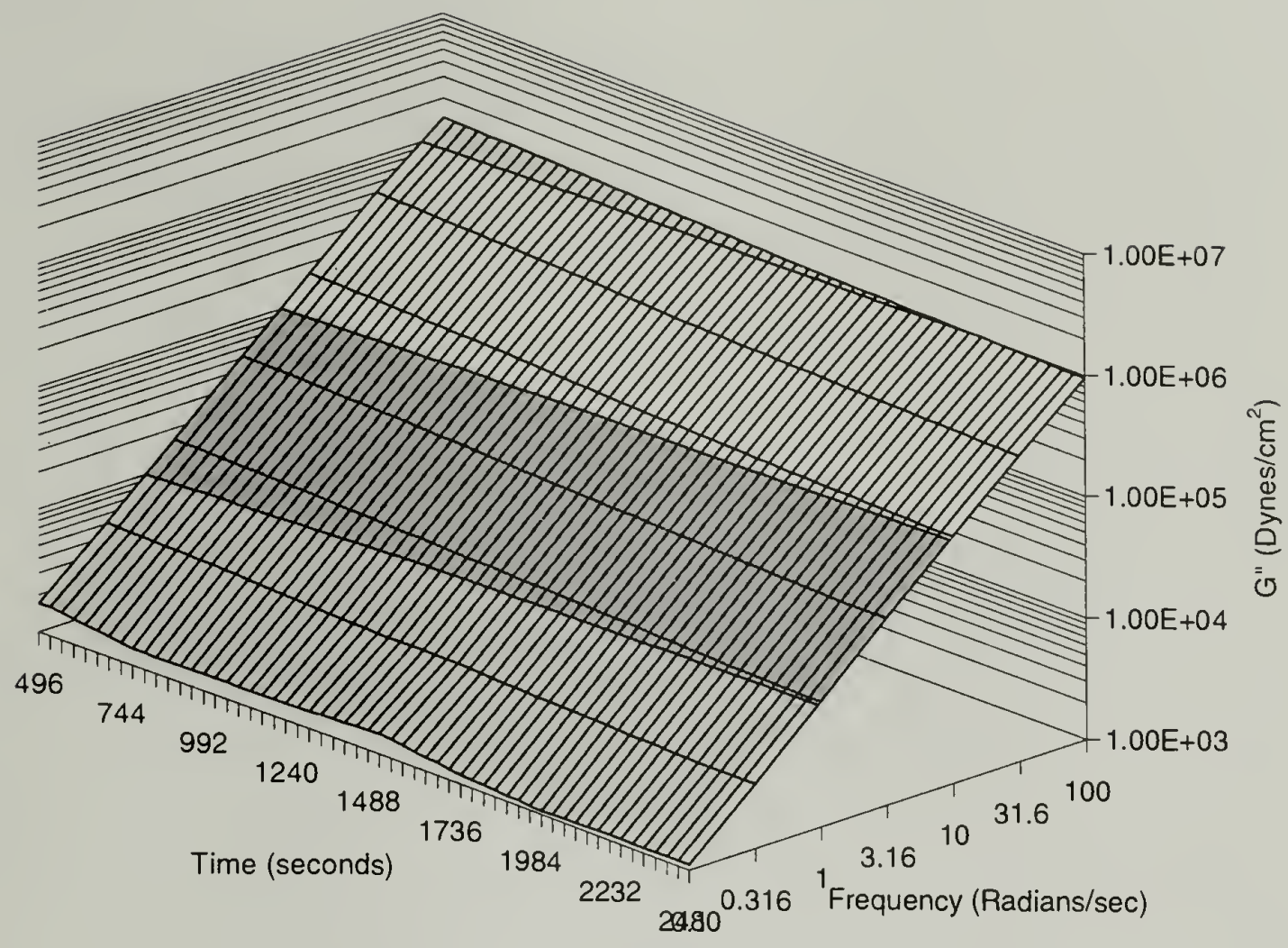


**Figure 6.29 Contour plot of Loss Modulus for VALOX 315 PBT at 250° C.**

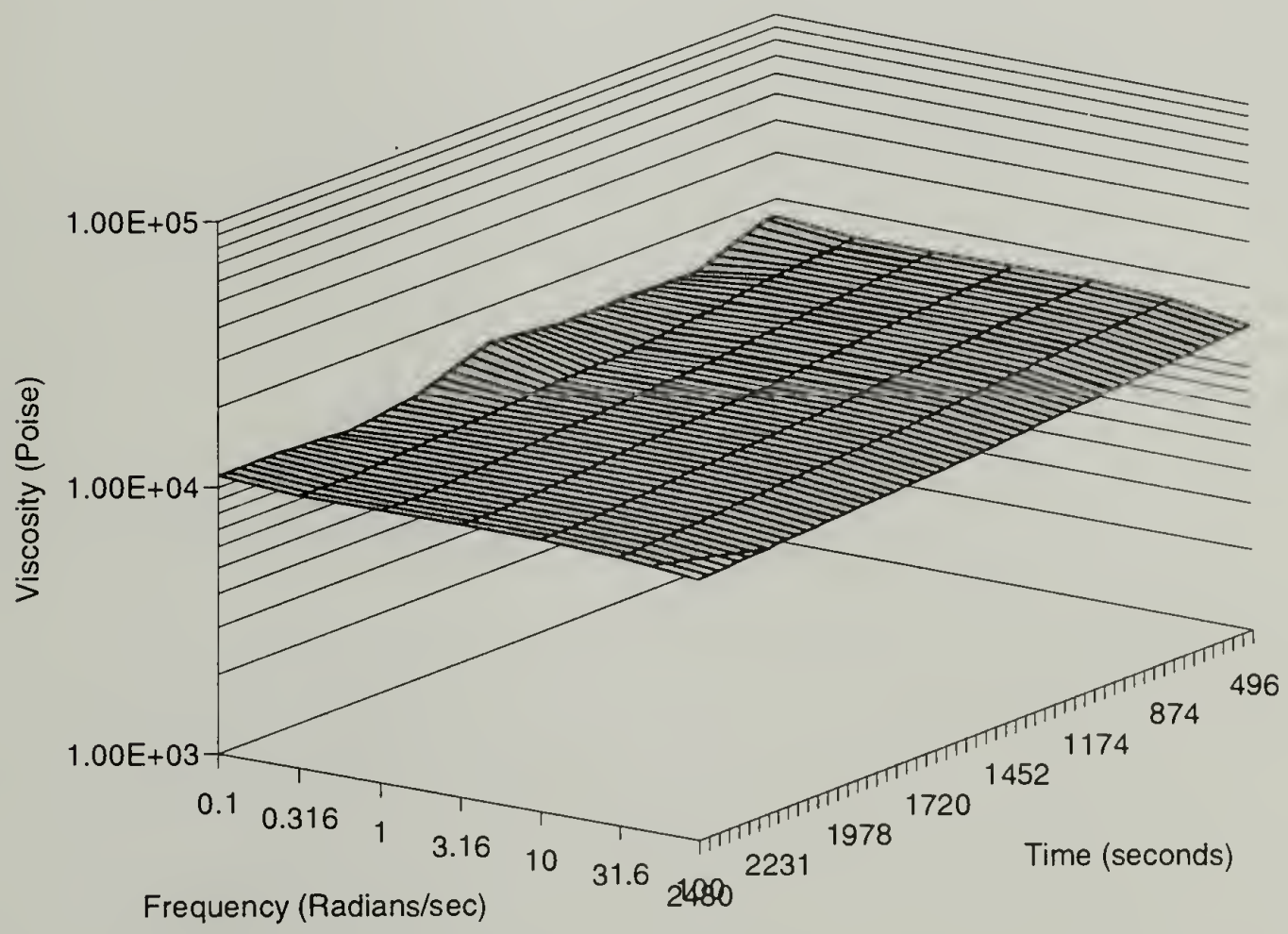


**Figure 6.30 Contour plot of Viscosity for VALOX 315 PBT at 250° C.**

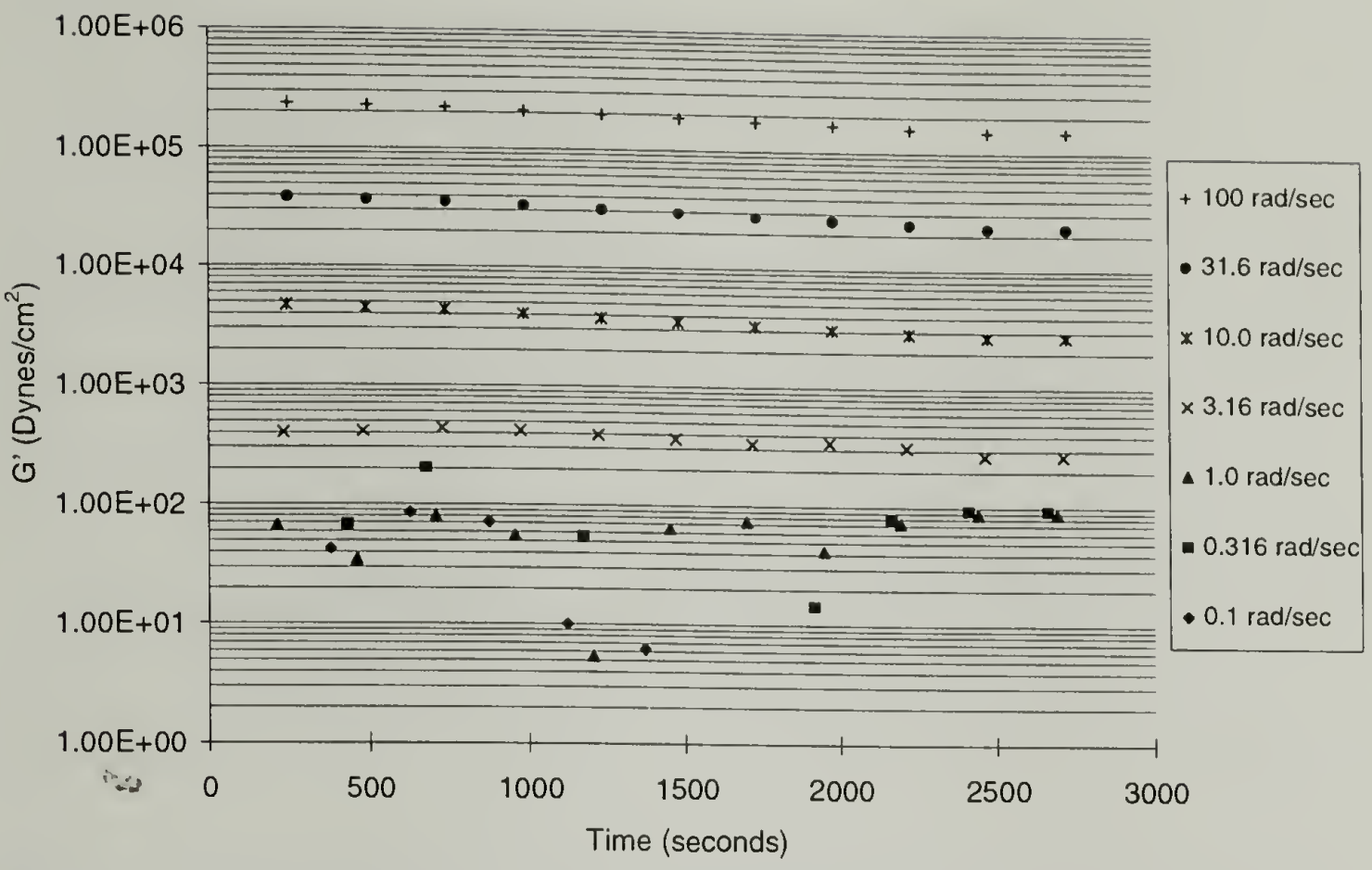


**Figure 6.31 Elastic Modulus of VALOX 310 PBT as a function of time and frequency at 250° C. Legend shows shear rates.**

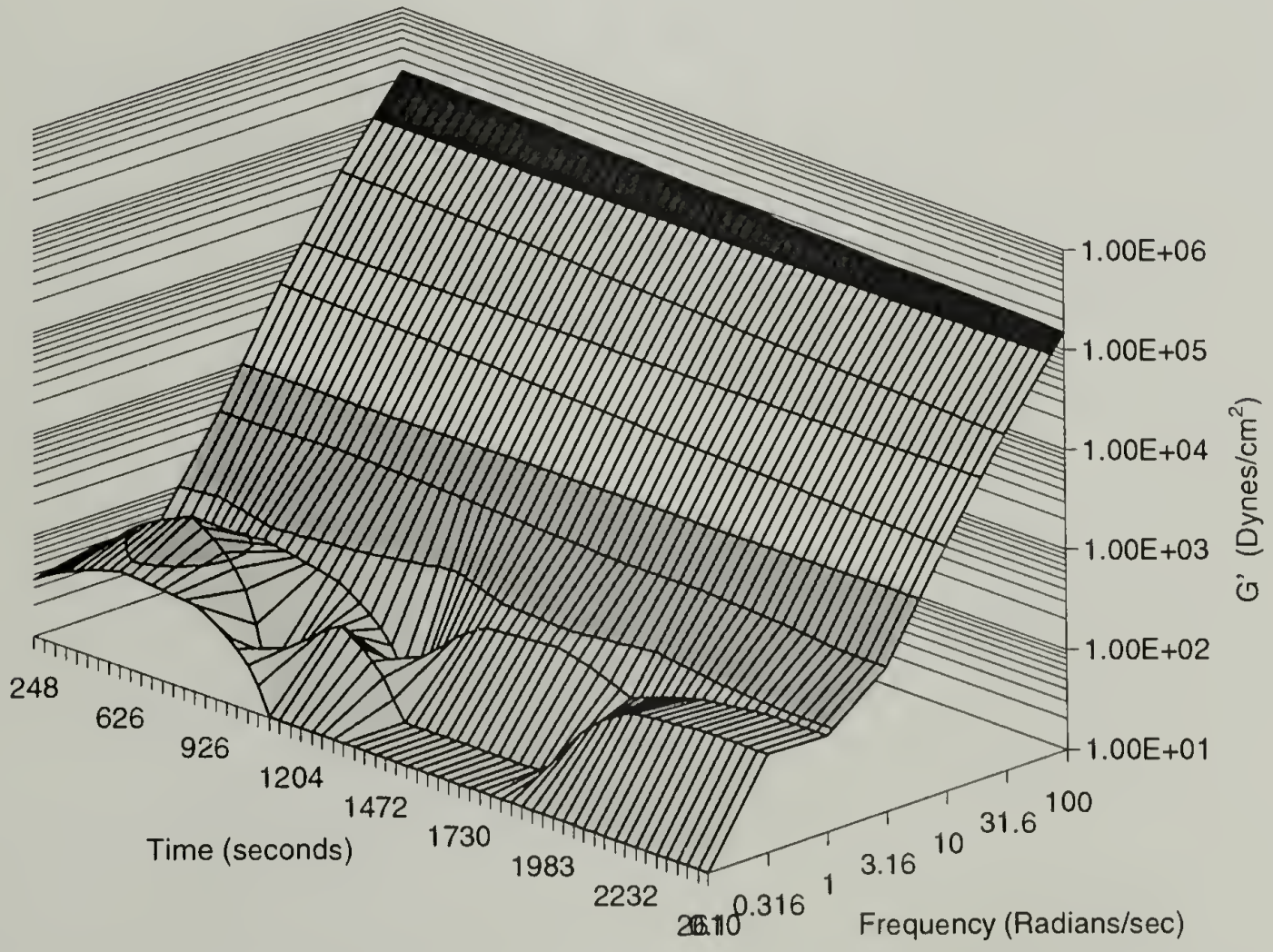


**Figure 6.32 Contour plot of Elastic Modulus for VALOX 310 PBT at 250°C.**

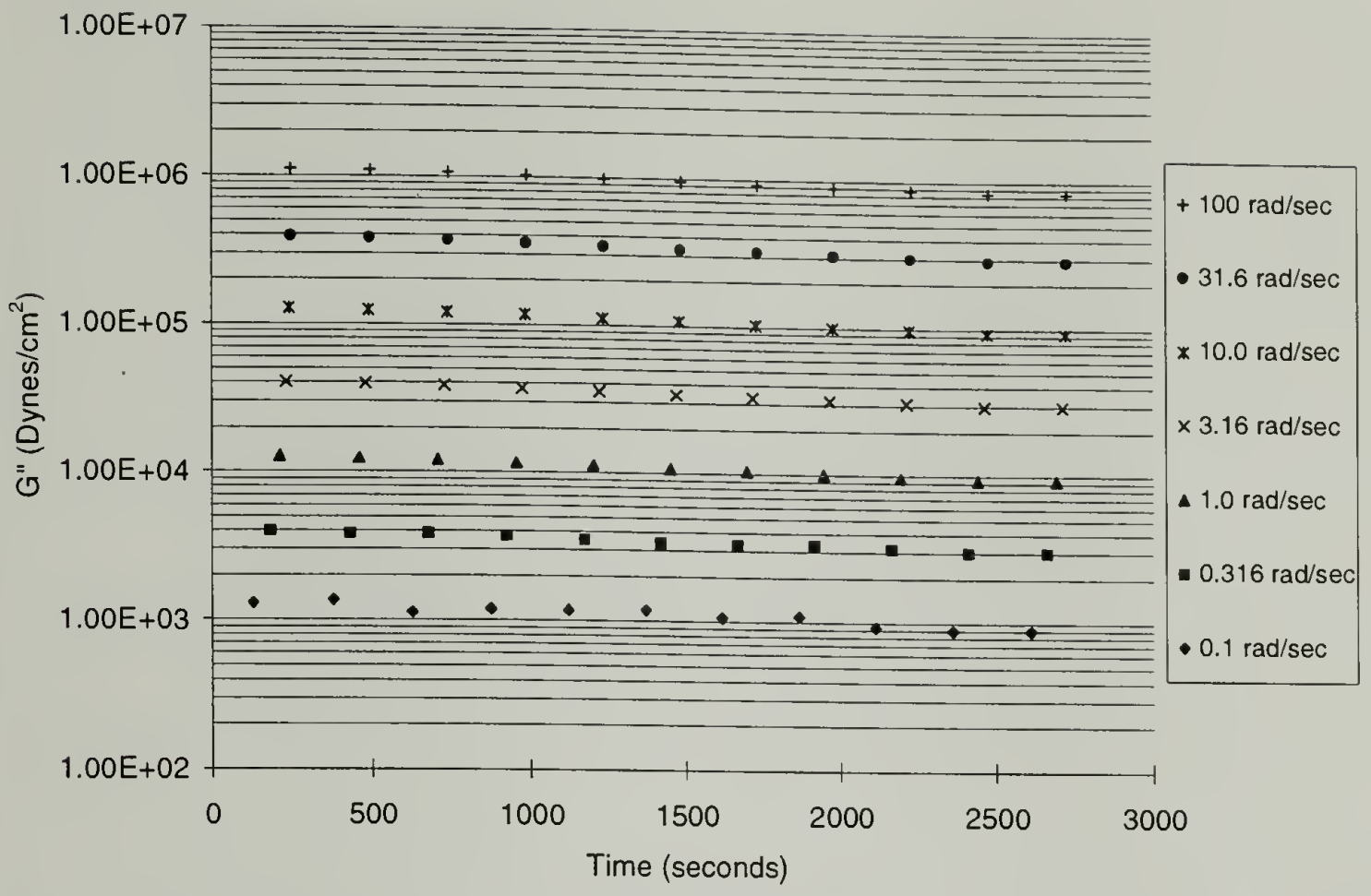


**Figure 6.33 Loss Modulus of VALOX 310 PBT as a function of time and frequency at 250° C. Legend shows shear rates.**

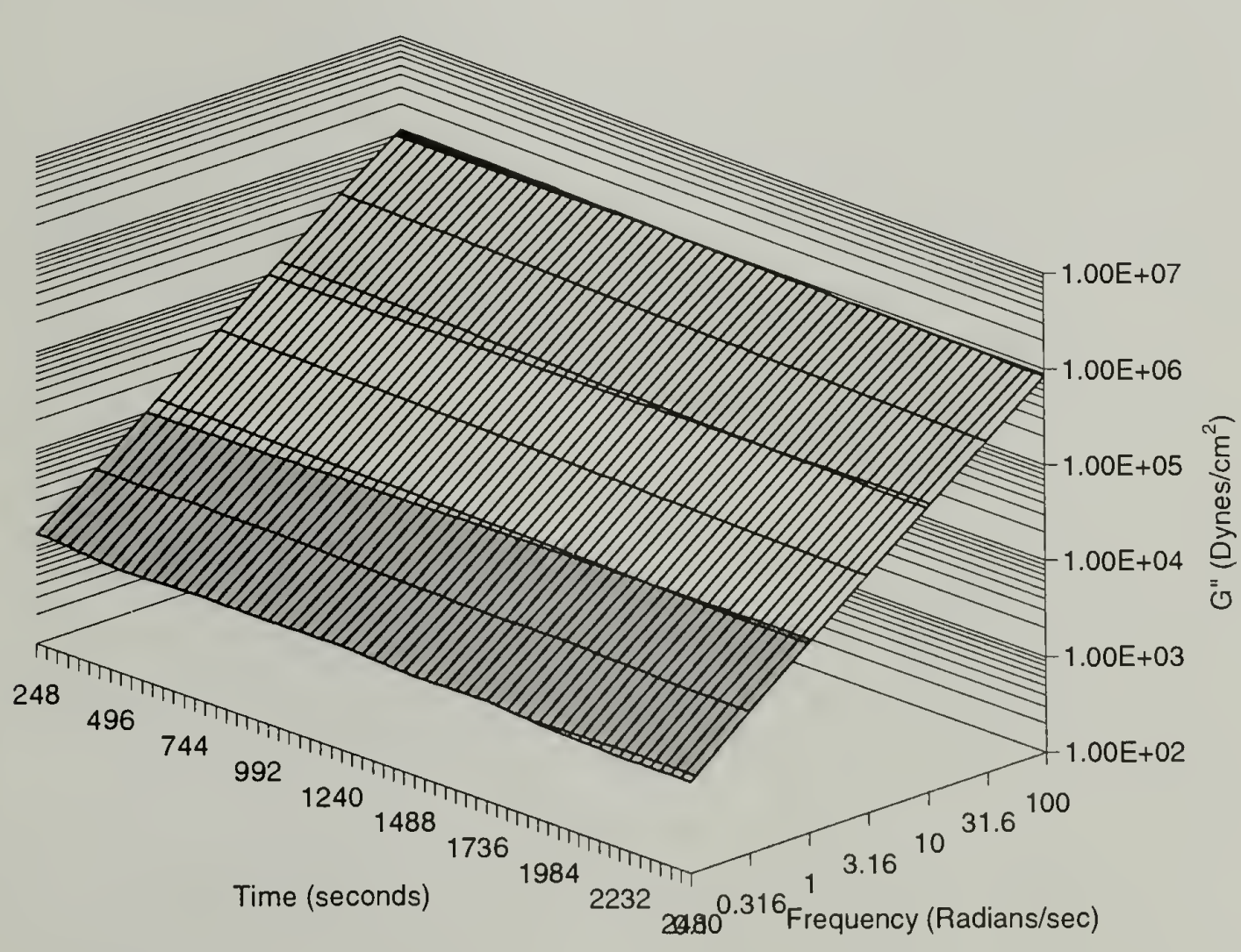


**Figure 6.34 Contour plot of Loss Modulus for VALOX 310 PBT at 250° C.**

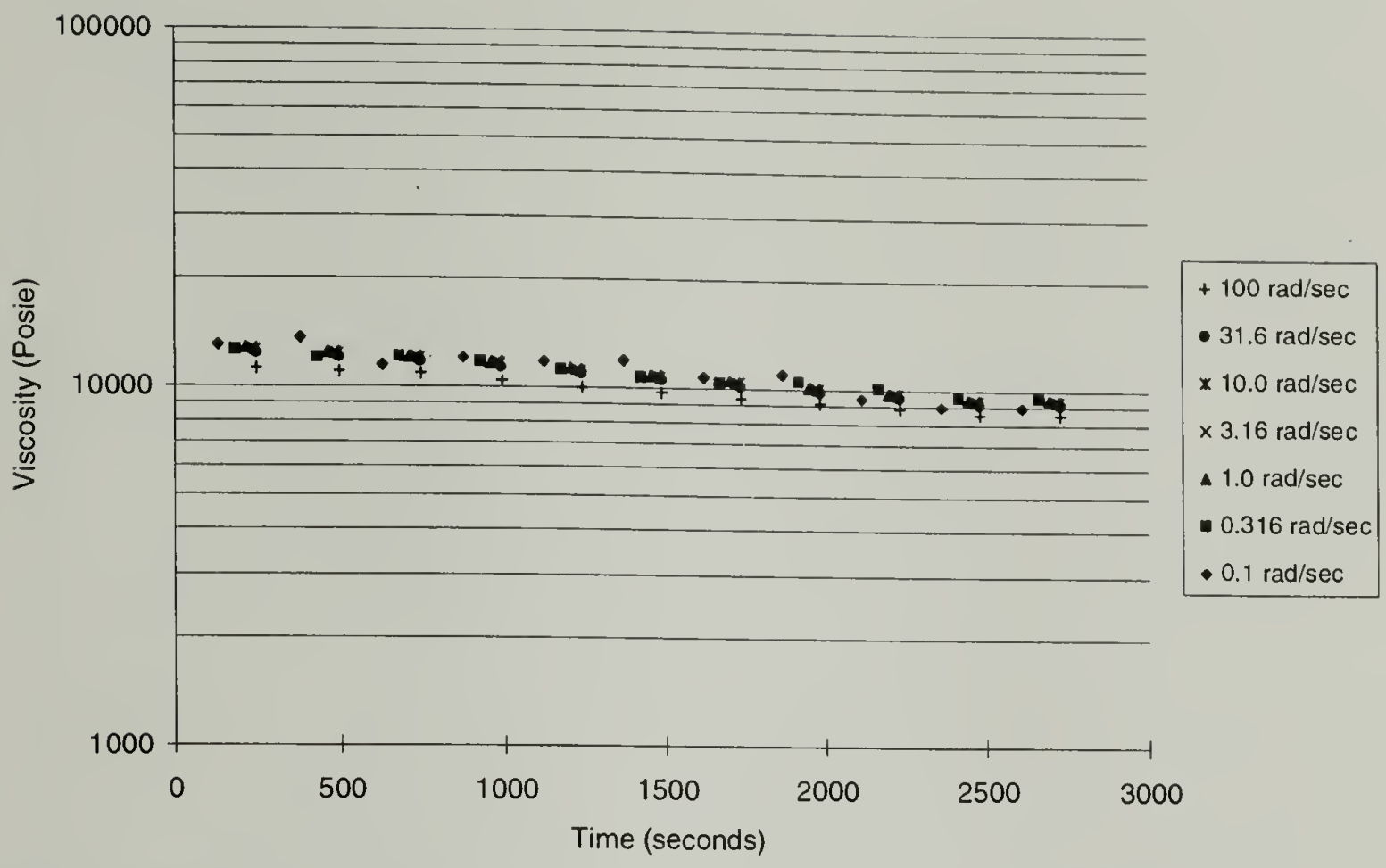


**Figure 6.35 Viscosity of VALOX 310 PBT as a function of time and frequency at 250° C. Legend shows shear rates.**

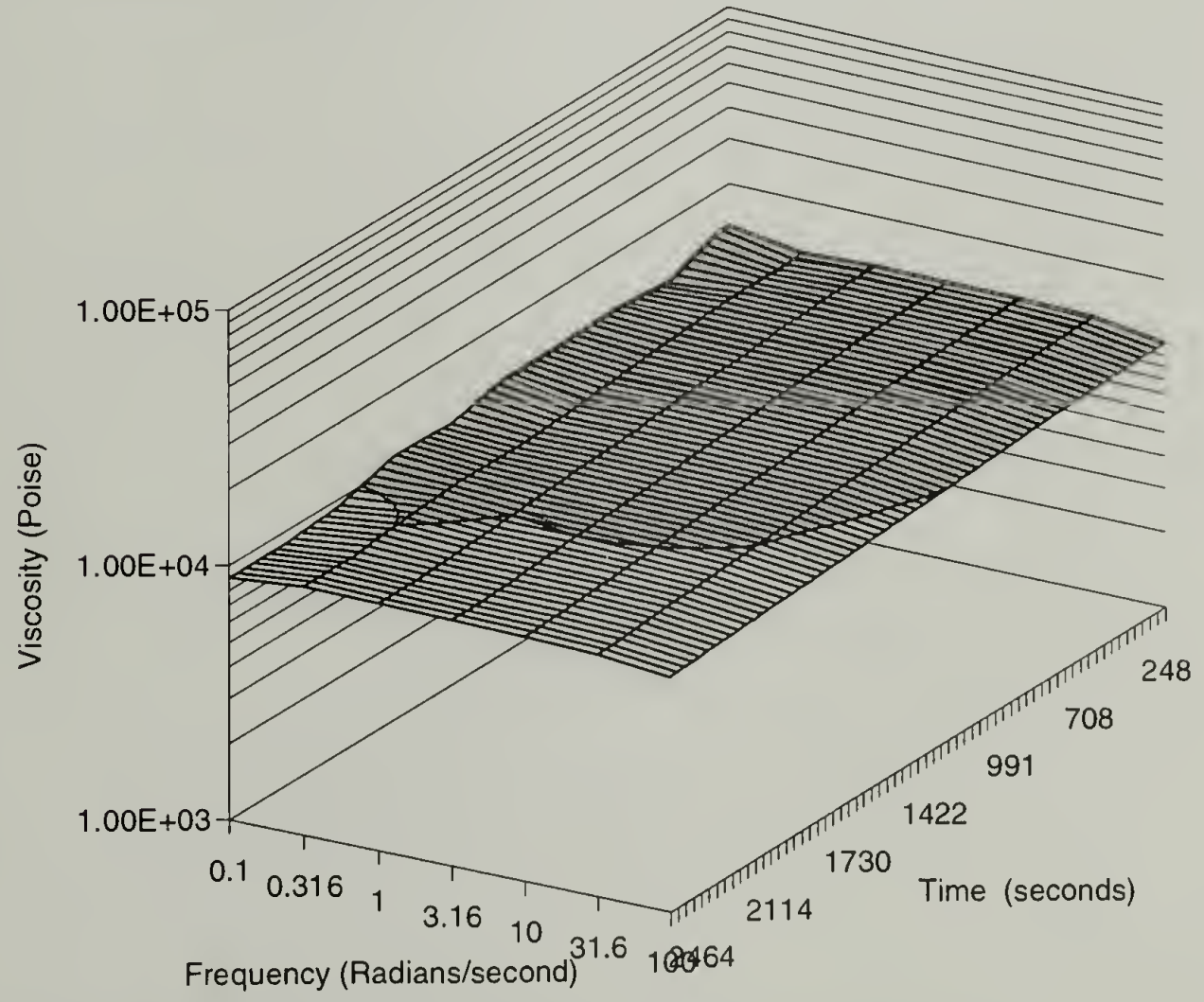


**Figure 6.36 Contour plot of Viscosity for VALOX 310 PBT at 250° C.**

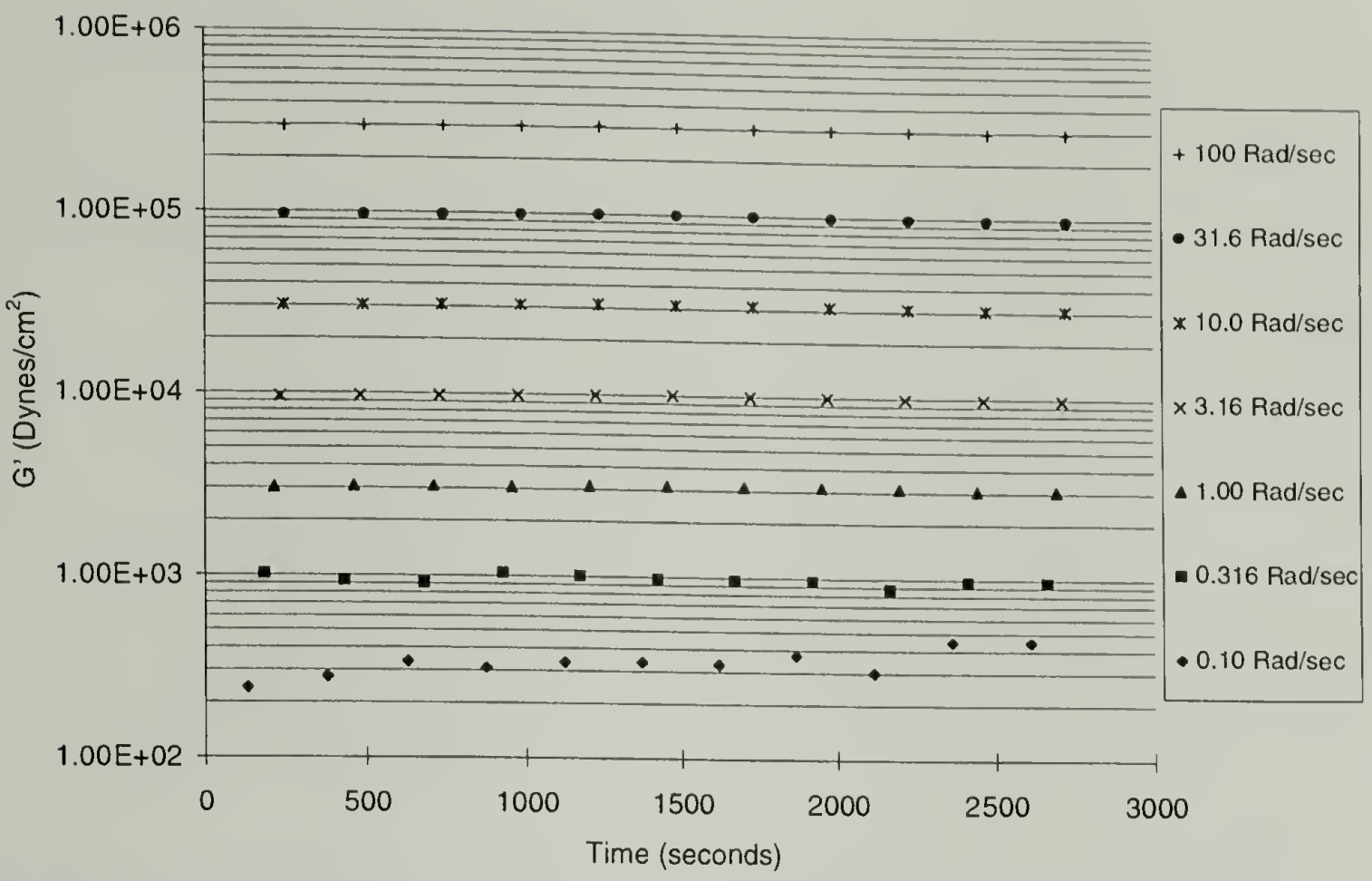


**Figure 6.37 Elastic Modulus of VALOX 295 PBT as a function of time and frequency at 250° C. Legend shows shear rates.**

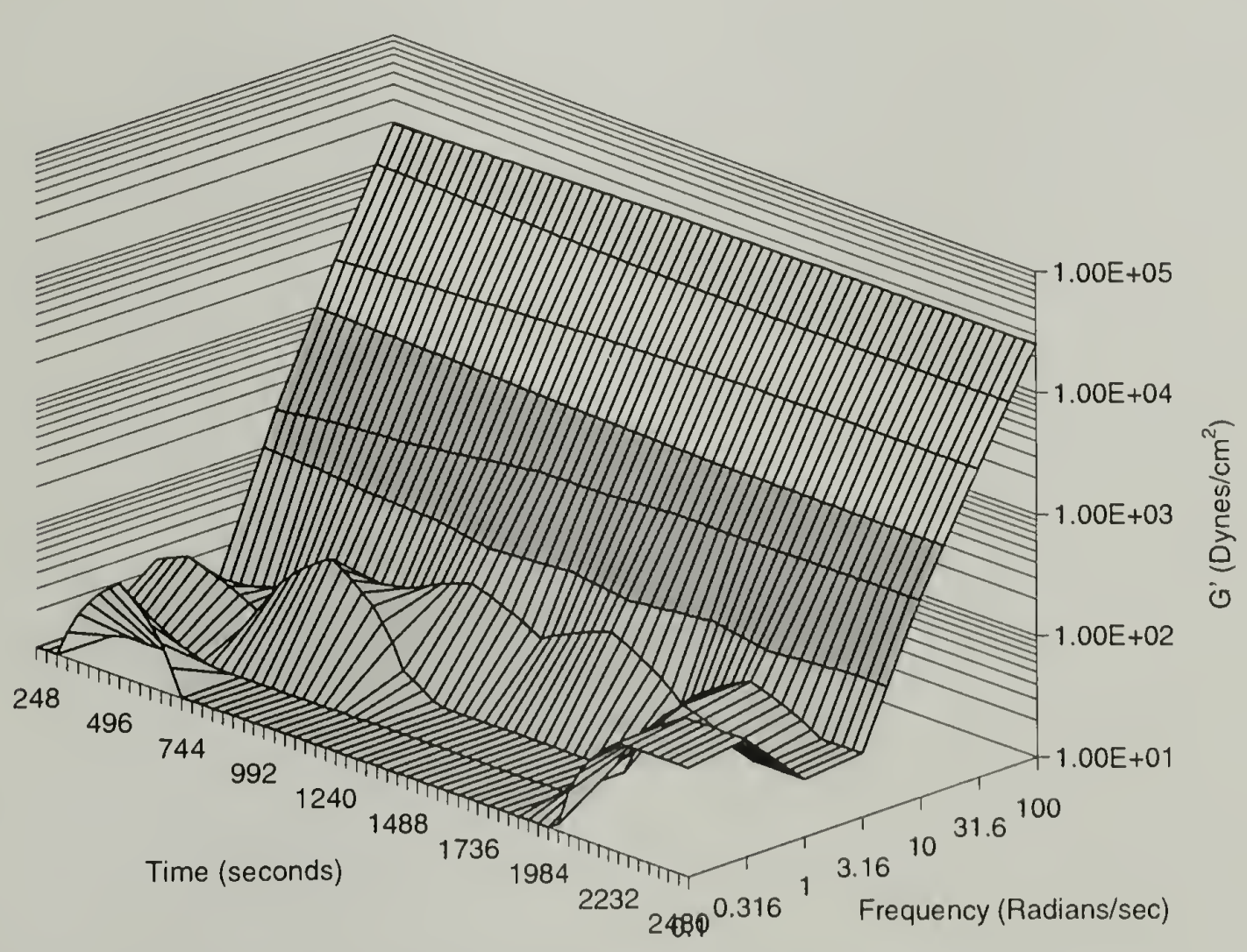


**Figure 6.38 Contour plot of Elastic Modulus for VALOX 295 PBT at 250° C.**

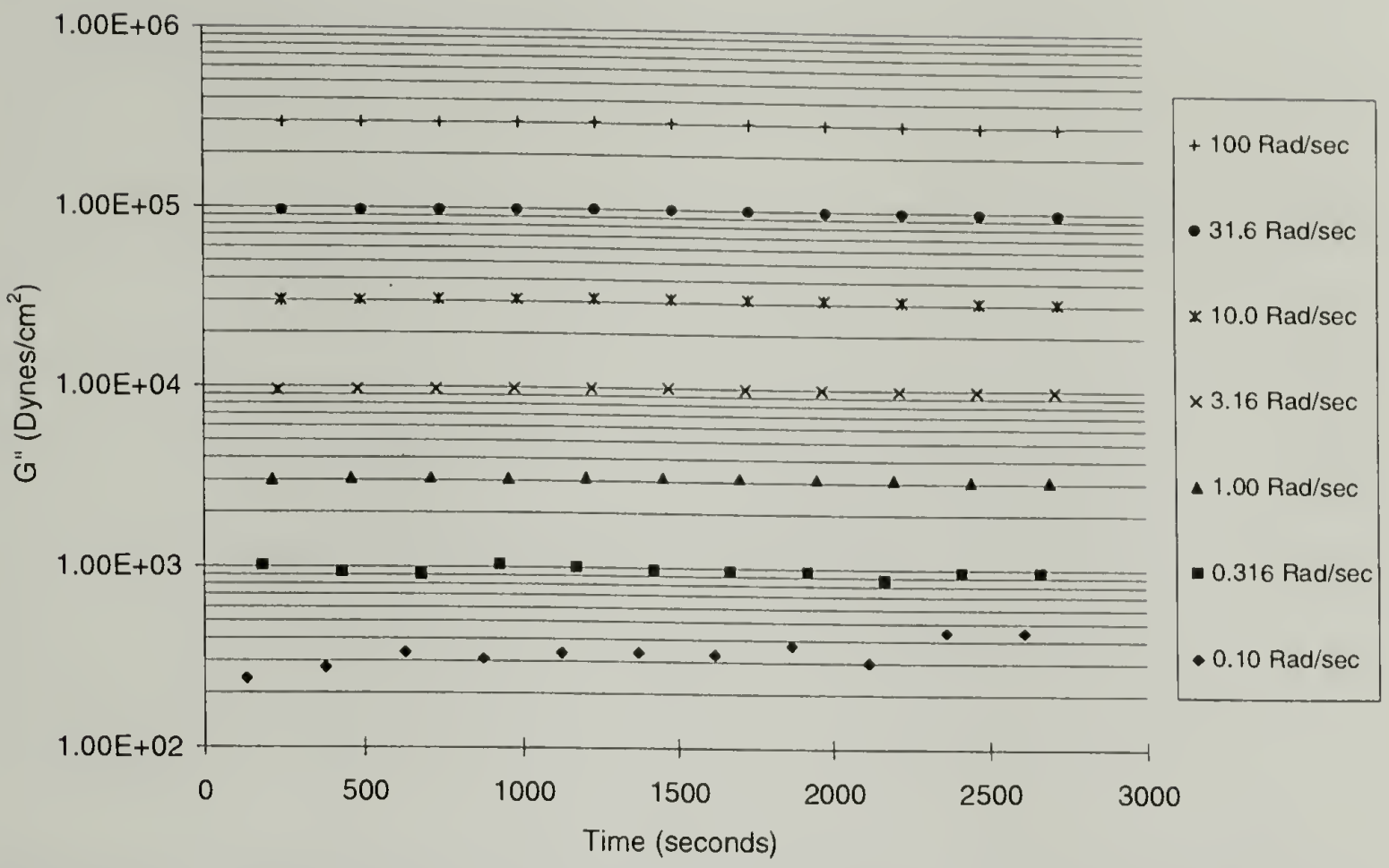


**Figure 6.39 Loss Modulus of VALOX 295 PBT as a function of time and frequency at 250° C. Legend shows shear rates.**

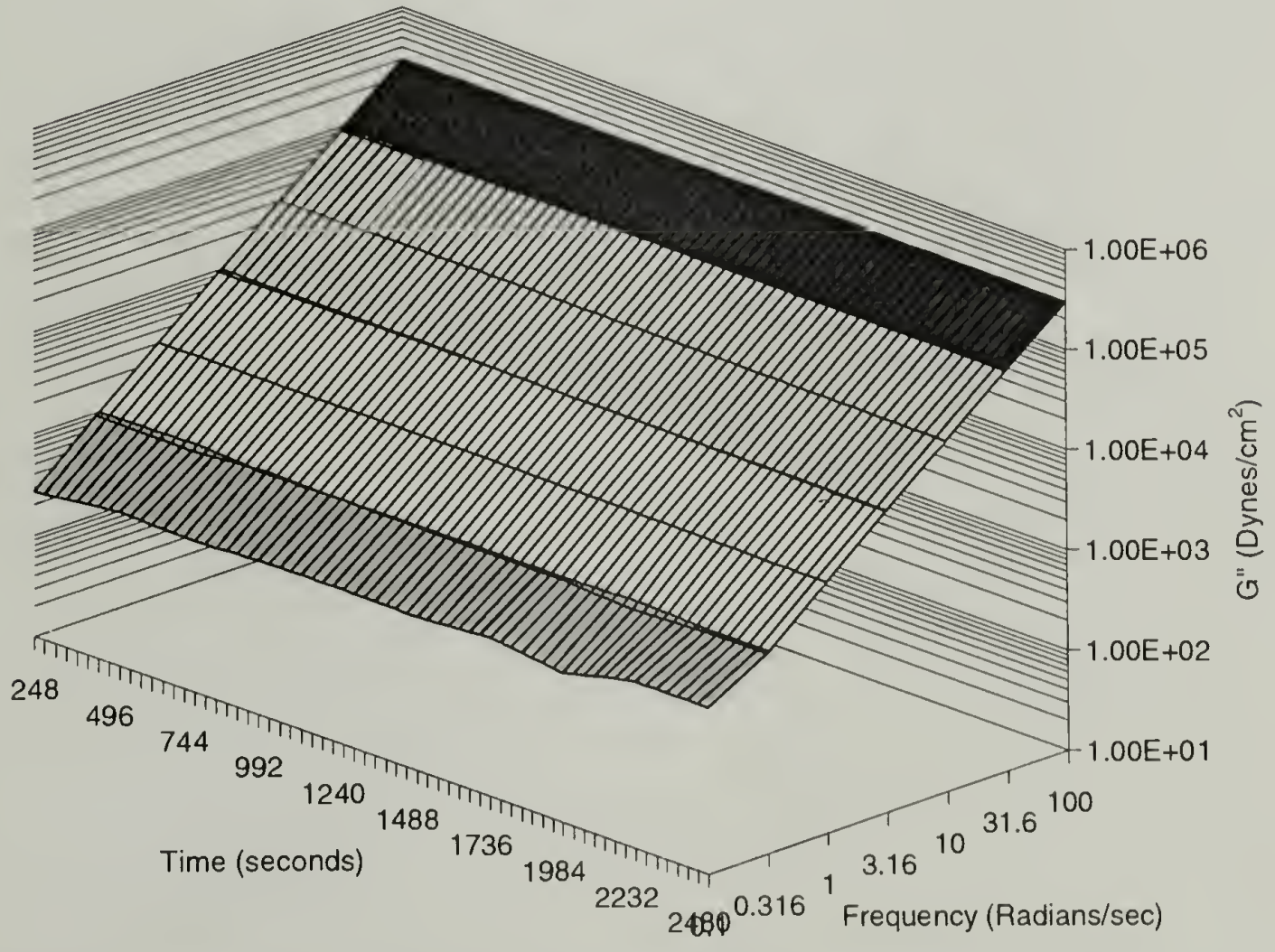


**Figure 6.40 Contour plot of Loss Modulus for VALOX 295 PBT at 250° C.**

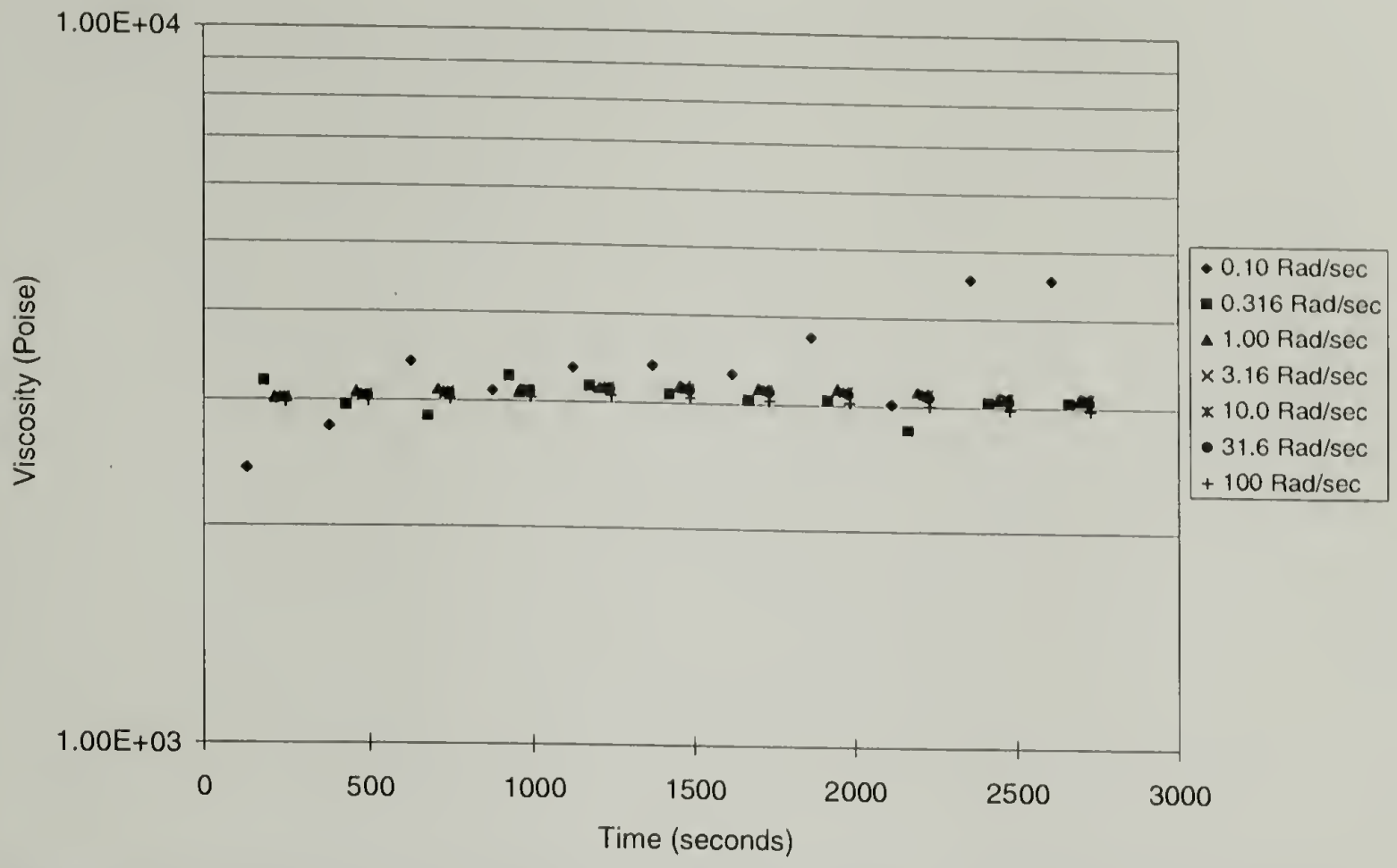


**Figure 6.41 Viscosity of VALOX 295 PBT as a function of time and frequency at 250° C. Legend shows shear rates.**

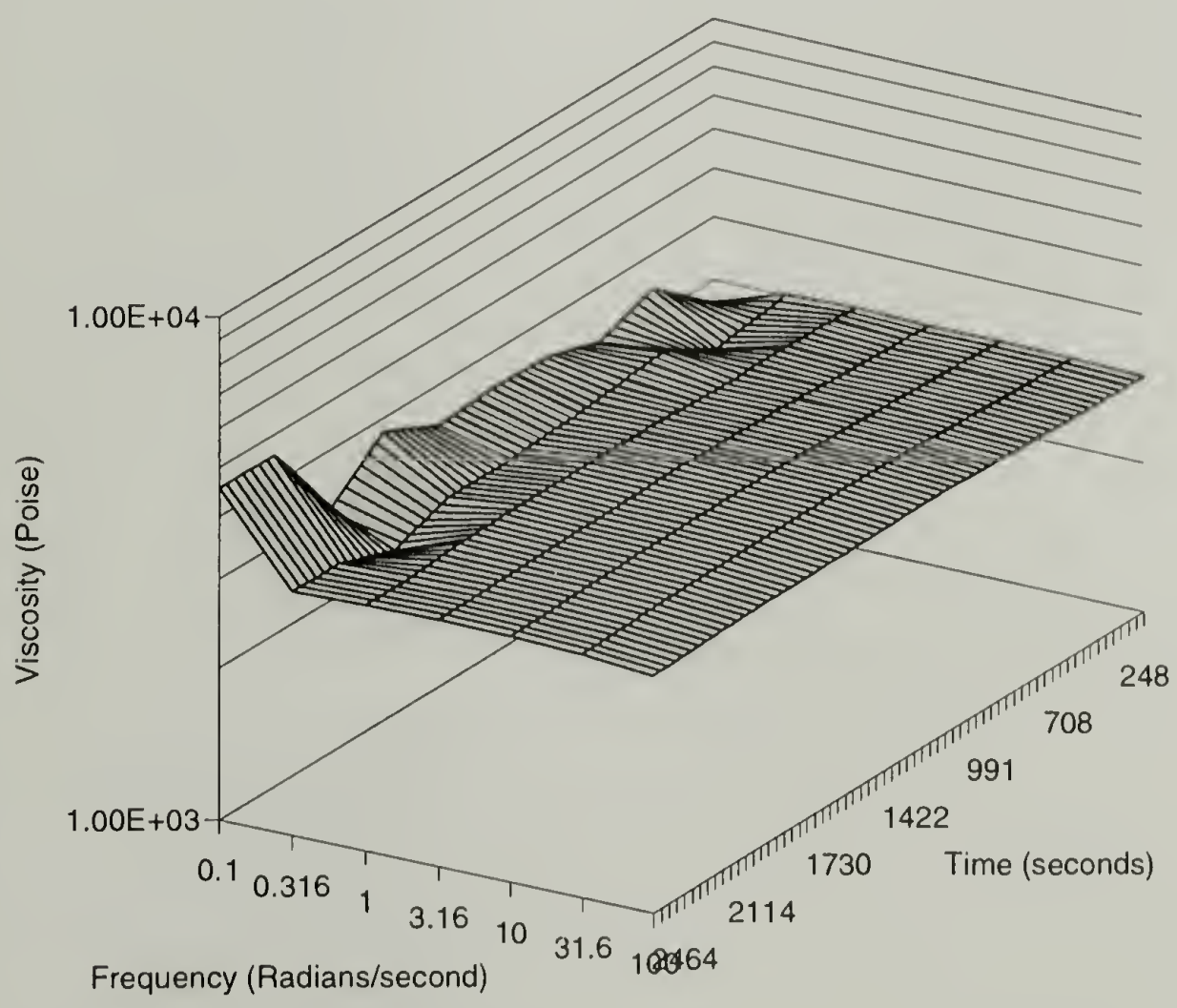


**Figure 6.42 Contour plot of Viscosity for VALOX 295 PBT at 250° C.**

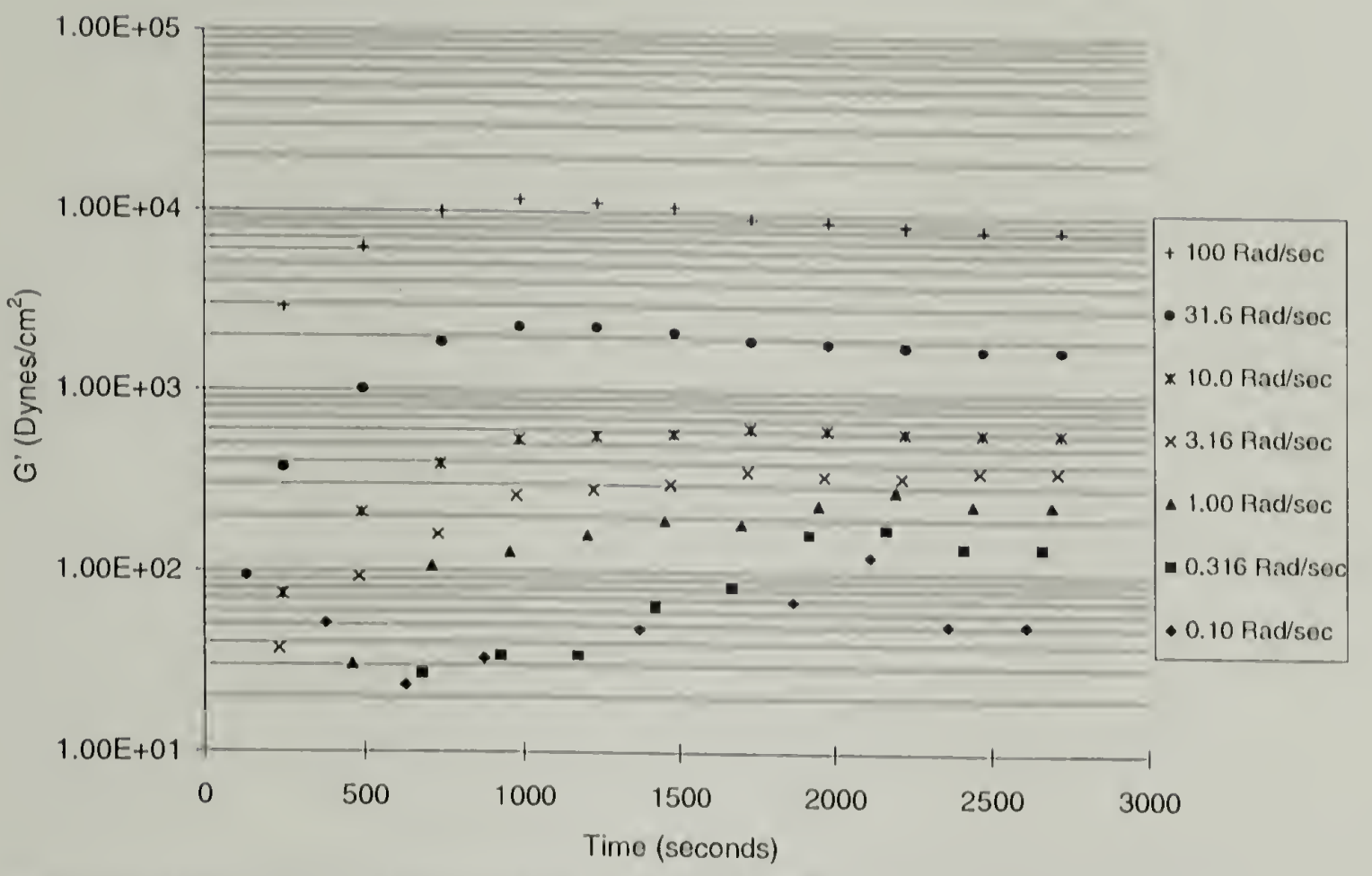


**Figure 6.43 Elastic Modulus of VALOX 195 PBT as a function of time and frequency at 250° C. Legend shows shear rates.**

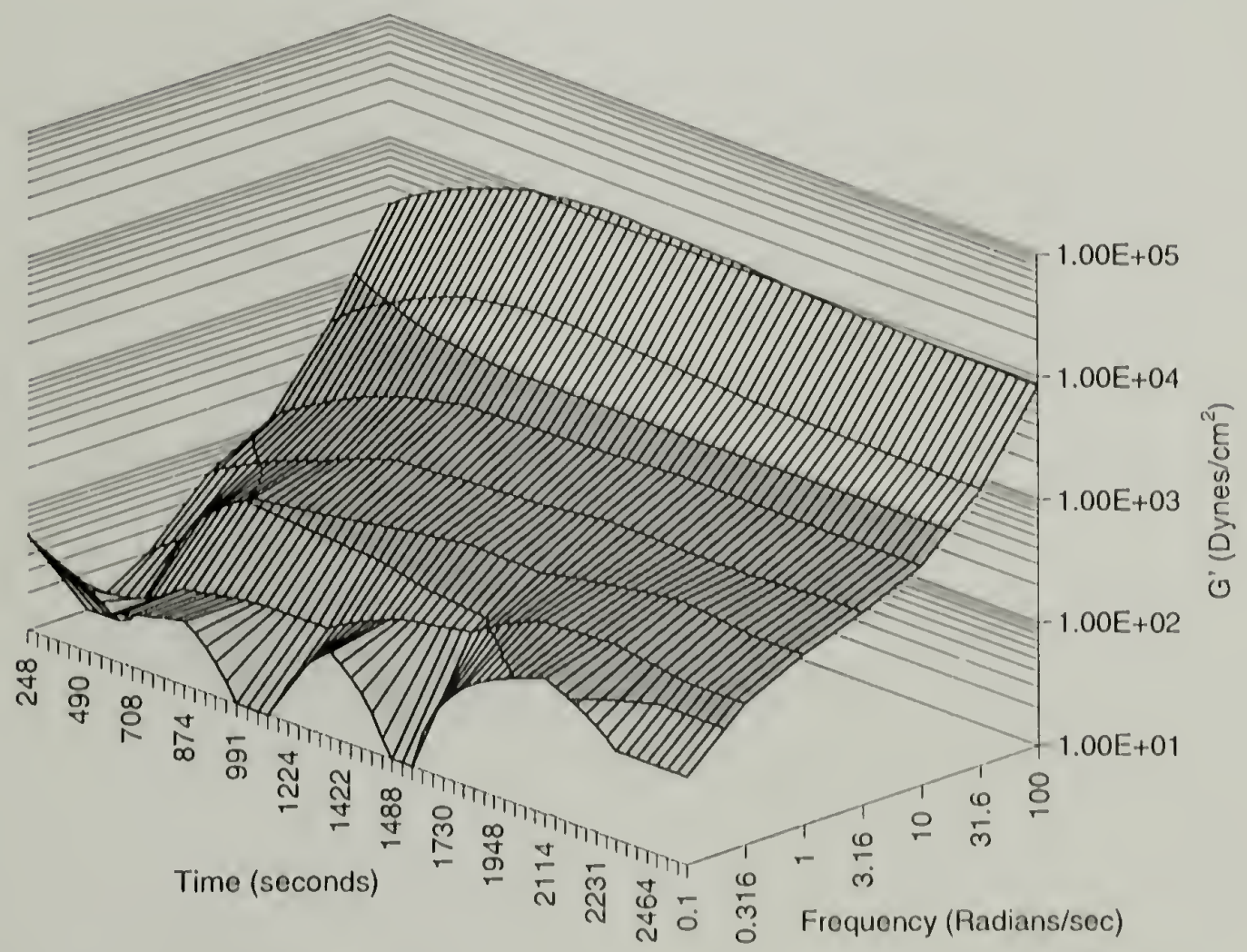


**Figure 6.44 Contour plot of Elastic Modulus for VALOX 195 PBT at 250° C.**

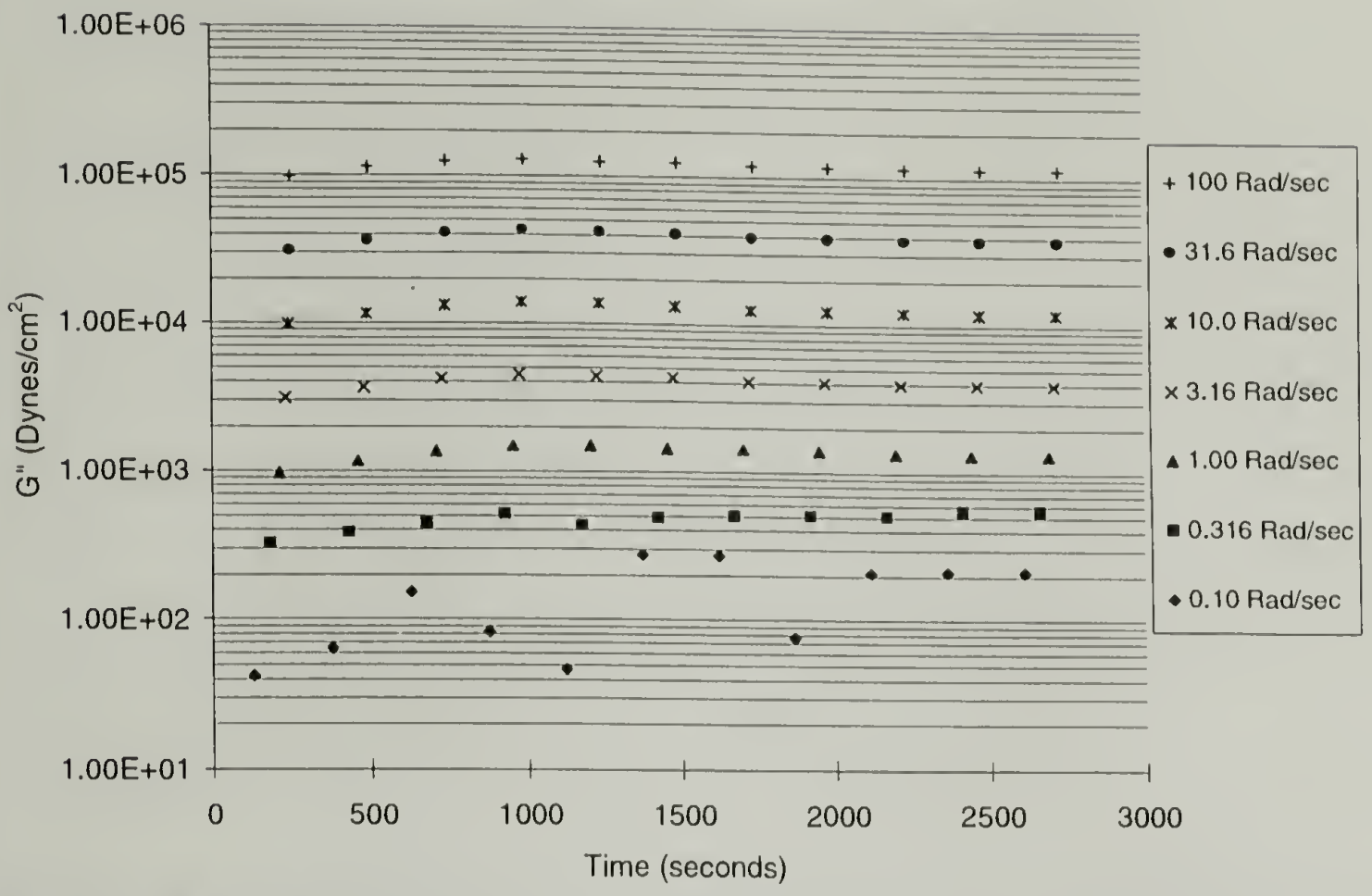


**Figure 6.45 Loss Modulus of VALOX 195 PBT as a function of time and frequency at 250°C. Legend shows shear rates.**

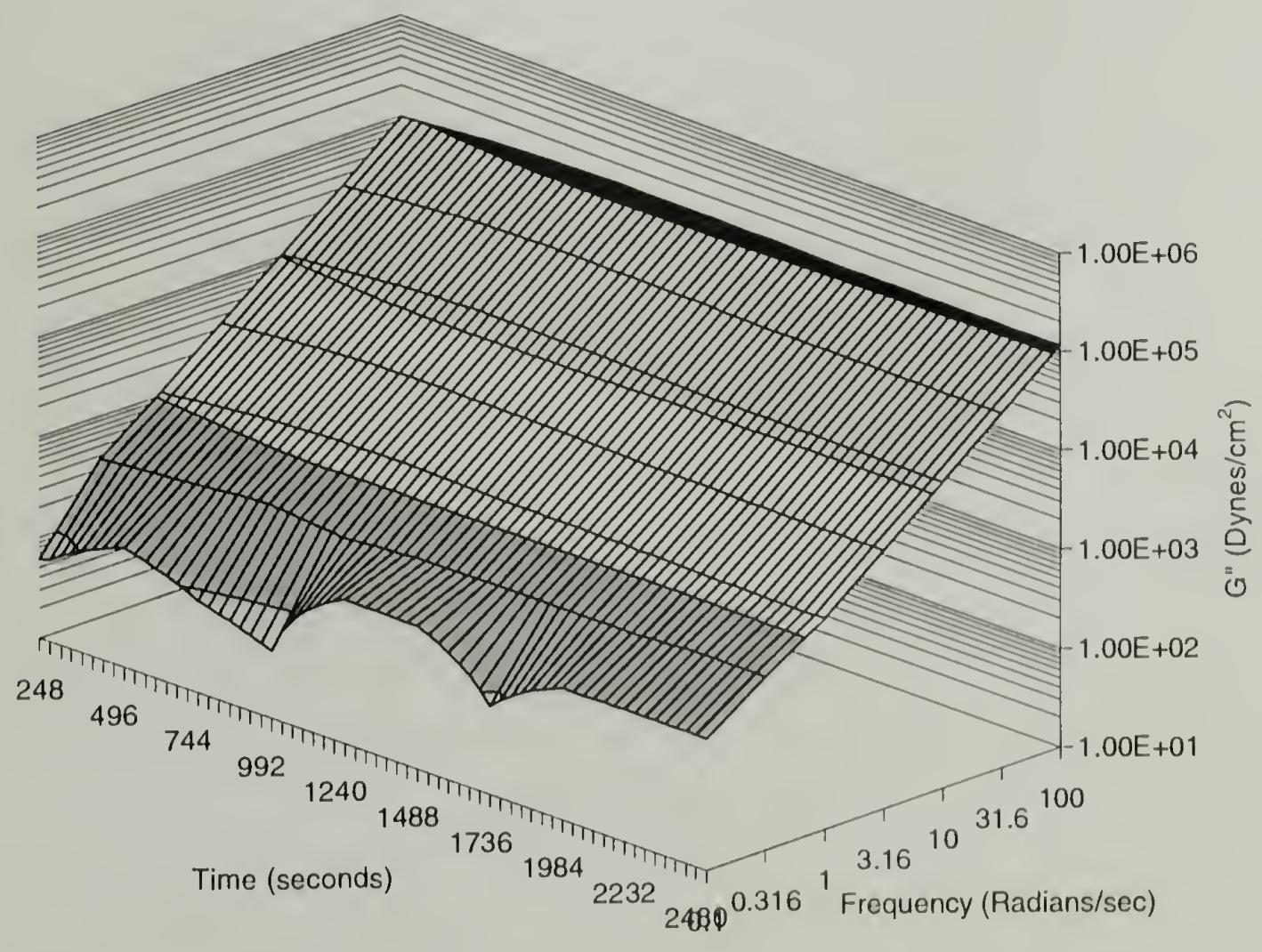


**Figure 6.46 Contour plot of Loss Modulus for VALOX 195 PBT at 250° C.**

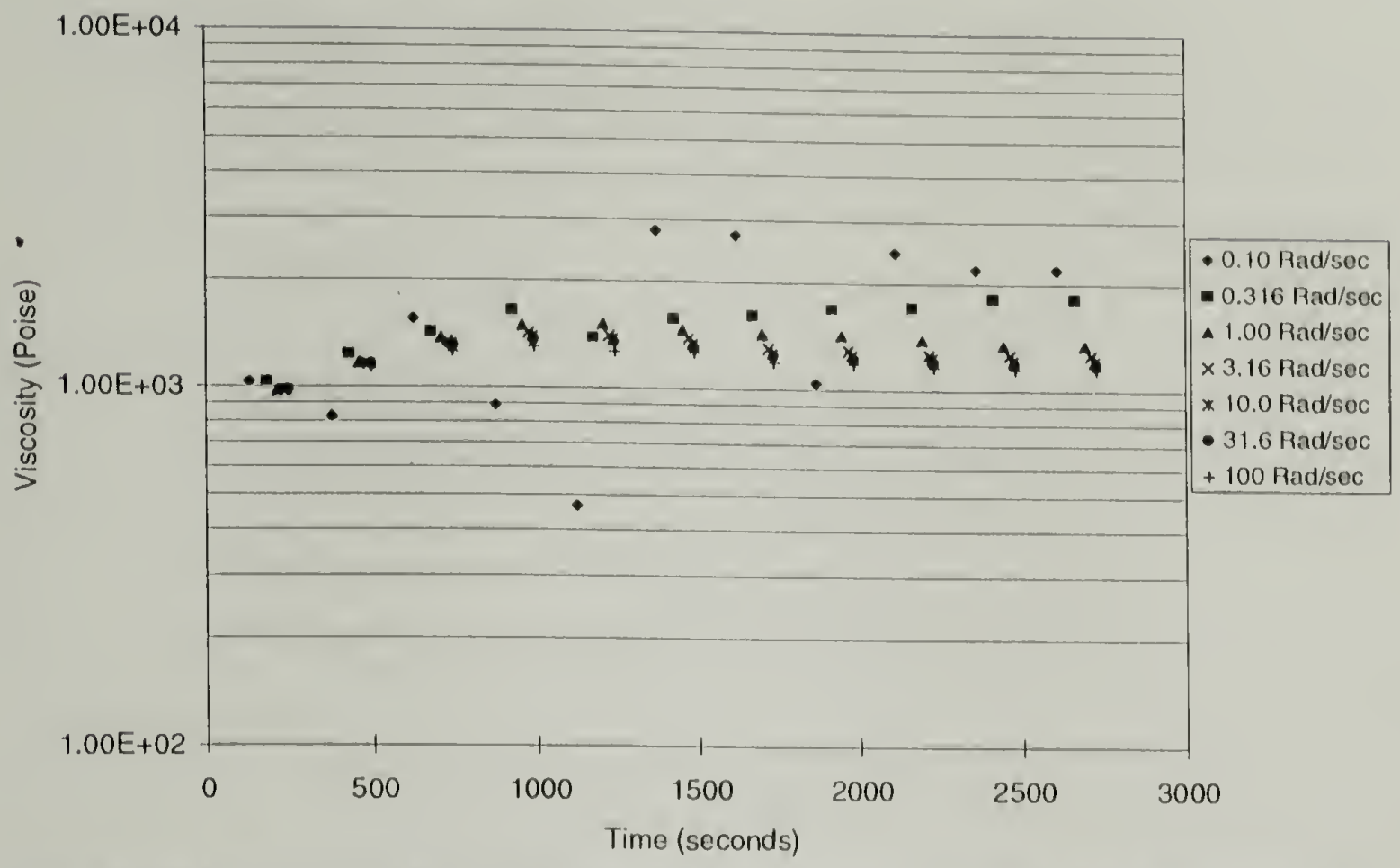


**Figure 6.47 Viscosity of VALOX 195 PBT as a function of time and frequency at 250° C. Legend shows shear rates.**

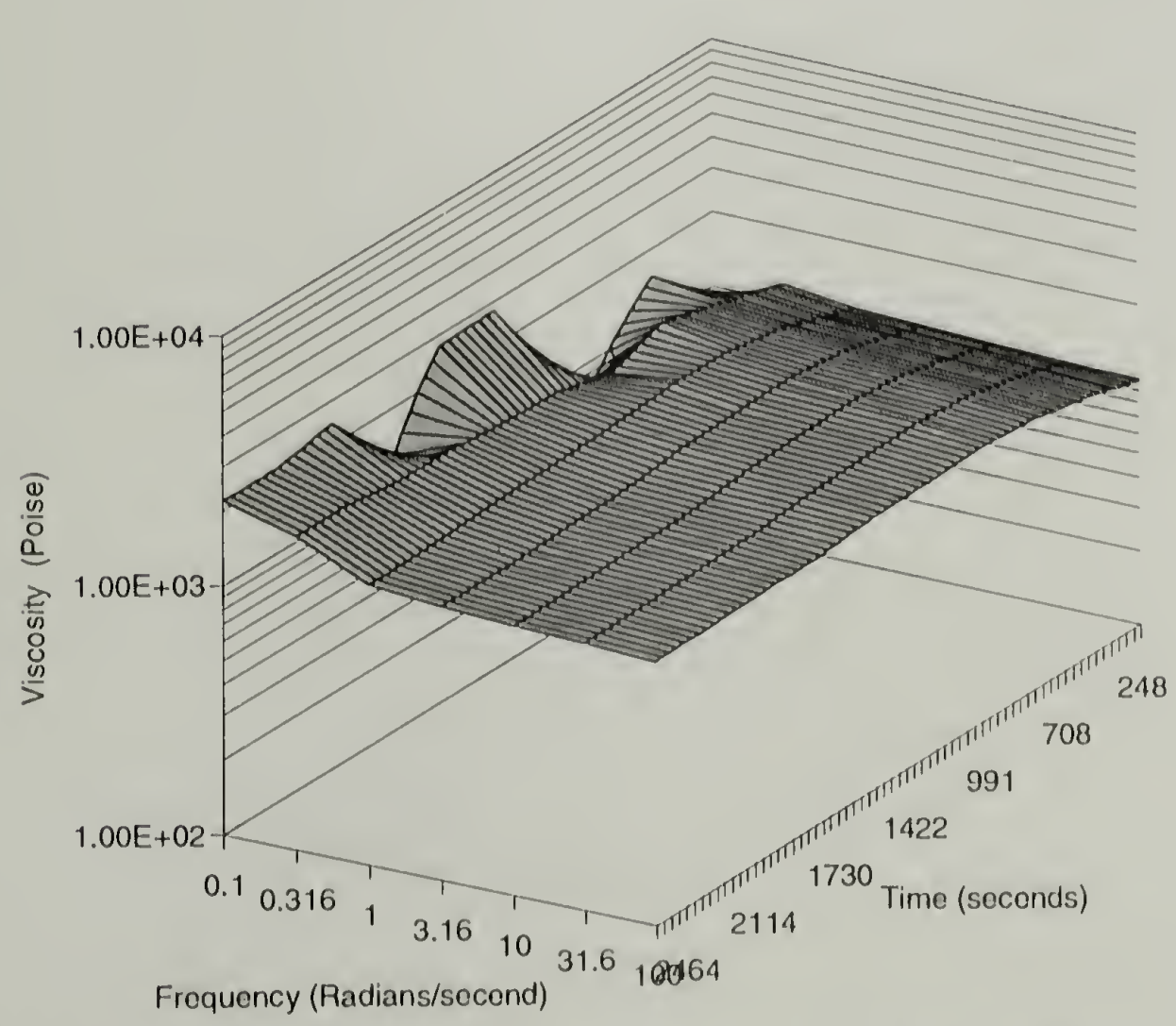


**Figure 6.48 Contour plot of Viscosity for VALOX 195 PBT at 250° C.**

### 6.3.1.3 Discussion of Linear Resin Thermal Stability

The thermal stability of the four linear resins is shown in a single plot of viscosity vs. time at 250° C in Figure 6.49. This plot represents a single slice of each viscosity contour plot at 1.0 radians / second. Since viscosity is controlled primarily by molecular weight under constant conditions, a change in viscosity with time indicates a change in molecular weight (and/or molecular weight distribution) with time under constant conditions. VALOX 315 PBT has the highest viscosity throughout the time frame of the rheology test, followed in order by VALOX 310 PBT, VALOX 295 PBT, and VALOX 195 PBT.

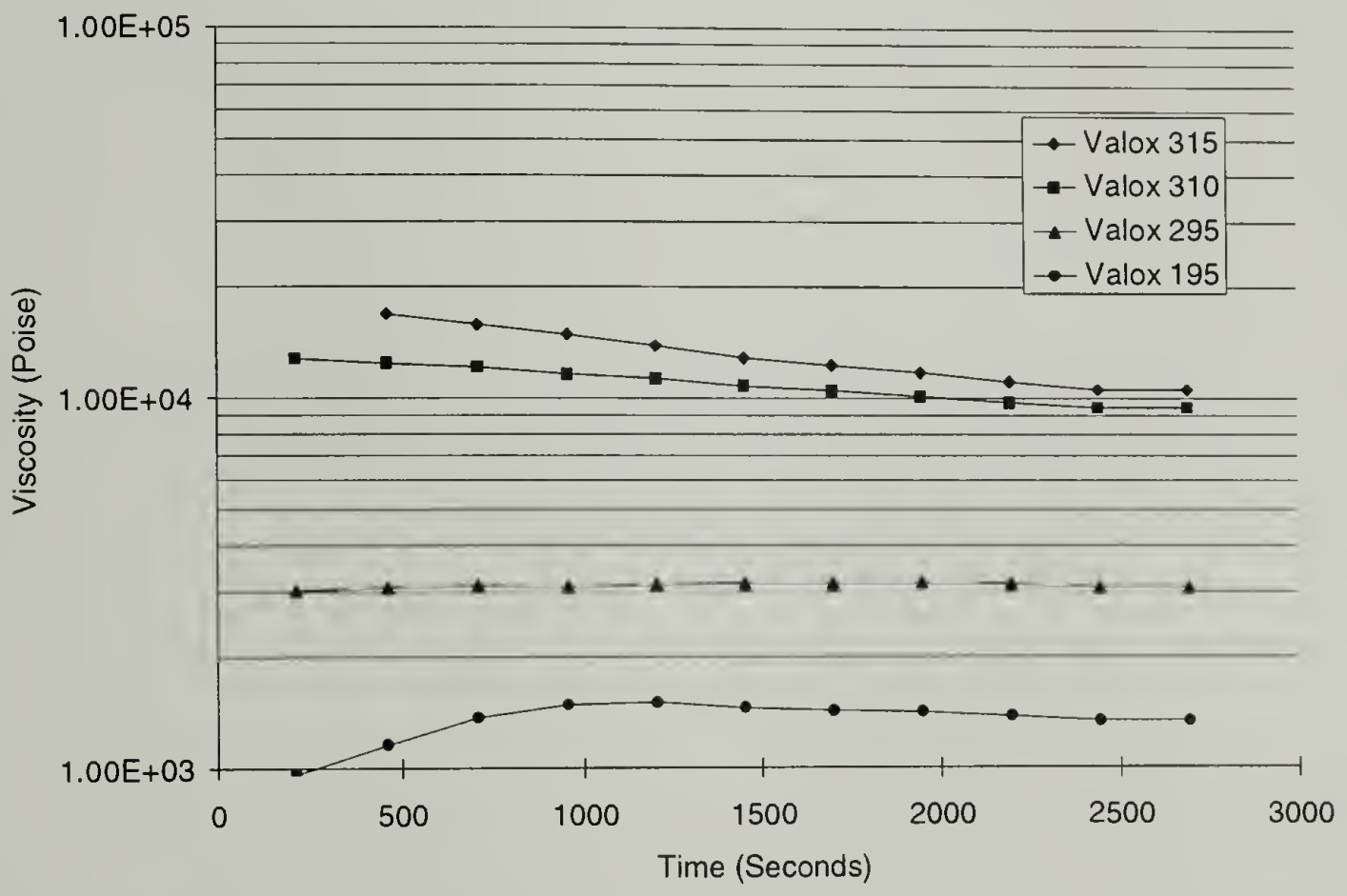


**Figure 6.49 Thermal Stability of linear PBT resins at 250°C.**

Based on rate of change in viscosity, VALOX 295 PBT appears to be the most stable resin as it shows the lowest slope over the time frame of the characterization. VALOX 310 PBT and VALOX 315 PBT each drop in viscosity at a nearly uniform rate; the resin of higher molecular weight has a slightly faster loss rate. VALOX 195 PBT

shows a rising viscosity curve that indicates either 1) the temperature is not stable but is decreasing slightly at the beginning of the test or 2) the polymer's molecular weight is continuing to increase through the first 15 minutes of testing.

(A continuing investigation into molecular association in PBT resins has brought to light a new explanation of this behavior for VALOX 195 PBT[6]. Although the details are proprietary at this time, the increase in viscosity is to be expected. These results cannot be disclosed in this thesis as they may be the basis for a new competitive process for producing PBT resins.)

Molecular weights were determined for each resin prior to and after the rheology test with the results shown in Table 6.3. Since these are commercial resins, the losses in average molecular weight with time in the melt are related to the amount and type of thermal stabilizer used in each formulation. Significant differences are seen in the stability of the resins based on Mw determinations, with VALOX 310 PBT being the most stable, followed by VALOX 295 PBT , VALOX 315 PBT, and then VALOX 195 PBT in that order. Chemical identities of the stabilizers are proprietary to General Electric Plastics and are not reported herein.

**Table 6.3 Molecular weight of PBT resins studied for thermal stability. All molecular weight data is based on GPC analysis using linear PS calibrants.**

| | Before Rheology Testing | | | After 50 minutes at 250° C | | |
|---|---|---|---|---|---|---|
| | $M_w$ | $M_n$ | PDI | $M_w$ | $M_n$ | PDI |
| VALOX 315 PBT | 89,800 | 43,400 | 2.12 | 80,900 | 30,200 | 2.68 |
| VALOX 310 PBT | 78,700 | 29,900 | 2.63 | 77,400 | 29,100 | 2.66 |
| VALOX 295 PBT | 57,500 | 20,000 | 2.88 | 54,300 | 22,300 | 2.43 |
| VALOX 195 PBT | 41,300 | 16,700 | 2.47 | 28,200 | 14,500 | 1.95 |
| SMII-60 | 290,000 | 122,000 | 2.39 | 131,000 | 56,600 | 2.31 |
| SMIII-75 | 156,000 | 57,300 | 2.72 | 85,800 | 30,600 | 2.81 |
| SMIII-102 | 527,000 | 46,700 | 11.3 | 136,200 | 41,900 | 3.25 |

### 6.3.1.4 Cyclic Resin Thermal Stability

The same rheological characterization as just described for linear PBT resins, was performed on three high molecular weight cyclic PBTs (designated as SMII-60, SMIII-75 and SMIII-102). Apparent molecular weights for these resins are included in Table 6.3. SMII-60 was found to produce very high shear stresses at shear rates above 10 radians/second. Above this shear rate, the shear stress in this macrocyclic system produced torques beyond the capacity of the equipment. Thus the rheology data shown in both two-dimensional and three-dimensional (contour) plots below is truncated at this 10 radians/second. This material is included because it accurately represents the material in the low shear ranges, where shear stresses are within the equipment capabilities. A useful correlation of zero shear viscosity vs. molecular weight was determined from the rheology data and the weight average molecular weight of this resin.

The other two macrocyclic resins were characterized for thermal stability at 250° C using lower shear strains to allow higher shear rate testing. The resin designated SMIII-102 is found to have an extremely high molecular weight and a very broad molecular weight distribution. The distribution is bimodal and heavily skewed toward the high molecular weight end. The $M_w$ reported from GPC analysis is the high molecular weight peak, which most strongly influences the melt viscosity. The reason for this skewed distribution appears to be incomplete polymerization in the laboratory oven prior to the rheology testing. Once heated to 250° C, the polymerization was quickly completed and the results below show that the high $M_w$ peak was representative of the resin once polymerization was completed. The resin designated SMIII-75, which was

produced with lower molecular weight by using a higher initiator content, shows a normal molecular weight distribution and a more reasonable PDI.

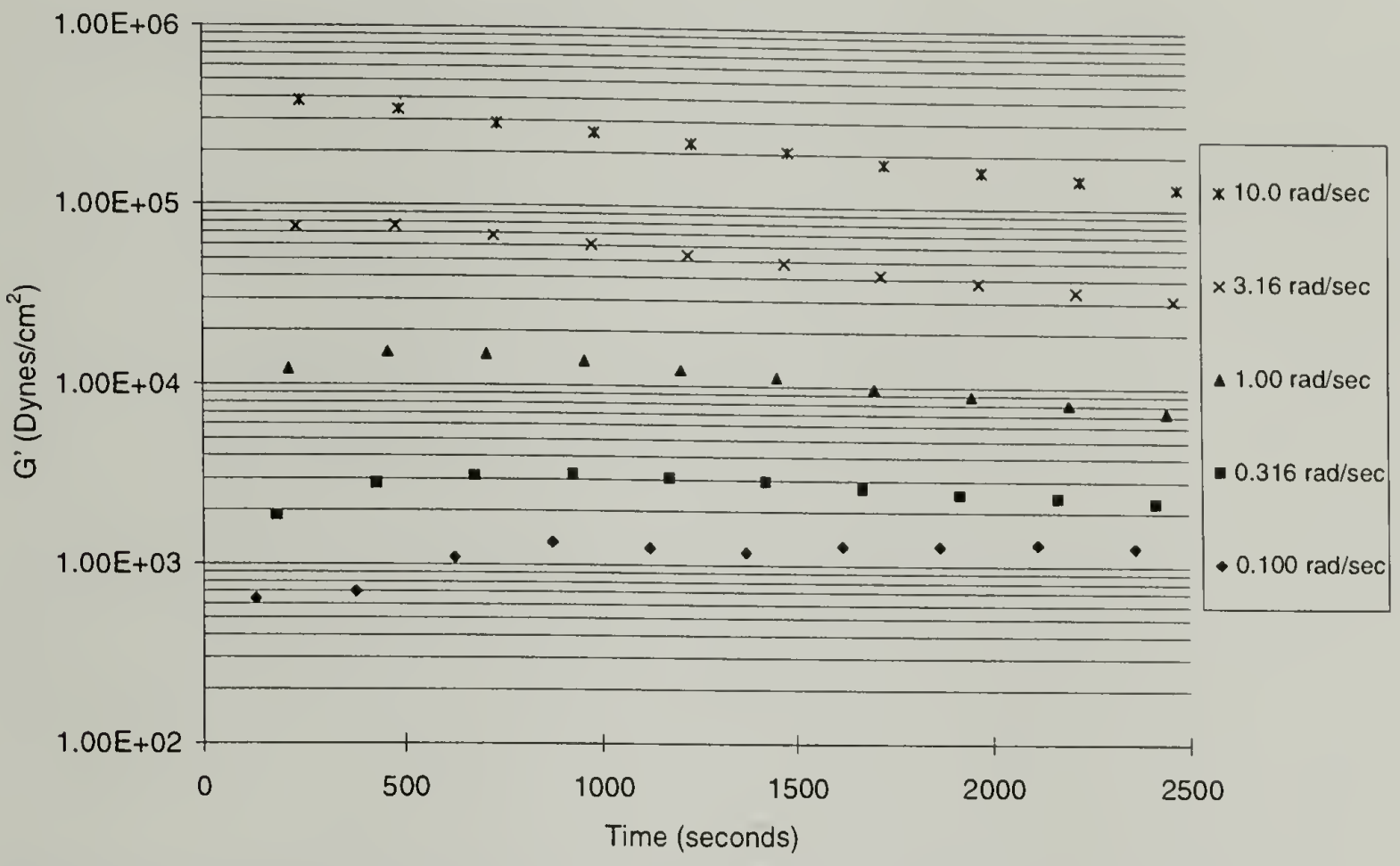


**Figure 6.50 Storage Modulus for SMII-60 at 250° C. Legend shows shear rates.**

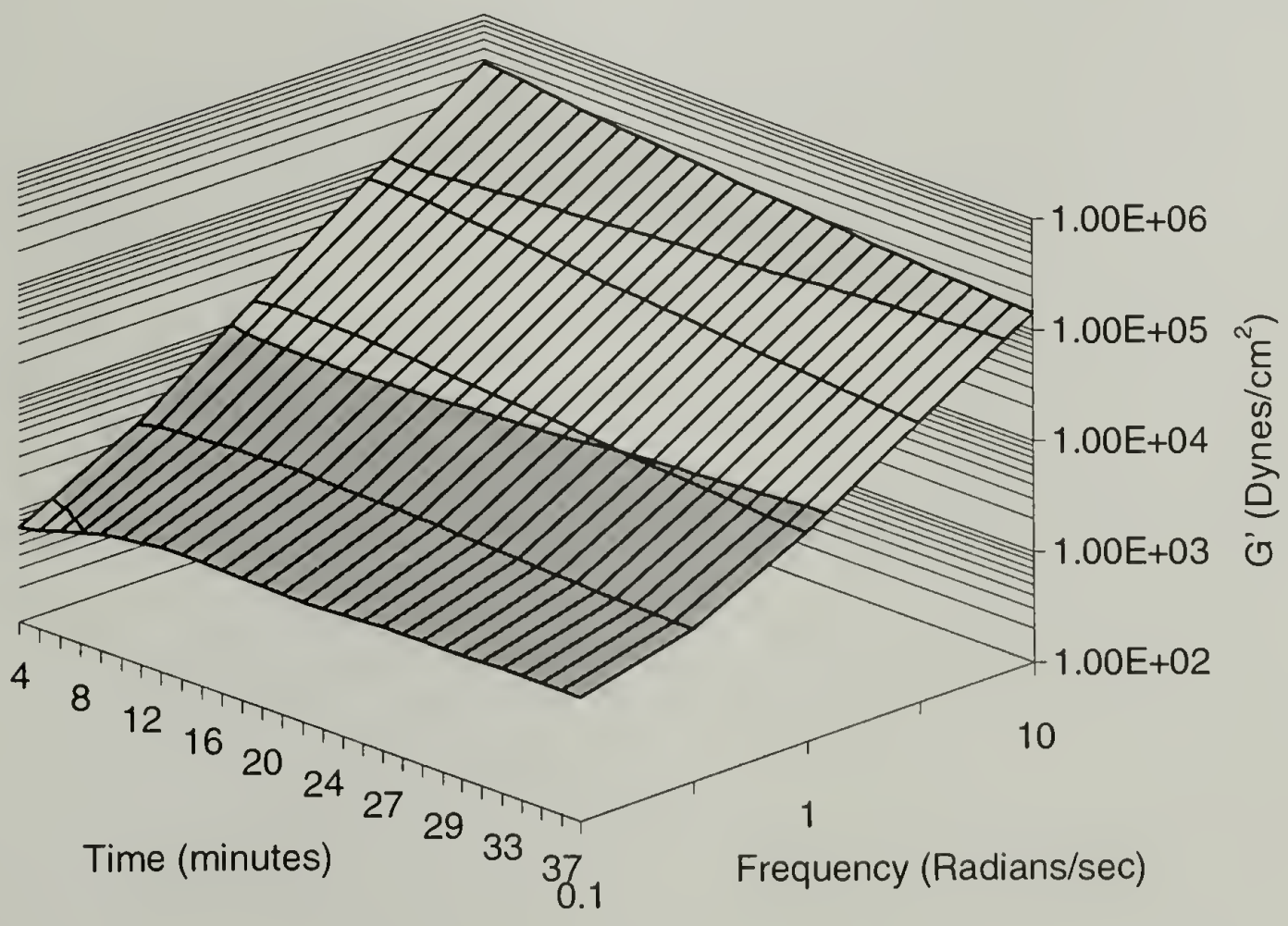


**Figure 6.51 Storage Modulus Contour SMII-60 at 250° C.**

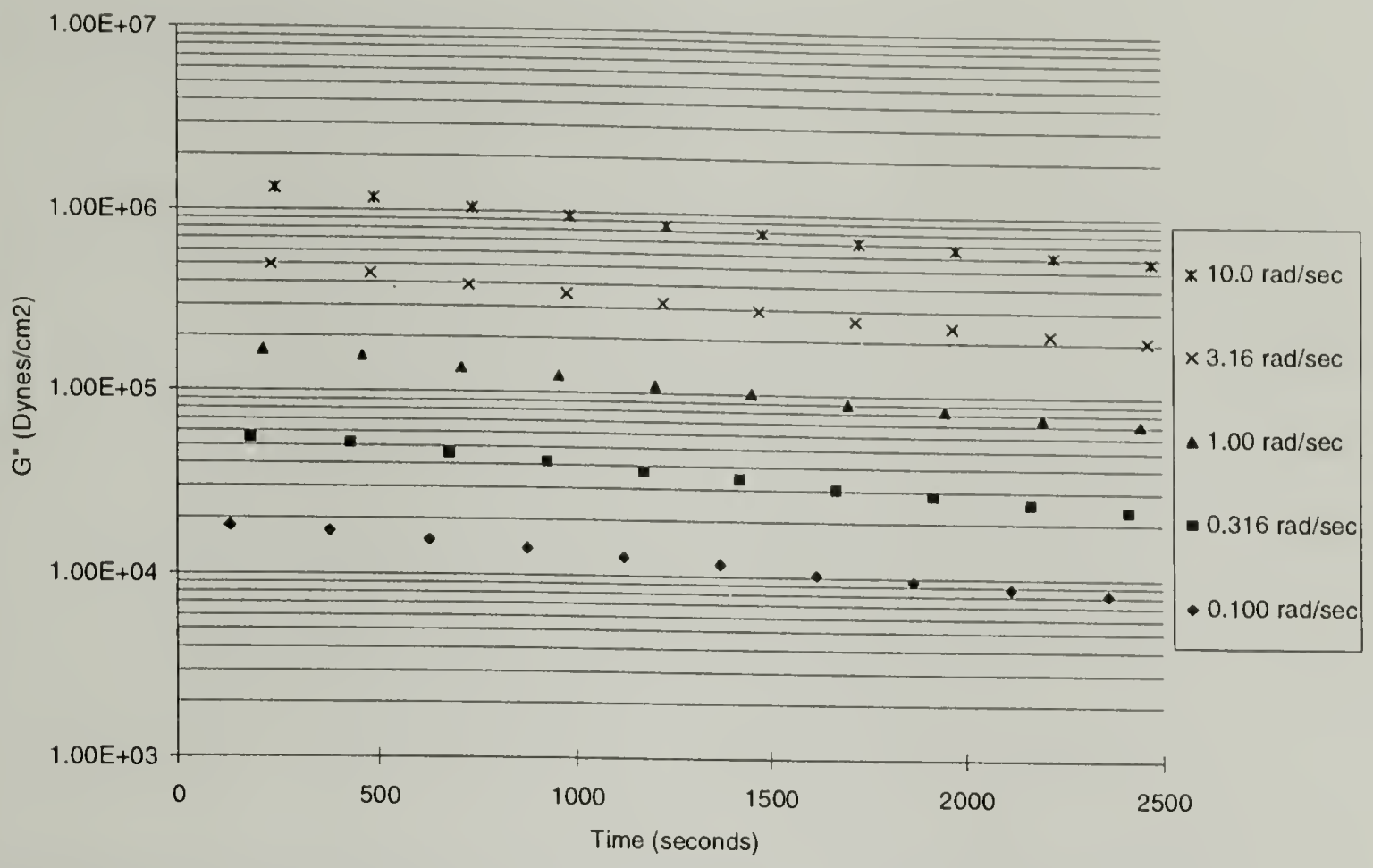


**Figure 6.52 Loss Modulus for SMII-60 at 250° C. Legend shows shear rates.**

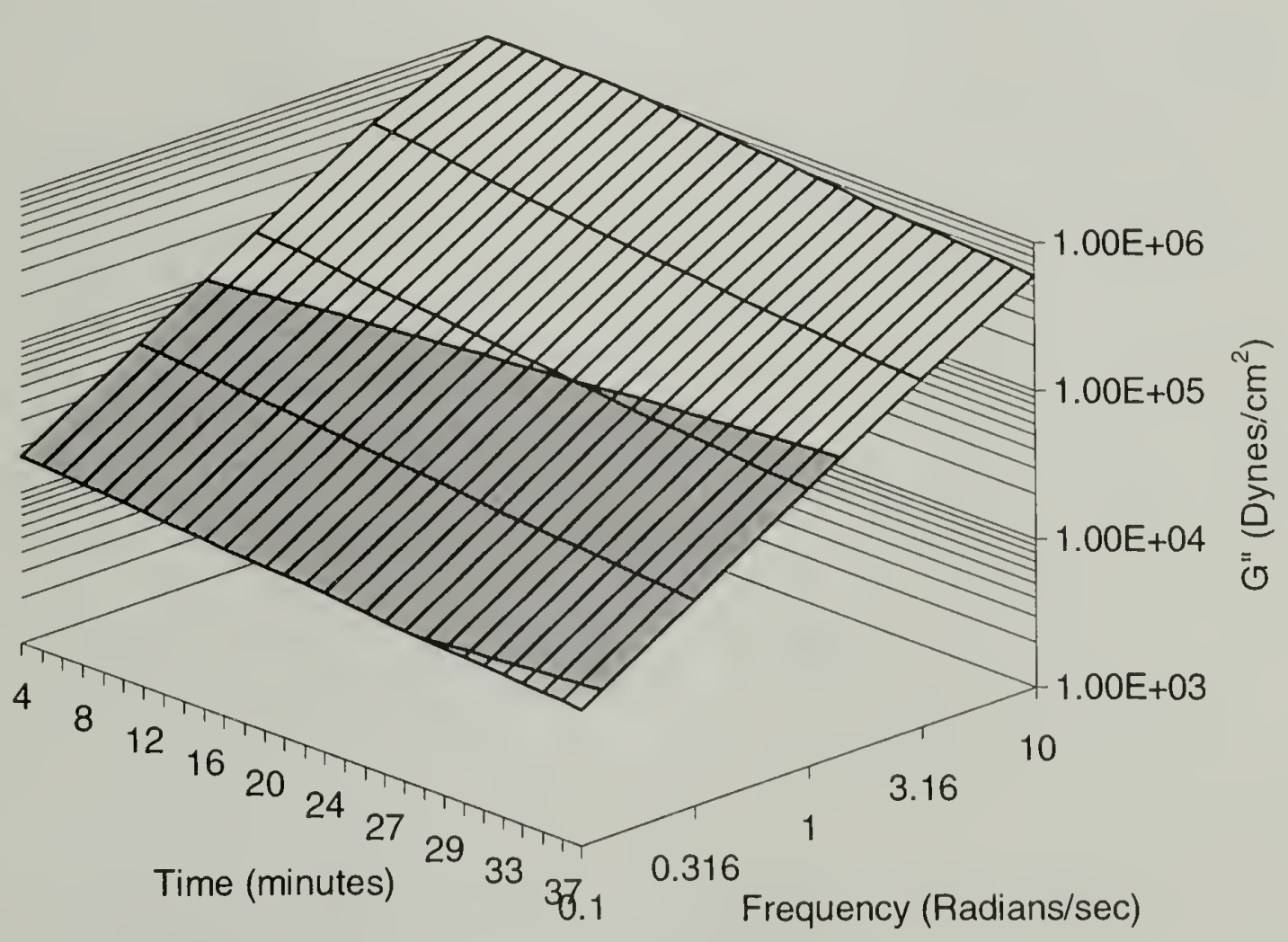


**Figure 6.53 Loss Modulus Contour for SMII-60 at 250° C.**

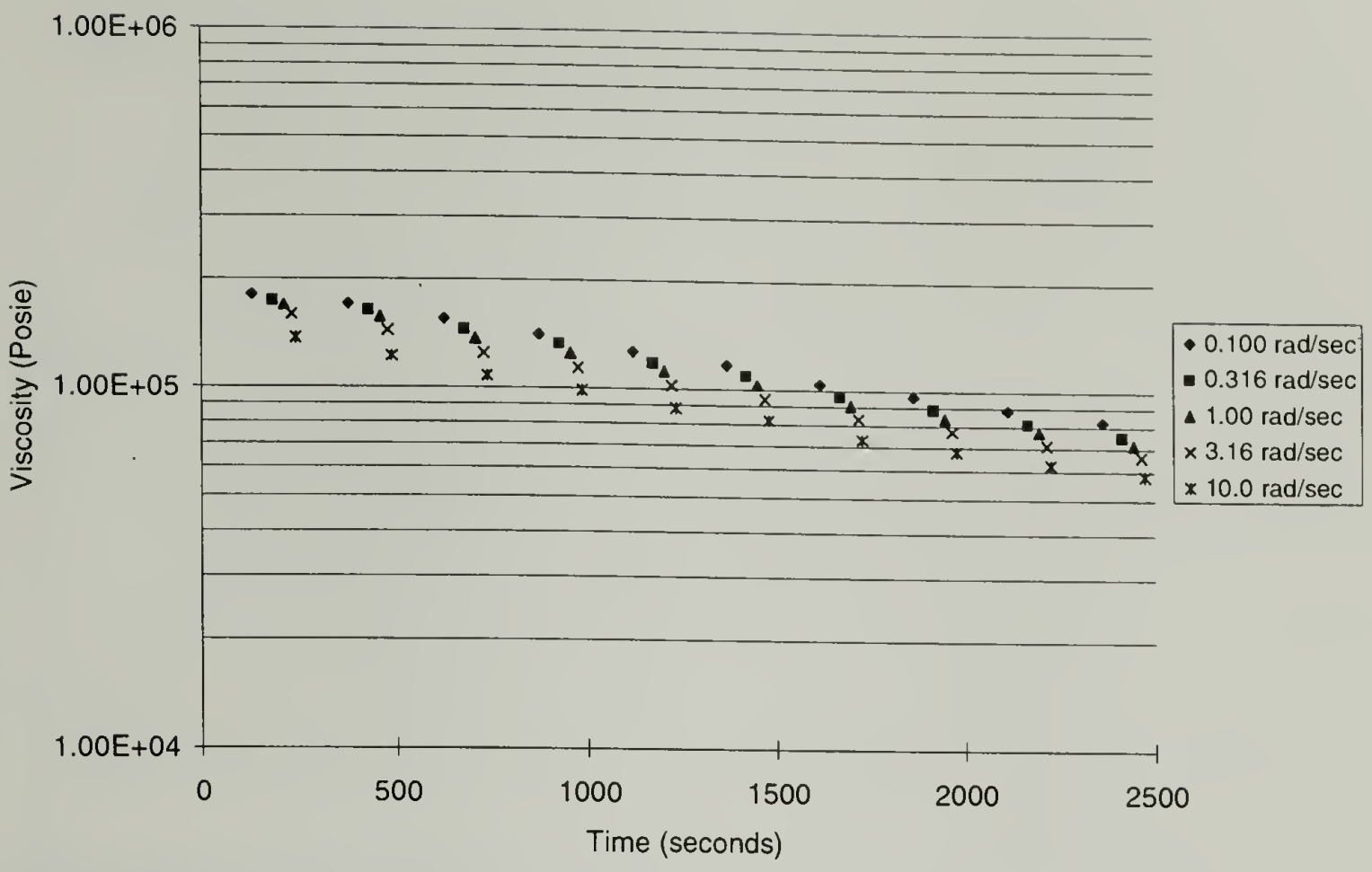


**Figure 6.54 Viscosity for SMII-60 at 250° C. Legend shows shear rates.**

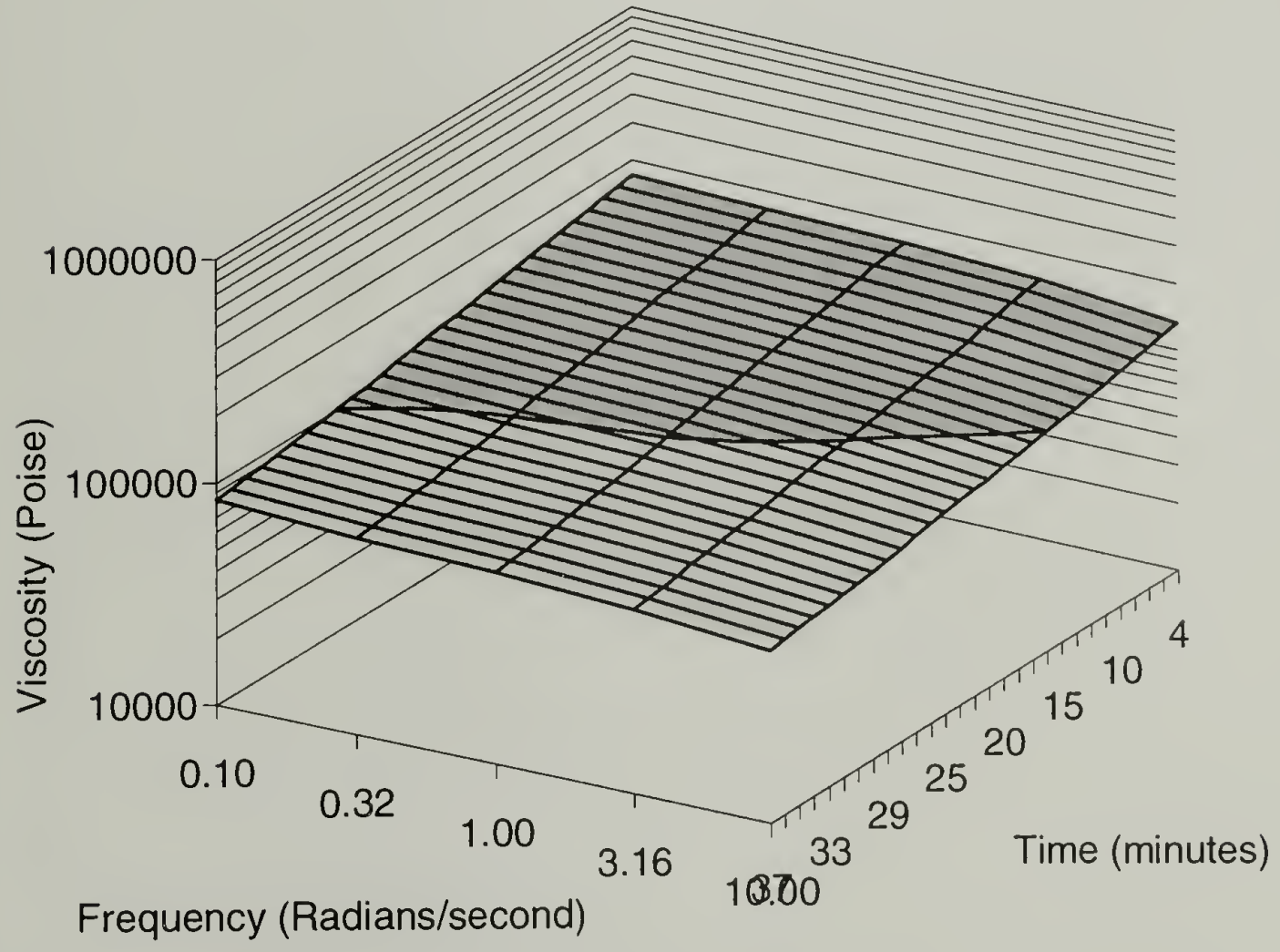


**Figure 6.55 Viscosity Contour for SMII-60 at 250° C.**

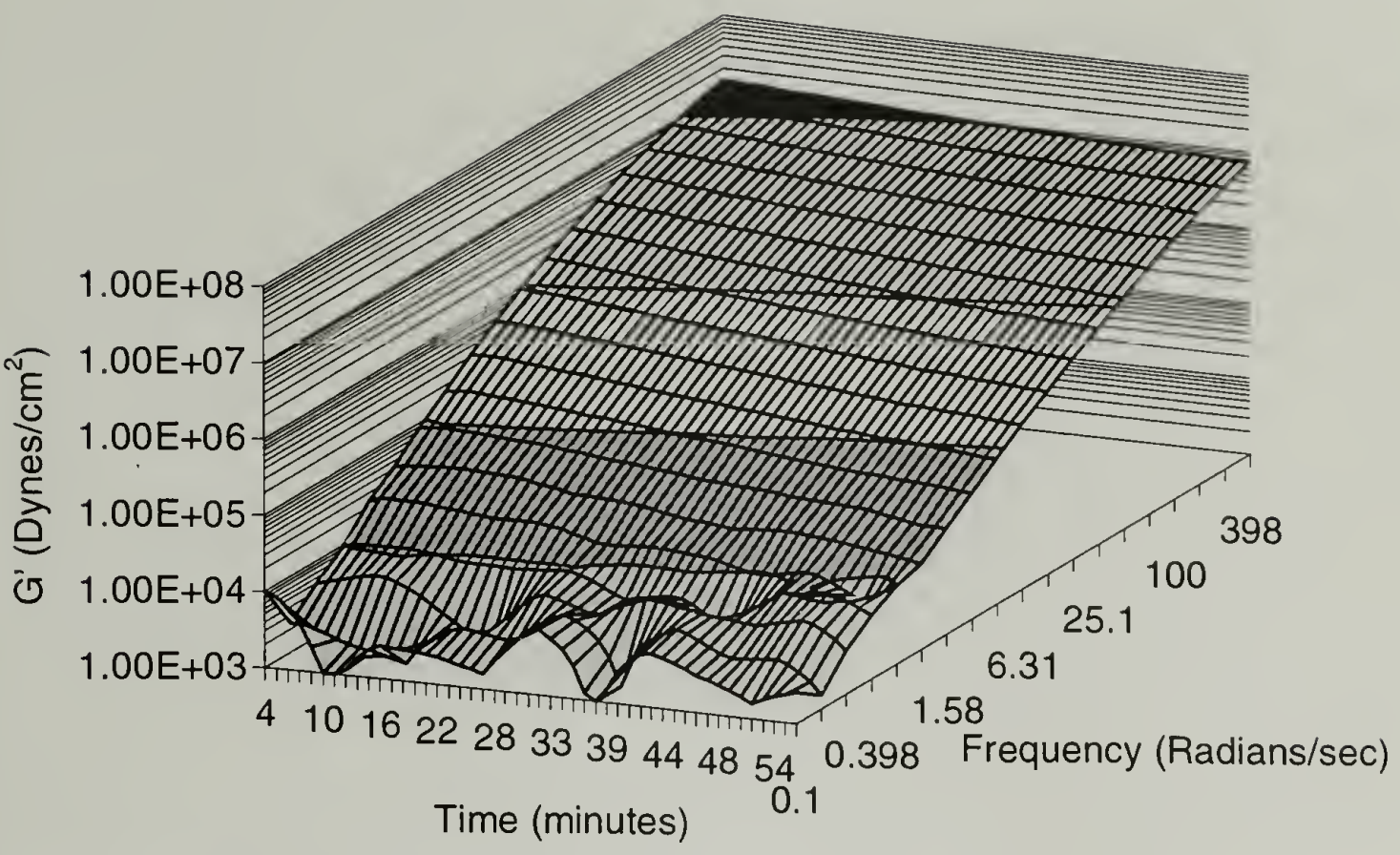


**Figure 6.56 Storage Modulus for SMIII-102 at 250° C.**

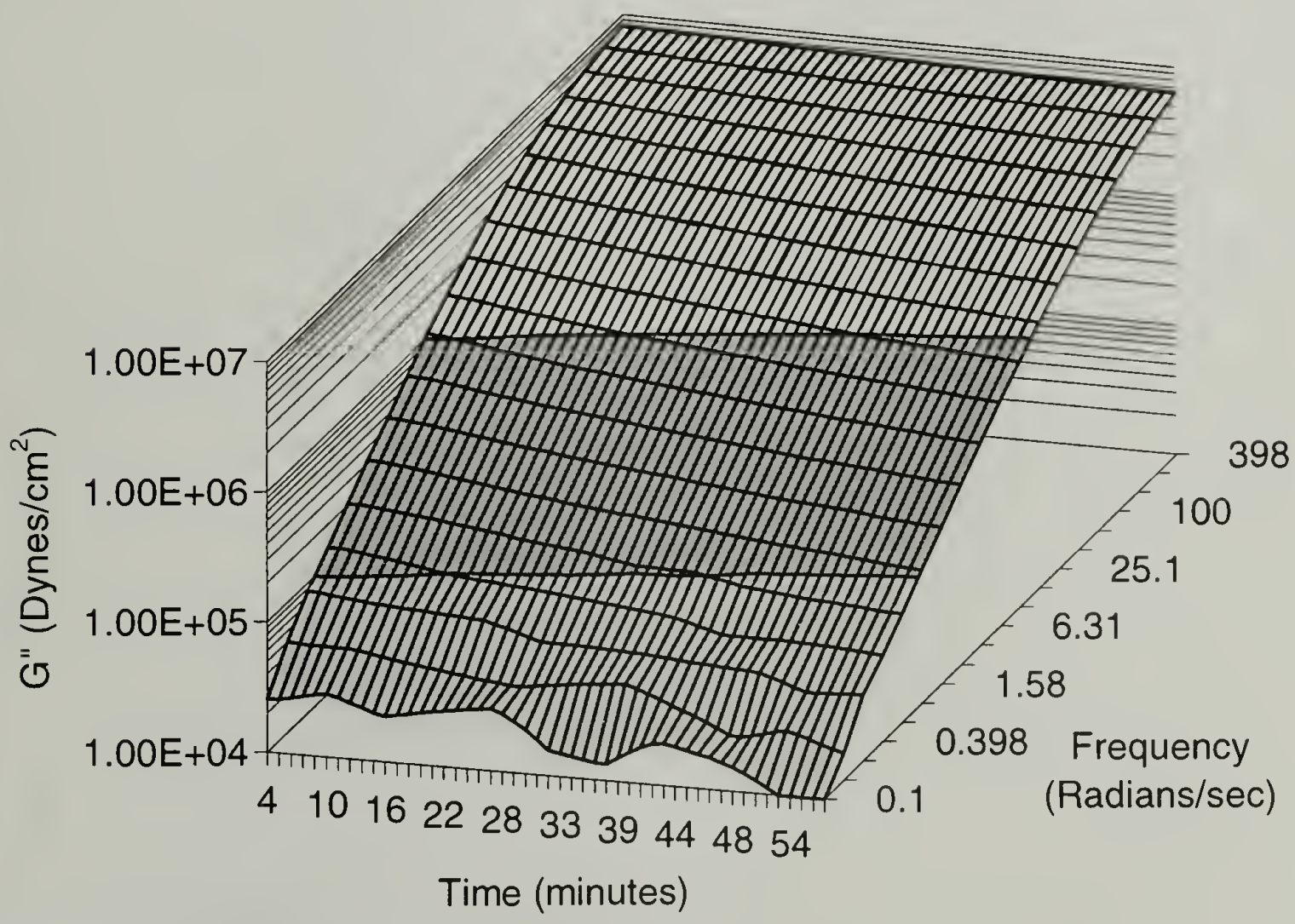


**Figure 6.57 Loss Modulus for SMIII-102 at 250° C.**

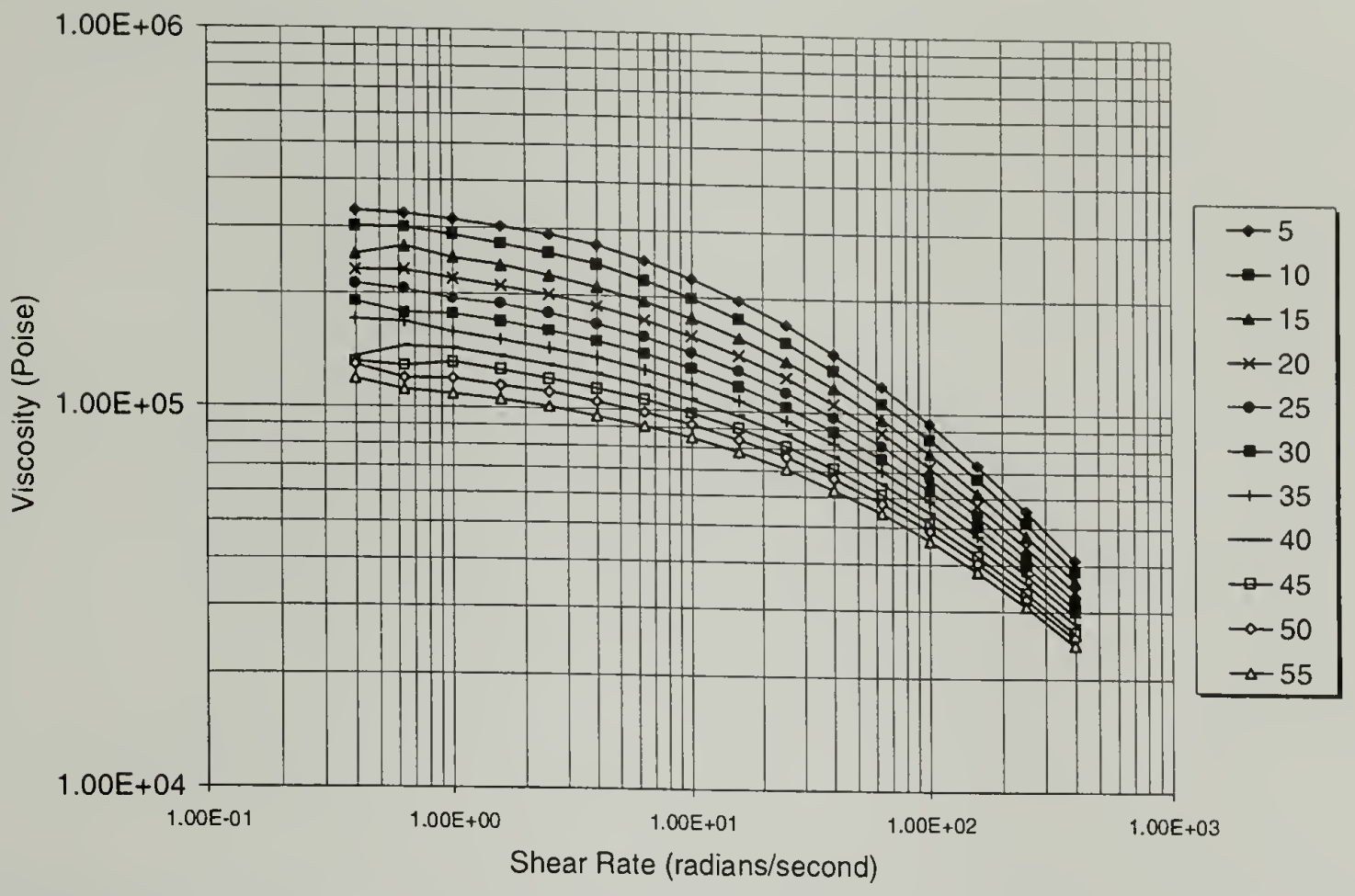


**Figure 6.58 Isochronus Viscosity Curves for SMIII-102 at 250° C. Legend gives times in the melt in minutes.**

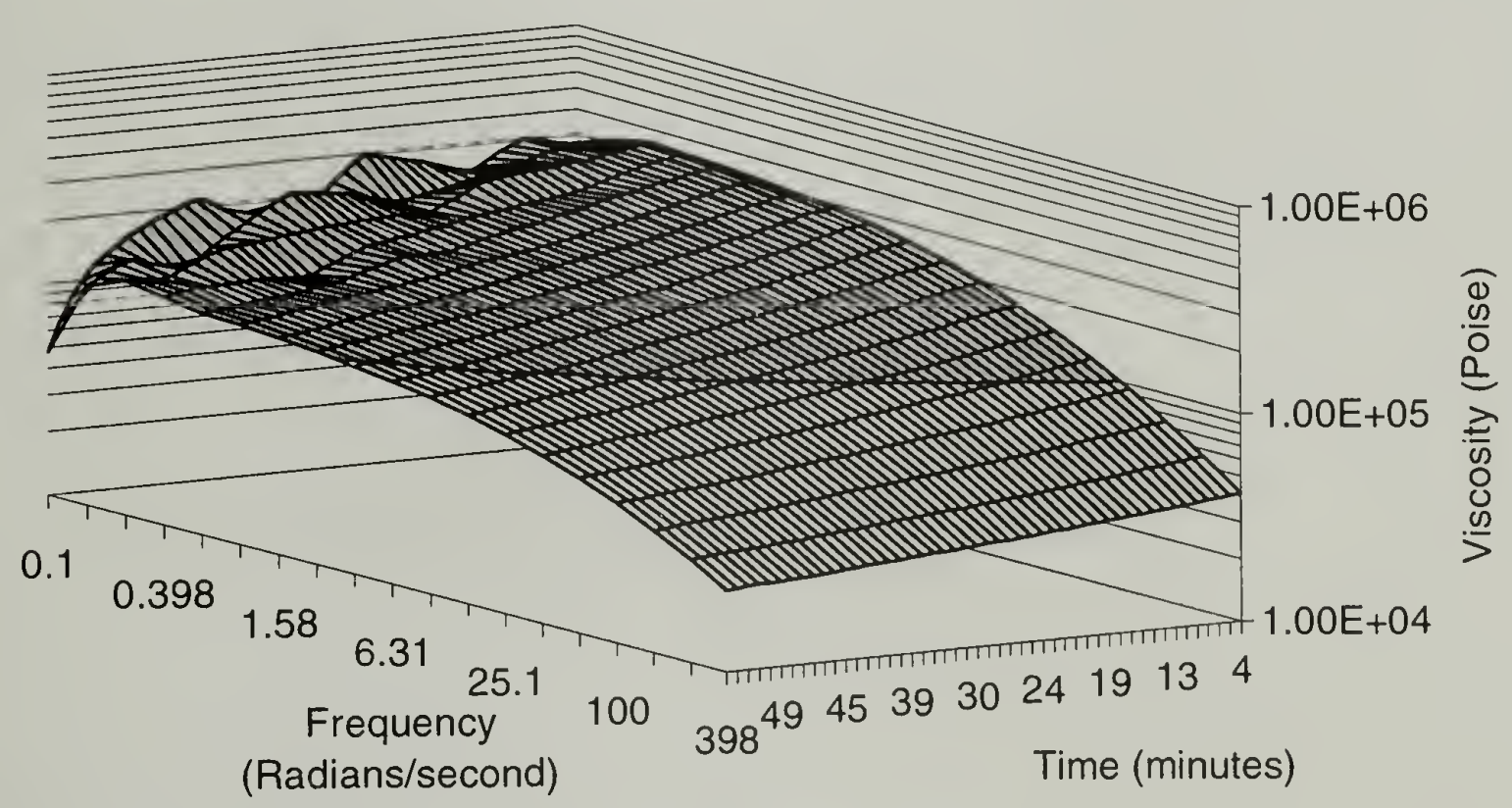


**Figure 6.59 Viscosity Contours for SMIII-102 at 250° C.**

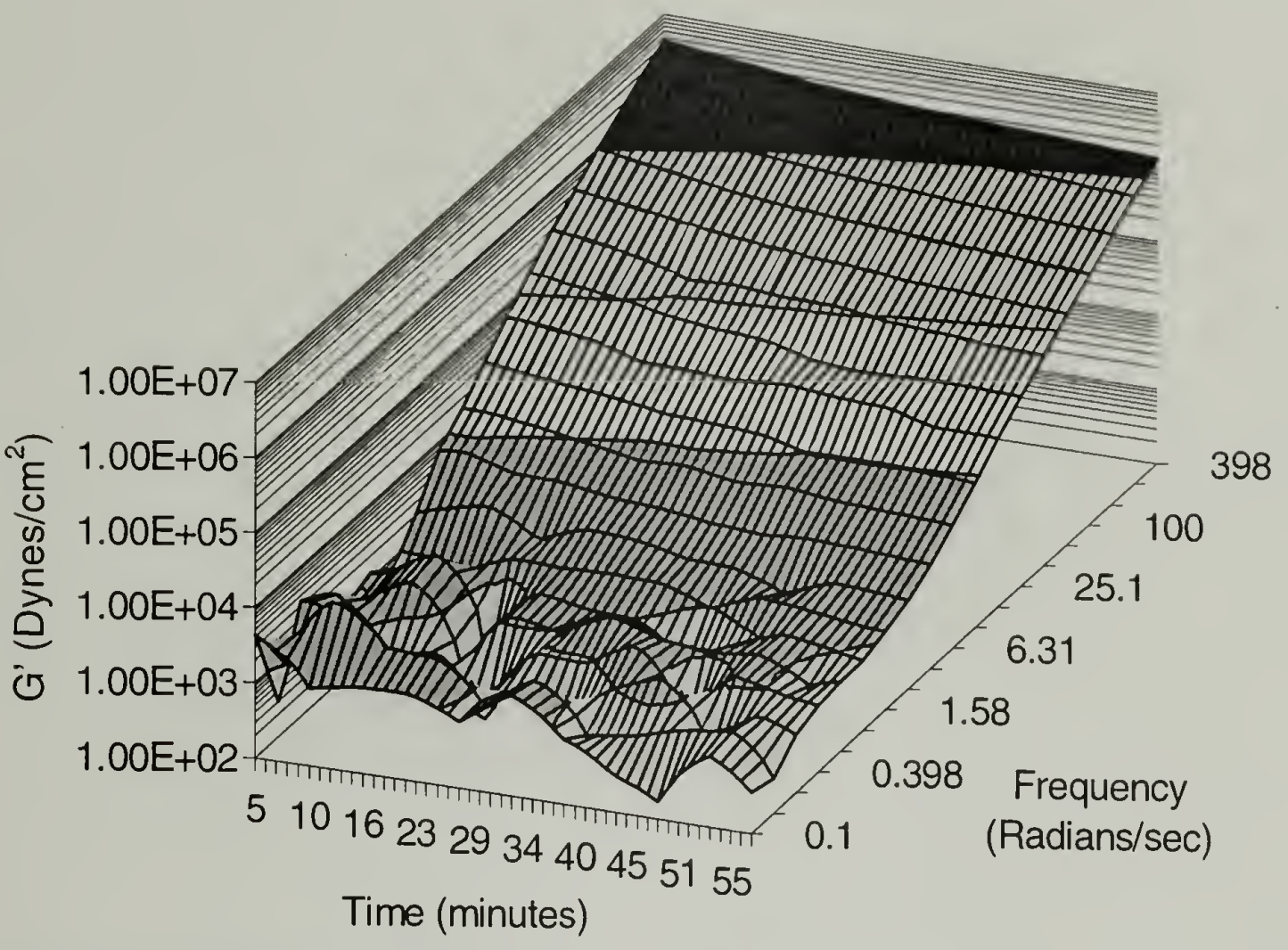


**Figure 6.60 Storage Modulus Contour for SMIII-75 at 250° C.**

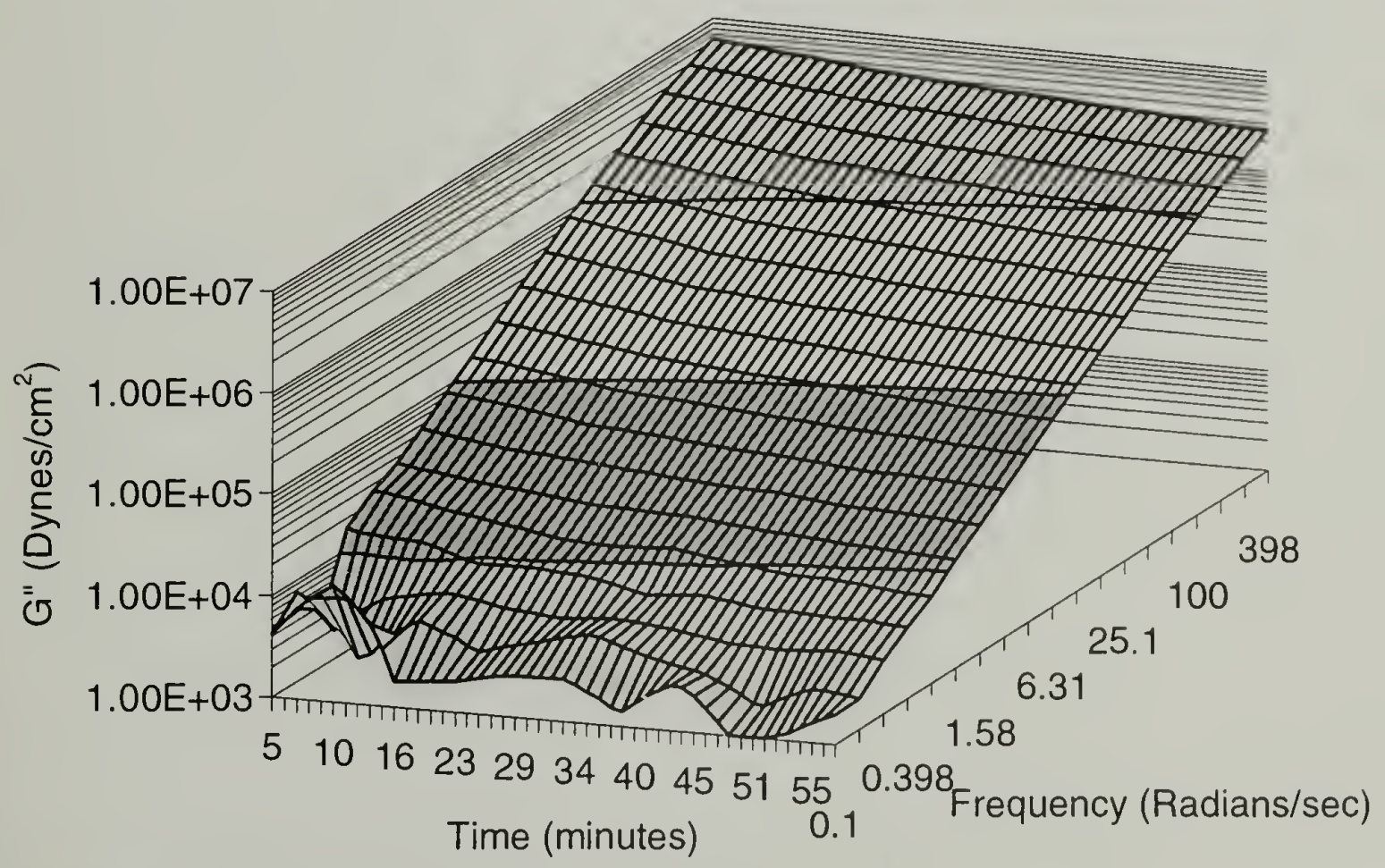


**Figure 6.61 Loss Modulus Contour for SMIII-75 at 250° C.**

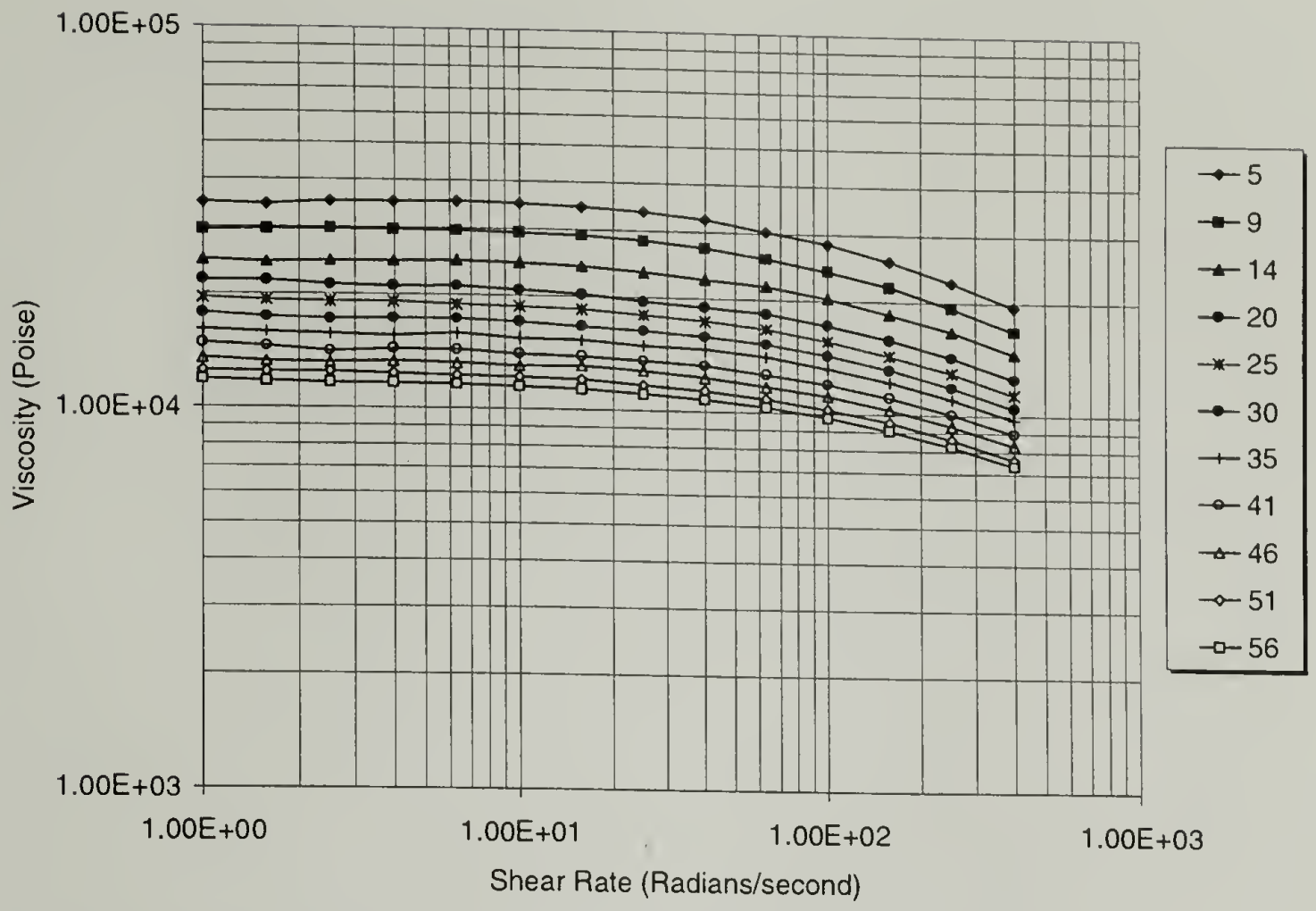


**Figure 6.62 Isochronus Viscosity curves for SMIII-75 at 250° C.**

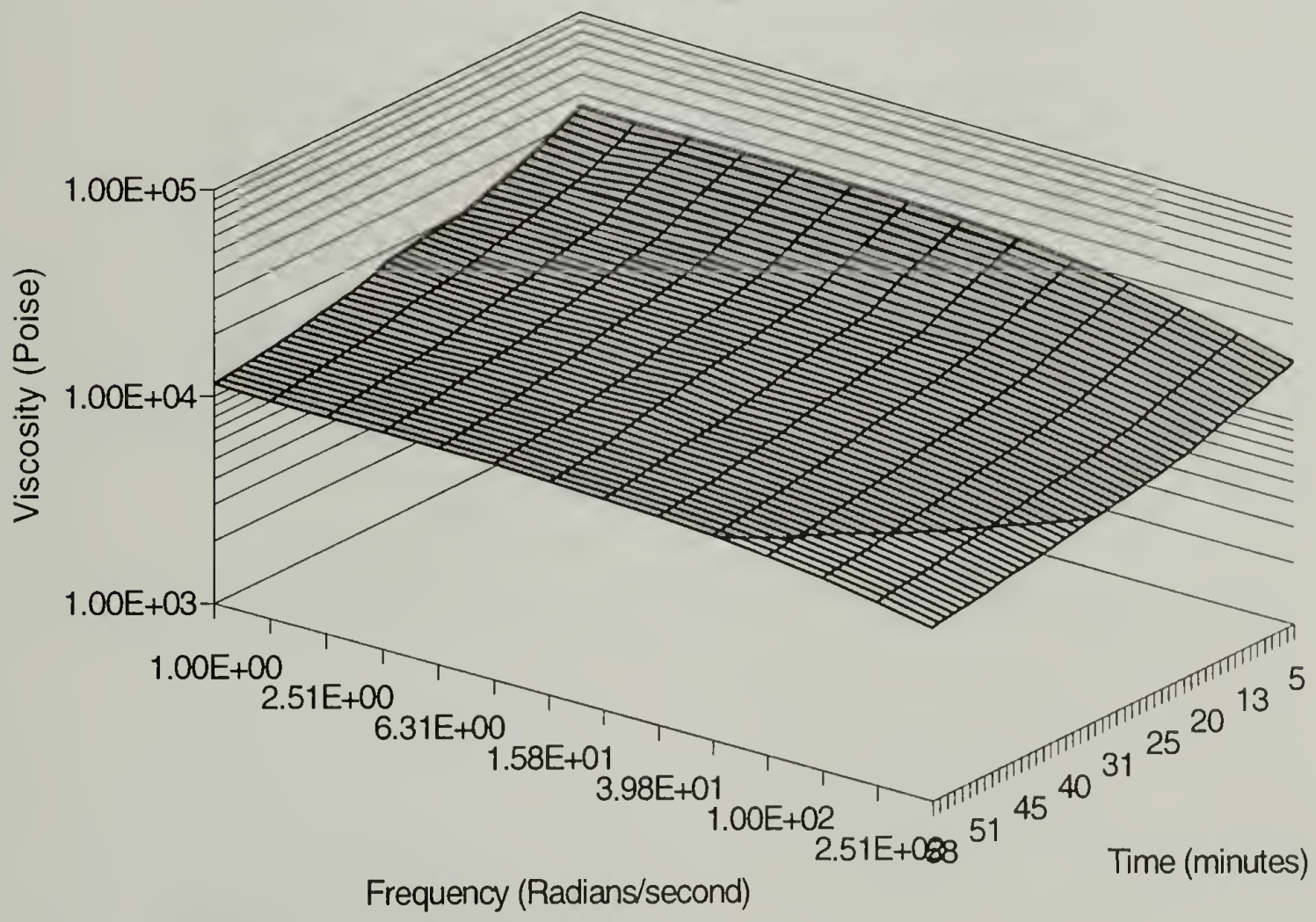


**Figure 6.63 Viscosity Contour for SMIII-75 at 250° C.**

The thermal stability for the three macrocyclic resins is compared in Figure 6.64. Here we find that the rate of viscosity loss is consistent, independent of molecular weight, indicating a slow decomposition of the polymer, related to the stability of the stannoxane initiator residue at this temperature[7]. (See also Section 5.1, Figures 5.4 and 5.5, for thermal stability of stannoxane).

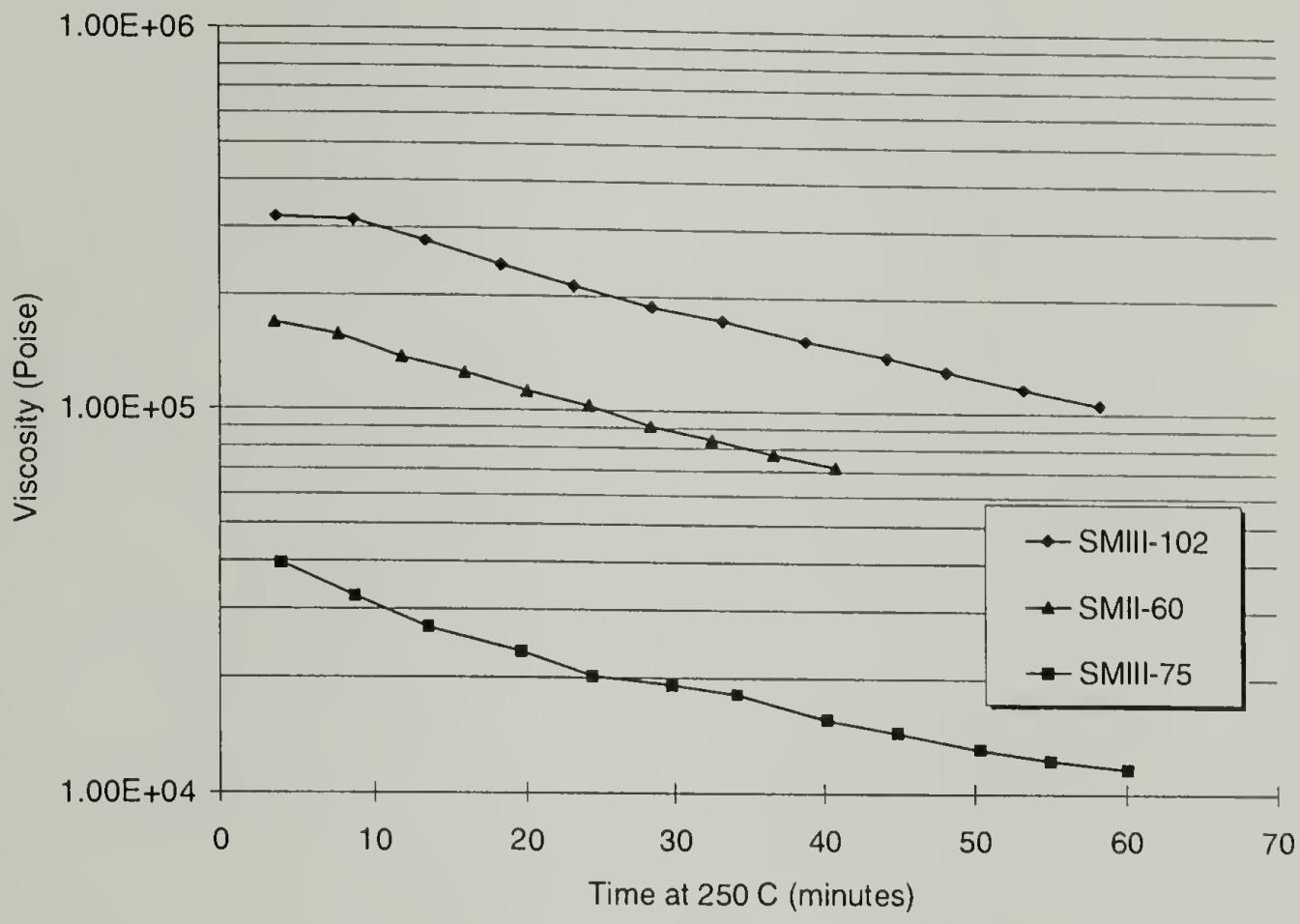


**Figure 6.64 Time dependence of the viscosity at 250° C for three c-PBT resins. Shear rate = 1 radian/sec. SMII-60 and SMIII-102 are polymerized using 0.12 mol % stannoxane, SMIII-75 is polymerized using 0.3 mol % stannoxane.**

The difference in viscosity for the two preparations having 0.12 mol % stannoxane (SMII-60 and SMIII-102) was initially thought to be due solely to the differences in the preparation of the specimens or due in part to a temperature effect. However, the temperatures recorded from a thermocouple placed in contact with the lower platen during the test shows that the later data (SMIII-102) were collected at 250.2° C, while the earlier data (SMII-60) were collected at 251.4° C.

The difference in viscosity is more than can be accounted for by this temperature difference alone. The time dependence of the melt viscosity at 1 radian/second at each of three temperatures is shown in Figure 6.65. The viscosity at zero time is determined at each temperature by extrapolation back to zero time. These "zero-time" viscosities are plotted vs. temperature in Figure 6.66. This graph allows an estimate of the temperature sensitivity of viscosity to be made. The 1.2° C difference in temperature between SMII-60 and SMII-102 from Figure 6.64 can only account for a shift of 3.3% in viscosity.

The much larger discrepancy is thought to be related to the molecular weight developed on polymerization. While both resins were polymerized in a nitrogen environment using a laboratory oven, the resin with the higher $M_w$ was polymerized at a lower temperature. The actual temperature of the first polymerization, resulting in a lower $M_w$, was only monitored using a surface thermocouple on the oven floor, while the second polymerization was monitored using a contact thermocouple on the specimen. The actual temperature difference between the two polymerizations is not known, but may have been as much as 20° C. Differences in polymerization temperature are known to result in different molecular weights as will be shown the following section on low temperature rheology (see Table 6.5 on page 155).

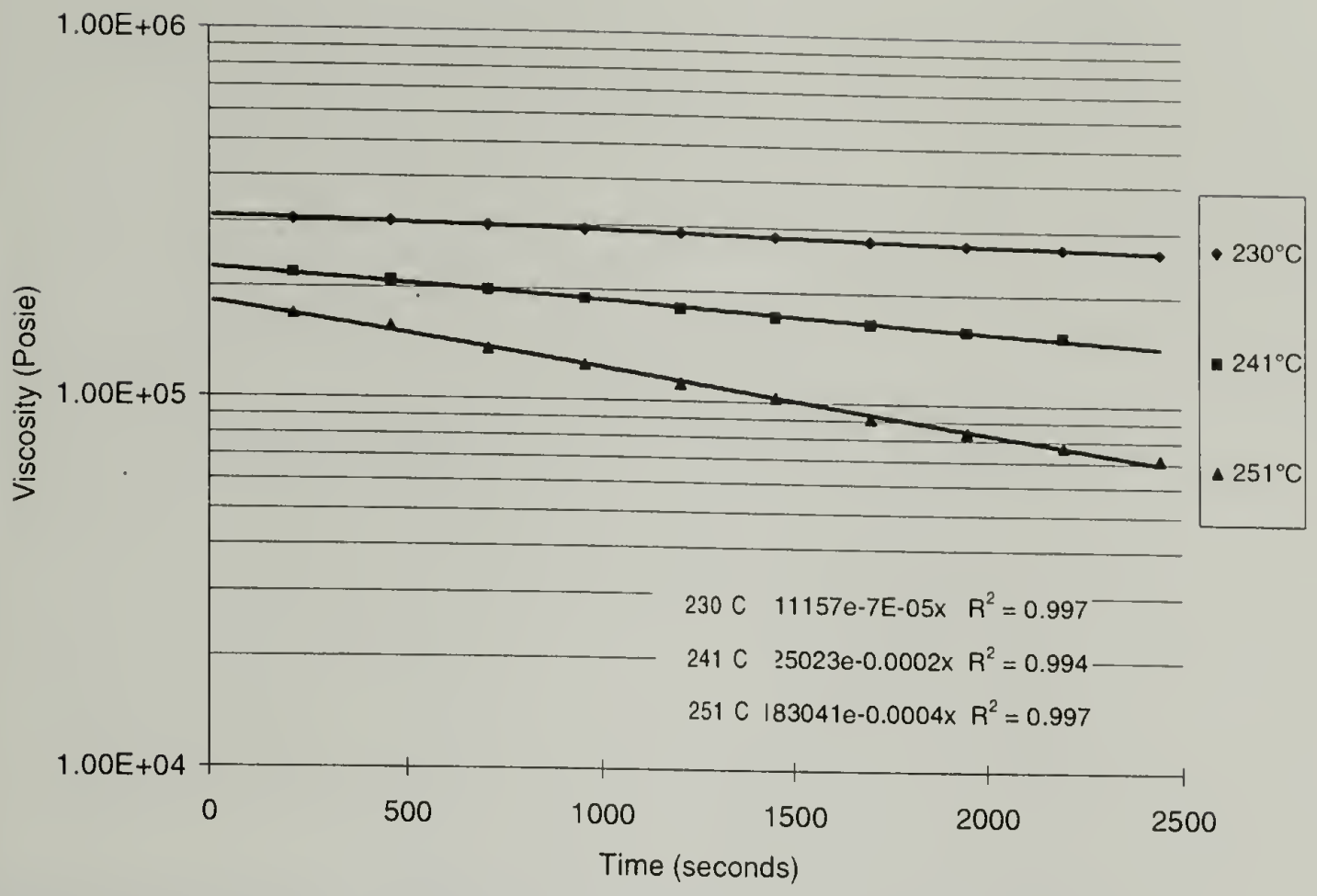


**Figure 6.65 Thermal Stability of SMII-60 at three temperatures.**

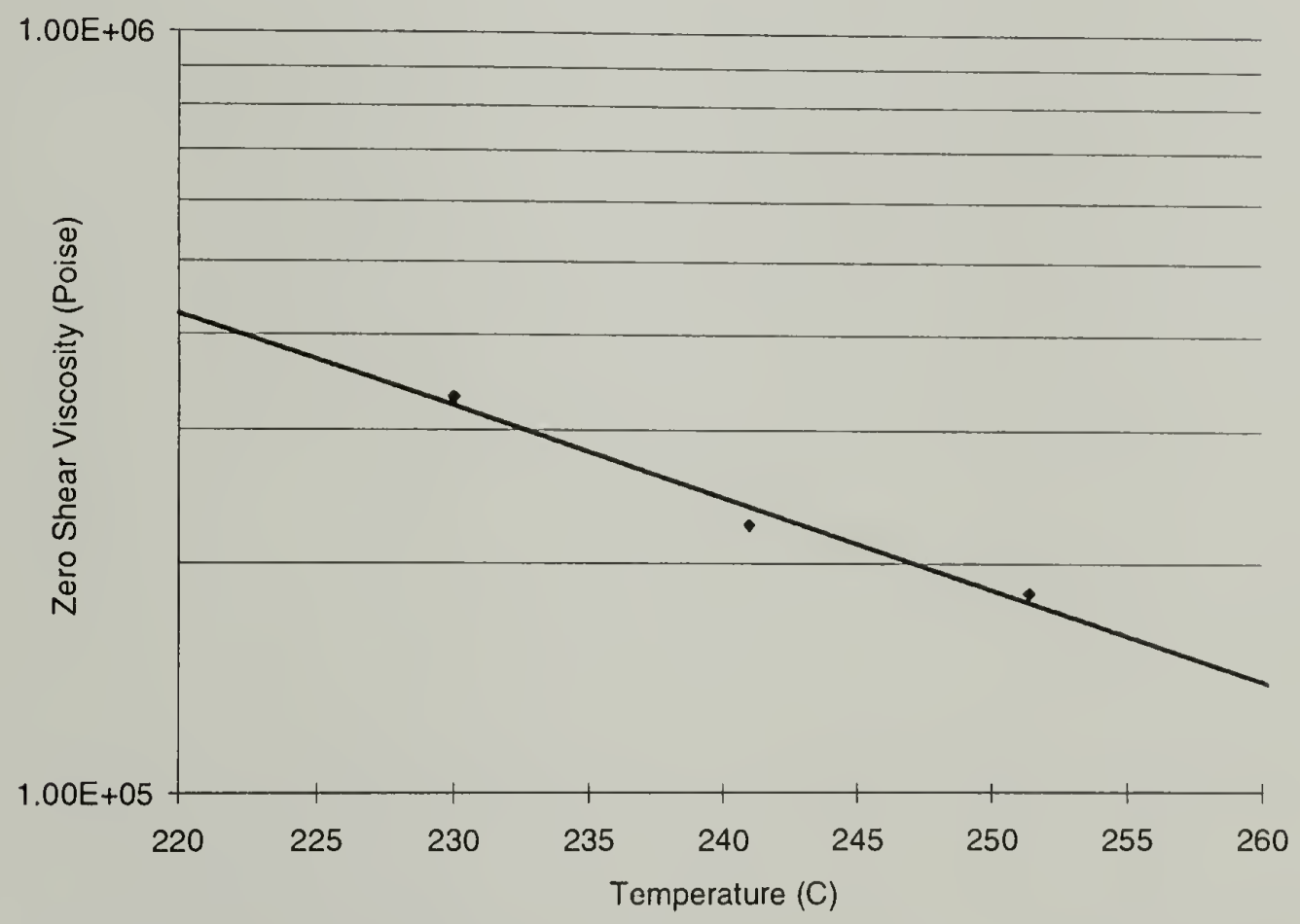


**Figure 6.66 Temperature sensitivity of the zero shear rate viscosity of SMII-60 extrapolated to zero time. Line represents an exponential fit of the data with the equation: $y = 2E+08e^{-0.0278x}$ , $R^2 = 0.9755$**

Molecular weights were determined for each of the specimens following the rheology measurements. Figure 6.67 shows the consistent loss of molecular weight after similar exposure times at increasing temperatures for SMII-60.

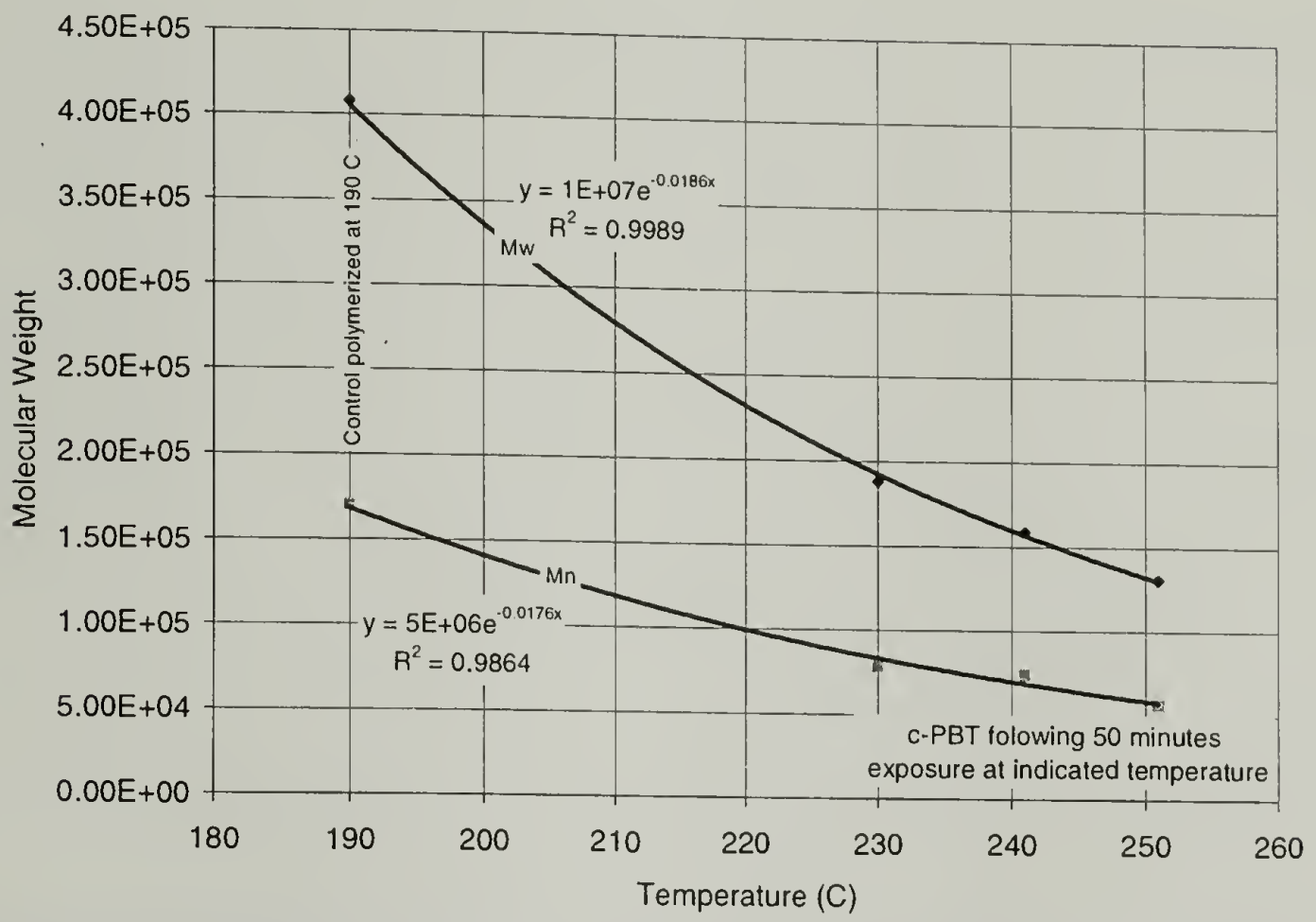


**Figure 6.67 Exponential dependence of the "corrected" molecular weight of SMII-60 and $M_w$ after 50 minutes of heat soaking at the indicated temperatures. (see Section 6.4.1)**

The drop in molecular weight from 400,000 to 130,000 following 50 minutes of heat soaking at 250° C implies that an average macro-ring of SMII-60 contained 3 to 4 stannoxane residues which split open to yield 3 or 4 separate linear chains. (At higher temperatures all PBT chains are thermally unstable, and further molecular weight loss with increased exposure temperature will result from conventional degradation within the PBT chain.)

Crystallinities of the SMII-60 rheology specimens following thermal exposure is shown in Figure 6.68. The heat of fusion of the control is seen to have decreased from

that of the nascent polymer to a value typical of high molecular weight linear PBT after 50 minutes exposure at 230° and 240° C. The low value of heat of fusion for the 250° C exposure is not understood. This may be the result of rapid cooling on opening the platens and removing the specimen from the rheometer. The specimen collected after the 250° C testing was very "stringy" when the rheometer platens were separated. A high cooling rate could effectively "quench" some of the crystallization which would have developed on slower cooling. Specimens from 240° and 250° C exposure exhibited a sharp, single melting endotherm with a peaks at 222.6° and 222.8° C, typical of the usual spherulitic structures found in injection molded linear PBTs. The specimen recovered from exposure at 230° C showed a major peak at 221.3° C, with a predominant shoulder just above 225° C, more typical of the changing crystalline structure (unusual to usual type spherulite structure) as described in Section 6.2.1.

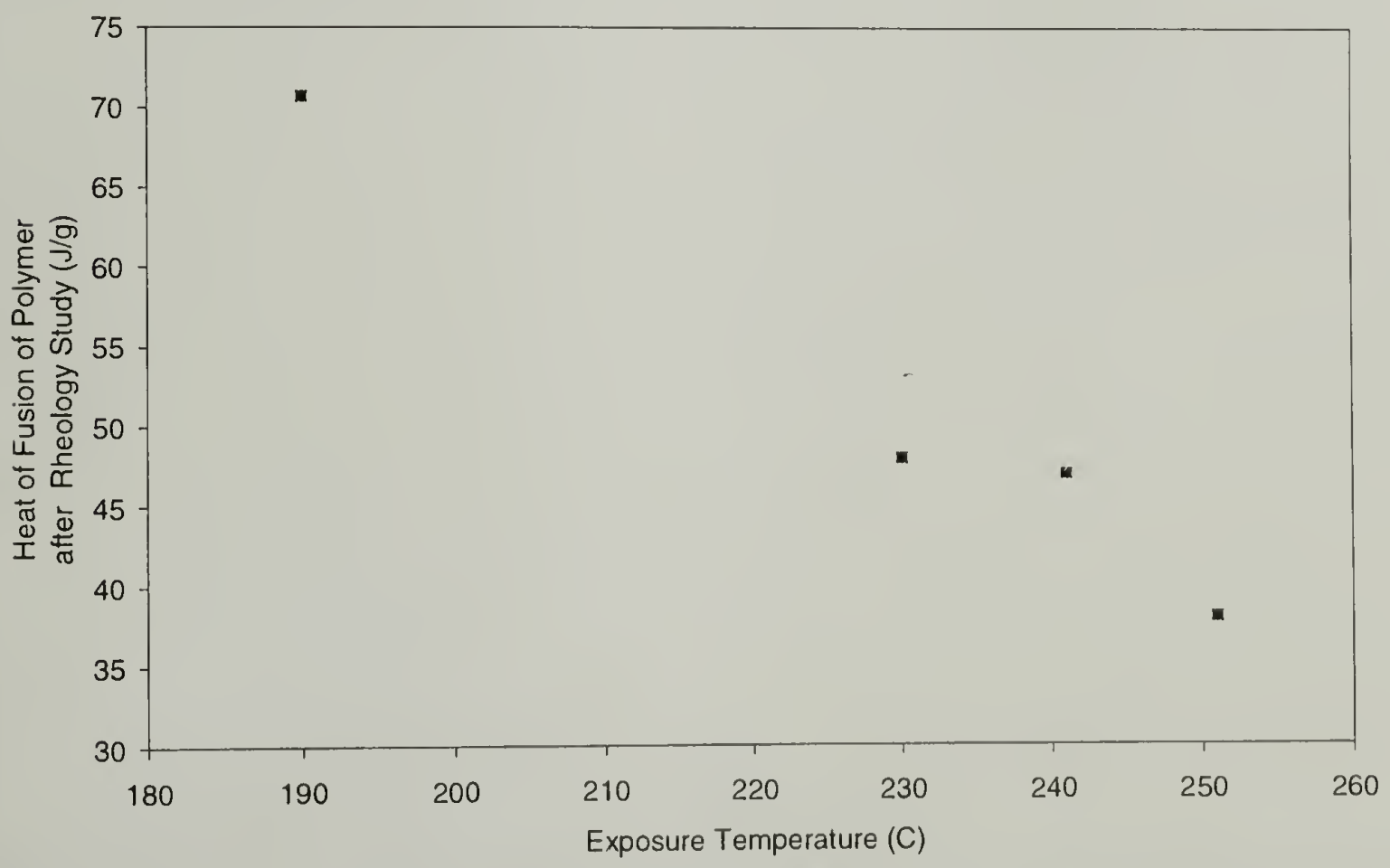


**Figure 6.68 Heat of Fusion of SMII-60 following 50 minutes thermal exposure at the temperatures indicated. Control was polymerized and crystallized at 190° C.**

### 6.3.1.5 Comparison of Macro-cyclic and Linear PBT Resins

When compared to the linear resins, the macro-cyclic resins are not as thermally stable; this is illustrated in Figure 6.69. The c-PBT resins are seen to have a greater negative slope, indicating a faster rate of degradation for these resins. This is expected since the stannoxane link in the macro-cyclic polymer is expected to be rapidly degrading at 250° C. The nearly linear loss of viscosity is surprising. This indicates that either 1) the stannoxane is degrading more slowly than expected, or 2) there is a continuing re-equilibration reaction in the melt, as the macrocyclics open to linear chains having residual reactive end groups which may continue to react into other chains, broadening the molecular weigh distribution, while also lowering the overall molecular weight of the polymer.

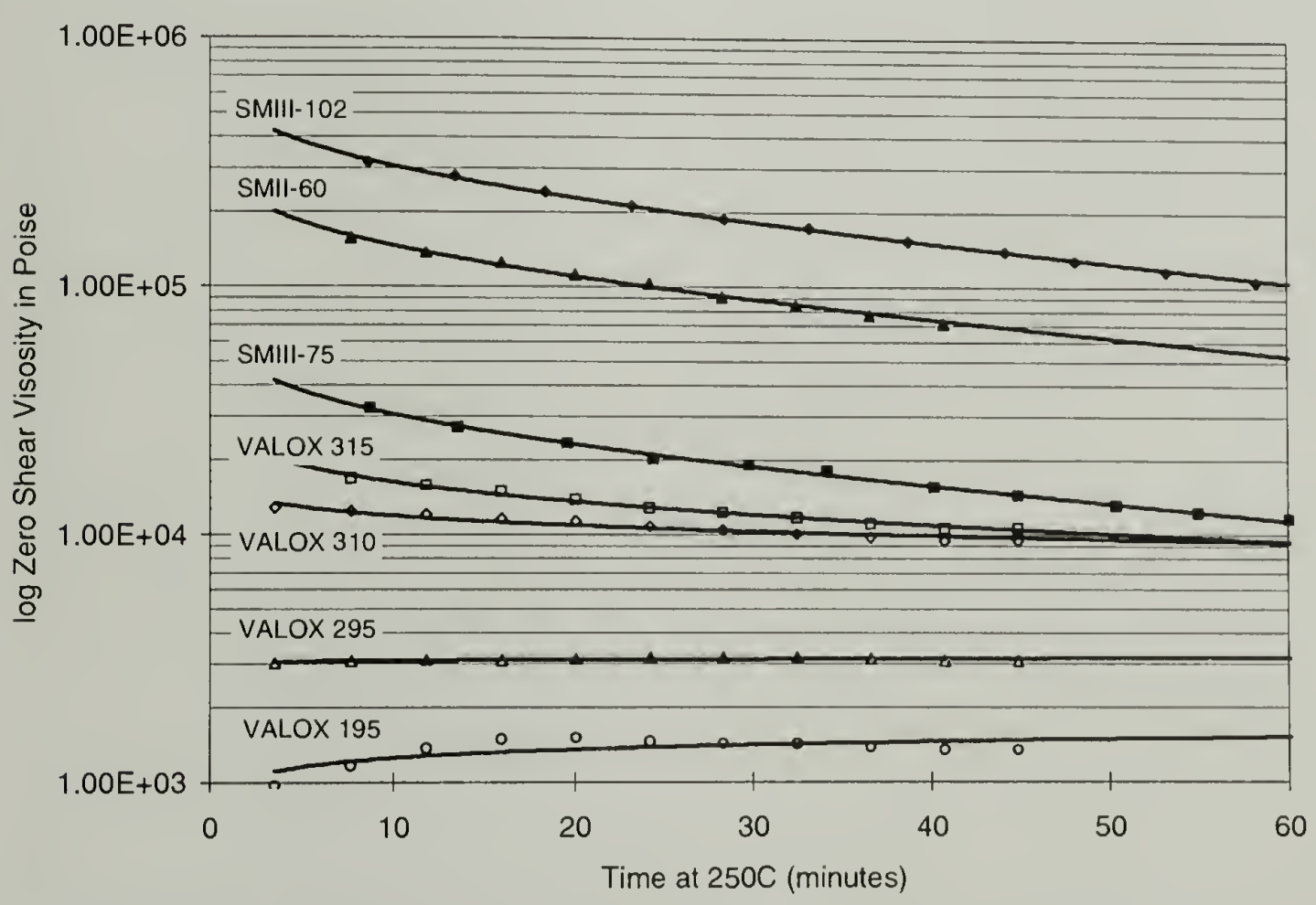


**Figure 6.69 Thermal Stability of conventional and cyclics-based PBT resins at 250° C. Lines shown represent best logarithmic fits through collected data points. Linear resins data is the same as shown in Figure 6.49 but with the addition of best fit log curves.**

The lines in Figure 6.69 were determined by fitting logarithmic curves. These curves are represented by the equations in Table 6.4. The coefficients in these equations represent the rate of degradation for the resins. The intercepts are representation of the zero shear viscosity. These data fits are used to calculate both the zero shear viscosity and the viscosity after each resin's appropriate degradation time at 250° C during the rheology studies. The zero shear viscosity data from VALOX 195 PBT is not included in the presentation charts which follow. Its behavior at short thermal exposure times is atypical of the other resins, resulting from a known reason, proprietary to GE Plastics,.

**Table 6.4 Logarithmic best fit curves for data points in Figure 6.69**

| | |
|---|---|
| SMIII-102 | y = - 111,800 ln(x) + 562,400 |
| SMII-60 | y = - 51,900 ln(x) + 265,500 |
| SMIII-75 | y = - 10,700 ln(x) + 55,300 |
| VALOX 315 PBT | y = - 3880 ln(x) + 25,200 |
| VALOX 210 PBT | y = - 1460 ln(x) + 15,300 |
| VALOX 295 PBT | y = + 36.5 ln(x) + 3000 |
| VALOX 195 PBT | y = + 144 ln(x) + 924 |

### 6.3.1.6 Correlation of Melt Viscosity and Molecular Weight

The most important structural variable in the determination of a polymer's flow characteristics is its molecular weight. Flory[8] first suggested that the log viscosity of a polymer would be proportional to the square root of the number of atoms in the polymer chain. Later studies by Fox[9] refined this relationship. Fox studied a range of polymer structures and determined that linear polymers have a more complex relationship between viscosity and molecular weight than simple molecules. He demonstrated the existence of a break in the molecular weight dependence on viscosity at an average chain length of about

600 atoms. Working at low shear rates, where the melts exhibited Newtonian behavior, he demonstrated that below a critical chain length the viscosity was nearly proportional to length, while above this length secondary forces dramatically increased the viscosity of the melt as the molecular weight increased. His measurements of a series of polymers showed that many linear polymers follow the relationship

$$\log(\eta) = 3.4\log(\overline{Z}_w) + k$$

above the critical molecular weight, where $Z_w$ is the weight average chain length and $k$ is a temperature dependent constant. Below the critical molecular weight, Fox determined that $\eta \sim Z_w^{1.75\text{-}2.0}$ while above critical molecular weight $\eta \sim Z_w^{3.4}$. This has since been confirmed in studies of a wide variety of polymers. It is of interest to see if this relationship holds true for macrocyclic resins prepared through ring expansion polymerization.

The data in Table 6.4 was used to calculate the zero shear viscosity for each resin at zero time. A plot of log (zero shear viscosity) vs. log (weight average molecular weight) for the linear resins is shown in Figure 6.70. Solid points in this plot represent the resins prior to testing while open points represent the resins after thermal exposure. The three high molecular weight linear resins all fall on a line having the predicted slope of 3.4. After degradation, the three high molecular weight resins show a reduced molecular weight and reduced viscosity, while still falling near the line of slope 3.4. Deviation from the theoretical prediction may be due to a broadening of the MWD during degradation. The dotted line is drawn to have a slope of 1.0 and placed in the chart such that it intersects the data point represented by degraded VALOX 195. The intercept of these

two lines gives an estimation of the entanglement molecular weight for PBT as about 55,000 Daltons. This critical molecular weight for entanglement is high for linear polymers, and falls just above the range of reported values for linear resins

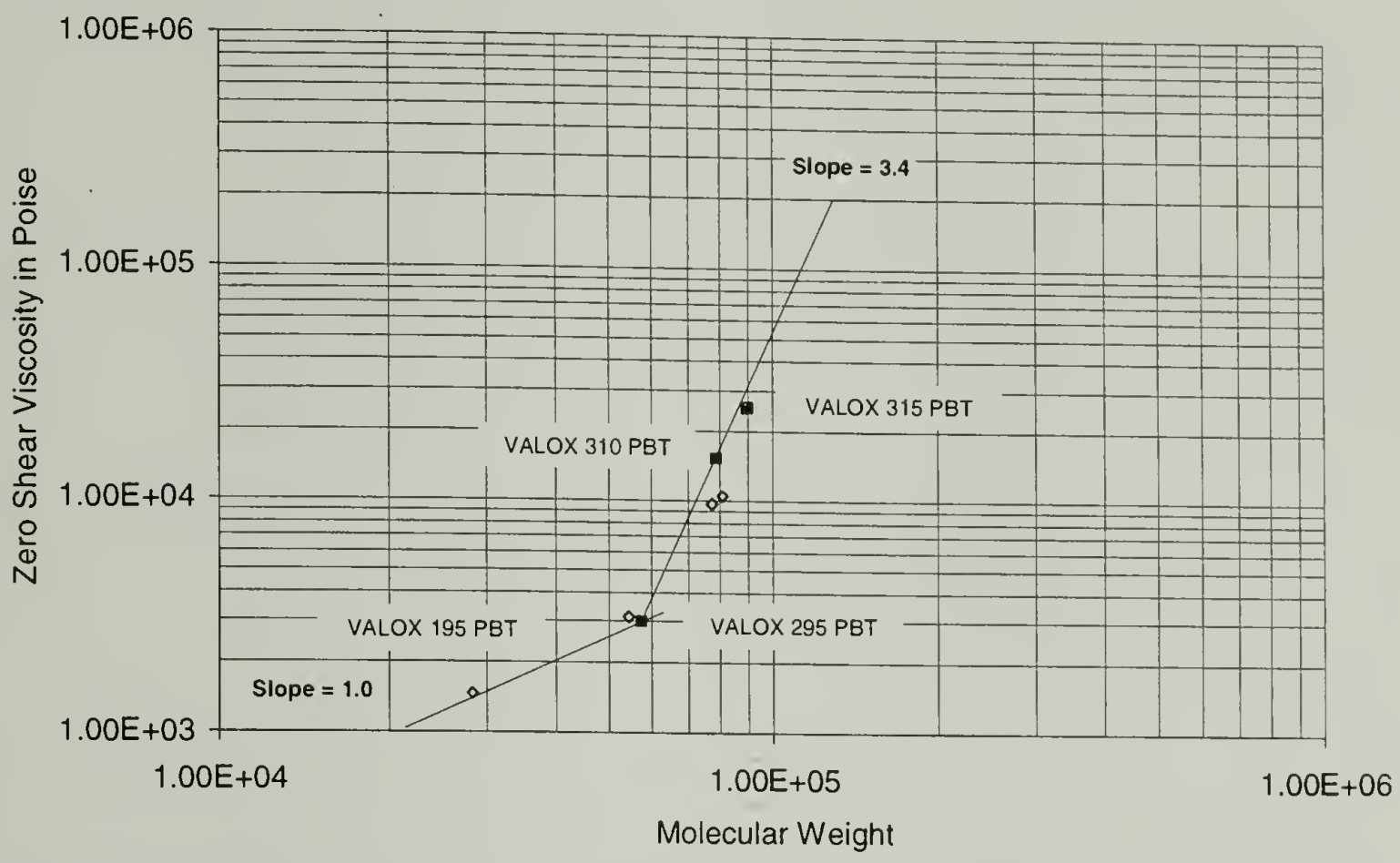


**Figure 6.70 Zero Shear Viscosity vs. Apparent Weight Average Molecular Weight for PBT resins at 250° C. Solid points are before degradation. Open points are after degradation. Molecular weight determined from GPC using PS standards.**

Figure 6.71 compares comparable data from c-PBTs with the data from the above plot. Prior to melt degradation the cyclic resins are seen to fall to the right of the predicted relationship. This suggests that the melt consisting of macrocyclic molecules has an inherently lower entanglement density and, under low shear rate deformation, the cyclic molecules are more easily disengaged in the melt than corresponding linear molecules (i.e. ones of equal molecular weight).

Another way of understanding the reduced melt viscosity of cyclic molecules is that the compactness of the individual molecules reduces long range stress transfer through the melt. An applied stress is transferred within a macrocyclic molecule but the

stress transfer between macrocyclic molecules is much reduced, in favor of intermolecular slip, resulting in a reduced viscosity of the bulk melt.

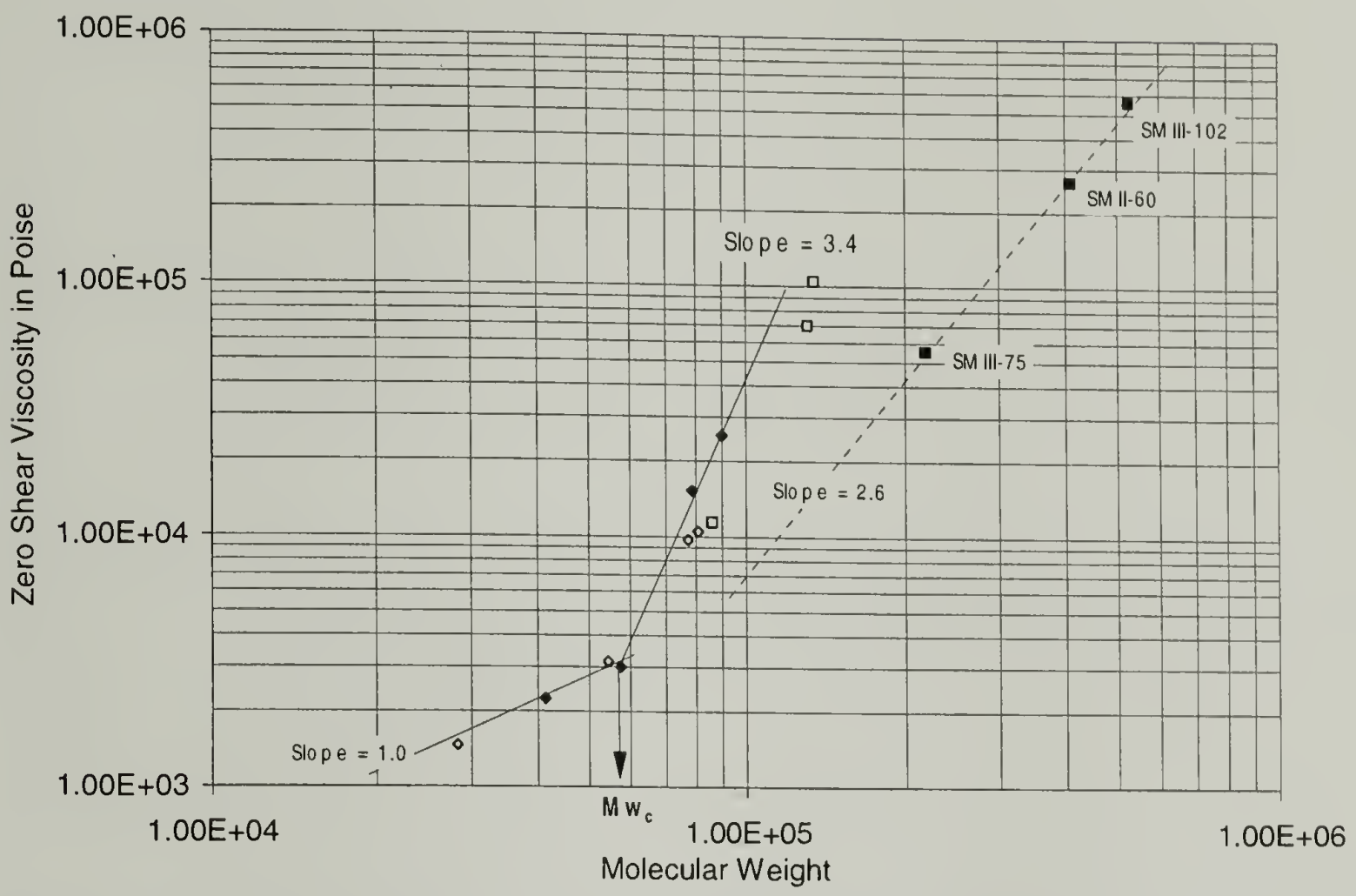


**Figure 6.71 Zero Shear Viscosity vs. Apparent Molecular Weight for both linear and macrocyclic PBT resins at 250° C. Solid points are prior to degradation. Open points are after degradation. Diamonds represent linear PBTs. Squares represent c-PBTs. Molecular weights were determined from gel permeation chromatography using PS standards. For linear resins, $Mw_c$ = 55,000 Daltons.**

The present finding on the reduction in melt viscosity for cyclic polymer chains relative to linear polymer chains confirms the findings of both Roovers[4] and McKenna[10] on the melt viscosities of cyclic and linear polystyrenes. It also suggests that the butane terephthalate cyclics produced by ring expansion constitute a purer cyclic system than do cyclics prepared by dilute solution ring closure reactions. Polystyrene cyclic molecules have been produced using bifunctional living precursors with an appropriate coupling agent at very low concentrations in solvents[4,10-12]. In the latest of these studies, McKenna

has calculated a shift factor that relates the cyclic polystyrene melt viscosity to that of the comparable linear polystyrene viscosity as

$$log\ \eta_{o,\ linear} - log\ \eta_{o,\ cyclic} = 0.11\ to\ 0.16$$

for molecular weights above the critical molecular weight for entanglement, the variation being dependent on temperature. Figure 6.72 includes a dashed line indicating how much the linear PBT data would be shifted upon conversion to equivalent macrocyclic PBT using McKenna's shift factor. This shift would be correct if the shift were only the result of a topology difference in the polymer chains.

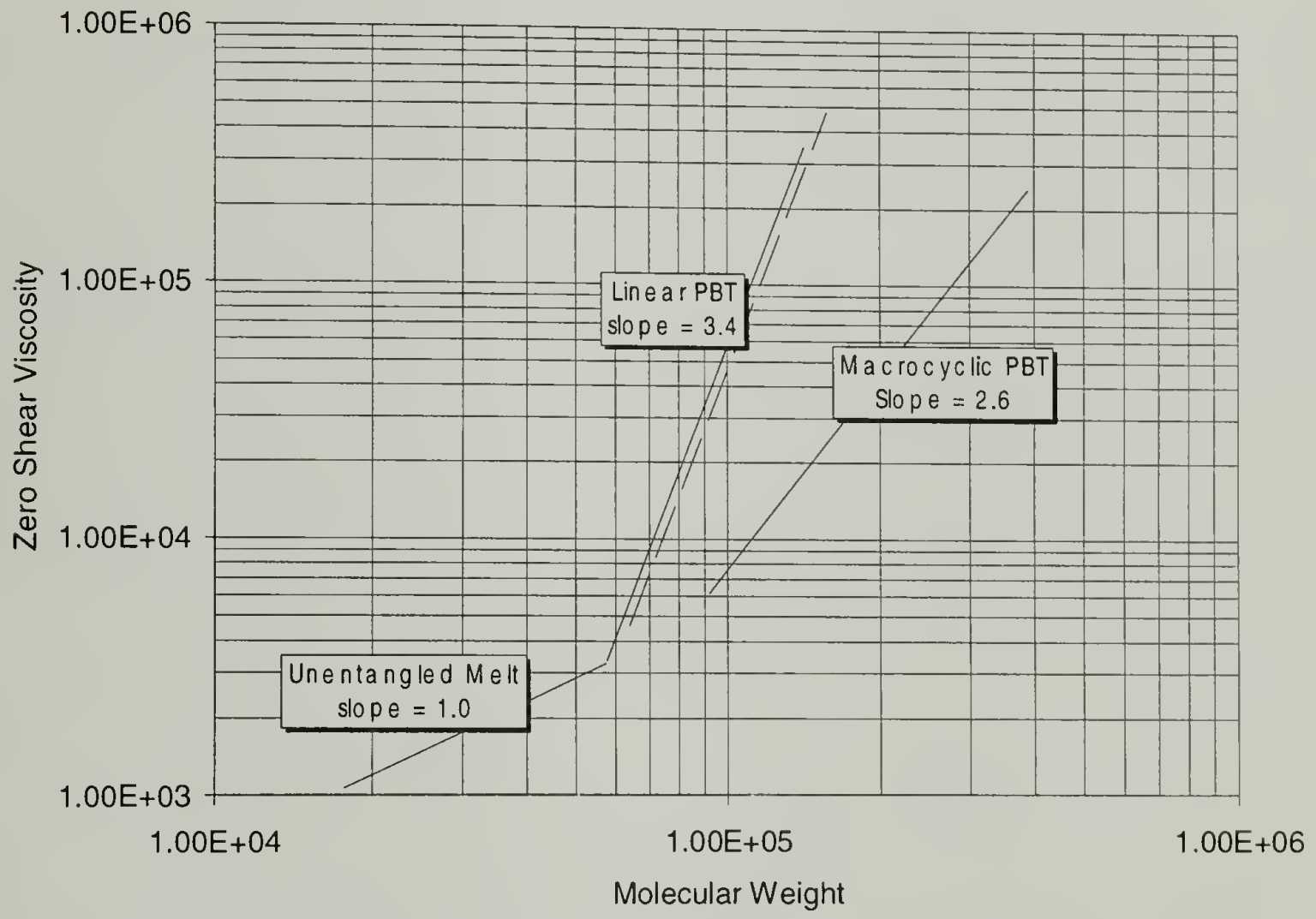


**Figure 6.72 Zero Shear Viscosity vs. Molecular Weight for PBTs. Dashed line represents the shift proposed by McKenna for cyclic vs. linear chain structures. Solid lines are from Figure 6.71.**

The present research shows a greater shift downward in viscosity at a given molecular weight than was determined using cyclic and linear polystyrenes. This is

believed to be the result of the ring expansion polymerization which cannot produce rings with knots or catenation. By contrast, any ring closure reaction must result in some degree of "pretzel" rings, since the ends are connected from a random coil after the final molecular weight is reached. The probability of forming these knotted rings increases as the molecular weight increases. The ring expansion mechanism on the other hand is capable of producing simple cyclic structures at all molecular weights. The small difference in viscosity shown in Figure 6.72 suggests that the polystyrene rings are to some extent catenated and knotted. It has also been reported that small amounts of linear contamination dramatically affects the viscosity of cyclic molecules by effectively tying together the cyclics through entanglements[13]. Linear contamination in the polystyrene studies would be the result of residual linears after fractionation of the cyclic resins. This linear contamination should be higher in specimens prepared by the method involving ring closure and subsequent fractionation than in specimens prepared by ring expansion polymerization at low polymerization temperatures.

In short, the large difference in zero shear viscosity between linear and macrocyclic PBT resins compared to the cyclic polystyrene results[10] suggests that ring expansion polymerization is a method for producing a purer system of large cyclic molecules, free from linear contamination or ring catenation and knotting, than has been realized before.

When the macrocyclic PBT structures are thermally degraded at 250° C, they become linear chains with broadened molecular weight distribution. The back biting mechanism suggested in Figure 5.2 could produce some large cyclic rings each of which has no stannoxane initiator fragment. These macrocyclics would be much more stable at

250° C, and would tend to broaden the distribution. The effect of this degradation is seen in both molecular weight and its effect on zero shear viscosity. Figure 6.71 shows that the viscosities of the degraded macrocyclic polymers are shifted from the line that correlates cyclic structure (having a slope of 2.6). The degraded polymers fall very close to the correlation line for the linear resins (having a slope of 3.4). The apparent shift of these data points to the right of the linear correlation line is better interpreted as a shift down in viscosity for each given molecular weight. The c-PBT resins upon degradation, have become a mixture linear chains of broad molecular weight distribution possibly still contaminated by some cyclic chains. The viscosities of these mixtures do not correlate with the viscosities of linear PBT resins that have a more narrow molecular weight distribution. The resulting shift in viscosity is in the same direction and magnitude as the shift reported for polystyrene cyclic resins that may contain some knotting, catenation, or linear contamination as discussed above.

Nielsen[5] discusses possible reasons for the decrease in slope of $\eta_o$ vs. $<M_w>$ curves above $Mw_c$. He suggests that a gradual decrease from the 3.4 power dependence at zero shear rate is the result of entanglements that cannot reform in the melt as fast as they are being destroyed by increased shear stresses at high molecular weights. While he only discusses linear polymer systems, the analogy to cyclic structures is apparent. As the shear stresses increase, the entanglement density in the melt is decreased by a limiting rate of entanglement formation, analogous to a diffusion rate. The cyclic resins, with slower self diffusion than linear resins[14-16], would therefore have a slower rate of re-entanglement under high shear stresses. The result is both a lower viscosity, and a less steep viscosity

dependence on molecular weight above $Mw_c$. This rationalization seems to correlate with the findings in this study.

### 6.3.2 Polymerization and Crystallization Rates of c-PBTs

The second rheological study in this research program was done to determine the polymerization and crystallization rates of c-PBT resins. Isothermal polymerization and crystallization studies in the DSC has shown that the polymer crystallizes rapidly to high polymer, however, because the polymerization is athermal, no indication of the polymerization rate can be sensed using this equipment. Using the rheometer to study the increase in viscosity during initial polymerization allows the polymerization rate to be determined. When crystallization occurs in the rheometer, it is evidenced by an increase in the storage modulus of the melt, concurrent with an increase in viscosity as the melt begins to solidify.

By working at low temperatures, where the stannoxane initiator is believed to be stable during the time frame of the test, the polymerization is slow enough to measure in the rheometer. The polymerization rates and melt viscosities were determined for both cyclic and linear resins produced from BTCs. In addition, the viscosities of commercial linear resins were determined under the same conditions of low temperature and low shear rate.

#### 6.3.2.1 Special Fixture for Rheology Study of Low Viscosity Melts

Rheology studies of low viscosity melts are difficult to perform using a parallel plate geometry because the low viscosity of the fluid results in a tendency to drool out of the gap between the platens during the test. If this happens, the test result is invalid since

the contact surface is decreased and the shear stresses and normal forces generated by the fluid are inaccurately determined.

A special fixture was used in these tests to keep the melt contained while the viscosity was very low, and still allow viscosity and modulus determinations after the polymerization had finished. The upper fixture utilized a standard 25 mm diameter plate, while the lower fixture consisted of a 50 mm platen to which a ring of silicone had been attached, leaving a well which could retain a specimen for low viscosity melt studies. This rheological geometry resembles that of the Couette flow cup commonly used in the oil and paint industries. However, in this series of studies, an attempt was made to maintain the upper melt surface in contact with the upper platen, without allowing the melt to climb the platen edges and coat the upper surface. Such a coating would thereby have artificially exaggerated the melt viscosity by increasing the resistance through greater surface area contact between the melt and the platen.

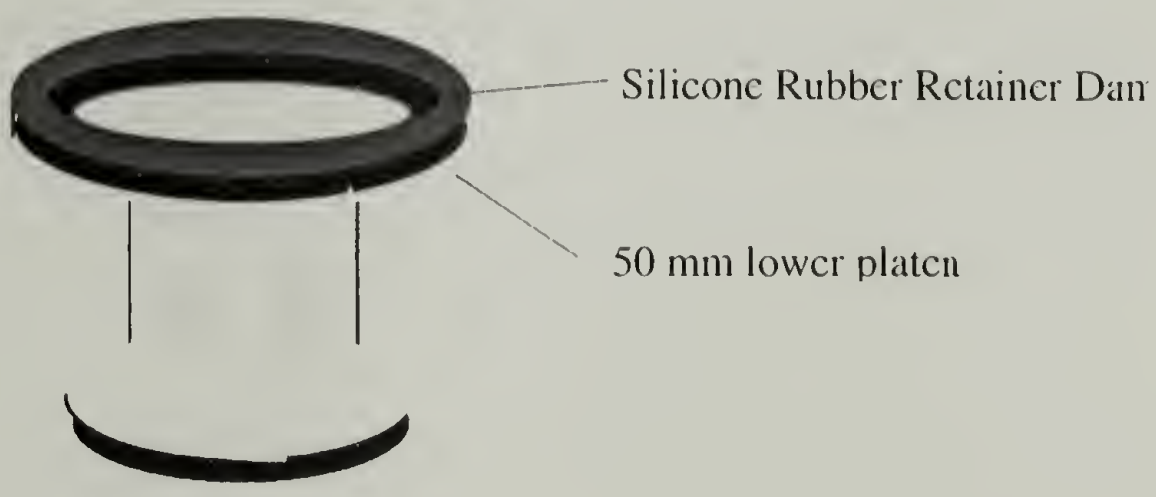


The retainer ring (dam) was punched from a sheet of high temperature red gasket rubber using concentric punches of 1 inch and 1.25 inches. The gasket material was placed on a backing substrate and the punches were driven by a Carver hydraulic press to compression cut the ring. The ring was then adhered to the platen surface using GE Red

High Temperature Silicone Sealant RTV-106® . After curing for four hours in a 100° C oven, the platens were cleaned thoroughly prior to use.

Some compromise was made in the measurement precision of the viscosity determination. While the upper platen contacted the fluid over a 4.90 $cm^2$ area, the lower platen had a necessarily larger contact area since the melt pool could flow to cover a larger surface on the lower platen. Reproducibility studies were done to determine the best specimen size and platen gap setting for each resin run using this special fixture.

#### 6.3.2.2 Isothermal Polymerization of Cyclic Oligomers in a Parallel Plate Rheometer

Polymerization studies were carried out under nearly isothermal conditions in the rheometer. Using the viscosity of the melt as a measure of the extent of polymerization allows monitoring changes in the molecular weight, or degree of polymerization, as a function of time. Under conditions where crystal nucleation and growth are within the time frame of the experiment, it is also possible to determine a crystal nucleation time.

As reported in Section 6.2.4.1 on isothermal polymerization in the differential scanning calorimeter, the polymerization is very fast at 190° C for stannoxane-initiated BTCs. The time to reach the peak of the crystallization exotherm was only two minutes at 180° C, and four minutes at 190° C. In each case, the crystalline structure that developed was found to have a high melting point (221° and 226° C respectively). Each specimen consists of high polymer based on the size of the resulting melt endotherm, showing that the polymerization is fairly advanced within the time frame of the crystallization exotherm.

---

® Silicone Sealant RTV-106 is a registered trademark of the GE Plastics Co.

While polymerization rate is known to increase with temperature, the crystallization rate is slowed at higher temperatures because of the reduction in the degree of undercooling with increased temperature. In order to measure a steady-state viscosity in the melt, the temperature must be high enough to retard any crystallinity developing during the measurement. For BTCs with 0.3 mol % stannoxane, DSC results show that the PBT crystallization is delayed to about twenty minutes when isothermally polymerized at 212° C (see Figure 6.8). Working within this time frame, and at temperatures above 210° C, an accurate measure of the viscosity was deemed possible.

By preparing a specimen consisting of oligomer and initiator, sintered at low temperature into a solid preform, it is possible to monitor the rate of polymerization under isothermal conditions. For this study, the rate of polymerization is taken as the slope of a *linear* plot of viscosity vs. time at the time when the viscosity reaches 200 poise. (On such a linear plot, the value of 200 poise is above the noise and therefore easily determined in all TBTE-initiated polymerization studies.) This low viscosity was selected for comparing relative rates of polymerization vs. a) initiators type, b) levels of initiator, and c) temperatures of polymerization. A viscosity of 200 poise was found to be low enough that the rates of polymerization are not limited by the diffusion of oligomer to the initiator sites, but being significantly above the oligomer viscosity for all studies.

Temperatures for isothermal polymerization studies were set sufficiently high that a value of the plateau viscosity could be determined after polymerization was completed but before crystallization began. Temperatures were limited to those below the temperature, c.a. 230° C, where the initiator begins to degrade. Polymerization studies

were attempted at temperatures as low as 210° C. However, at this low temperature the polymer began to crystallize before the melt viscosity reached a plateau as shown in Figure 6.73. For an initiator loading of 0.3% stannoxane, G' is seen to increase continuously, becoming greater than G" after only 12 minutes at 210° C. This indicates that crystal nucleation has begun and the crystal structure has grown sufficiently within this time to cause the melt to develop some solid character.

Based on the DSC results run at 212.5° C, the degree crystallinity is very low after 12 minutes, since the crystallization exotherm is barely beginning to develop at 10 minutes and the onset time (intercept of the onset slope with the baseline) is 20 minutes. (At 212.5° C, the crystallization exotherm for this material takes 110 minutes to reach a peak.) The rheometer, used to monitor viscosity, is more sensitive to the effects of a low degree of crystallinity than is the DSC which only shows the exothermic heat of crystallization. As shown in Figure 6.73, the shape of the viscosity curve changes at the crossover point to reflect the increase in crystallinity in the melt. The viscosity curve, which initially follows the shape of G" (while the melt characteristics dominate) shifts to follow the G' curve when the crystal content becomes significant. By twelve minutes into the test, this polymer shows sufficient crystal development that the viscosity reflects the elastic rather than the dissipative modulus of the melt.

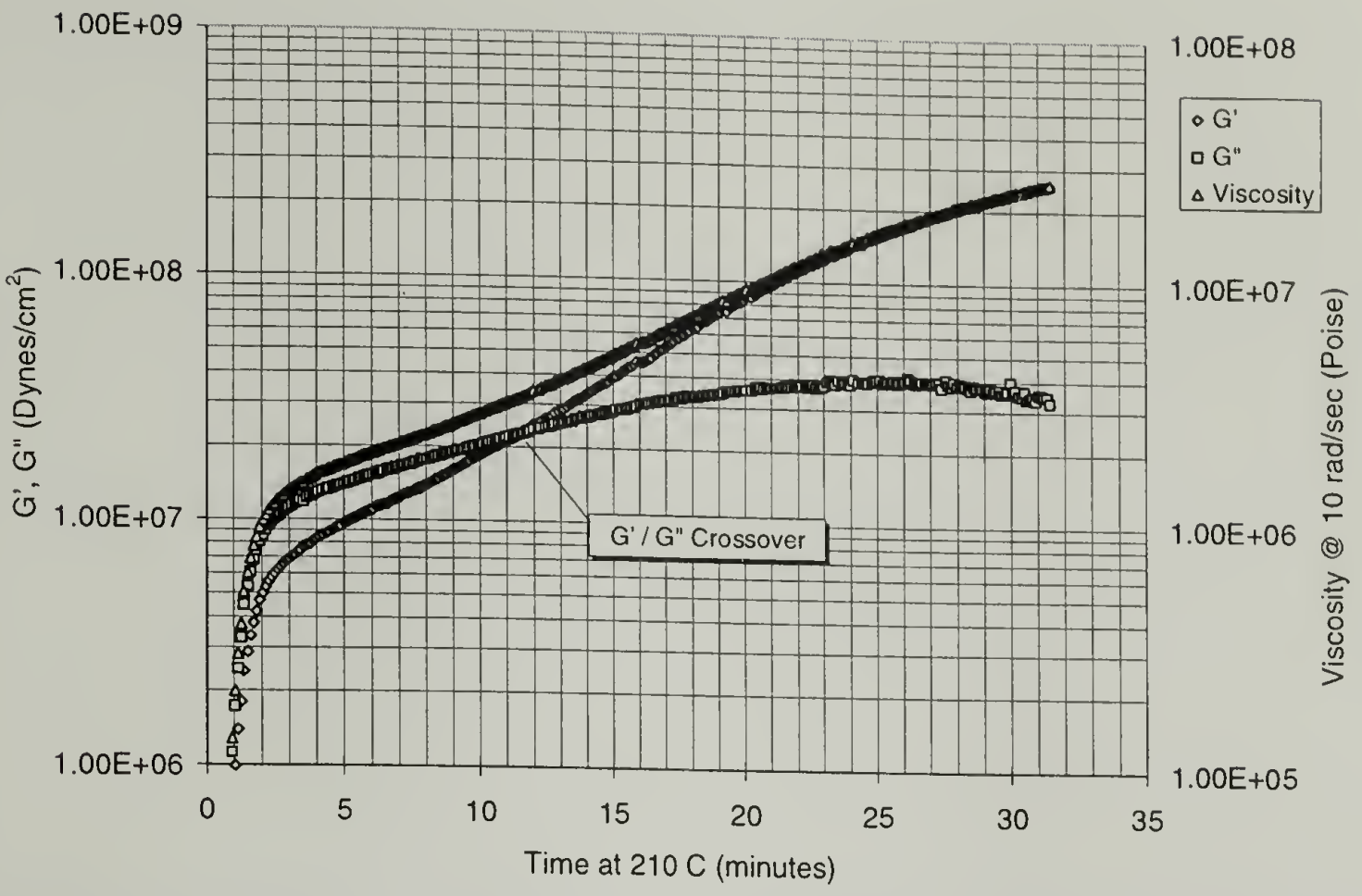


**Figure 6.73 Evidence of crystallization occurring in BTCs initiated using 0.3 mol % stannoxane during isothermal polymerization at 210° C.**

At higher polymerization temperatures, the polymerization rate increases, and the crystallization rate decreases. Also, the crystal nucleation time increases at higher temperatures as discussed earlier, making a stable measurement of viscosity possible within ten minutes as shown in Figure 6.74. In this figure, the viscosity at 210° C continues to increase as crystallization progresses over thirty minutes. The viscosity at 220° C is stable for about 10 minutes, but also begins to rise slowly after 10 minutes as crystallization begins to develop slowly. The viscosity at 226.5° C is stable for 10 minutes, but this temperature is near the range in which the stannoxane initiator becomes unstable.

To determine a viscosity for the resin it is only necessary to find an isoviscous plateau. Isothermal polymerization studies were therefore run between 215° C and 226.5° C.

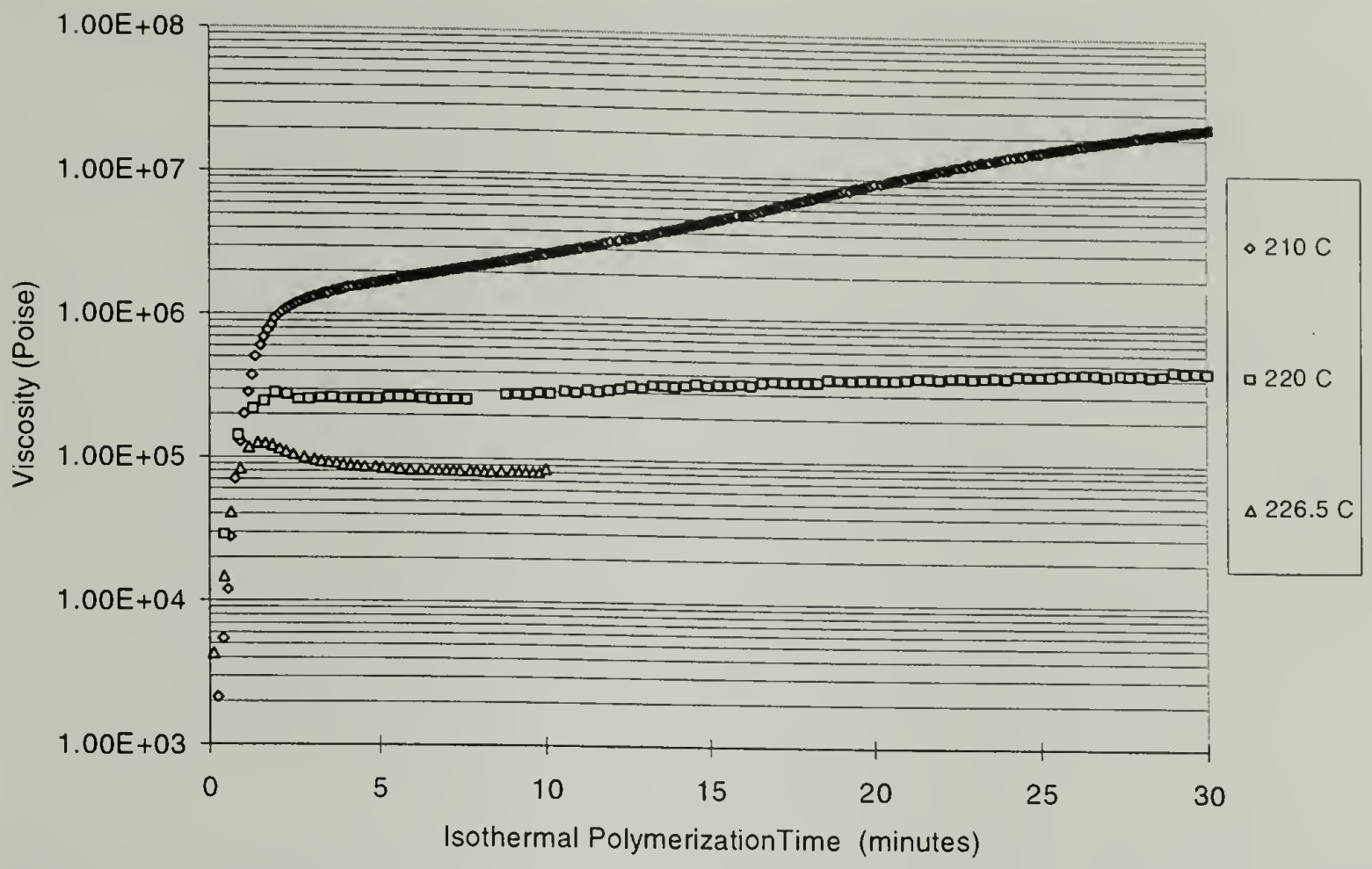


**Figure 6.74 Viscosity of 0.3 % stannoxane initiated BTCs at three temperatures during polymerization.**

The concentration of stannoxane initiator present during polymerization was found to be the most important factor in determining in the molecular weight, and therefore the viscosity of c-PBTs. Stannoxane concentrations from 0.3 mol % to 1.2 mol % were investigated with the results shown in Figure 6.75. As expected, the higher initiator levels produce lower viscosity resins, based on the concentration of monomer to concentration of initiator (the [M]/[I] ratio) which determines the molecular weight. The results in Figure 6.75 suggest that using half the initiator level produces a greater than four fold increase in melt viscosity. This non-linear dependence is expected for polymers above the entanglement molecular weight.

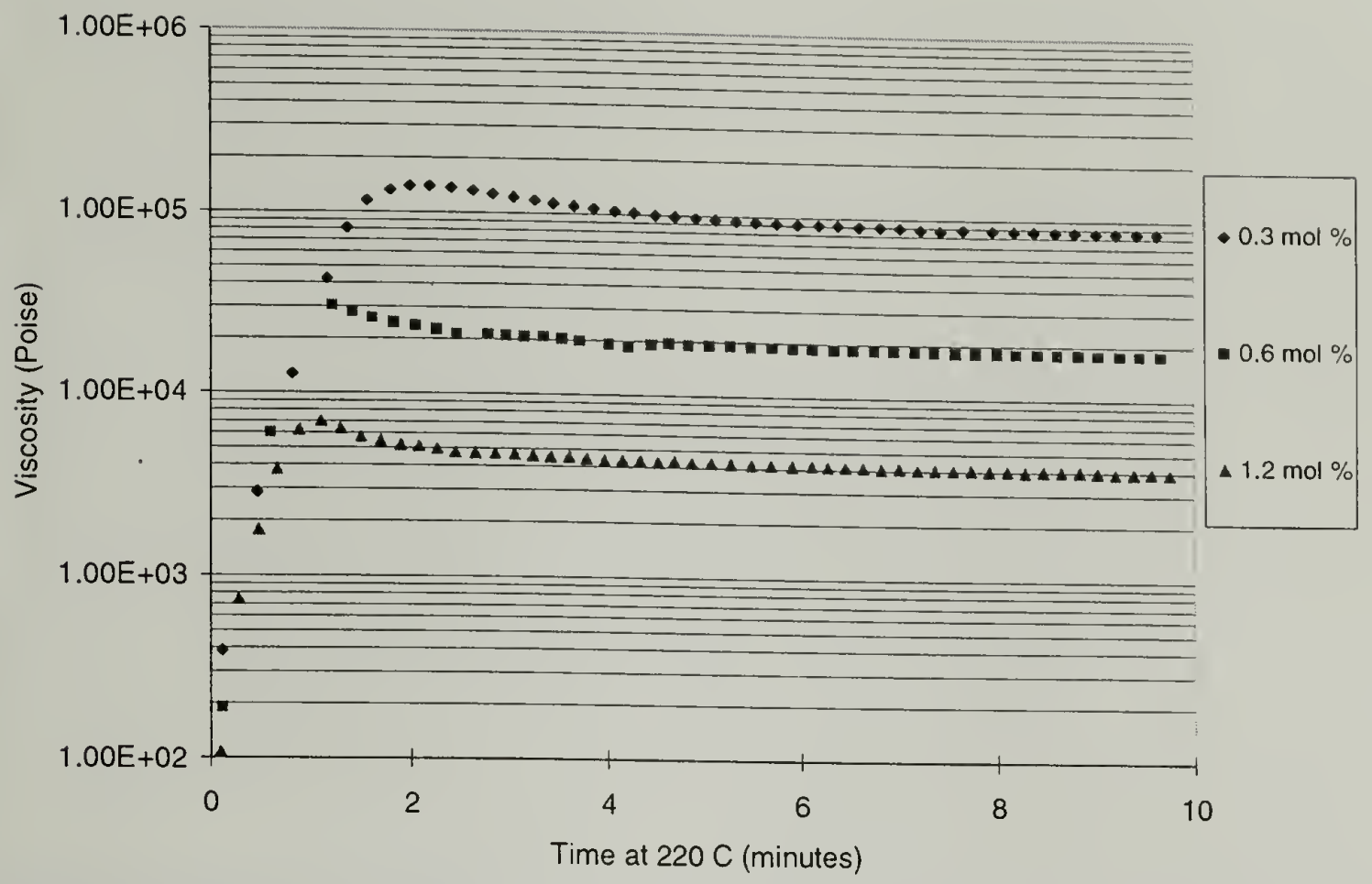


**Figure 6.75 Effect of stannoxane concentration on melt viscosity of c-PBT at 220° C.**

When using the TBTE initiator to polymerize BTCs, the same rates of crystallization (and presumably polymerization) were found as were seen earlier in the DSC studies. TBTE is found to be a considerably slower initiator for polymerization than is the stannoxane initiator. The viscosities of the polymer were found to be inversely related to the level of initiator as demonstrated for two temperatures in Figures 6.76. and 6.77.

The viscosity of the linear PBT made from cyclic oligomers with the TBTE initiator is found to be higher than the viscosity of macrocyclic c-PBT produced using stannoxane initiator at an equivalent molar initiator content. A direct comparison of the results of using the two initiator systems is shown in Figure 6.78.

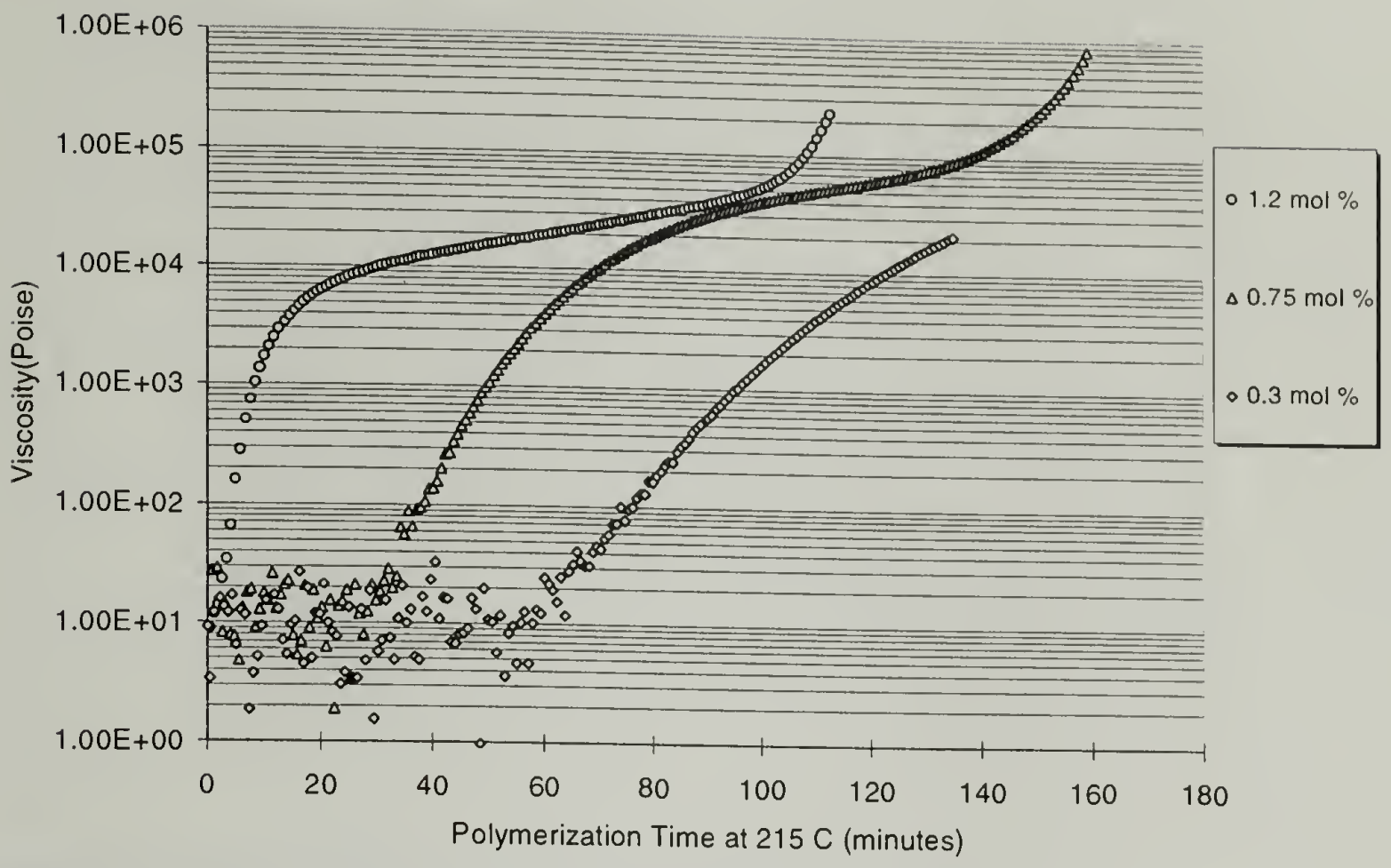


**Figure 6.76 TBTE-initiated polymerization of BTCs at 215° C.**

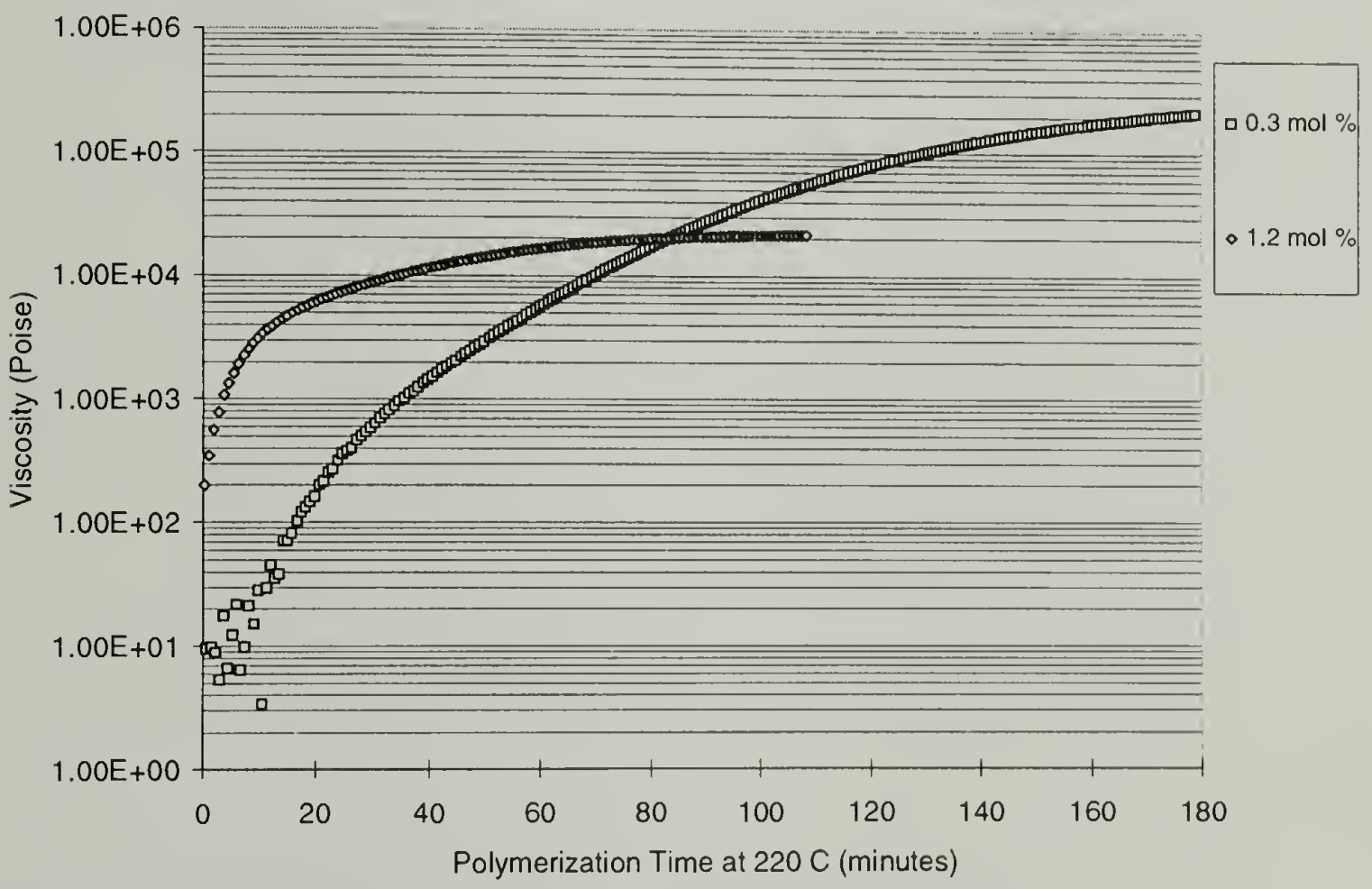


**Figure 6.77 TBTE-initiated polymerization of BTCs at 220° C.**

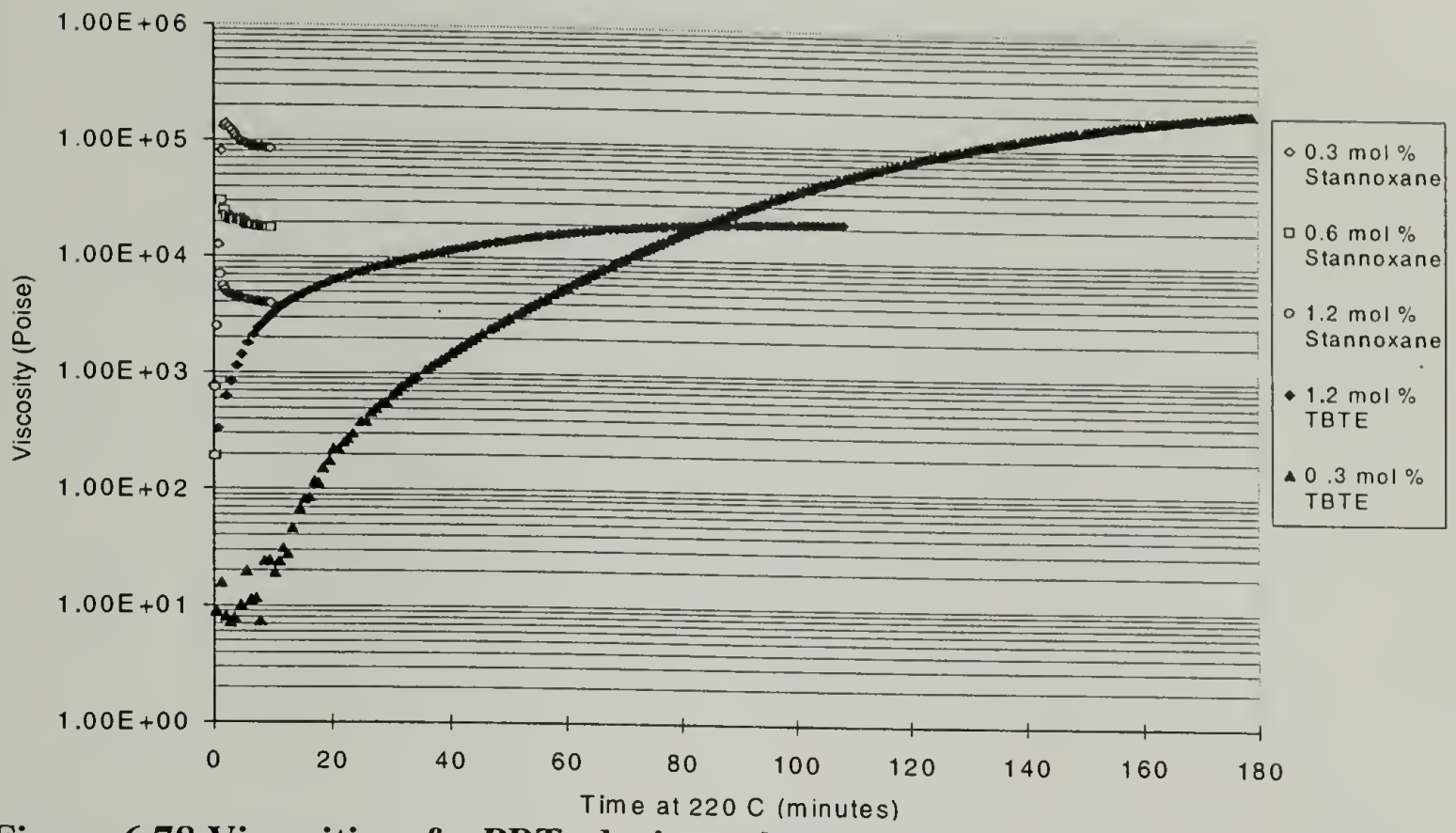


**Figure 6.78 Viscosities of c-PBTs during polymerization at 220° C. (Showing the combined data from Figures 6.75 and 6.77 on the same time scale.)**

Here the stannoxane initiator is seen to polymerize BTCs much faster than does TBTE initiator at all mol ratios. PBTs of equal viscosity result from polymerizing with 0.6 mol % stannoxane and 1.2 mol % TBTE. However at these concentrations, the molar ratio of active Sn-O linkages in the BTC/stannoxane is twice the ratio in the BTC/TBTE. The higher Sn-O content probably accounts for part of the higher polymerization rate found with the cyclic initiator.

However, the rate with the cyclic initiator is seen to be higher by several orders of magnitude. The stannoxane tin is also more electropositive than the TBTE tin; resulting from the two strongly electron withdrawing oxygens and two weak electron donating butyl groups on a stannoxane tin atom vs. one oxygen and three butyl groups on the TBTE tin atom. This relative electron deficiency in the stannoxane tin appears to result in a much higher coordination potential for the carbonyl oxygen in the PBT, resulting in a much higher probability of polymerization, manifested as an increased polymerization rate.

### 6.3.2.3 Low Temperature Rheology of Commercial Linear PBT Resins

For the commercial linear PBT polymers with melting points in the range of 222° - 230° C, it was necessary to run comparative rheology studies below their normal crystalline melting points. This was possible over a range of small undercoolings, by first melting the resins at 250° C to destroy all crystallinity, then dropping the temperature rapidly to the study temperature, and completing the viscosity characterization before crystal growth occurred. At 220° C, the viscosity of the melted resins was found to be stable, i.e. free from effects of crystallization, for at least 10 minutes after cooling from 250° C as shown in Figure 6.79. These data suggest that a plateau viscosity measurement is valid once the viscosity stabilizes. When compared to the rheological curves of the c-PBTs, these viscosity traces differ in shape as they rise over the first few minutes as the melt is cooling from a higher temperature. (See Figure 6.75 for a comparison with the c-PBT response at short times).

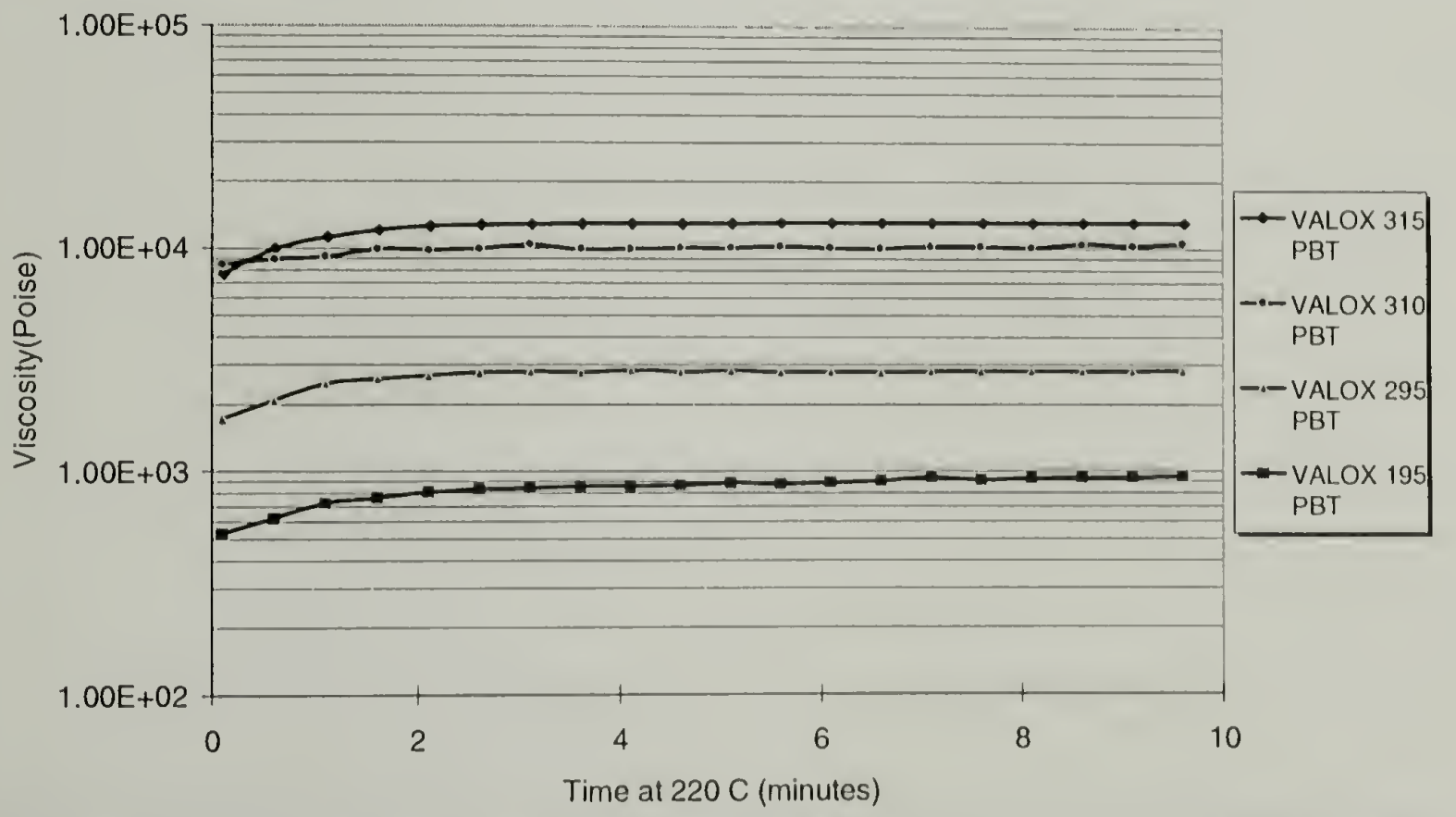


**Figure 6.79 Stable plateau viscosity measurements for molten VALOX PBT resins at 220° C (small undercoolings) after rapid cooling from 250° C.**

### 6.3.2.4 Results of the Polymerization and Crystallization Rate Study

Based on the type of characterization shown in the previous section, a series of polymerization and crystallization studies was completed at over a range of temperatures. Specimens were collected for molecular weight determination after each test. The results of these studies are shown in Table 6.5.

**Table 6.5 Summary of Polymerization and Crystallization Studies.**

| Material | Temp (C) | Time at Temp (min) | Plateau Viscosity (poise) | <Mw> after test | Polymerization "Rate" (Poise/min) | Polymerization Initiation Time (minutes) | Crystallization "Rate" Dynes/cm$^2$/min | Crystallization Initiation Time (minutes) |
|---|---|---|---|---|---|---|---|---|
| 0.075% Stan | 219.5 | 95 | 200,000 | 220,000 | - | - | - | - |
| 0.3% Stan | 210 | 33 | 2,000,000 | 134,000 | - | - | 4,040,000 | 11.6 |
| 0.3% Stan | 213 | 30 | 470,000 | | - | - | 25750 | 15 |
| 0.3% Stan | 215 | 30 | 119,000 | | - | - | 1080 | - |
| 0.3% Stan | 220 | 10 | 85,000 | 115,600 | - | - | - | - |
| 0.3% Stan | 220 | 10 | 63,000 | 126,300 | - | - | - | - |
| 0.3% Stan | 220 | 10 | 59,600 | 114,700 | - | - | - | - |
| 0.3% Stan | 220 | 60 | 60,000 | | - | - | - | - |
| 0.3% Stan | 220 | 30 | 50,000 | 113,000 | - | - | - | - |
| 0.3% Stan | 220 | 10 | 47,000 | | - | - | - | - |
| 0.3% Stan | 220 | 180 | | 103,000 | - | - | - | - |
| 0.3% Stan | 226.5 | 60 | 80,000 | 82,000 | - | - | - | - |
| 0.6% Stan | 220 | 10 | 18,000 | 53,700 | - | - | - | - |
| *0.6% Stan | 226.5 | 30 | 500,000 | 292,000 | - | - | - | - |
| 1.2% Stan | 220 | 10 | 4000 | 40,600 | - | - | - | - |
| 1.2% Stan | 220 | 10 | 5200 | 46,600 | - | - | - | - |
| 0.3% TBTE | 215 | 135 | >100000 | | 26 | 82 | - | - |
| 0.3% TBTE | 220.2 | 180 | 200,000 | 182,000 | 29.8 | 20.3 | - | - |
| 0.75%TBTE | 215 | 160 | 50000 | 110,000 | 56.4 | 41.5 | 114000 | 157.2 |
| 0.75%TBTE | 220 | | 22000 | | | | - | - |
| * 0.75%TBTE | 230 | 60 | 30000 | 97,000 | 88.9 | 23.6 | - | - |
| 1.2% TBTE | 215 | 113 | 50000 | 93,300 | 150 | 5.3 | 32500 | 100.8 |
| 1.2% TBTE | 220 | 110 | 21000 | 90,500 | 164 | 0.2 | - | - |
| VALOX 195 | 220 | 30 | 950 | 42,500 | - | - | - | - |
| VALOX 295 | 220 | 30 | 1400 | 61,000 | - | - | - | - |
| VALOX 310 | 220 | 30 | 10000 | 78,000 | - | - | - | - |
| VALOX 315 | 220 | 30 | 10400 | 90,000 | - | - | - | - |

* Data collected without using drying cartridge on inlet nitrogen stream.

Rate of polymerization could not be measured for the stannoxane-initiated polymerization studies. The polymerization was so fast at these temperatures that it was completed before the temperature could stabilize. Figure 6.80 shows a polymerization

using 0.3 mol % stannoxane at 215° C. This is one of the lowest temperatures in this study so the polymerization rate is the lowest at this temperature. The specimen was inserted into the rheometer once the oven temperature was stable by opening the oven door and placing the solid specimen on the lower platen. The door was closed quickly and the platens brought together as the specimen melted. The timer was started when the two platens reached the preset gap, as the specimen now was just melted sufficiently to flow and fill the gap. Viscosity and melt moduli as well as temperature of the lower platen were monitored throughout the test. As can be seen in Figure 6.80, the temperature took nearly five minutes to recover to 215° C and stabilize. By this time, the polymer had reached its plateau viscosity; the early small drop in viscosity reflects the final heating of the specimen as it stabilizes at the test temperature. It is obvious that polymerization was completed prior to temperature recovery and therefore no measure of polymerization rate was possible in the stannoxane system.

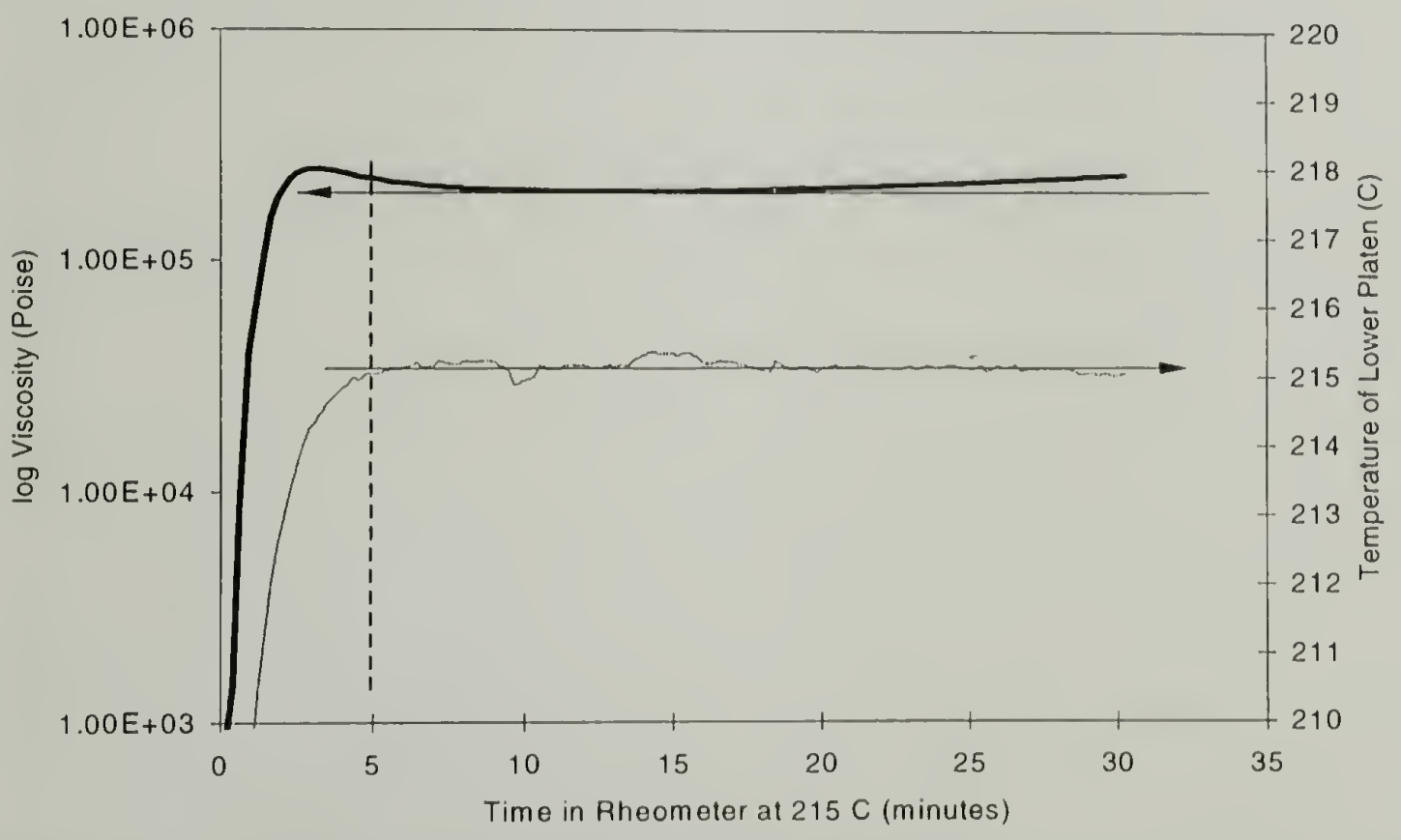


**Figure 6.80 Temperature recovery of the rheometer and viscosity build during a 0.3 mol % stannoxane initiated polymerization of BTCs at 215° C.**

As opposed to the stannoxane initiated polymerizations, polymerization rates could be determined for TBTE initiated polymerizations. The initiation time is found to be a function of the initiator loading, with higher initiator content producing a measurable viscosity at a shorter time. This shows that the viscosity is not controlled by a few high molecular weight chains in an solvating solution of oligomers, but by many chains reaching sufficient length to increase the viscosity over that of the oligomers. Figure 6.81 also shows a strong temperature sensitivity in the onset of polymerization, in that it takes four to five times longer to initiate with only a five degree drop in polymerization temperature.

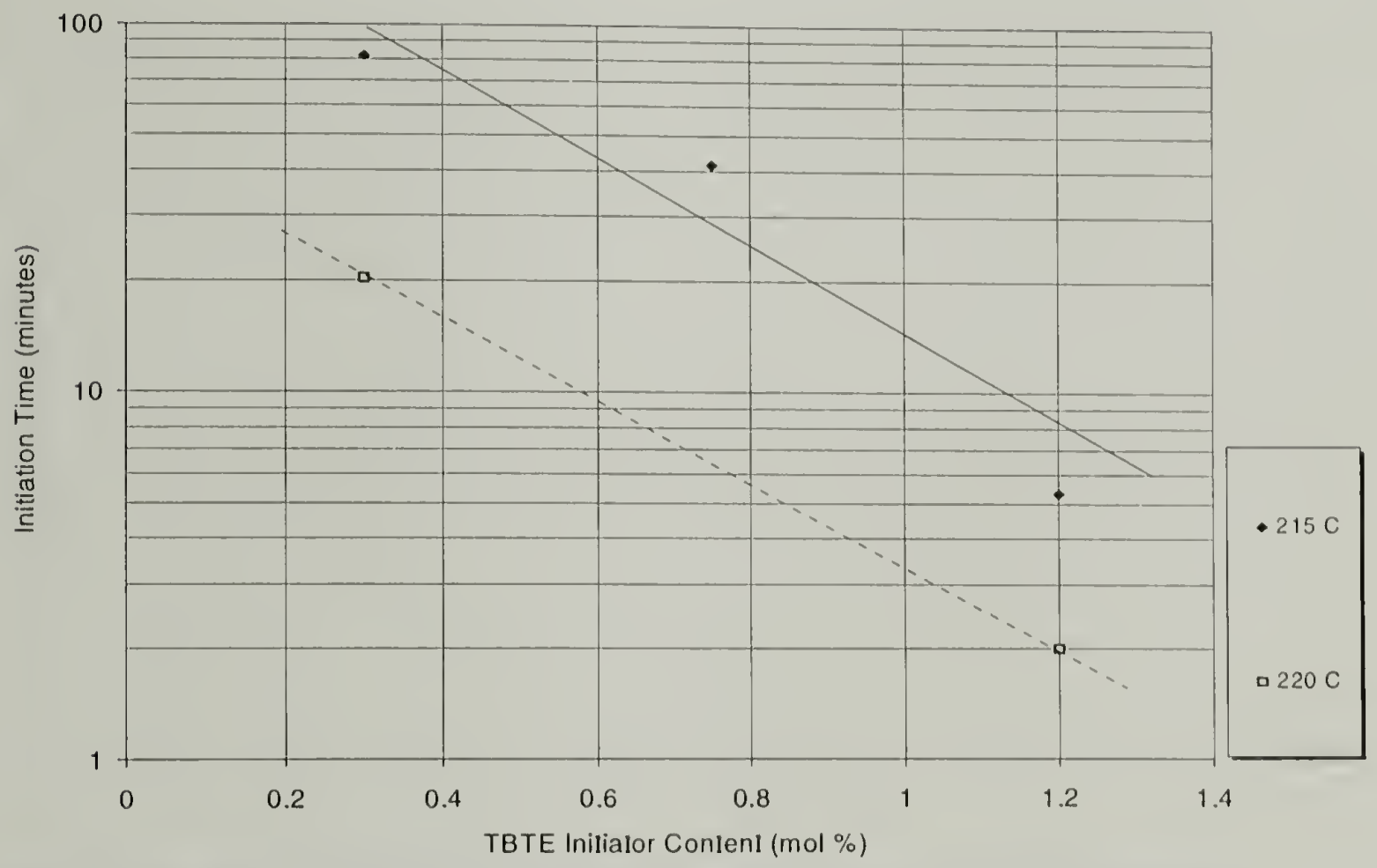


**Figure 6.81 Effect of initiator content on initiation time for TBTE initiated polymerization of BTCs.**

Because polymerization rates were the focus of this study, crystallization rates were only determined in a few of the runs, i.e. those in which the material was left in the rheometer until crystal development was obvious. Figure 6.76 shows an upturn in the

viscosity for two of the TBTE initiated polymerization curves, indicating crystallization was beginning after an extended time following the end of polymerization. The crossover of G' and G' was found to be a reproducible time which marked the onset of crystallization. Crystallization rates were determined at this time as the derivative, dG'/dt. at crossover. As shown in Figure 6.82, the crystallization rate is found to be an inverse function of initiator content. This is because low molecular weight chains take longer to begin to crystallize. The explanation appears to lie in the viscosity difference between the two different $<M_w>$ polymers during polymerization. The polymer with the lower rate of polymerization has at least twice the viscosity, based on its higher $<M_w>$ following polymerization (Figure 6.76). This implies that the $<M_w>$ not only controls the viscosity of the melt, but has a secondary effect on the crystallization rate. That is, the higher the $<M_w>$, the lower the crystallization rate, because of the lower diffusion rate for high molecular weight polymer segments to reach the growing crystal front. (The same result is found for commercial linear crystalline resins. On cooling at constant rate from the melt, the crystallinity is found to be higher for the lower $<M_w>$ resins as shown earlier in Figure 6.5)

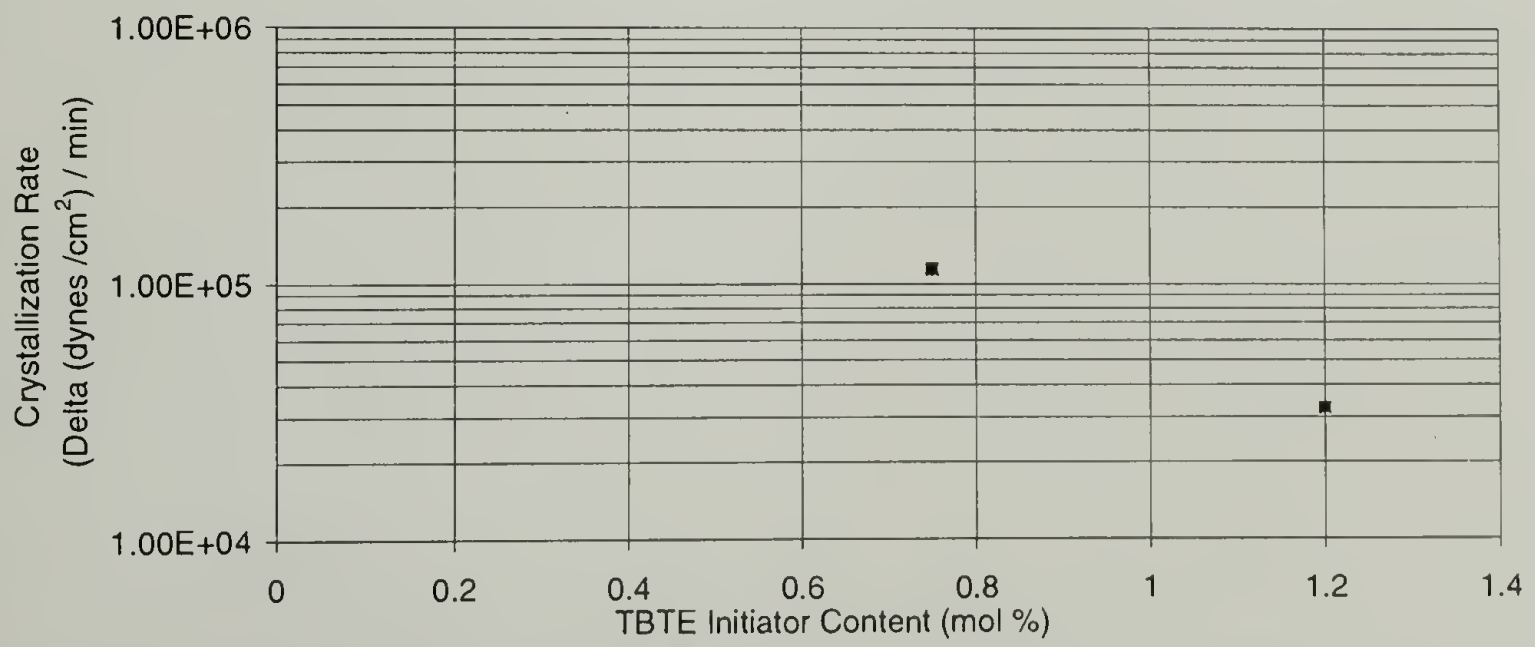


**Figure 6.82 Crystallization rate as a function of TBTE initiator content at 215° C.**

### 6.3.2.5 Correlation of Viscosity and $<M_w>$ at Low Temperatures.

An analysis similar the one reported in Section 6.3.1.6 was attempted using the lower temperature viscosity data at 220° C. Table 6.5 reports plateau viscosities for a range PBT resins, both linear and cyclic, of different molecular weights. The linear VALOX PBT resins were found to have a slightly higher viscosity dependence on molecular weight at 220° C (Figure 6.83) than was found at 250° C (Figure 6.70). The greater slope (3.7 at 220° C vs. 3.4 at 250° C) for these resins, near but slightly below the crystalline melting point, is not yet understood.

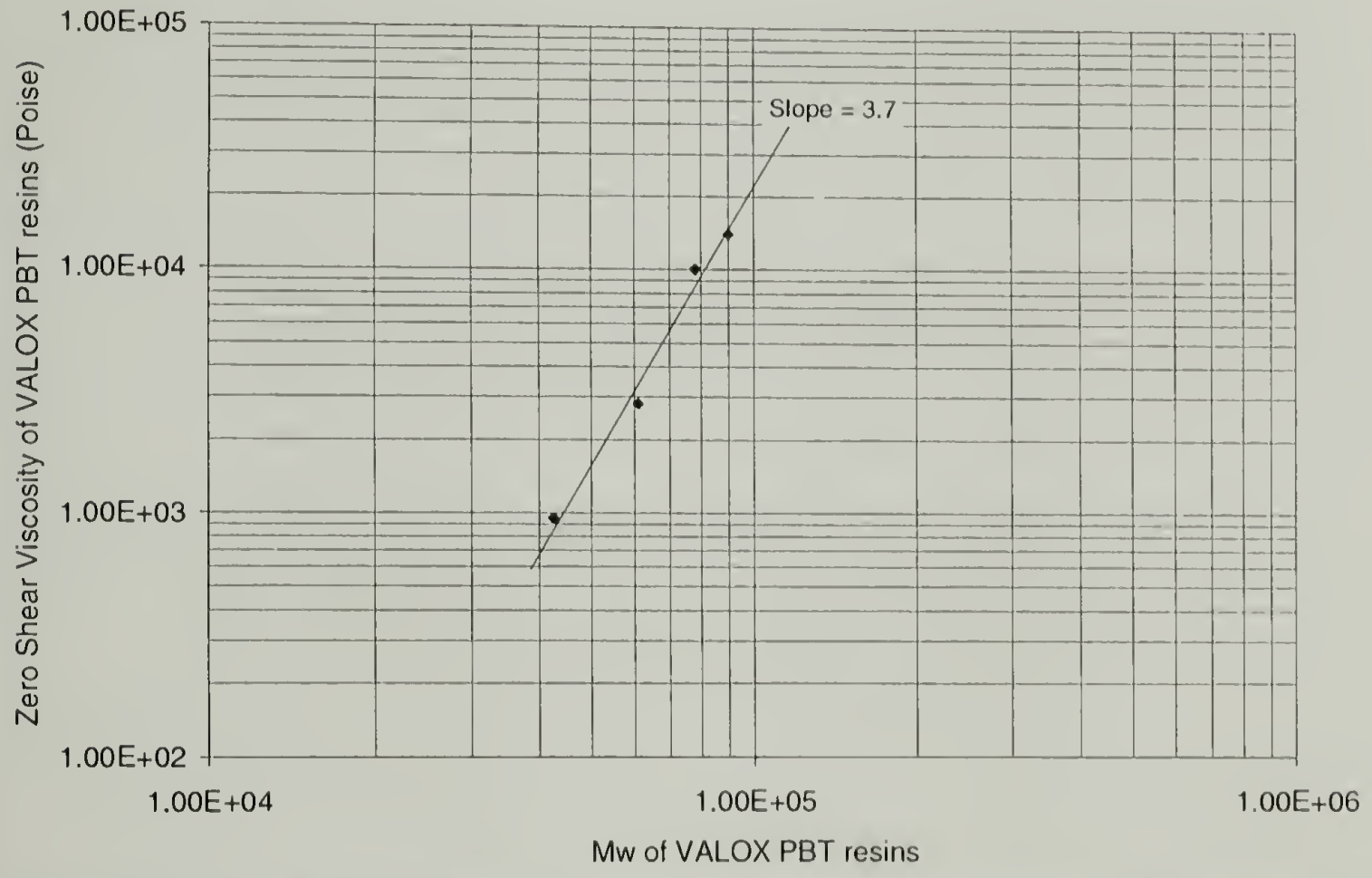


**Figure 6.83 Correlation of zero shear viscosity and $<M_w>$ for linear PBTs at 220° C.**

The viscosities of the cyclic resins are found to have the same slope at 220° C as was shown earlier at 250° C. This slope (2.4) may be the result of a lower effective entanglement density for the molten cyclic resins vs. that of the molten linear resins. At

high molecular weight, these molecules are more compact[17], transferring less shear stress and producing lower melt extension under an applied shear field. This result is shown in Figure 6.84 for a series of stannoxane-initiated c-PBTs. The lowest viscosity resins, with the lowest $<M_w>$, are from the 1.2 mol % polymerizations. The lowest $<M_w>$ resin shown below has a molecular weight in the range reported earlier to be the critical entanglement molecular weight for linear PBT resins. At the highest $<M_w>$ is a resin produced from 0.075 mol % stannoxane.

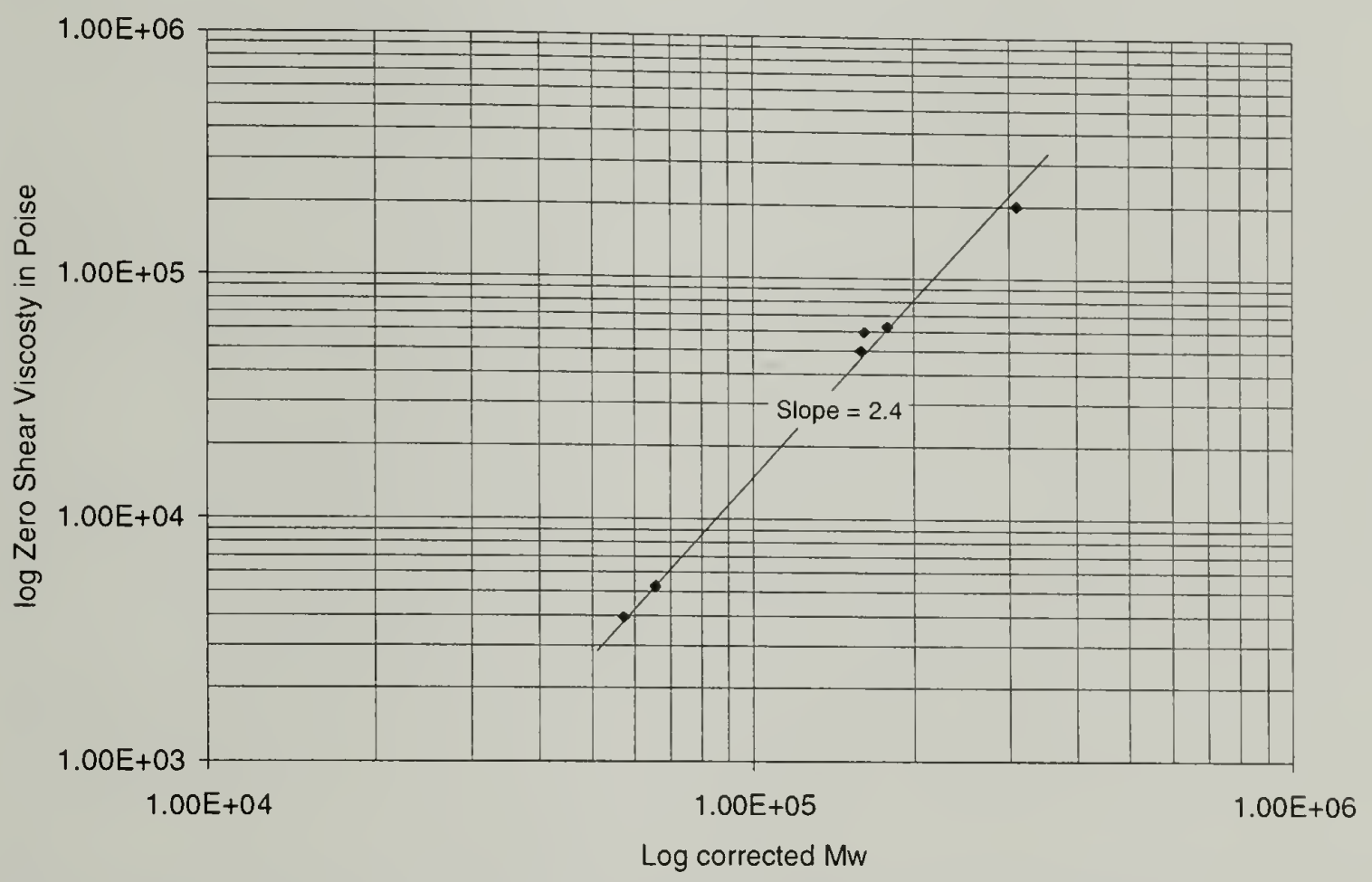


**Figure 6.84 Correlation of zero shear viscosity and $<M_w>$ for c-PBT cyclic resins at 220° C.**

Combining the two above plots gives a result similar to the plot at 250° C. Figure 6.85 shows the comparison. Two points are worth noting from this plot. First, the lowest molecular weight linear resin, VALOX 195 PBT, falls on the same correlation line as the other resins. At the higher temperature, this resin was found to have a peculiar behavior, the result being that it appeared to fall below critical molecular weight for entanglement.

The data at 220° C suggests that this resin is entangled, and the 250° C data shows a chemical reactivity associated with this particular resin. As VALOX 195 PBT is a commercial resin, currently under study by GE researchers, the analysis of this data cannot be discussed further in this thesis.

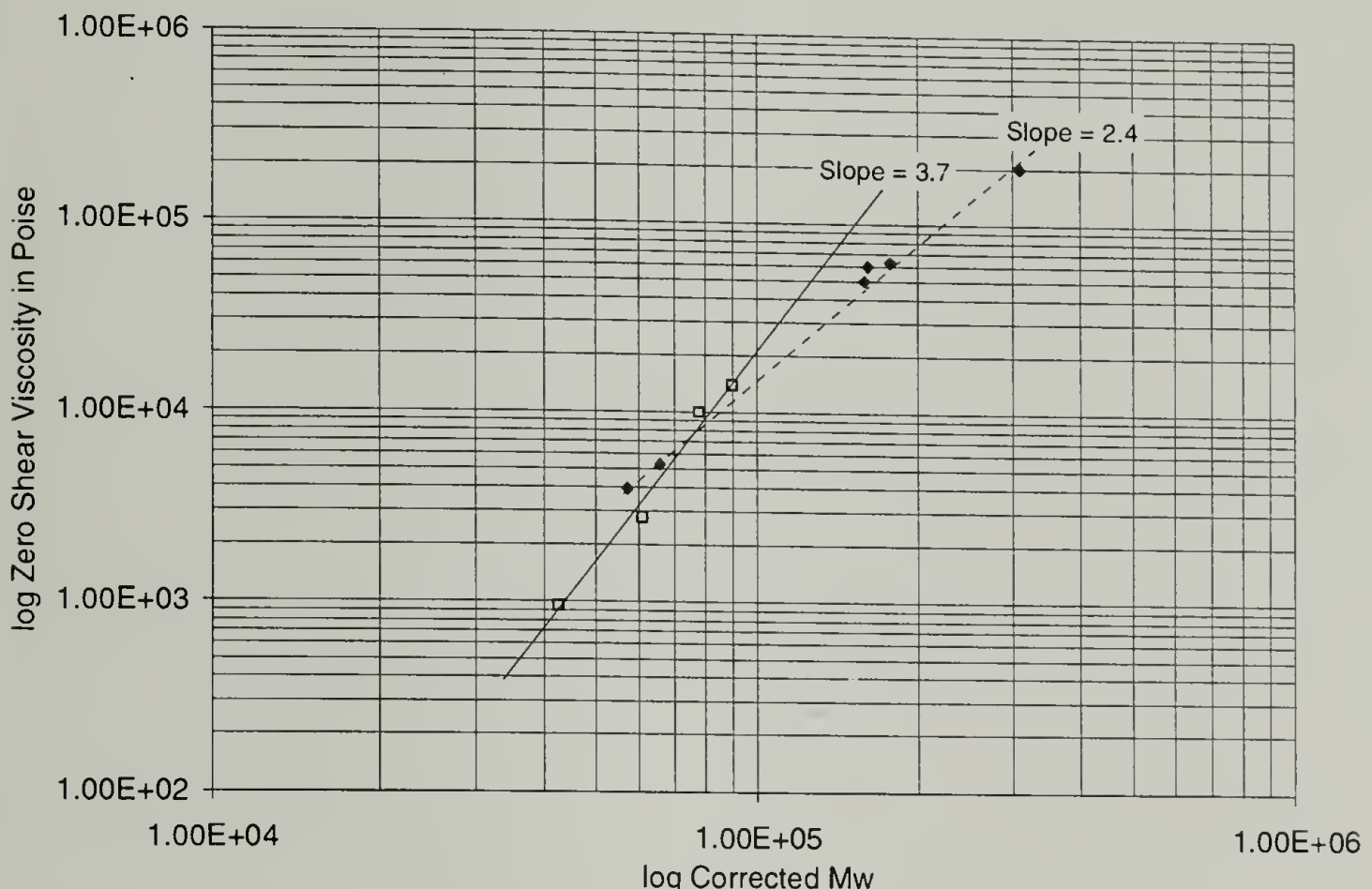


**Figure 6.85 Zero shear viscosity vs. <$M_w$> correlation for linear and cyclic PBT resins at 220° C. Open squares represent linear PBT resins. Closed diamonds represent cyclic c-PBT resins. (Cyclic resin molecular weights are corrected to linear equivalents.)**

Second, the low molecular weight cyclic resins fall in the same viscosity range as the low molecular weight linear resins. This would suggest that at low molecular weight, the cyclic molecules have nearly the same intramolecular entanglement density as the linear resins. This finding is significant in understanding the degree of entanglement vs. the radius of gyration for these cyclic molecules.

Consider a model of a single cyclic macromolecule of very high <$M_w$>. In this model, the molecule has the shape of a ball with a diffuse surface. This molecular ball will

have some characteristic dimension where the center becomes dense. Above this characteristic dimension, the density decreases radially, as the outer regions become more diffuse near the least probabilistic maximum dimensions for the cyclic molecule. Below this dimension, the center of this molecular ball has a constant density. The inner melt density cannot continue to increase as the radius decreases, but reaches a characteristic melt density, being that of the bulk melt. The inner region consists only of polymer chain segments which are part of this single cyclic molecule. In a melt of many such cyclic molecules, only the surface of the molecules are involved in intermolecular entanglements. The cyclic molecule therefore is less entangled with neighboring molecules than a linear molecule of equivalent molecular weight. If we decrease the $<M_w>$ of this model cyclic molecule, we will reach a $<M_w>$ where the characteristic dimension vanishes, and the entire molecular ball consists of only the diffuse surface. At this lower molecular weight, the entire cyclic molecule is involved in intermolecular entanglement, and is therefore not differentiated from a linear chain. At molecular weights near the critical entanglement molecular weight, the linear and cyclic molecules are not differentiated by viscosity. This appears to be the case for the different types of PBT molecules shown in Figure 6.85. To confirm this hypothesis, even lower $<M_w>$ cyclic resins need to be prepared. These low molecular weight cyclic polymers would show whether the correlation continues with a slope of 2.4 or the cyclic resins begin to show a slope closer to the 3.4 - 3.7 which is found for linear resins.

### 6.3.3 References for Rheology


1)Miller, M. L. *The Structure of Polymers*; Reinhold Book Corp:, **1968**.
2)Dodgson, k.; Bannister, D. J.; Semlyen, J. A.,*Polymer* **1980**, *21*, 663-667.
3)Bloomfield, V.; Zimm, B. H.,*Journal of Chemical Physics* **1966**, *44*, 315-323.
4)Roovers, J., *Macromolecules* **1985**, *18*, 1359-1361.
5)Nielsen, L. E. *Polymer Rheology*; Marcel Dekker, Inc.: New York, NY, **1977**.
6)Banach, T. M., Personal Communication.
7)Kambour, R. P.; Banach, T. E.; Carnahan, J. C.; Garbauskas, M. F.; Gundlach, P. E.; McAlea, K. P.; McCracken, L. L.; Todt, M. L.; Takekoshi, T. "Macrocyclic Polybutylene Terephthalates: PBT Variants of Unusually High Crystallinities via the Ring Expansion Polymerization of Butylene Terephthalate Cyclic Oligomers Using a Cyclic Stannoxane Initiator," Manuscript in preparation,**1998**.
8)Flory, P., *Journal of the American Chemical Society* **1940**, *62*, 1057-1070.
9)Fox, T.; Gratch, S.; Loshaek, S. *Rheology - Theory and Applications, Chapter 12: Viscosity Relationships for Polymers in Bulk and in Concentrated Solution*; 1st ed.; Academic Press: New York, **1956**; Vol. 1.
10)McKenna, G. B.; Hadziioannou, G.; Lutz, P.; Hild, G.; Strazilelle, C.; Straupe, C.; Rempp, P.; Kovacs, A. J., *Macromolecules* **1987**, *20*, 498-512.
11)Hild, G.; Kohler, A.; Rempp, P., *European Polymer Journal* **1980**, *16*, 535-527.
12)Hild, G.; Strazielle, C.; Rempp, P., *Eur. Polym. J.* **1983**, *19*, 721-727.
13)McKenna, G. B.; Plazek, D. J., *Polymer Communications* **1986**, *27*.
14)Tead, S. F.; Kramer, E. J., *Macromolecules* **1988**, *21*, 1513-1517.
15)Mills, P. J.; Mayer, J. W.; Kramer, E. J.; Hadziioannou, G.; Lutz, P.; Strazielle, C.; Rempp, P.; Kovacs, A. J., *Macromolecules* **1987**, *20*, 513-518.
16)Tead, S. F.; Kramer, E. J.; Hadziioannou, G.; Antonietti, M.; Sillescu, H.; Lutz, P.; Strazielle, C., *Macromolecules* **1992**, *25*, 3942-3947.
17)Hadziioannou, G.; Cotts, P. M.; tenBrinke, G., *Macromolecules* **1987**, *20*, 493-497.

## 6.4 Molecular Dimensions

Several attempts were made to determine the dimensions of the cyclic macro molecules produced from polymerization of the cyclic oligomers. In each case, conventional linear PBT materials were characterized by known techniques, and the techniques evaluated for suitability in the macrocyclic systems. Although no technique discussed below gave acceptable results, the strengths and weaknesses of the techniques are discussed with hope that future research on similar macrocyclic semicrystalline polymers may find a more acceptable method of determining the molecular dimensions.

### 6.4.1 Gel Permeation Chromatography

Gel Permeation chromatography (GPC), more precisely named size exclusion chromatography (SEC), is the primary technique in use by today's laboratories for determining the molecular weight of a long chain natural or synthetic polymer. This technique makes use of the size of a polymer molecule in very dilute solution to promote the separation of polymer chains of various length through diffusion of the smaller molecules into a "molecular sieve" while larger molecules that cannot enter the small passageways are passed more quickly through the separation column of the instrument. By making the path length through the separation column the determinant of column elution time, a sequence of molecular weights are eluted from the column. Comparing the characteristics of the eluted solution against a pure solvent stream (using differential optical density), a distribution of molecular weights may be inferred from the output signal based on time for any particular molecular size to be eluted from the column.

The absolute molecular weights are then determined by comparison with a series of known standards of monodisperse polystyrene which have been previously run through the equipment using the same separation columns and solvent. Based on a correlation of these monodisperse results, a calculation of the molecular weights and molecular weight distribution may be made on any polystyrene sample. In addition, these molecular weight parameters may be obtained for any other polymer that has the same molecular weight / hydrodynamic volume relationship as polystyrene through application of a universal calibration calculation and published values of constant parameters for the polymer / solvent system in question. The empirical Mark Houwink equation allows for molecular weight determination in any polymer with similar molecular structure to polystyrene.

The molecular weight and molecular weight distribution of linear PBT has traditionally been determined through the GPC technique described above. Both PBT and PS polymers have similar chain architecture in that they have linear backbones and free chain ends. Macrocyclic polymers, while having linear backbones, do not have free chain ends. Since the molecule is cyclic, it may be thought of as a linear polymer chain whose ends have been connected. This chain configuration has a reduced entropy by comparison with the linear chain of equivalent molecular weight. In addition, the entire chain must have a smaller radius of gyration than the equivalent liner chain. Several researchers have studied the molecular dimensions of cyclic and linear molecules from the same monomers. Zimm and Stockmeyer[1] predicted that the root mean square radius of gyration of a flexible linear polymer is related to the root mean square radius of gyration of the equivalent flexible ring polymer by $Rg_{linear} = 2^{1/2} Rg_{ring}$.

It has been reported[2-5] that cyclic molecules exhibit a longer elution time than do linear molecules of equivalent molecular weight. This is believed to be the result of the smaller dimensions for the cyclic polymer chains compared to the linear chains.

Benoit[6] has suggested that polymers with different molecular architecture but composed of the same structural units should fit a universal calibration curve when the logarithm of the product of (intrinsic viscosity · molecular weight) is plotted against elution volume. For this relationship to hold, the intrinsic viscosity is measured under θ-conditions. Geiser[7] shows that this relationship applies for cyclic and linear polystyrenes in cyclohexane at 34.5° C, but the relationship is less applicable if different solvents and temperatures (i.e., conditions other than θ-conditions) are used for the measurement.

Roovers[8] reports that there is a parallel delay in the elution volume ($V_e$) for ring polystyrenes vs. the equivalent linear polymers over a wide range of molecular weights as evidenced by a linear plot of $V_e$ vs. $\log(M_w)$. Using polystyrenes of molecular weight between 5,000 and 500,000 the apparent molecular weight of the rings was

$$(M_{ring})_{apparent} = 0.71\,(M_{ring})_{true}.$$

True molecular weights in this study were obtained from light scattering measurements in cyclohexane at 35° C (θ-conditions). In other words, *the actual molecular weight of macrocyclic polystyrene is 41 % larger than the value determined through GPC.*

This reported increase in molecular weight, which is used to relate a true $<M_w>$ from a GPC $<M_w>$, is believed to be true for other polymers as well. The effect seen here is based on the topology of cyclic molecules, and their higher probability of being retained in the porous gel packing of the GPC columns, vs. their linear counterparts. The same

relationship is used throughout this study of cyclic PBT molecules. In sections where the viscosities of cyclic and linear PBT polymers are compared and related to their molecular weights, this relationship has been evoked. The results of these studies make it clear that the calculated molecular weights of macrocyclic PBT, increased by 41 % over the GPC determined values, are more reasonable for interpretation of the results.

One additional interesting note is found in the theoretical degradation of a cyclic molecule through a single bond cleavage. On opening a single bond in a cyclic molecule, the cyclic molecule becomes linear. The molecular weight of this molecule does not change by this single bond opening, rather the GPC molecular weight of a group of such molecules would appear to increase, as the hydrodynamic radii (proportional to the radii of gyration) are increased though a single degradation step. In practice, based on GPC results, the average macrocyclic molecules from stannoxane initiated polymerization of BTCs contained several residual O-Sn-O links which open on thermal degradation, thereby producing several shorter linear chains from each macrocyclic molecule.

### 6.4.2 Intrinsic Viscosity as a Determinant of Molecular Dimensions

The limiting viscosity number, also known as the intrinsic viscosity (IV or [η]), is widely used as a determinant of molecular weight for polymers based on the existing empirical relationships which relate these two factors. The presence of polymer molecules in a particular solvent gives rise to a dramatic increase in the viscosity of the solution, because of the great difference in dimensions between the solvent molecules and the polymer molecules. As the interactions between the solvent and polymer become more favorable, the polymer coil expands and in the presence of a good solvent, and the

viscosity increase is even greater. (In terms of viscosity, the solvent-expansion of the coil is analogous to coil expansion through an increase in molecular weight.) The viscosity of a solution depends not only on the relative attractions between the two types of molecules (solvent and polymer), but also on the temperature, the concentration of polymer, and the length of the polymer chain. While no acceptable theory has been developed to describe the molecular interactions, there are existing empirical relationships that have been widely accepted. The Mark-Houwink relationship relates the intrinsic viscosity to the viscosity average molecular weight through two constants; $[\eta] = K\ M^a$, where $K$ and $a$ are experimentally determined constants related to the specific polymer and solvent under study. Borman[9] has reported values of $K = 6.25 \times 10^{-5}$ and $a = 0.847$ for a wide range of molecular weights of linear PBT samples tested in a mixture of 60:40 phenol-tetrachloro ethane at 30° C. To date, no measurements of the $[\eta]$ or molecular dimensions of cyclic PBT have yet been published.

Roovers[10] has reported that a series of linear and a series of cyclic polystyrenes respectively produce plots of log $[\eta]$ vs. log M having different slopes. For linear PS in cyclohexane (at θ-conditions = 35° C) he finds $K = 8.3 \times 10^{-4}$ and $a = 0.50$. Cyclic PS (at θ-conditions = 28.5° C) gives a value of $a = 0.40$, increasing to 0.46 at 35° C, and 0.50 at 40° C. The constant, a, is also found to increase with increasing $\langle M_w \rangle$. As a consequence, the viscosity ratio, defined as $g' = ([\eta]_{ring} / [\eta]_{linear})_M$, decreases with increasing molecular weight, going from 0.67 at low molecular weight to 0.57 at high molecular weight.

The viscosity ratio is also found to be affected by the solvent, good solvents causing a more dramatic expansion of the linear chain, and thereby decreasing $g'$. By comparison, one would expect that a poor solvent would increase the value of $g'$, making the differentiation of cyclic and linear polymers more difficult in poor solvents. Geiser[7] has measured molecular weight and intrinsic viscosity of linear and cyclic polystyrenes in a series of solvents. He finds that the ratio $[\eta]_{ring} / [\eta]_{linear}$ decreases when moving from a θ-solvent to a "good" solvent such as toluene. The results suggest that the good solvent influences the volume of the linear molecule more than the volume of the cyclic molecule, the linear becoming more expanded that the corresponding cyclic in better solvents. Although Geiser's study did not examine the effect of "bad" solvents directly, the implication of his work is that the poorer the solvent, the more the volume of the linear chains becomes reduced, and the more they behave like cyclic molecules.

This effect prevents the use of intrinsic viscosity for $<M_w>$ determinations for macrocyclic PBT. A poor solvent, such as tetrachloroethane (TCE), does not show a good distinction between the linear and cyclic polymers. Good solvents for PBT, such as hexafluoroisopropanol (HFIP) and the phenol/TCE solution described above, contain free hydroxyl groups that will open the Sn-O linkage in the cyclic molecules[11], rendering the viscosity results useless. Thus an acceptable solvent for cyclic PBT has not been found. Such a solvent would have the following characteristics: 1) it would be a sufficiently "good" solvent that the differences in random coil sizes due to configurational differences are not masked by contractions in the coils caused by unfavorable polymer-solvent interactions, and 2) the solvent would be chemically inert and would not produce chemical chain scissions. Until such a solvent is identified, intrinsic viscosity remains an elusive

goal for determining the molecular weights of cyclic PBT molecules polymerized using stannoxane initiator.

### 6.4.3 End Group Determinations

Another approach to determining the "cyclicity" of polymers is to measure the concentration of end groups relative to the molecular weight of polymer. Several methods are available for this determination including acid titration for carboxylic acid end groups and infrared (IR) spectroscopy or nuclear magnetic resonance (NMR), both of which can identify the presence and concentration end groups. Of these, solid state IR transmission spectroscopy and solution NMR were selected as having the capability for not only identifying suspected end-capping species, but also being able to identify any unexpected, but important, species in the samples.

#### 6.4.3.1 Infrared Spectroscopy

Specimens for solid state IR spectroscopy must be sufficiently transparent to allow transmission of infrared energy. Naturally transparent polymers are well suited to this technique, while naturally crystallizing polymers must be inhibited from crystallization which could scatter or block the radiation. Polybutylene terephthalates are known to be among the most rapidly crystallizing of the common polymers. The resulting spherulitic structure is of sufficient size to completely block both light and IR transmission. Thus to be made usable for IR spectroscopy, the PBT polymers must be quenched rapidly from an amorphous melt into a glassy state. This is only possible by dropping the temperature of the melt below the glass transition temperature so fast that crystal nucleation in the

polymer does not have time to occur. Hobbs[12] has reported that the crystallization half times for PBT are 30 seconds at 200° C and 15 seconds at 190° C. Therefore to prevent PBT crystallization, specimens were prepared from crystallized polymers by first heating above the upper melting temperature (as determined from DSC heating traces), squeezing the polymer into thin films, and quenching the films into a bath of hexane and dry ice. This bath was used to avoid any potential hydrolysis of the c-PBT from a water-based quench bath.

#### 6.4.3.1.1 Preparation of Thin-film Specimens via Compression Molding

Prior to molding, a predetermined amount of stannoxane initiator was predispersed in the BTC oligomers through solution blending in methylene chloride. Once dissolved, the methylene chloride was slowly evaporated until the mixture was nearly dry, then placed under vacuum to finish drying. After vacuum drying overnight at 50° C, the BTC mixture was powdered and redried. (Very dry conditions are necessary when polymerizing BTCs to macrocyclics using stannoxane initiator, because of the rapid hydrolysis of the stannoxane molecule at the temperatures of polymerization.) A BTC plaque containing 0.3 mol % stannoxane was allowed to polymerize isothermally for 30 minutes in a 3" x 5" tool under low pressure in a 190° C preheated compression press. The plaque was formed under low pressure, i.e. 15 psi, and cooled in the compression press under the same pressure at a programmed rate of 200° C/minute. When the press reached 110° C, i.e. just above the glass transition temperature, the press was opened, and the plaque tool removed. The specimen was removed from the tool while still hot, thereby

avoiding the buildup of excess stresses in the specimen by cooling under pressure to a temperature below $T_g$.

To form films for IR spectroscopy, small pieces of the plaque were cut out and thinned by remelting and compressing between Teflon®-coated heavy aluminum foil sheets supported by ferrotype plates. Samples for film forming weighed about 0.3 grams. These samples were preheated at 240° C for two to three minutes, then compressed at 200 pounds pressure for one minute. Quenching was done by opening the press, sliding the aluminum sheet and molten polymer "sandwich" from between the ferrotype plates, and immediately dropping it into the quench bath. Quenching the polymer from 240° C to below $T_g$ was thereby accomplished quickly. Upon separating the aluminum sheets, the polymer specimen was found to be slightly hazy, but thin enough to transmit light. The haze is attributed to surface roughness from molding against the matte surfaces of the PTFE sheets. All specimens were subsequently dried for 16 hours at 135° C under vacuum to remove residual surface water. This drying process, while crystallizing the polymer, produced a sheet which was nearly transparent, and thereby was usable for IR spectroscopy.

Three materials were prepared for analysis. The standard c-PBT polymer from BTCs using 0.3 mol % stannoxane was selected as the basis for the experiment. A premolded slab of polymer identified as SMII-228 was selected. The experiment was designed to answer the following questions: 1) Does stannoxane-initiated c-PBT from BT cyclics contain a significant amount of OH endgroups? 2) Can such polymer be "linearized" by selective methanolysis of the Sn-O bonds? and 3) does thermal degradation

result in a similar linearization of the polymer, with a measurable increase in OH endgroups?

For a control specimen, the polymer was melted and compressed within 3 minutes at 240° C, thereby minimizing degradation. To produce a thermally degraded specimen, another film was melted and held at 250° C for 30 minutes prior to quenching. The methanol degradation was done by immersion a thin film, prepared like the control, for 5 hours in refluxing methanol.

#### 6.4.3.1.2 IR Technique

The IR technique used for OH endgroup measurement is a proprietary method developed by Banach[13]. This method uses an internal peak to determine the specimen thickness. By subtractive techniques, the unknown sample is compared to a similar film containing no OH endgroups at a normalized thickness. The intensity of the resulting OH peak is a direct quantitative measure of the hydroxyl endgroups present in the unknown specimen. By this technique, the results of the three experimental films were as follows:

**Table 6.6 Results of IR determination of OH content for various c-PBTs.**

| **Material** | *Thickness (mm) (overtone method)* | *[OH] after subtraction* | ***Calculated [OH] meq/Kg*** |
|---|---|---|---|
| Control | 0.571 | 0.0271 | 17.9 |
| Methanol Degraded | 0.219 | 0.065 | 70.2 |
| Thermally Degraded | 0.22 | 0.048 | 50.5 |

The hydroxyl content increase from both the methanolysis and thermal degradation implies that the stannoxane link is readily degraded by both techniques. The hydroxyl endgroup content measured in the control is significantly higher than could be expected

form fully cyclic resin. This may imply that there was some linearization in the specimen prepared by the relatively mild compression molding conditions. These results appear inconsistent with the earlier reports of c-PBT maintaining a high degree of crystallinity after relatively short excursions into the melt[4].

The current results lead two possibilities that could rationalize the high hydroxyl content in the control film. The first possibility is that the stannoxane link is readily degraded at short times in the melt, but the diffusion of the newly formed linear chain is too slow to affect the crystallizability of the polymer. This reasoning would suggest that diffusion is very slow for PBT at 240° C. However at this temperature, the molten resin is at least 180° C over $T_m$ and any diffusion should be very fast.

Another possibility is that residual water has degraded the stannoxane link during the quenching process. In an earlier experiment aimed at using infrared spectroscopy to determine OH content, a specimen was quenched directly into an ice water bath. This specimen was subsequently measured as having 50 meq/Kg OH content, the same as the specimen which was thermally degraded. These results suggest that the degradation is occurring in the melt, where any residual moisture in the air or on tooling surfaces can degrade the stannoxane link, which becomes especially evident in these thin films.

#### 6.4.3.2 Nuclear Magnetic Resonance

Over the past twenty or thirty years, Nuclear Magnetic Resonance (NMR) has become the most valuable tool available for detailed analysis and understanding of organic compounds It complements both infrared spectroscopy, which is used to determine what

functional groups are present in an unknown organic material, and mass spectroscopy which is used to determine the molecular weight and formula.

Certain atomic nuclei behave as though they are spinning about an axis and as such, their individual electric fields give rise to individual magnetic fields. Within a PBT molecule, the carbon and hydrogen atoms both have isotopes present that are detectable by NMR. These are the $^{1}H$ isotope for hydrogen, and the low concentration $^{13}C$ isotope for carbon. Stannoxane-initiated c-PBTs also have an identifiable isotope,$^{119}Sn$.

Without any external magnetic interference, these isotopes spin in random orientations, however their spin axis will become aligned by the application of a strong magnetic field. Under this condition, the isotope axis will either take on an orientation parallel to the external magnetic axis, or against the external magnetic axis. Because the parallel alignment is lower energy, most of the nuclei are found in this position.

When a secondary energy source is imposed, the lower energy state nuclei absorb additional energy and "spin-flip" to the higher energy state. This is accomplished by pulsing an orthogonally applied alternating radio frequency (rf) signal into the system. Various frequencies of energy are resonant to different protons, which flip and then decay back to their original spin states. The energy loss to absorption can be detected and used to determine which types of nuclei have absorbed the additional energy.

The IR experiment suggested that there is a considerable number of endgroups in what was believed to be cyclic c-PBT, which had been prepared at 190° C, after re-melting the polymer at 240° C for less than three minutes to produce a film specimen. To confirm that the cyclic structure could be degraded by very mild conditions in melt processing, a thin specimen was prepared using 0.3 mol % initiator in a compression press

at 232° C for 2 minutes. The pre-polymerization and remelting was similar to that described for IR specimen preparation in the previous section with the only differences being the lower temperature and shorter time in the melt. The specimen was dissolved in $d_2$-TCE by heating gently with a hot air gun. Once dissolved, the specimen was inserted into the NMR, heated to 70° C to maintain the solution, and data was collected for four hours.

The OH endgroup signal, which appears at $\delta = 3.6$ ppm downfield, was too small to measure after the first 30 minutes. With time in the NMR this weak signal continued to grow. After four hours, the signal was integrated and the OH endgroup concentration was determined to be 60.6 meq/Kg. This concentration of OH is just above the concentration determined by IR for thermally degraded c-PBT. Residual moisture in the solvent is suspected as a hydrolyzing agent, because of the time dependent appearance of the endgroup signal. A repeat of this experiment, using molecular sieve to pre-dry the $d_2$-TCE also showed a lower level of hydroxyl endgroups, growing to 25.8 meq/Kg after 12 hours at 70° C. This lower level suggests that there was still sufficient residual moisture in the dried solvent to hydrolyze the stannoxane when the solution is maintained at 70° C for an extended period.

While not proving that the stannoxane initiated c-PBT was free from linear polymer, this experiment gives an indication of the ease of hydrolysis of the cyclic polymer. When c-PBT, prepared by isothermal polymerization and rapid crystallization at 190° C, is either re-melted or put into solution, any residual moisture in the environment will hydrolyze the Sn-O linkages, opening the rings and resulting in linear polymer. Both

ends of the linear polymer produced by hydrolysis will have a hydroxyl endgroup as shown earlier in Figure 5.6.

A second NMR experiment was attempted to better understand the degradation mechanism of the Sn-O linkage. A c-PBT specimen identified as SMIII-54 was prepared and polymerized at 190° C using 6.0 mol % stannoxane. This high level of initiator was used to produce sufficient tin content in the polymer that the weak $^{119}Sn$ isotope could be monitored. Three materials were analyzed in this experiment: 1) a specimen of the pure stannoxane initiator, 2) SMIII-54 after remelting for 2 minutes at 232° C and, 3) SMIII-54 after remelting for 15 minutes at 250° C.

The stannoxane specimen was dissolved in $CDCl_3$ and run at room temperature. the polymer specimens were dissolved in $C_2D_2Cl_4$ and run at 85° C. A 500 MHz NMR was used for this experiment. The results of the analysis are shown in Figure 6.86 and Table 6.7.

**Table 6.7 $^{119}Sn$ NMR shifts for stannoxane degradation experiment.**

| Specimen | NRM Shifts (ppm) | | | |
|---|---|---|---|---|
| Stannoxane initiator | | | -137.1 | |
| c-PBT Remelted at 232° C | -91.5 to -91.7 | | -139.0 to -139.3 | -182.4 to -184.7 |
| c-PBT Degraded at 250° C | | -117.5 to -118.4 | -137.0 to -137.1 | |

Stannoxane initiator alone is found to produce a single shift, at -137 ppm upfield. This shift therefore represents the local electron environment of the tin atoms in the stannoxane molecule. This environment results from the pull from two oxygen atoms, and the electron donation from two butyl groups on the tin atom. When polymerized using stannoxane initiator, c-PBT is found to produce a triplet peak, centered at the same upfield shift as the tin signals found in the pure stannoxane analysis. This triplet, with

relative intensities of 1:2:1 is characteristic of spin splitting. This type of peak is known to result from two different interactions with the tin[15]. The minor peaks are nearly symmetrically located at +/- 45 ppm from the main peak. The two different electron attractions may result from the local short-segment interactions on the tin atom as described above, with the addition of local carbonyl oxygens in the PBT segments. When this polymer is thermally degraded to linear chains, a single peak similar to the pure initiator is found, but the secondary attractions are absent. The implication is that the singlet again represents a uniform electron environment around the tin isotope, with the same electron deficiencies found in the original stannoxane molecule

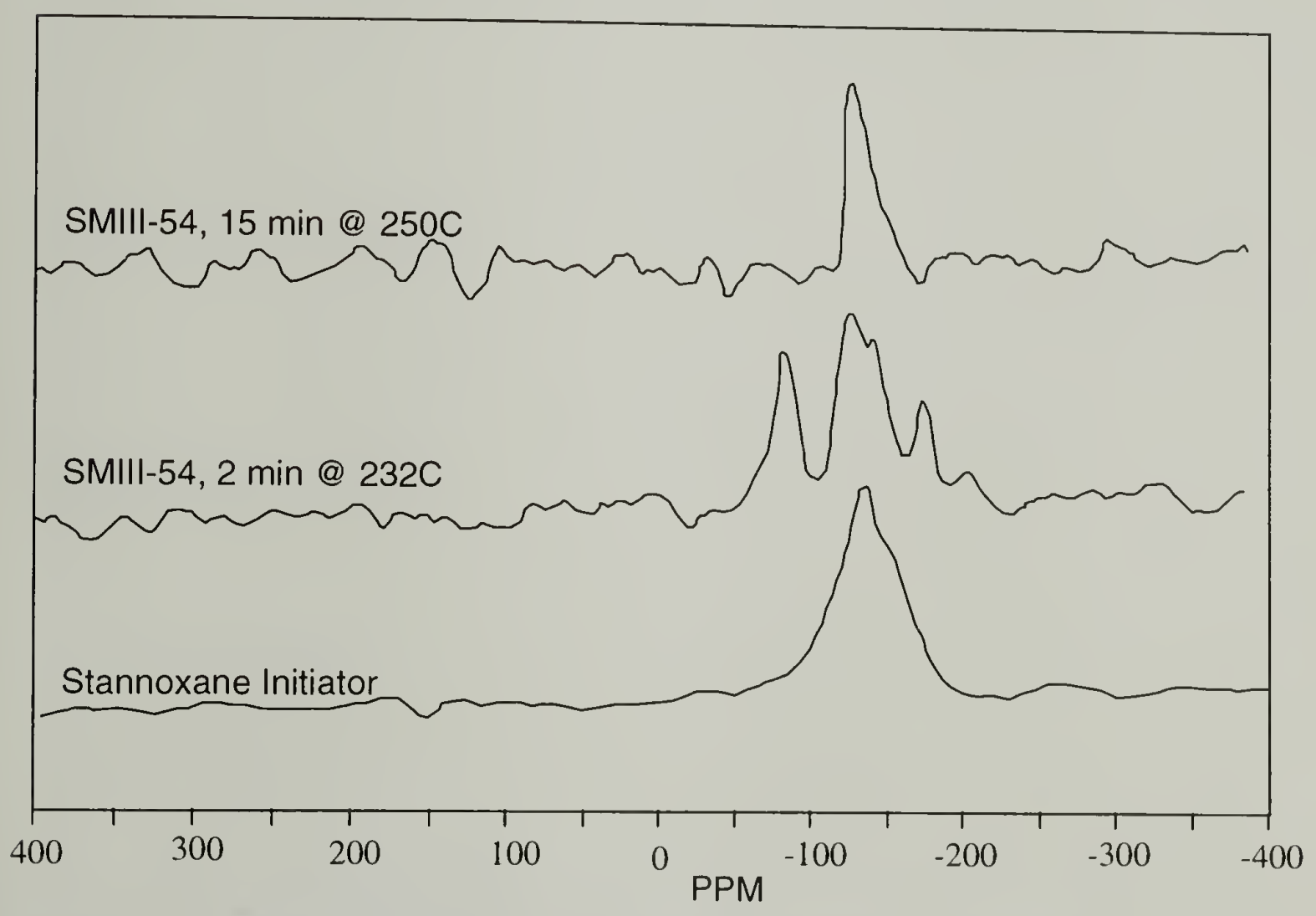


**Figure 6.86 $^{119}$Sn NMR peaks for stannoxane degradation experiment.**

The original singlet is produced by a symmetric attraction of electrons about the tin in the stannoxane molecule. Both tin atoms have the same electron environment and the signal is reinforced by this symmetry. When polymerized, the tin atoms are in the same

local environment along the polymer chain, but there is an additional attraction between the tin atoms and the carbonyl oxygens from the PBT linkages in the polymer. These attractions are both intramolecular and intermolecular. At this high initiator loading, the cyclic molecules have low molecular weight, resulting in many coordination sites in the molecule. Thermal degradation changes the ability of the tin to coordinate to the carbonyl oxygens. The complex chemistry of stannoxane degradation is not understood, but this experiment suggests that the tin atom is again in an electron environment identical to what is found in the initiator molecule. The small peak located 20 ppm downfield from the main peak is not identified, but is only found in the thermally degraded specimen, suggesting that there is some minor coordination between the tin and another moiety in the degraded polymer. The degradation appears to be either straight chain oxidation or disproportionation[13].

### 6.4.4 References for Molecular Dimensions


1)Zimm, B.; Stockmeyer, W., *J. Chem. Phys.* **1949**, *17*, 1301.
2)Edwards, C. J. C.; Stepto, R. F. T.; Semlyen, J. A., *Polymer* **1982**, *23*, 869-872.
3)Hild, G.; Strazielle, C.; Rempp, P., *Eur. Polym. J.* **1983**, *19*, 721-727.
4)Ishizu, K.; Kanno, H., *Polymer* **1996**, *37*, 1487-1492.
5)Semlyen, J., *Pure and Applied Chemistry* **1981**, *53*, 17971804.
6)Benoit, H.; Grubisic, Z.; Rempp, P.; Decker, D.; Zilliox, J., *J. Chim. Phys. Phys.-Chim. Biol.* **1966**, *63*, 1507.
7)Geiser, D.; Hocker, H., *Macromolecules* **1980**, *13*, 653-656.
8)Roovers, J.; Toporowski, P., *Macromolecules* **1983**, *16*, 843-849.
9)Borman, W. F. H., *Journal of Applied Polymer Science* **1978**, *22*, 2119-2126.
10)Roovers, J., *Journal of Polymer Science: Polymer Physics Ed.* **1985**, *23*, 1117-1126.
11)Brunelle, D. J., Personal Communication.
12)Hobbs, S.; Pratt, C., *J. Applied Polymer Science* **1975**, *19*, 1701-1705.
13)Banach, T. M., Personal Communication.
14)Kambour, R.; Barnes, J.; Garbauskas, M.; Gundlach, P.; McCracken, L. "Microstructure, Morphology, and Crystallinity Level in Polybutylene Terephthalates Produced from Cyclic Oligomers: A Progress Report.," Manuscript in preparation.
15)Atkins, P. W. *Physical Chemistry*; 3d ed.; W H Freedman and Co.: New York, NY, **1986**.

## 6.5 Mechanical Testing

The mechanical properties of any polymer solid are the result of its basic molecular and morphological properties. Peterlin[1] suggests these parameters for a semi-crystalline polymer of good physical properties must be:

1) strong covalent bonds between the atoms along the backbone of the polymer,
2) van der Waals intermolecular forces within the polymer crystal, i.e. forces that are weak in comparison to the covalent bonds,
3) a region of amorphous material, usually less than 50% of the total structure, where weaker van der Waals forces are present (based on shorter coordinated sections between adjacent molecules and greater separation of these molecules), and
4) tie segments that exist in the amorphous regions and connect the lattices of adjacent crystals. These tie segments provide small elastic resistance at low strains, and high energy-elastic forces at high elongations, as the tie molecules become strained to nearly their full extension.

With this well accepted framework as a model, a series of mechanical evaluations have been undertaken on the PBTs of present interest.

For any given polymer the covalent bonding forces are fixed and the van der Waals forces depend on the way the chains are distributed within the solid structure. Variation in the properties of a semi-crystalline polymer with spherulitic morphology are the result of changes in two structural parameters within the solid polymer, the degree of crystallinity and the number of interlamellar tie chains that stabilize the crystalline structure. When the degree of crystallinity is increased, there is an associated increase in modulus. These increases in crystallinity and modulus are commonly the result of annealing of semi-

crystalline polymers which treatment causes the modulus over the entire temperature range of the solid to be increased. The transition temperatures (Tg and Tm) however remain constant[2].

The interlamellar tie chain density is a more elusive parameter to determine. Keith[3] suggests that the most important function of interlamellar tie chains is to transmit stress between the crystallites. The existence of intercrystalline tie chains is believed to be critical to strength and ductility in semi-crystalline plastics.

Within this context, four linear PBT resins and two macrocyclic PBT resins have been tested in both tension and compression up to their failure stresses, to determine both elastic responses and ultimate properties. Small variations between test results for these polymers are correlated to differences in crystallinity and tie chain density. Because each polymer necessarily had a different degree of crystallinity, the crystallinity of each specimen was measured by taking a section of the core of the specimen and determining its heat of fusion on first melting. In addition, the same mechanical and thermal testing was carried out on a series of linear PBT specimens that had been annealed to increase the crystallinity and bring them into the crystallinity range of the c-PBT.

### 6.5.1 Tensile Studies

The response of a polymer to a tensile load is the most common type of test used in characterizing the mechanical performance of the material. Strength, modulus, and elongation at failure are all obtained from this single experiment. When these fundamental parameters are not well characterized, they may lead to the misapplication of a material for a mechanical or structural design.

The stress developed in a polymer under a given applied strain is a function of intensive variables in the polymer such as molecular weight and chain strucutre, and is also affected by the polymer's current local environment and environmental history. Thermal aging and prior exposure to solvents can affect the degree of crystallinity and degree of plasticization in the polymer. In addition the stress-strain behavior will be determined by extensive variables such as temperature and deformation rate. To minimize the effect of these variables, standard conditions for specimen preparation, conditioning, and testing are specified by regulatory agencies such as American Society of Testing and Materials (ASTM), the British Standards Institute (BSI), the German standards group Deutschen Institut für Normen (DIN), the Japanese International Standards Organization (JISO), or the more recent International Standards Organization (ISO). An accurate comparison of materials, even within the same generic material type, requires a complete consideration of the material's response to a variety of loading situations. As a starting point, differences in the response to a simple uniaxial tensile force can help the researcher identify subtle differences in the material under evaluation.

Tensile characteristics are generally reported in terms of "engineering stress" vs. "engineering strain". This simplification in testing allows for stress to be calculated from the force and the dimensions of the original cross section of the test specimen (engineering stress) and strain to be calculated from the length under stress divided by a nominal gage length, i.e. the length of the specimen gage before deformation (engineering strain). More rigorous deformation data are produced by attaching gages to the specimen to monitor true strains in the specimen during deformation. By using strain gages in both the extension direction and transverse direction, the volume strain is determined, and

Poisson's ratio is easily calculated. This additional information gives insight into the mechanisms of volume change in the material under evaluation.

Four linear PBTs covering a wide range of molecular weights were evaluated in tension using two strain gages to monitor the axial and transverse strains during extension. Specimens were prepared to conform with the ASTM D638 Type I geometry by carefully routing the "dog bone" shapes out of injection molded plaques. Edges were smoothed using Emory paper to remove any residual nicks or scratches from the cutting operation.

Tensile specimens of c-PBT were cut from a compression molded plaque of SMII-60 (0.12 mole % stannoxane initiated c-PBT). This plaque was polymerized in the compression press at 190° C for 20 minutes in a 4" by 5" by 0.95" thick "open-frame" tool, then cooled to room temperature under constant pressure. A foil liner was used in the tool, as described earlier, to minimize material loss prior to polymerization. (See the Section 6.1.1 on molding c-PBT.)

A typical trace of engineering stress vs. axial strain for a linear PBT is shown in Figure 6.87 and a comparison trace of engineering stress vs. transverse strain for PBT is shown it Figure 6.88. Both of these traces are for a ductile PBT which develops a stable propagating neck after yield. The drop in stress at the yield point is typical of a semicrystalline polymer. Analogous traces were generated for each resin. PBTs of lower molecular weight broke in tension before necking was observed.

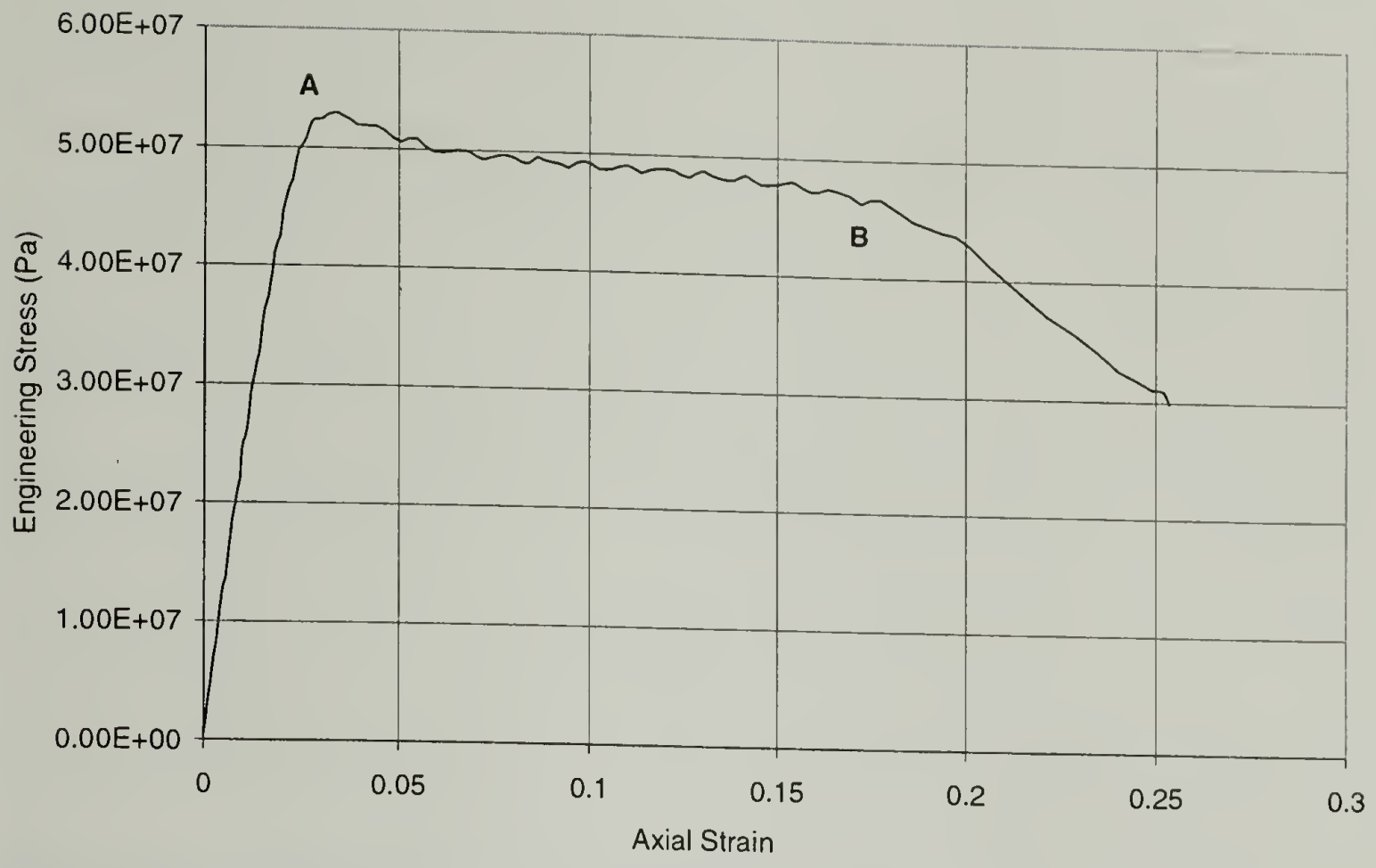


**Figure 6.87 VALOX 315 PBT Engineering Stress vs. Axial strain. Point A is the yield point. Point B is the onset of stable neck formation and drawing.**

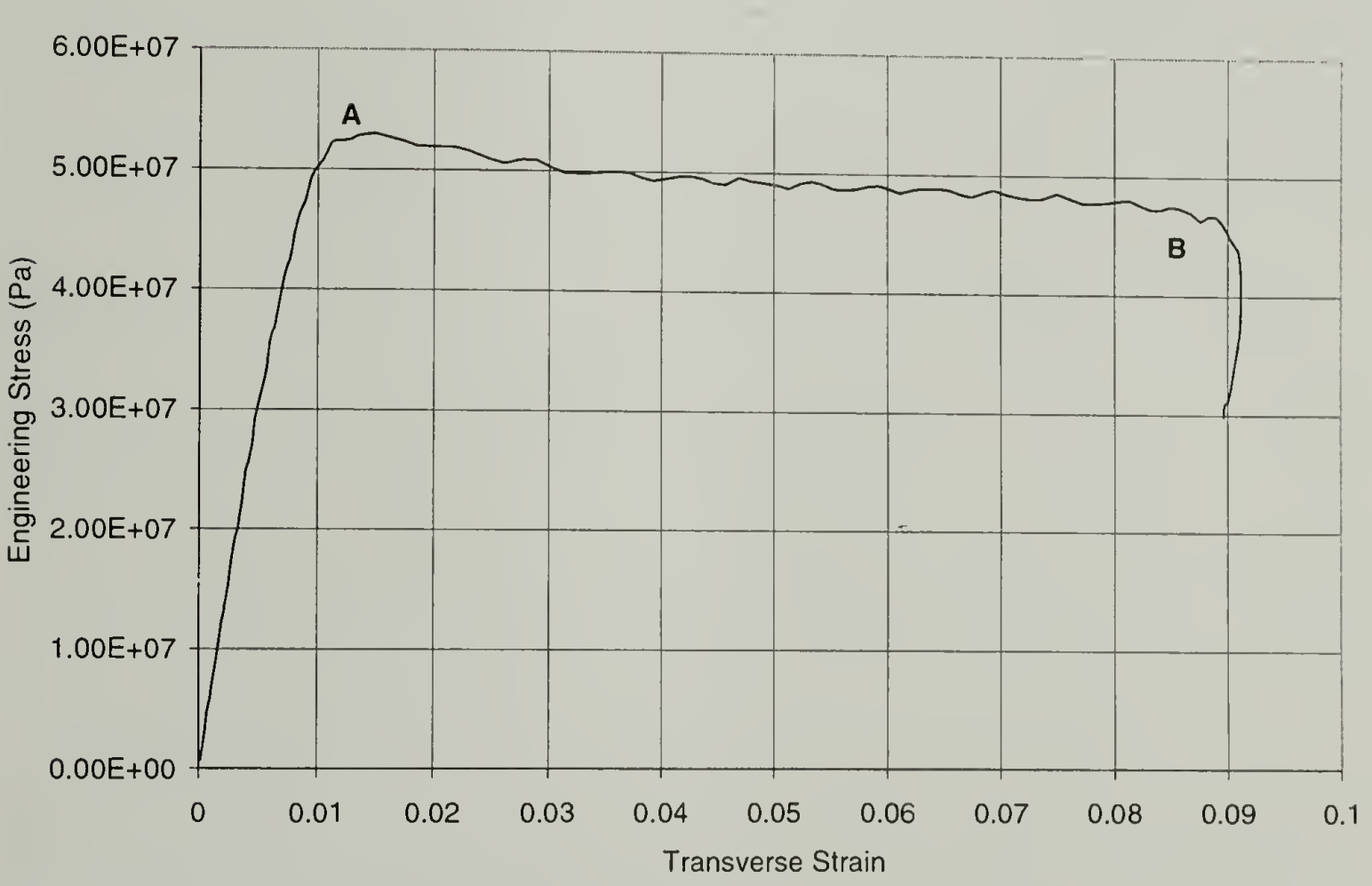


**Figure 6.88 VALOX 315 PBT Engineering Stress vs. Transverse Strain. Point A is the yield point. Point B is the onset of stable neck formation and drawing.**

Poisson's ratio is determined from a ratio of the elastic strains;

$$\nu = \frac{\varepsilon_{transverse}}{\varepsilon_{axial}}.$$

(Note that both strains are here defined as positive. Transverse strain is conventionally defined as a collapse, or negative strain as related to the extensional strain in the axial direction. By convention then, Poisson's ratio is the negative ratio of these strains.) Poisson's ratio is shown graphically in the linear elastic deformation region in Figure 6.89. A plot of transverse strain vs. axial strain at higher strain levels reveals a volume dilation in the polymer at the onset of plastic deformation. As shown in Figure 6.90, the lower slope in the linear elastic region is followed by an slower increase in transverse strain for a continued incremental increase in axial strain. This nonlinear behavior is the result of volume dilation in the polymer during yield.

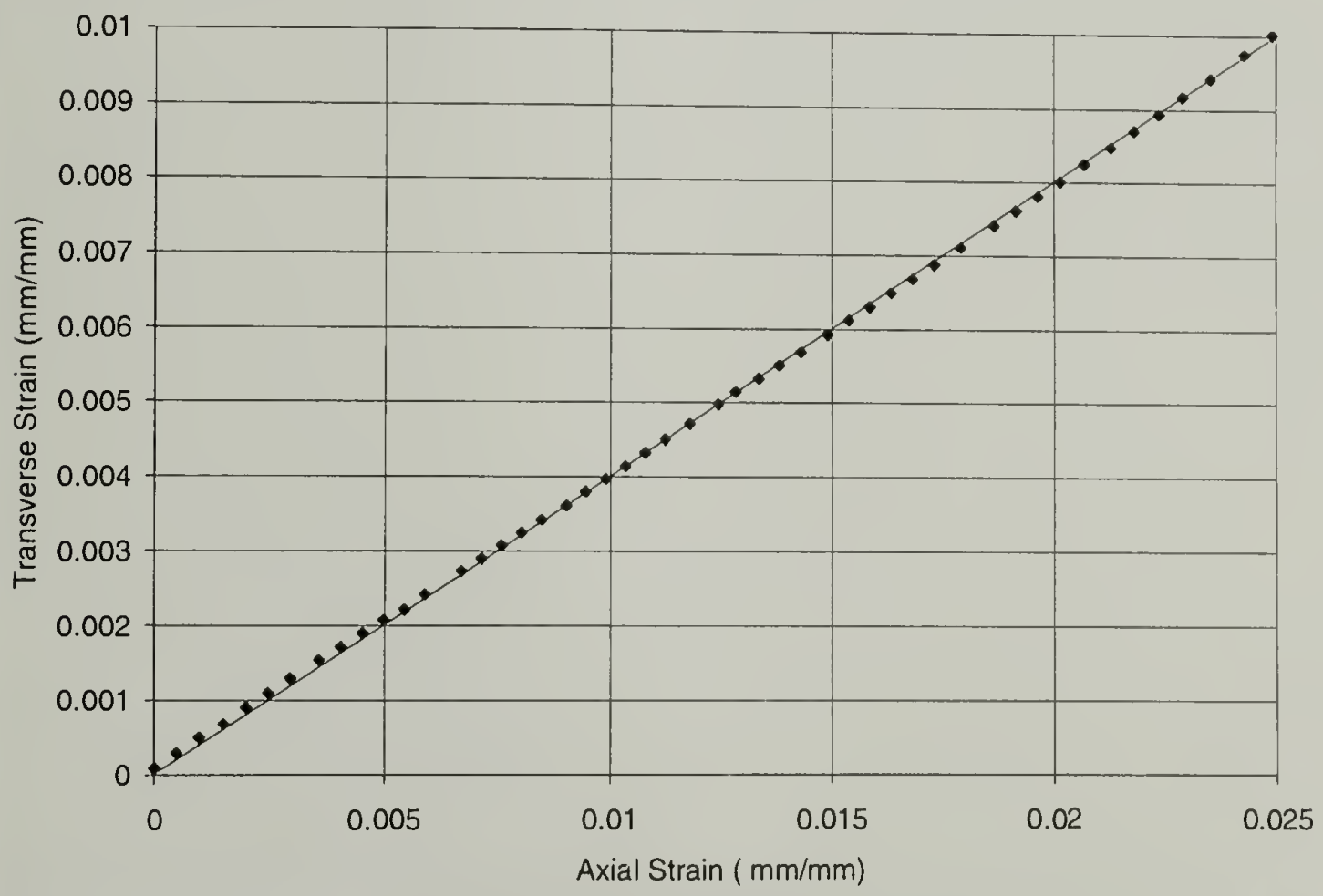


**Figure 6.89 Poisson's Ratio for VALOX 315 PBT. Slope is Poisson's Ratio = 0.392**

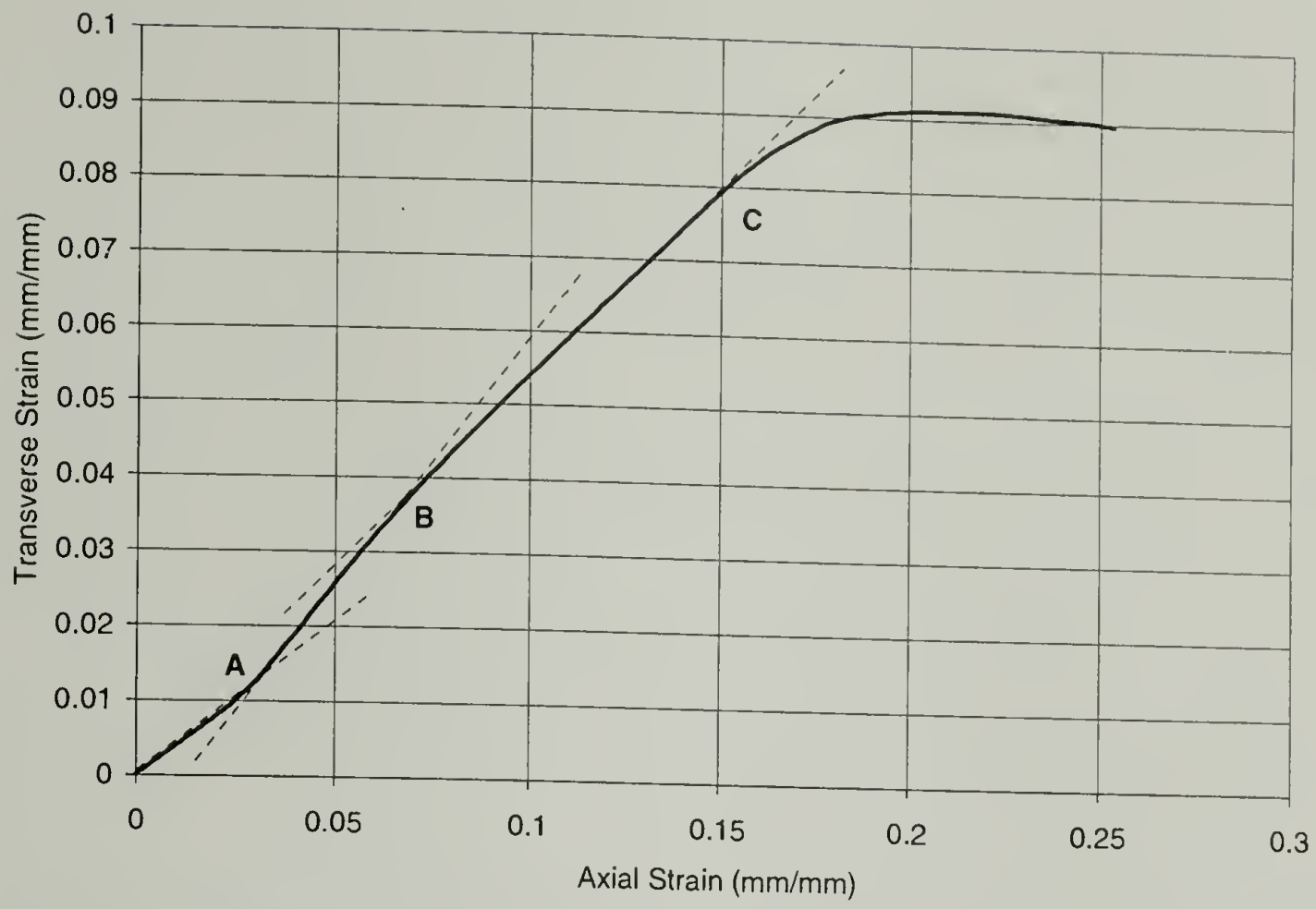


**Figure 6.90 Differential Volume of VALOX 315 PBT at high strains. Point A marks the end of the elastic region, and the yield point. Between point A and point B is the region of volume increase during yield. From point B to point C is the stable draw zone beyond yield. Point C marks the onset of neck formation. Beyond point C is stable drawing of the neck.**

Beyond yield (between points B and C in Figure 6.90), the polymer continues to draw with a strain ratio corresponding to that of the elastic region (Poisson's ratio) until the neck forms. Once the neck is stabilized, this high molecular weight PBT will continue to draw in a ductile manner. The data collection was stopped once the neck was well formed. A nearly identical differential volume change is seen in VALOX 310 PBT as it yields and begins to deform plastically as shown in Figure 6.91.

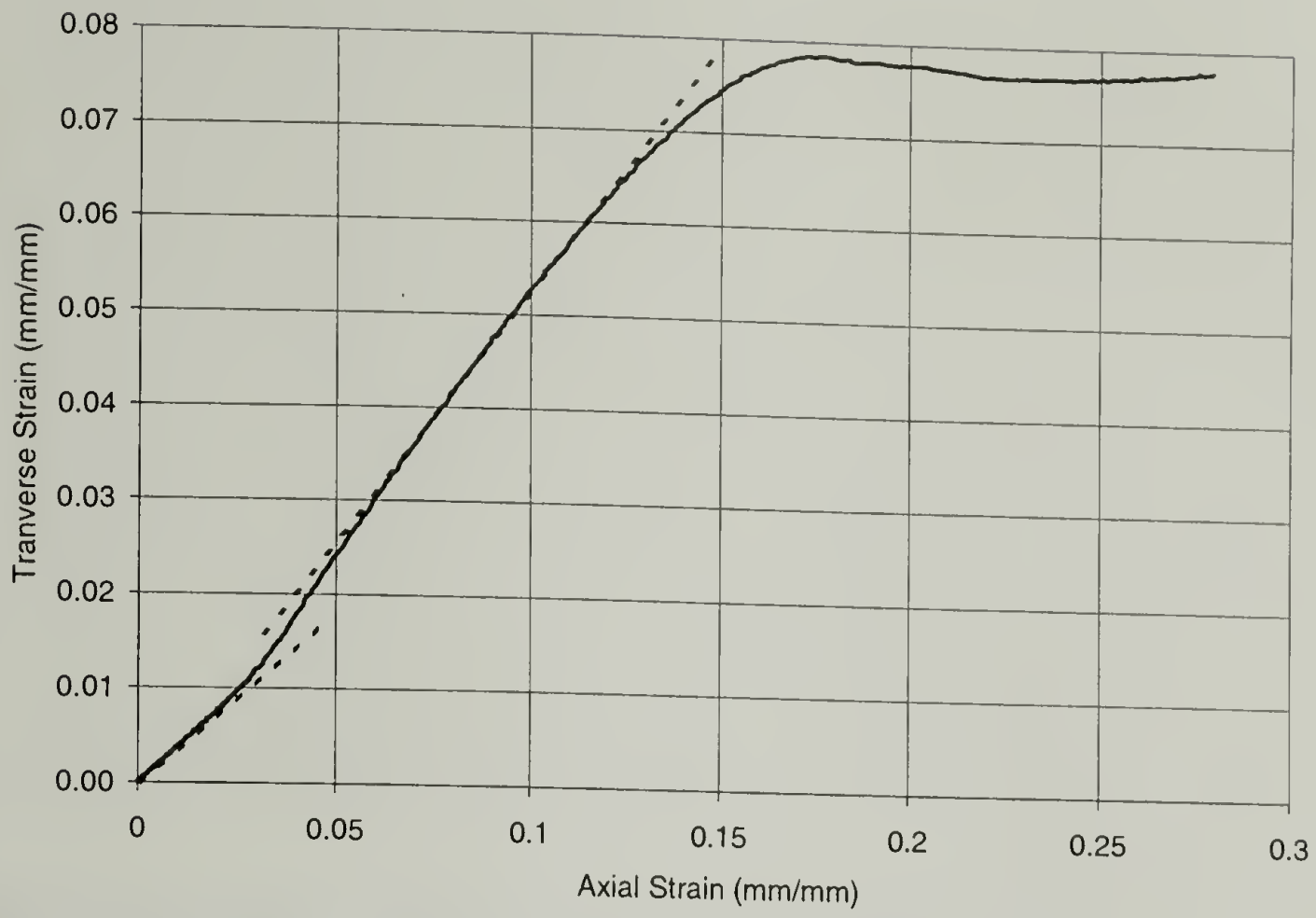


**Figure 6.91 Differential Volume of VALOX 310 PBT at high strains.**

The stress vs. strain trace for each of the five PBT resins is shown in Figure 6.92 Reduced data from these curves are compiled in Table 6.8. The resins are seen to all have similar moduli, differentiated by and dependent on differences in the degree of crystallinity. These resins differ more in terms of their elongations to failure and their Poisson's ratios. Linear resins with high molecular weight (above 70,000 Daltons) show a ductile yield, followed by development of a stable neck that draws through the full length of the specimen's gage section. Specimens of linear resin with $<M_w>$ between 50,000 and 70,000 Daltons begin to yield but fracture before necking. Low molecular weight linear PBT specimens ($<M_w>$ less than 50,000) break in a brittle manner before yielding. This resin (VALOX 195 PBT) also has a higher modulus than the other linear resins, because of its higher crystallinity (see Figure 6.93). Another factor in the brittleness is that VALOX 195 PBT is found to be below the critical molecular weight for entanglement as determined in low shear rate melt viscosity measurements as discussed in Section 6.3.1.6.

This resin is found to crystallize more rapidly and to a higher final crystallinity, with higher modulus and lower toughness (as determined by the integrated area under the stress strain curve at break) than is the case for the higher molecular weight PBTs. By contrast, the cyclic PBT resin exhibited the same strain to failure and same toughness as low molecular weight linear resin, although it has the highest molecular weight of any of the resins evaluated.

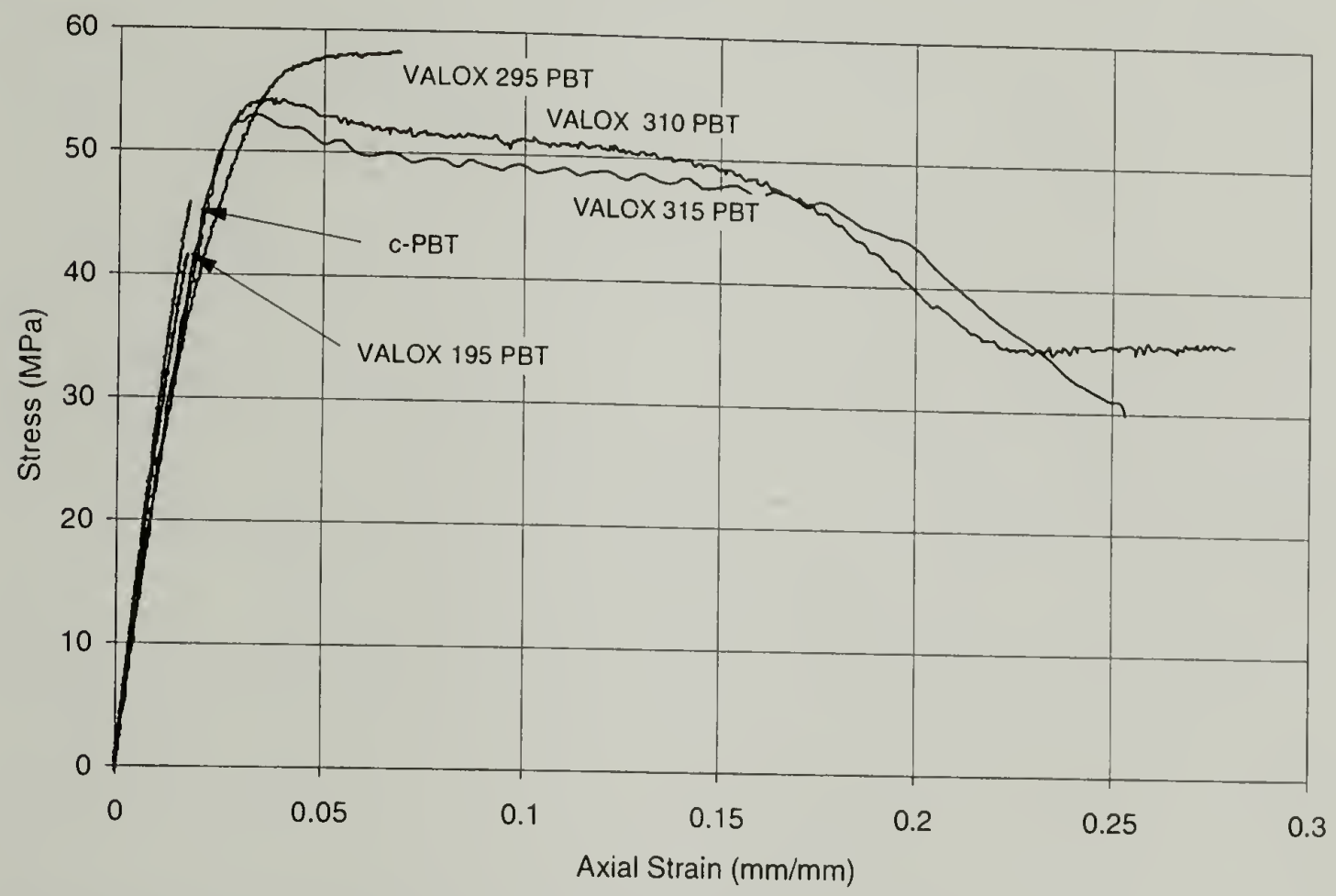


**Figure 6.92 Full Tensile Curves for PBT resins.**

**Table 6.8 Tensile Characteristics of PBT resins.**

| Resin | Modulus (MPa) | Poisson's Ratio | Yield Stress (MPa) |
|---|---|---|---|
| VALOX 195 PBT | 2740 | 0.41 | 41.6* |
| VALOX 295 PBT | 2450 | 0.42 | 58.3 |
| VALOX 310 PBT | 2420 | 0.37 | 54.3 |
| VALOX 315 PBT | 2430 | 0.39 | 53.0 |
| c-PBT (SMIII-60) | 3020 | 0.34 | 45.9* |

* Brittle Fracture prior to Yield

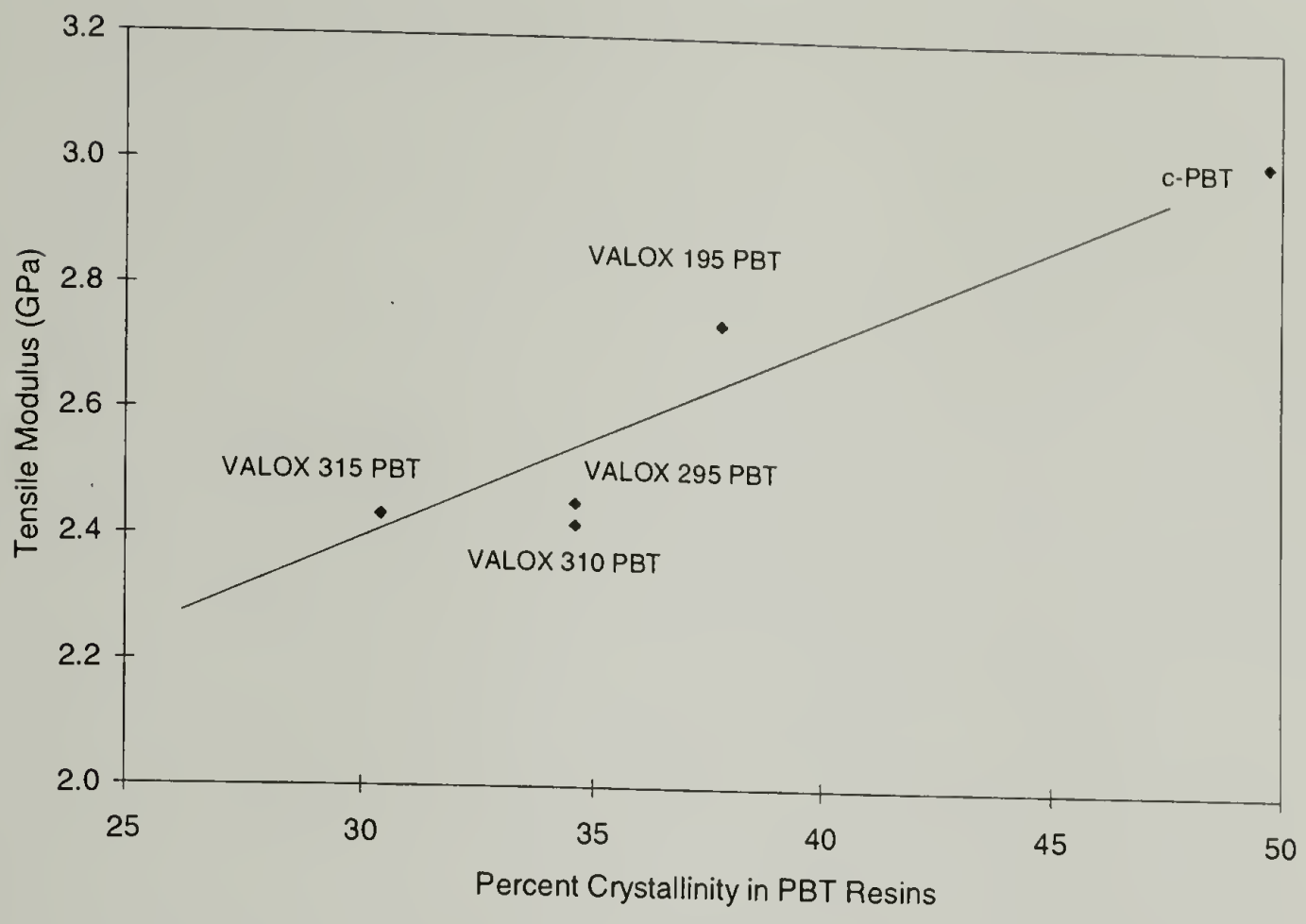


**Figure 6.93 Tensile Modulus increase with Crystallinity for PBT resins.**

Cyclic PBT appears to have the same extent of toughening mechanisms as VALOX 195 PBT. In Peterlin's model[1], a critical element of these toughening mechanisms for a crystalline polymer is the tie molecules that connect adjacent lamellae, and stabilize the spherulitic structure against crack initiation under a slowly applied tensile force. The influence of the tie molecules is greatest when the non-crystalline fraction of the crystalline polymer is above its glass transition temperature. At temperatures far below $T_g$, the glassy intercrystalline layers resist deformation. (Creep mechanisms would allow for a slow deformation of the glass, but this type of deformation is negligible at the elongation rates used in tensile testing.) The $T_g$ of purely amorphous PBT to be about 30° C, which is 7° C above the test temperature used in these tensile evaluations. The proximity to the amorphous $T_g$ allows high molecular weight linear PBT to be drawn and necked at low strain rates without brittle fracture. Peterlin[4] also suggests a deformation

model for semi-crystalline polymers (above $T_g$) on which the tie molecules become stretched under a tensile load. Given the right combination of draw rate and temperature, the tie molecules will begin to reorient the crystalline structure by first tilting the crystallites by slipping the chains, then pulling chains from developed crystals, reorienting the chains in the draw direction, and reforming crystal structure with the chains aligned to better carry the load. This model results in a higher number of tie chains in the oriented polymer, which is then capable of withstanding loads beyond the yield stress. A high density of amorphous tie molecules is believed[5] to be responsible for the toughness and stable neck formation under high strains for the high molecular weight PBT resins. The lack of toughness in low molecular weight PBT would then be the result of fewer intercrystalline tie chains. Macrocyclic PBT, rapidly polymerized to high molecular weight and crystallized at 190° C, has high crystallinity but apparently has few tie chains, and consequently low toughness.

Nielsen[6] reached a similar conclusion based on published results[7] of linear and branded polystyrenes. Tensile strength for the two different molecular architectures was found to correlate with melt viscosity but not with molecular weight, because of branching. Nielsen's analysis concludes that molecular entanglements not only have a strong effect on melt viscosity but also on the strength of solid polymers.

For crystalline polymers, the degree of crystallinity is known to be inversely proportional to the molecular weight. Low molecular weight polymer also tends to collect at the boundary between spherulites, reducing the number of inter-spherulitic tie molecules. Thus low molecular weight polymers tend to be brittle and weak. For crystalline polymers, it is generally difficult to separate the behaviors resulting from

molecular weight and the behaviors resulting from degree of crystallinity which may change with molecular weight.

Poisson's ratio gives additional insight into the molecular structure of these PBT resins. For a soft polymer such as polyethylene under tension at a low strain rate, volume is conserved and Poisson's ratio is equal to 0.50. As the material becomes less plastic, the transverse strain becomes smaller with respect to the axial strain and Poisson's ratio decreases to a value of 0.33 for a hard plastic[8]. Van Krevelen[8] suggests that there is a direct relationship between Poisson's ratio and the maximum elongation to break for a wide range of linear polymers. Poisson's ratio is a measure of the liquid-like character of a material, and lower Poisson's ratio implies less liquid-like characteristics. Macrocyclic PBT, being highly crystalline and with few tie molecules, exhibits a Poisson's ratio lower than typically found for thermoplastic polyesters. Only glasses such as acrylic and thermosetting resins such as phenolformaldehyde have a Poisson's ratio in this range.

### 6.5.2 Tensile Modulus as a Function of Temperature

Above $T_g$, amorphous intercrystalline material becomes rubbery, and the modulus of a semicrystalline polymer could be expected to correlate to its intercrystalline tie chain density. Dynamic mechanical thermal analysis (DMTA) was used to investigate this hypothesis for two linear and two macrocyclic PBT resins. The DMTA technique allows a simple determination of the elastic modulus, E', and loss modulus, E", in tension as a function of temperature while working at low strains and low frequency. The response to a steady state sinusoidal stress is a steady sinusoidal strain at the same frequency, but with

a phase shift which is related to the energy loss in the system. Thereby, a mechanical relaxation $T_g$ can also be characterized by this technique.

The complex modulus, $E^*$, is the sum of the components of the elastic modulus, E', and loss modulus, E", i.e. $E^* = E' + i E''$ , with magnitude $E^* = ( E'^{\,2} + E''^{\,2})^{1/2}$.

Thus, $E' = | E^* | \cos \delta$ , $E'' = | E^* | \sin \delta$ , and their quotient, $\frac{E''}{E'} = \tan\delta$. Loss modulus and tan δ both exhibit a maxima in the region of the glass transition[9]. Below $T_g$, the modulus is dependent on the rigidity of the glassy phase and the degree of crystallinity for a semicrystalline polymer. Since glassy polymers have all roughly the same modulus, the only correlation of differences in moduli for semi-crystalline polymers is expected to be in their degree of crystallinity. As the temperature is increased to above $T_g$, the amorphous intercrystalline polymer softens, and applied stresses must be carried by the tie chains which link the crystallites. To this end DMTA might be expected to show a difference in the moduli of PBTs of constant crystallinity, arising from differences in their tie chain densities.

The results of the elastic modulus determined by DMTA, from room temperature to just below the melting temperature, are shown for PBTs in Figure 6.94 Loss Modulus and Tan δ over this temperature range are shown in Figures 6.95 and 6.96.

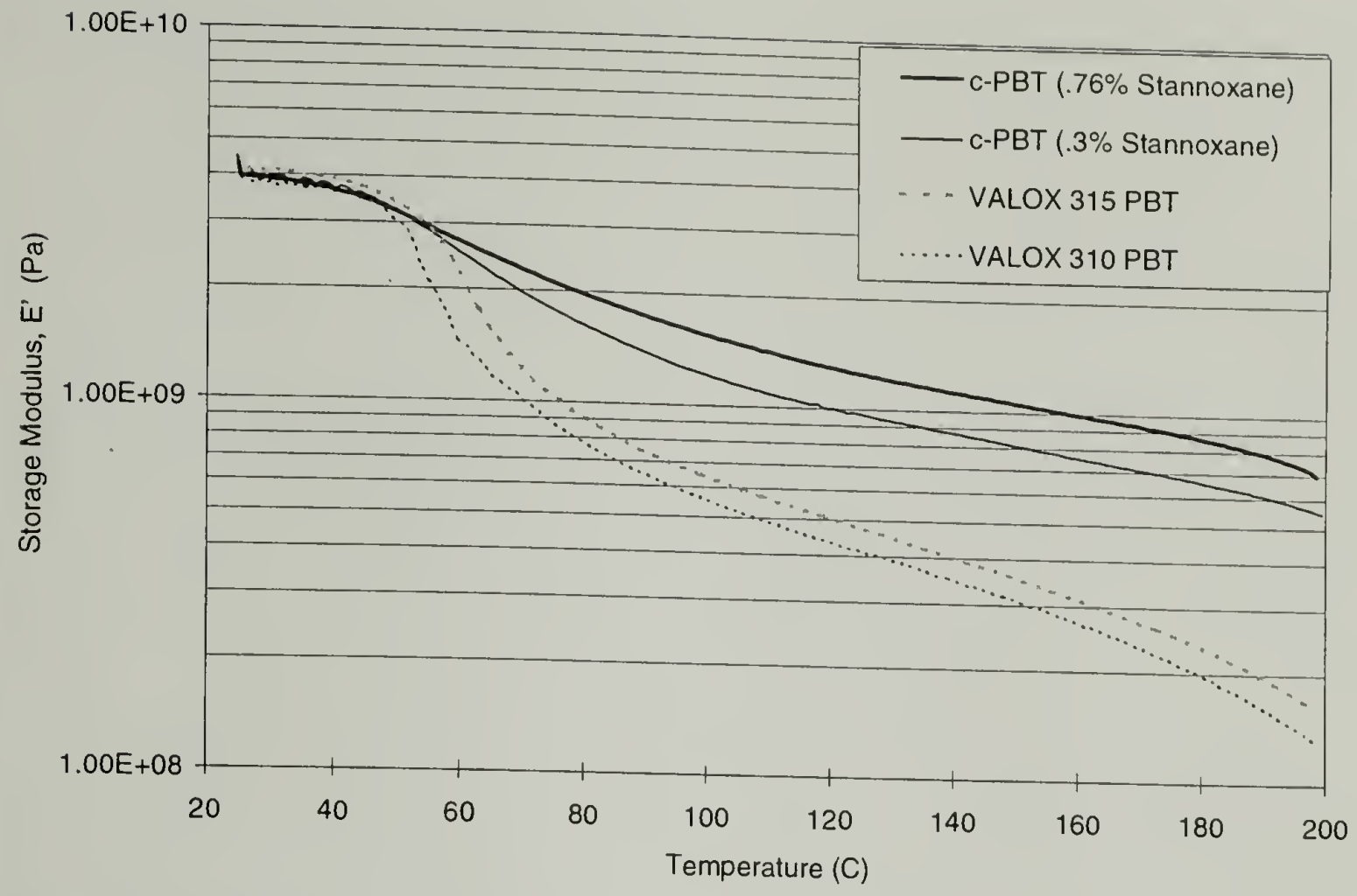


**Figure 6.94 Elastic Modulus vs. Temperature for 4 PBT resins.**

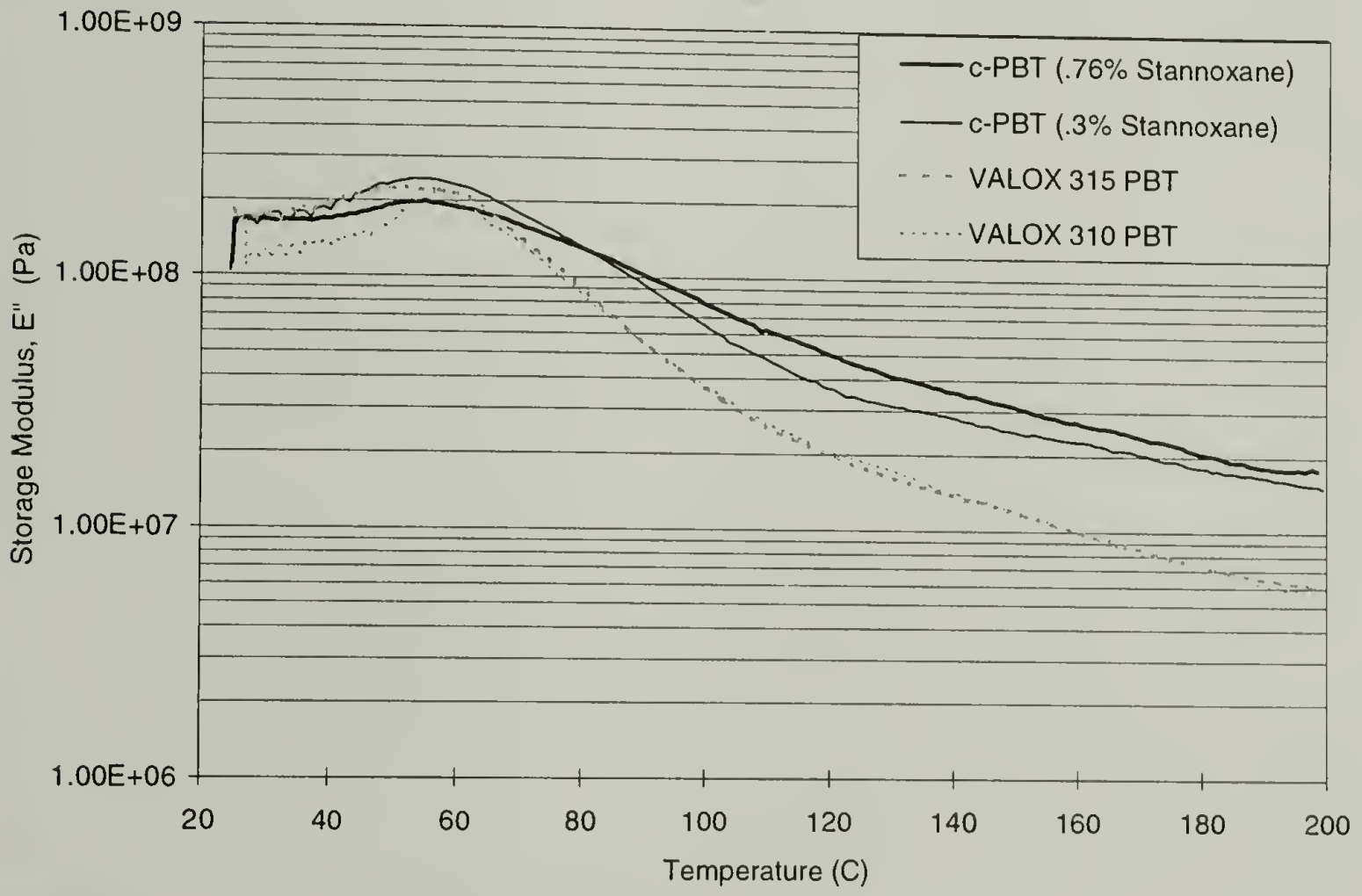


**Figure 6.95 Storage Modulus for 4 PBT resins.**

Unexpectedly, the elastic moduli of the macrocyclic resins were retained above $T_g$ better than for the linear resins. In hindsight, this is believed to be the result of the higher

crystallinity of the macrocyclic resins. Increasing the crystallinity of the linear resins (through slow cooling from the melt) could reduce the amount of intercrystalline amorphous material and raise the modulus over the entire temperature range[2,10]. This would minimize the amount of amorphous material, which is of interest in this study. A better experiment for comparing these two resins would be to reduce the crystallinity of the macrocyclic structure. We have not succeeded in doing this without degrading the cyclic topology, so no result related to tie chain density has been derived from DMTA analysis.

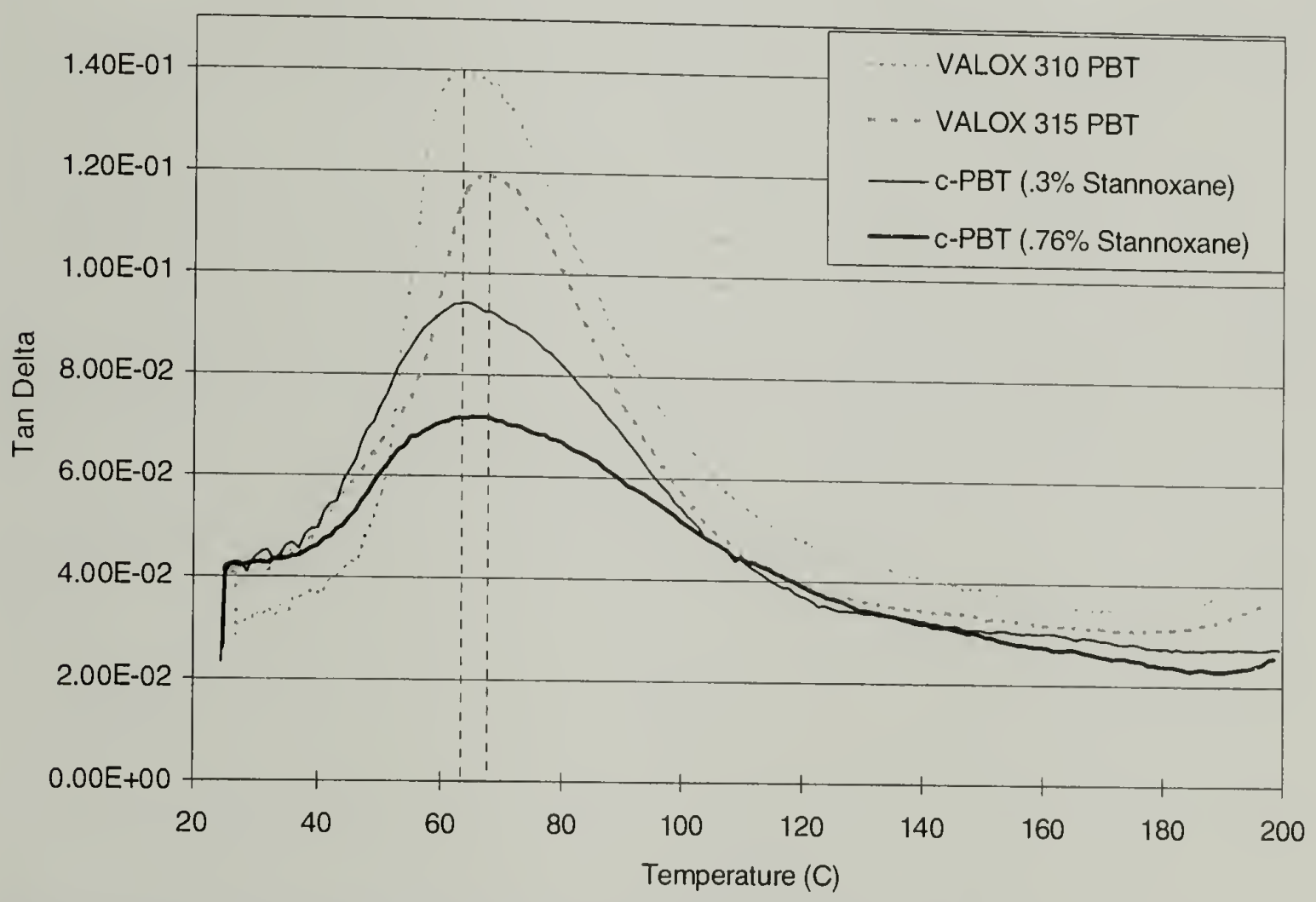


**Figure 6.96 Temperature Dependence of Tan δ for 4 PBT resins.**

$T_g$, as determined from the peak of the curve of tan δ vs. temperature, is not affected by the chain architecture in PBT (Figure 6.96). $T_g$s of all four materials fall within a 5° C range, with the $T_g$ of the linear resins bracketing the $T_g$ of the two macrocyclic resins.

### 6.5.3 Compression Studies

Young's modulus (elastic modulus) is a fundamental parameter for structural materials and is equally valid when determined from tensile or compressive tests. Moreover, the basic calculations for fracture toughness require a knowledge of a material's modulus, as well as Poisson's ratio. Although tensile modulus is the most commonly measured and reported modulus for polymers, constraints arising from the small quantities of c-PBTs available made modulus measurement in compression the method of choice. For fracture toughness correlations in c-PBT, it was necessary to determine the change in modulus resulting from the crystallinity decrease caused by thermal aging in the melt. To this end, compressive modulus test specimens were simply taken from portions of the same compression moldings that were evaluated in SENB fracture tests (see Section 6.6).

A series of specimens of c-PBT were treated under conditions that were designed to cause degradation to increasing fractions of the stannoxane links holding the macro-cyclic rings together with increasing time of thermal aging. As these links open, the macro-cyclic rings are converted to linear chains, with the resulting molecular weight being dependent on the number of stannoxane links which open in the cyclic ring. Toughness differences in the heat treated c-PBTs could only be accurately determined with knowledge of the each specimen's modulus following its thermal conditioning period.

DSC results have shown that the crystallinity achievable on subsequent cooling is progressively and irreversibly lost as c-PBT is held in the melt (see Section 6.2). Thus, this series of compression tests was based on compression molded specimens that had been subjected to a range of "heat soak" times at 250° C.

As referenced in Section 6.1, the specimens for mechanical compression tests and the SENB fracture specimens were prepared by a different process and using a different compression tool than described earlier for other mechanical test specimens. To make mechanical test specimens it was necessary to find a way to overcome the leakage problem caused by the low viscosity of the cyclic oligomers of PBT while holding the melt at 250° C for extended times. When heated in a compression tool, the cyclics and low viscosity polymer are quickly exuded through the tooling vents.

To overcome this problem, the powdered cyclic oligomers, containing predispersed stannoxane initiator, were first polymerized under a nitrogen atmosphere in a small laboratory oven. Sieved powder of the oligomer containing the initiator was placed at a uniform depth of 0.5 inches inside a "boat" formed from Teflon® coated heavy aluminum foil. The boat was then set on the insulated oven shelf and left for 45 minutes. Temperature during this process was monitored using a surface thermometer placed on an insulated shelf inside the oven. The thermometer was stable at 190° C and accurate to 5° C. After polymerization the block of polymer was found to have a density of 0.68 g/cc which is roughly half the density of the well consolidated c-PBT specimens.

The block of polymer was then cut into 0.5 inch-wide strips using a band saw with a new blade. Each strip weighed about 15 grams. The strips were fully consolidated in a preheated compression tool. The tool was first prepared by covering the upper and lower slides with a layer of self adhering Teflon® coated heavy aluminum foil to prevent sticking and allow shrinkage immediately upon release of the pressure.

The compression tool was first heated to 250° C between the heated platens of a Tetrahedron "Evencool" MTP-14 24 ton hydraulic press. Temperature was controlled to

within 0.5° C. To begin the c-PBT consolidation, the heated tool was removed from the press, a polymerized strip placed into the tool, the heated top placed onto the tool, and the tool returned to the oven, all within 30 seconds. The platens were closed until the tool just touched the upper platen and the timer was started. After the predetermined "soak" time had elapsed, the platens were opened slightly and the tool moved up to the cool side of the press. The press was then closed to a pressure of 2000 pounds, and a surface thermocouple attached. The tool was allowed to cool under pressure until the surface reached 110° C. This temperature was found to be cool enough to allow complete crystallization, while being warm enough that the polymer was well above $T_g$, so that the specimen could be removed from the tool without fracturing from high pressure and restricted shrinkage.

The control specimen was moved from the hot side to the cold side of the press immediately on evidence of melting. (which was determined by a small amount of flash at the upper vent). Specimens were removed from the compression tool by placing the frame of the tool on blocks in a Carver press and driving the core of the tool out. Immediately upon removal from the Carver press, the specimen was separated from the slides using a razor blade. Specimens prepared by this process were well consolidated as evidence by few visible voids, showed little loss of polymer due to flash, and could be prepared in thick sections without developing cracks.

Compression specimens of VALOX PBT resins were machined across the flow direction of injection molded plaques having a nominal thickness of 0.25 inches. Prior to testing, all cut edges were sanded flat and parallel. Compression specimens of c-PBT resin were taken from broken sections of compression molded bars after they had served

as single edge notched bending specimens in fracture mechanics testing. Each of these specimens was examined prior to compression testing and each was selected for having sufficient length to get an acceptable slenderness ratio* as well as having no visible voids caused by shrinkage. Compression testing was done using an Instron Servohydraulic Model 8502A Universal testing machine at a crosshead rate of 0.10 inches per minute. All testing was done at room temperature.

The maximum stress attainable was not reproducible as the specimens would develop signs of fracture near this stress. Therefore the yield stress was determined two ways; a) from a 0.2 % offset tangent and b) from a 1.0 % offset tangent. Both of these yield stresses are shown graphically in Figure 6.97. Up to the 1.0 % "yield" stress, duplicate specimens gave reproducible results. In this way, a compressive modulus and compressive yield stress were accurately determined. To assure reproducibility, two specimens were tested for each molding condition.

Axial compression of a uniform rectangular specimen was used to determine the room temperature modulus of each material. A typical compression curve is shown in Figure 6.97. Compressive modulus and the two offset yield stresses were determined according to ASTM D695-96[11]. All specimens showed linear stress/strain behavior up to three percent strain, followed by a deviation from linearity as anelastic behavior at high stresses resulted in yielding as the specimens began to develop shear deformation and buckling. A compressive modulus was determined for each specimen by finding the longest linear portion of the stress/strain curve below the proportional limit. Stresses are

---

* Slenderness Ratio is the ratio of the length of a rectangular specimen to its least radius of gyration. For the geometry used herein, the radius of gyration is 0.289 times the thickness of the specimen. Slenderness Ratio is to be between 11.0 and 16.1 according to ASTM D695.

expressed as force per unit area based on the initial cross-sectional area. A yield stress was determined at each of two offset strains. Working close to the end of the elastic region, a 0.2% tangent offset stress was obtained. A second tangent offset yield stress at 1.0 % strain was recorded: the latter stress reflects both elastic and anelastic or plastic contributions to the strain. Both yield stresses are a valid determinants of the end of elastic behavior and differ in the degree of plasticity in the specimen. The following correlations will make it clear as to which yield stress is being considered.

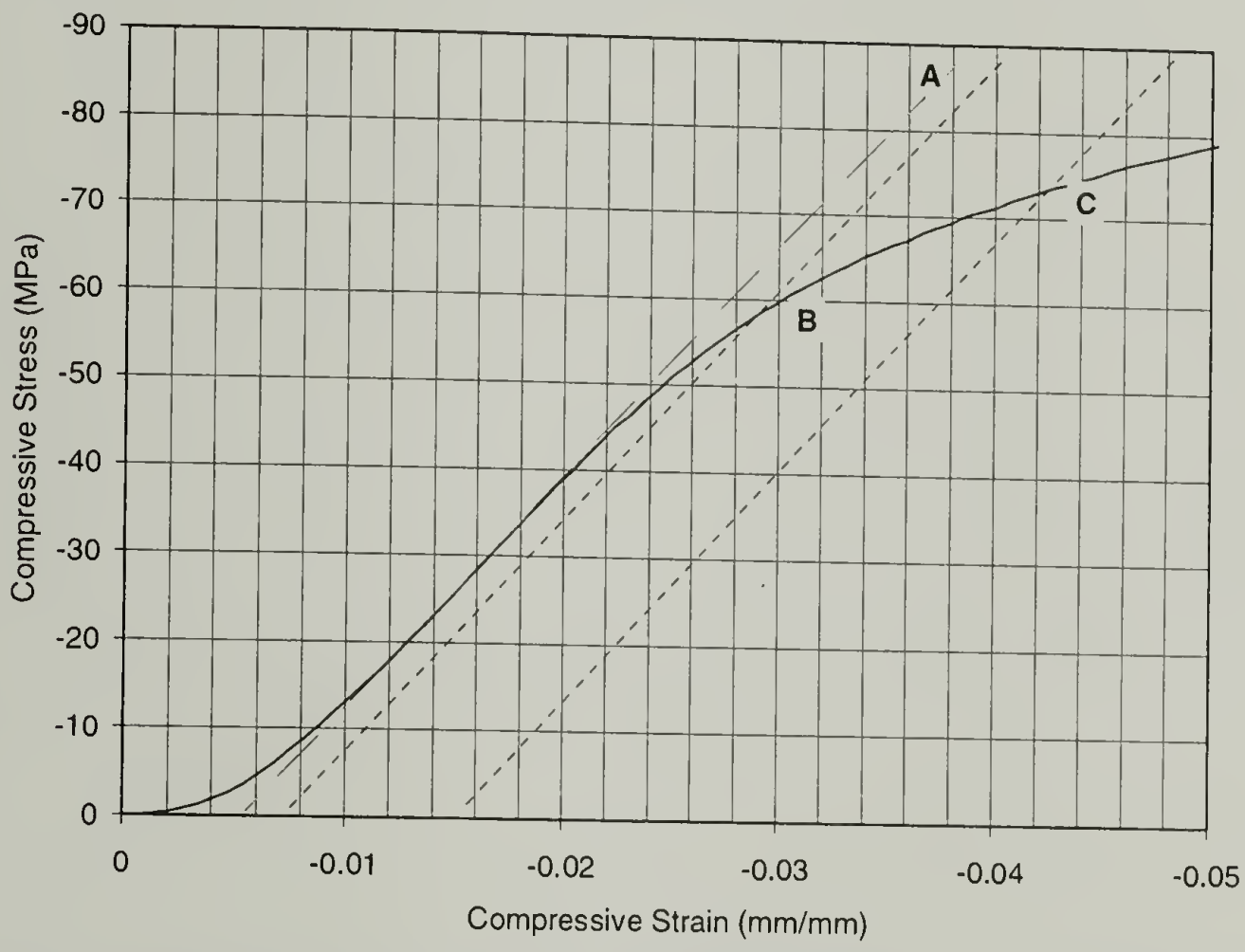


**Figure 6.97 Compressive Stress / Strain curve for c-PBT polymerized with 0.3 mol % stannoxane. Slope of line A is the compressive modulus. Point B shows the 0.2 % offset yield stress. Point C shows the 1.0 % offset yield stress.**

Linear resins were evaluated before and after annealing for 15 hours at 150° C to increase the crystallinity to the same range as the macrocyclic resins. Crystallinity was determined from GPC and calculated from Illers[12] reported value of 142 J/g for 100 % crystalline PBT. The modulus, yield data, and crystallinity results are given in Table 6.9.

A correlation of crystallinity and compressive modulus in Figure 6.98 shows that crystallinity is the prime determinant of modulus below $T_g$. This is the same result obtained in both room temperature tensile testing as reported above in Sections 6.5.1.

**Table 6.9 Compressive Moduli, Yield Stresses, and Crystallinity of PBTs used in fracture studies.**

| | Modulus (GPa) | 0.2 % Yield Stress (MPa) | 1.0 % Yield Stress (MPa) | Heat of Fusion (J/gram) | Crystallinity (%) |
|---|---|---|---|---|---|
| VALOX 195 | 2.12 | 59.8 | 66.8 | 53.8 | 37.9 |
| VALOX 195 | 2.16 | 57.0 | 66.3 | 53.8 | 37.9 |
| VALOX 295 | 2.30 | 59.1 | 68.0 | 49.2 | 34.6 |
| VALOX 295 | 2.11 | 57.0 | 65.6 | 49.2 | 34.6 |
| VALOX 315 | 2.09 | 59.4 | 62.2 | 43.2 | 30.4 |
| VALOX 315 | 2.10 | 55.0 | 63.7 | 43.2 | 30.4 |
| VALOX 195 Annealed | 2.37 | 68.0 | 79.0 | 65.2 | 45.9 |
| VALOX 195 Annealed | 2.33 | 64.6 | 74.2 | 65.2 | 45.9 |
| VALOX 195 Annealed | 2.29 | 67.3 | 76.9 | 65.2 | 45.9 |
| VALOX 295 Annealed | 2.40 | 78.3 | 68.7 | 65.5 | 46.1 |
| VALOX 315 Annealed | 2.33 | 63.9 | 73.2 | 55.3 | 38.9 |
| VALOX 315 Annealed | 2.41 | 66.0 | 74.2 | 55.3 | 38.9 |
| c-PBT 2 min @232* | 2.50 | 57.7 | 75.2 | 80.0 | 56.3 |
| c-PBT 2 min @232* | 2.63 | 59.8 | 74.2 | 80.0 | 56.3 |
| c-PBT 0 min @250* | 2.13 | 54.3 | 73.2 | 62.0 | 43.7 |
| c-PBT 10 min @250* | 2.19 | 55.0 | 64.6 | 60.8 | 42.8 |
| c-PBT 20 min @250* | 2.17 | 49.5 | 59.4 | 51.8 | 36.5 |
| c-PBT 20 min @250* | 2.21 | 52.9 | 61.6 | 51.8 | 36.5 |
| c-PBT 35 min @250* | 1.96 | 52.2 | 59.8 | 51.6 | 36.3 |
| c-PBT 35 min @250* | 2.18 | 56.1 | 65.3 | 51.6 | 36.3 |

** Indicates heat soak time (in minutes) at temperature (in C)*

Figure 6.98 shows the modulus dependence on crystallinity for PBT resins. Both cyclic and linear resins fall on the same line, suggesting that at low strains, deformation resistance is not affected by differences in the topology of the chains. With the wide range of crystallinity represented in this graph, it is possible to make a rough prediction of the moduli both the crystalline and the amorphous regions of PBT. When extrapolated to zero % crystallinity, the amorphous modulus is determined to be 1.59 GPa. When extrapolated to 100 % crystallinity, the crystalline modulus is determined to be 3.33 GPa.

Thus, the crystallites have twice the modulus of the glassy region for PBT. No prior report of this determination has been found in the literature.

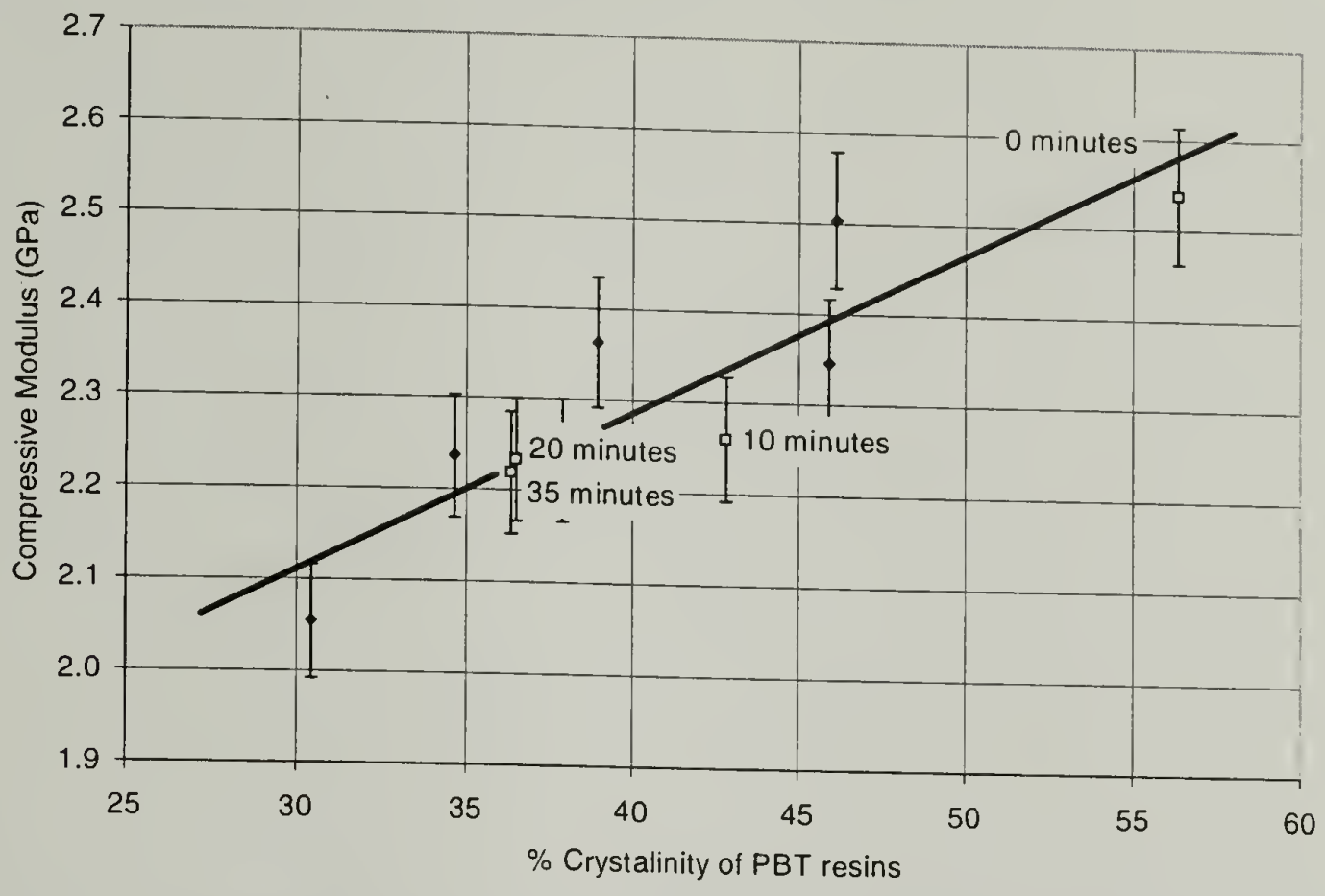


**Figure 6.98 Compressive Modulus vs. Crystallinity for PBT resins at 21°C. Open squares are c-PBT showing time at 250° C, filled diamonds are commercial linear PBTs. Error bars represent +/- 3% of average modulus at each condition. Line represents best linear fit: Modulus (GPa) = 0.0174( % Crystallinity) + 1.59.**

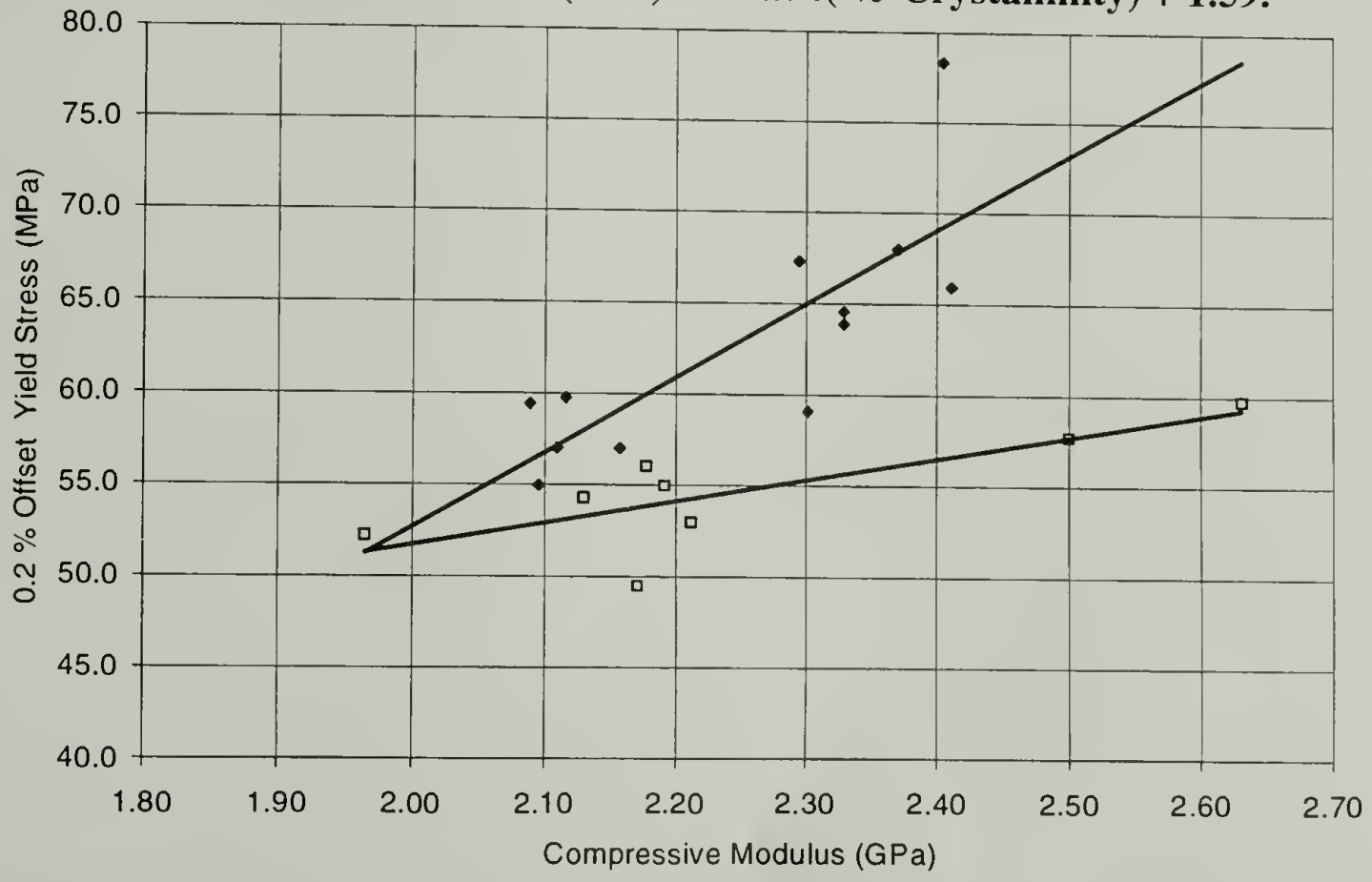


**Figure 6.99 Correlation of 0.2 % Yield Stress with Compressive Modulus. Open squares are c-PBT, filled diamonds are commercial linear PBTs.**

Under low stress, the modulus of either cyclic or linear PBT is only a function of the crystallinity. However, as the stress is increased, macrocyclic PBT begins to yield sooner than linear PBT, even though the modulus of the former is higher as shown in Figure 6.99. When the 0.2% offset yield stress is plotted as a function of crystallinity, this difference becomes even clearer (Figure 6.100).

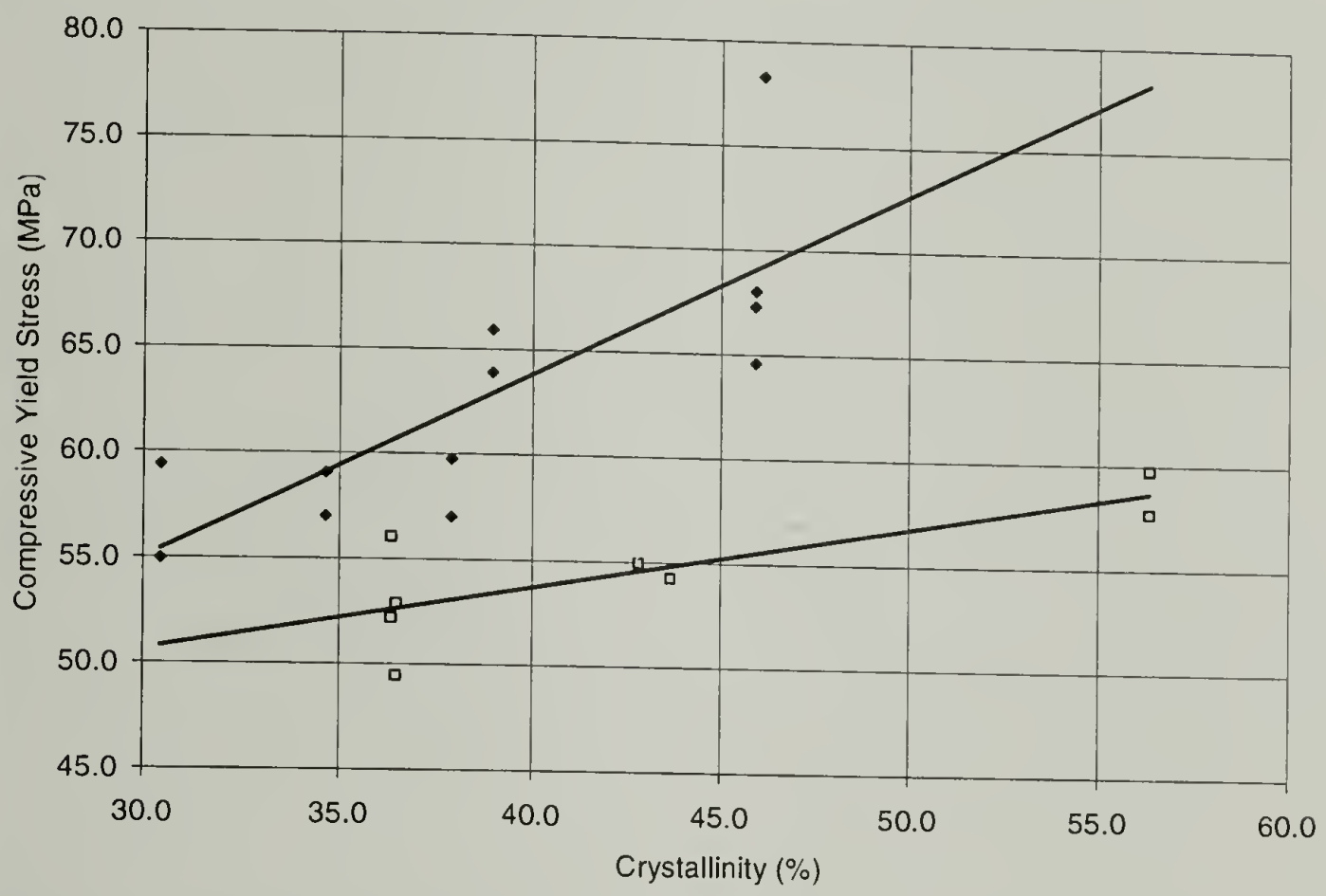


**Figure 6.100 0.2% Compressive Yield Stress vs. % Crystallinity for PBTs. Filled diamonds are linear PBT resins, open squares are c-PBTs.**

The cyclic polymer, perhaps because it has fewer tie molecules, is not as capable of resisting high stresses. While still below $T_g$, the cyclic structure begins to deform at stresses where the linear polymer is still elastic. This is not merely a function of the increased crystallinity of the macrocyclic structure. At the highest crystallinity, where the c-PBT is the most representative of a macrocyclic PBT, the linear resin is predicted to have a 35 % higher yield strength than the cyclic resin. As the c-PBT is degraded to linear

resin, its crystallinity is lowered, and the resulting polymer begins to approach the modulus vs. yield stress correlation of the linear resins.

Annealing the linear PBTs did not raise the crystallinity above 46 %. Slow cooling from the melt should increase the crystallinity of the linear resin to higher levels. This would allow for linear PBTs to be obtained which have the same levels of crystallinity that exist in nascent cyclic c-PBT. If this were done, the yield stress would need to be obtained in compression as this level of crystallinity will make the linear resins too brittle for tensile yielding.

In Figure 6.100, only one data point is represented by what is believed to be a macrocyclic resin. This data point, at the highest crystallinity shows the greatest deviation from the correlation represented by the linear resins. All other points on the line which is used to correlate the c-PBT resins are the result of testing cyclic resins which had been thermally degraded. The longer this thermal degradation, the lower the crystallinity of the specimen, and the closer the compressive yield comes to the line representing the linear PBT resins.

Note that the two lines in Figure 6.100 appear that they would converge somewhere between 20 % and 25 % crystallinity. Were it possible to prepare macrocyclic resins of lower crystallinity, it seems reasonable that the two lines representing linear and cyclic resins should be more nearly parallel, as they should not intersect until the crystallinity reaches zero In the glassy state, it is reasonable to expect that all of these resins would have nearly the same yield stress.

### 6.5.4 References for Mechanical Testing


1)Peterlin, A., *Journal of Polymer Science, Part A-2* **1969**, *7*, 1151-1163.
2)Takemori, M., *Polymer Engineering and Science* **1979**, *19*, 1104-1109.
3)Keith, H.; Padden, F.; Vadimsky, R., *Journal of Applied Physics* **1971**, *42*, 4585-4592.
4)Peterlin, A. *The Role of Chain Folds in Fibers*; Mark, H., Atlas, S. M. and Cernia, E., Ed.; John Wiley and Sons: New York, **1967**, pp 283-340.
5)Lustiger, A.; Markham, R. L., *Polymer* **1983**, *24*, 1647-1654.
6)Nielsen, L. E. *Mechanical Properties of Polymers and Composites*; Marcel Dekker, Inc: New York, NY, **1974**; Vol. 2.
7)Toggenburger, R.; Newman, S.; Tremontozzi, Q. A., *Journal of Applied Polymer Science* **1967**, *11*, 103.
8)Krevelen, D. v. *Properties of Polymers - Their Estimation and Correlation with Chemical Structure*; Elsevier Scientific Publishing Co.: New York,**1976**.
9)Aklonis, J. J.; MacKnight, W. J. *Introduction to Polymer Viscoelasticity*; 2nd ed.; John Wiley and Sons: New York NY, **1983**.
10)Kambour, R. P.; Banach, T. E.; Carnahan, J. C.; Garbauskas, M. F.; Gundlach, P. E.; McAlea, K. P.; McCracken, L. L.; Todt, M. L.; Takekoshi, T. "Macrocyclic Polybutylene Terephthalates: PBT Variants of Unusually High Crystallinities via the Ring Expansion Polymerization of Butylene Terephthalate Cyclic Oligomers Using a Cyclic Stannoxane Initiator," Manuscript in preparation.
11)ASTM *Standard Test Method for Compressive Properties of Rigid Plastics*, **1996**.
12)Illers, K., *Colloid and Polymer Science* **1980**, *258*, 117-124.

## 6.6 Fracture Studies

The selection of fracture techniques was primarily based on the amount of cyclics-based materials available for study. With only six pounds of BTC powder available for evaluation and the necessity of developing a technique for preparing solid specimens that were sufficiently thick to be used in fracture studies, it was imperative to use specimens having small volumes. The commercial linear polymers from which comparative data were acquired, were obtained in pellet form and injection molded into 6 inch x 8 inch plaques with a nominal thickness of 0.25 inch. The injection molding parts were produced using the set up conditions recommend by the manufacturer of the resins.

Before attempting to understand the fracture of composite materials, it is important to first develop an understanding of the fracture characteristics of the polymer matrix. Entanglement of the macromolecules gives the polymer its characteristic properties in both the melt and solid state. The toughness of a glassy linear polymer is affected by the extent of intermolecular entanglement within the solid mass, the extent of which is dependent on the polymer's molecular weight. Low molecular weight glassy polymers, with lower degrees of entanglement, exhibit low toughness[1]. As the molecular weight is increased, the extent of molecular entanglement increases, and the material becomes tougher. Crystalline polymers have an additional physical strengthening mechanism resulting from their crystalline structure. The crystallites physically cross link the intercrystalline amorphous polymer and are believed to be interconnected by tie chains[2] that transfer stress throughout the whole structure. Thus, the effective degree of entanglement is related to more than just the molecular weight in a crystalline polymer. The toughness of PBT, as with all crystalline polymers, is also influenced by the degree of

crystallinity in the specimens under evaluation. Increasing the crystallinity tends to make the polymer more brittle[3], as the crystallites themselves have higher modulus, are less deformable, and thus concentrate the strain energy in the amorphous regions when stressed.

Polymers that have crystallized may be considered as systems with two semi-independent phases. (For details, refer to the model of crystallization given in Section 6.2.5.) The crystalline phase consists of ordered domains of chains that rely on their low energy configurational state to maintain structural integrity while the second phase consists of an amorphous mass of polymer chain segments. Ordered segments in the crystal are not entangled therein, but may be connected to entangled segments outside of the crystalline domains, i.e. at lamellar surfaces. These entanglements serve to connect the lamellae to the amorphous regions but may not transfer stress effectively between adjacent lamellae. Other amorphous chains segments may traverse the amorphous regions, and connect adjacent lamellae, i.e. a single chain may be incorporated into more than one crystallite. Such chains are called interlamellar tie chains and these chains can effectively transfer stress between the lamellae[4]. As the crystallinity of a polymer is increased, an increasing fraction of the molecular mass becomes incorporated into crystal structure and the toughness of the polymer decreases. The net effect of annealing is to increase both the degree of crystallinity and the order in the crystal, at the expense of reducing the amount of amorphous interlamellar material. Both effects tend increase the modulus and concentrate any (shear) stress in the remaining amorphous regions, effectively lowering the toughness of the bulk polymer[5].

Because both linear and macrocyclic PBT are crystalline to varying degrees, it was important to characterize both the molecular weight and the degree of crystallinity of fracture test specimens. To compare the toughness' of linear and macrocyclic PBT at the same level of crystallinity, it was necessary to increase the crystallinity of the linear polymers. Two sets of fracture specimens of linear PBTs were evaluated; the first set taken from freshly injection molded plaques (with amorphous surfaces as described by Hobbs[6]), and the second set from plaques after 15 hours of annealing in a 150° C oven. Table 6.9 shows the crystallinity at the cores of these specimens as measured by DSC at a standard heating rate of 20° C per minute.

A primary goal of the fracture toughness study was to determine the effect of chain topology on the opening mode stress intensity factor, $K_I$. The concept of stress intensity factor is central to linear elastic fracture mechanics[7]. The stress intensity factor is a measure of the critical resistance to propagation of a sharp crack. While three unique modes of crack opening are commonly described, $K_I$ is generally the most important for the performance of a material, the easiest to determine, and therefore the most widely reported value in characterizing fracture resistance. This type of specimen is defined by the direct separation of the fracture surfaces perpendicular to the direction of the crack. The resulting fracture is termed a Mode I crack. Mode II cracks are characterized by the shear displacement of the crack faces in a direction normal to the crack front. In Mode III fracture, the crack faces are separated via a shear displacement parallel to the crack front. These three modes of fracture are illustrated in Figure 6.101.

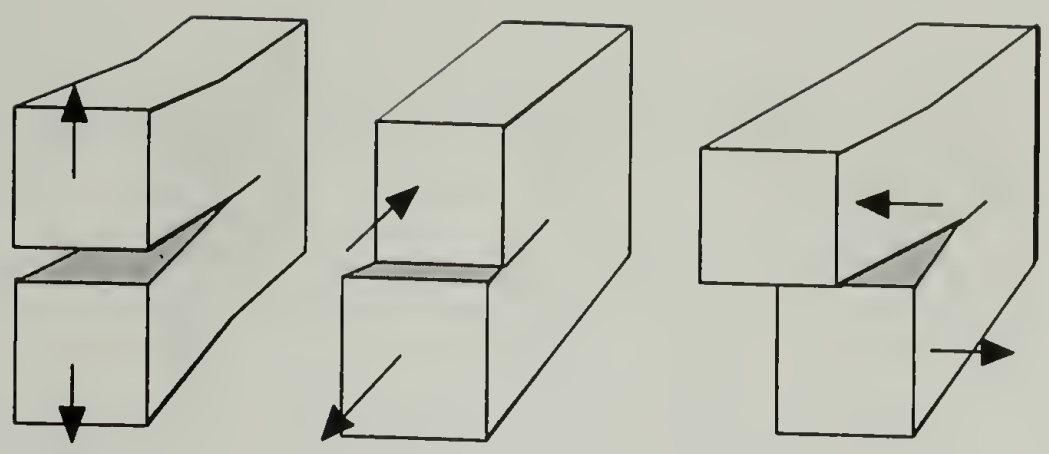

Mode I Mode II Mode III

**Figure 6.101 Three Fracture Modes resulting in Crack Extension: Mode I is tensile or opening mode, Mode II is in-plane shear or sliding mode, Mode III is out of plane shear or tearing mode.**

Mode I opening is the most commonly described mode, and is the easiest to control in testing. The stress intensity, K, for each mode is defined for each mode by

$$K_I = \sigma(\pi a)^{1/2} \qquad K_{II} = \sigma(\pi a)^{1/2} \qquad K_{III} = \sigma(\pi a)^{1/2}.$$

The term $\pi^{1/2}$ has been commonly omitted from the definition, particularly in early work on fracture[8]. Stress intensity is only a function of the applied stress,$\sigma$, and crack length, $a$.

These simple descriptions of the failure modes are only useful in describing fractures in which the energy consumed in fracture is only dissipated in creation of new fracture surfaces. In these fractures, the specimen deforms in a fully elastic manner up to the point of fracture, except for a plastic zone at the crack tip which is small when compared to the specimen dimensions. To make use of these simplifications, care is taken to design the fracture specimen with such geometry that the crack is predominantly formed in a state of plane strain. "Plane strain" means that all displacements at the crack tip, plastic or elastic, occur in one plane only. Under this condition, the $K_I$ is a measure of the resistance to a brittle fracture under conditions of critical flaw size in the material.

Plane strain conditions are considered applicable[7] when the specimens has a thickness across the fracture plane which meets the condition

$$\text{thickness} > 2.5\ (K_I/\sigma_y)^2.$$

When the specimen is thinner than the above condition, significant amounts of energy during crack propagation may be consumed in plastic deformation processes, and a different measure of fracture toughness applies. Yielding processes become the dominant energy absorption processes in plane stress failures. Plane stress is characterized by volume conservation under strain, resulting from lack of constraints on the specimen under uniaxial or biaxial loading. For example, in a thin plaque specimen of a solid material, the lateral surfaces are not constrained from displacement normal to the surface plane when the plaque is stretched, thus the material at the center of the plaque remains in a state of plane stress. By increasing the plaque thickness with respect to its other dimensions, the stress state within the center of the plaque is changed from plane stress to predominantly plane strain. While transverse strain is always present at unconstrained surfaces, it's effect at the crack tip is diminished in thick specimens. The transverse strain diminishes with distance inward from the surface, becoming negligible for very thick specimens which are thus considered to be essentially in a state of plane strain[9].

The transition from plane stress to plane strain fracture is characterized by a change in the appearance of the fracture surface. The plane stress fracture surface found in a fracture specimen from a thin sheet appears to have an oblique shear-type fracture[10]. As the specimen is thickened there is a flattening of the fracture surface, more characteristic of plane strain. In thick specimens, the stress distribution just ahead of the crack tip is that of triaxial tension. In reality there is always some anelastic or plastic zone

development at the crack tip as this portion of the specimen undergoes non-elastic deformations during loading prior to fracture. It has been found empirically that the value of the critical stress intensity, $K_c$, will reach a finite lower limit, $K_{Ic}$, if the specimen's width and length in the crack direction are selected such that each is greater than 2.5 times $K_c^2/(2\pi\sigma_y^2)$. [11]

When a flaw or defect is present in a material subjected to an external stress field, the local stresses in the vicinity of the flaw are increased. This may be visualized as a local increase in the density of the lines of force in the loading direction, which must concentrate to accommodate the flaw. More classically, this is seen as an increase in the local stress related to the geometry of the flaw. If the flaw is assumed to be an elliptical crack of major and minor axes *a* and *b*, the stress concentration at the crack tip will be

$$\sigma = \sigma_o ( 1+ 2a/b)$$

where $\sigma_o$ is the stress far from the defect. Thus the ratio $\sigma$ / $\sigma_o$ defines the stress concentration at the tip of the crack. When a sharp notch is intentionally cut in a sheet, and an far-field stress applied, the local stress will be a function of the radius of the notch. For most polymers, there is a lower limit to the effective or "intrinsic" flaw size such that the stress concentration does not go to infinity. This limit is about 0.07 mm for PMMA and about 1.0 mm for polystyrene[12]. These dimensions represent a "natural flaw size" for these materials, below which size the failure stress is independent of flaw size.

A notch cut into a fracture specimen constitutes a mechanical defect in the material. From the above equation it is seen that sharper the notch, the higher will be the stress concentration at the notch tip. In most notched thermoplastics subjected to high stress, a plastic zone will develop beyond the root of the notch prior to failure. The

formation of such a plastic zone will consume some of the energy absorbed during the fracture process. Moreover, as the crack propagates, plastic deformation will continue in front of the crack tip. However, if this zone size is small with respect to the specimen dimensions, it is still possible to apply the methods of linear elastic fracture mechanics and determine the plane strain fracture characteristics of a material as described below.

In applying the classic Griffith analysis of the forces existing in the area of a flaw in a stressed body, the external forces which do work on a body must be balanced by both the elastic strain energy within the body and the work done against the cohesive forces which resist fracture in the body[13]. This may be expressed as

$$\partial U + \partial W - \partial F = 0$$

or the condition for fracture must be such that the external forces exceed the sum of the recoverable strain energy and non-recoverable fracture energy in the body

$$\partial F > \partial U + \partial W .$$

The Griffith calculation involves a balance of the energy consumed in growing a sharp crack with the release of stored energy occurring with increasing crack length. An estimate of this energy could be made by considering that the crack completely relieves the stresses which exist in a circular zone around an internal crack having a length 2 $a$. This volume at unit thickness is $\pi a^2$, and the strain energy within this volume under a stress of $\sigma_o$ is $(\sigma_o{}^2)/2E$ where E is Young's modulus.

Griffith showed that in a brittle (elastic) plate containing an internal crack of length 2 $a$, or a surface crack of depth $a$, the maximum stress that a plate could withstand under plane strain conditions without fracture would be

$$\sigma = \sqrt{\left(\frac{2E\gamma_s}{a\pi}\right)}$$

where $\gamma_s$ is the surface energy per unit area of new crack. For plane stress this condition would become

$$\sigma = \sqrt{\left(\frac{2E\gamma_s}{a(1-\nu^2)\pi}\right)}$$

were ν is Poisson's ratio.

This result was later modified independently by Irwin[14] and Orowan[15] to account for plastic deformations in the area of the crack tip resulting in the modified Griffith equation for plane strain fracture

$$\sigma = \sqrt{\left(\frac{2E(\gamma_s + \gamma_p)}{a\pi}\right)}$$

where $\gamma_p$ is the plastic and anelastic energy absorbed in a region close to the crack tip during its propagation. The variables in the Griffith equation are σ and $a$, whereas E, $\gamma_s$, and $\gamma_p$ are considered to be material constants. By separation of these quantities we see

$$\sigma\sqrt{a\pi} = \sqrt{2E(\gamma_s + \gamma_p)} \equiv K_I$$

$K_I$ is known as the Mode I stress intensity factor and characterizes the state of stress at the crack tip. $K_I$ is dependent on both the stress level and the crack length and it has the units of stress times length$^{1/2}$. $K_I$ may sometimes be given a geometric correction factor, α*, which allows for the correlation for various geometric shapes of specimens used in testing. The term $2\gamma_s$, or $2(\gamma_s + \gamma_p)$, represents the surface energy for both halves of an extending crack and is commonly termed the (total) fracture energy, G.

As the crack extends, the strain energy release rate is *dU/da* for each end of the crack or *½ dU/da* for an edge crack. Rearranging the above equation in terms of surface energy we find a constant elastic energy release rate which is the crack driving force, $G_r$ such that

$$2\gamma_s = G_r = \pi \sigma^2 a / E$$

expressed in terms of energy per unit crack width per unit crack extension. The condition for fracture is that $G_r$ increases with increasing stress, until it reaches a critical value, $G_c$, the critical strain energy release rate.

The stress intensity factor is related to the strain energy release rate through Young's Modulus[7]: $K_I^2 = G_I E$. Fracture in a tensile specimen occurs when the stress intensity factor, $K_I$, exceeds the critical value given by $\sqrt{G_c E} = K_c$, known as the critical stress intensity factor or the fracture toughness.

In the discussion section on the fracture toughness of c-PBTs it will be shown that the fracture toughness is dependent on the extent of degradation of the cyclic structure. This degradation, caused by thermal soaks of the c-PBT polymer at a temperature above the known degradation temperature for stannoxane, results in a toughening of the polymer, even though the crystallinity of the polymer is decreased by the thermal treatment. It is important to understand that under conditions where the modulus of the polymer is roughly constant, large increases in fracture toughness can only result from increases in the fracture energy, $G_c$. This must be the result of a tendency toward plane stress deformations in the vicinity of the crack tip prior to fracture, which may be caused by an increase in the number of effective amorphous chains supporting the stresses, i.e. an increase in tie chain density or an increase in chain entanglement density.

### 6.6.1 Fracture Specimens

Several types of fracture specimens were fabricated and evaluated to assure that the values obtained were reproducible and representative of the fracture character of PBTs of different inherent toughness'. Three factors shaped the selection of the type of fracture specimens for this study: 1) as noted above, there was a limited quantity of cyclic oligomers available, 2) sharp starter cracks should be able to be easily produced in the test specimens, and 3) it was necessary to produce specimens using simple tooling and a compression press. Because the same types of specimens would be used to compare the fracture characteristics of high and low molecular weight linear PBTs to various c-PBTs, it was anticipated that the wide range of toughness existing in the various materials would make it necessary to evaluate toughness using several different geometries of test specimens.

Two specimens were selected based on their common acceptance as standards for fracture toughness measurements. These were the Compact Tension (CT) specimen and the Single Edge Notched Beam (SENB) specimen. Each specimen is very conservative of material in that each requires only about 15 grams of material per test specimen. However, each of these specimens gives only a single value of fracture toughness, $K_{Ic}$.

Each of these specimens also suffers from the same problem in that the toughness result is dependent on the sharpness of the crack and thus a function of the method used to insert the "starter" crack from which the fracture initiates. Standardized specimen geometries and test methods are published for these two specimens by the American Society for Testing and Materials[16]. By this standard, the specimens are prepared according to a prescribed range of geometric details such that the fracture toughness is

calculable as a product of the stress and a geometric expression in the form of a polynomial. The details of each of these specimen geometries are covered in the following sections.

Two other specimens were selected based on their capability to yield stable, controllable crack growth. These two specimens are the Double Cantilever Beam (DCB) specimen[17,18] and the Outwater Dual Torsion (DT) specimen[19-23]. These specimens each consumed considerably more material, the DT specimen weighing approximately 130 grams and the DCB specimen weighing about 50 grams.

However, in specimens having these alternative geometries it was often possible to drive "controlled" cracks in certain of the PBT materials. That is, the geometry of the specimen is such that at fixed displacement, an increment of crack growth causes a reduction in stress at the crack tip and a tendency for the crack to stop growing. The DCB specimen requires that the crack length be known at all times as it is used in the calculation of $K_c$. Because of the opacity of semicrystalline PBT, this length is difficult to determine accurately by direct inspection. However it can be determined indirectly. First, the compliance of the test specimen, i.e., the slope of the deformation/force trace at loads below those causing crack propagation, is measured as a function of crack length. Second, from a separate specimen in which a saw cut of progressively increasing length is made, an empirical relationship between cut length and specimen compliance is generated. This relationship is then used to convert the set of compliances from the crack test specimen to the desired set of crack lengths.

The DT specimen is unique in that the crack length is independent of the load. However, PBT specimens having this geometry were prone to developing ductile yield

zones ahead of the crack tip, thus reducing the utility of this specimen geometry for $K_c$ determinations.

The idealized behavior of each specimen during testing is sketched below.

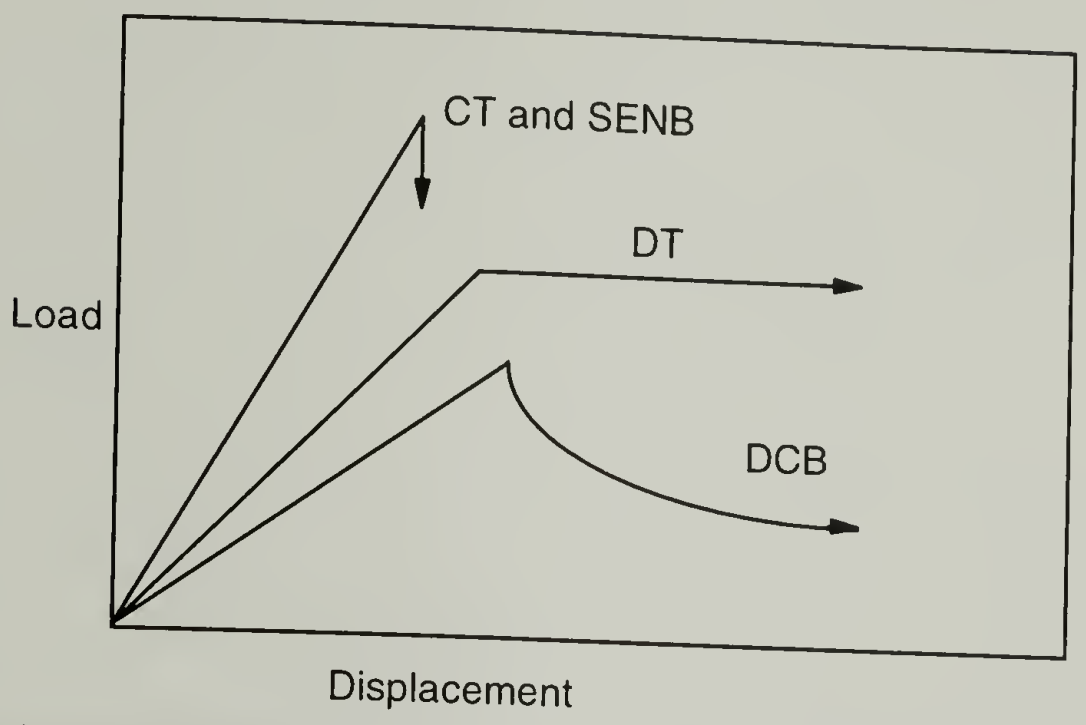


**Figure 6.102 Loading and failure behavior of various fracture specimens.**

Notice that only a single peak reading is obtained in the CT and SENB specimens whereas a stable crack front develops for both the DT and DCB specimens. (In this graphic representation, the relative loads at crack initiation are not intended to be an indication of the relative Kc values obtained from these specimens.) All four of these specimens were easily cut from molded plaques or prepared by compression molding bars of polymer.

### 6.6.2 Compact Tension Specimens

The compact tension specimen was produced as prescribed by ASTM D5045. The specimen geometry is shown in Figure 6.103. To assure plane strain conditions are operable using this specimen, the following condition must be met for the combination of material and geometry selected:

$$B, a, (W-a) \quad \geq 2.5\left(K_Q/\sigma_y\right)^2$$

$K_Q$ is a conditional or trial $K_{IC}$ value which must be determined to see if the geometries of the test can result in a valid determination of $K_{IC}$, and $\sigma_y$ is the yield stress of the material at the temperature and rate of testing.

The plane strain condition assures that a significant fraction of the energy consumed in the fracture initiation and propagation is not consumed in ductile deformation elsewhere in the specimen, i.e. in processes such as shear flow. Under plane strain conditions, the lateral surfaces of the fractured specimen will show no plastic deformation. If this is true, it can be assumed that the calculated fracture energy is a true indication of the energy used in creation of the new surfaces, and is areproducible material parameter.

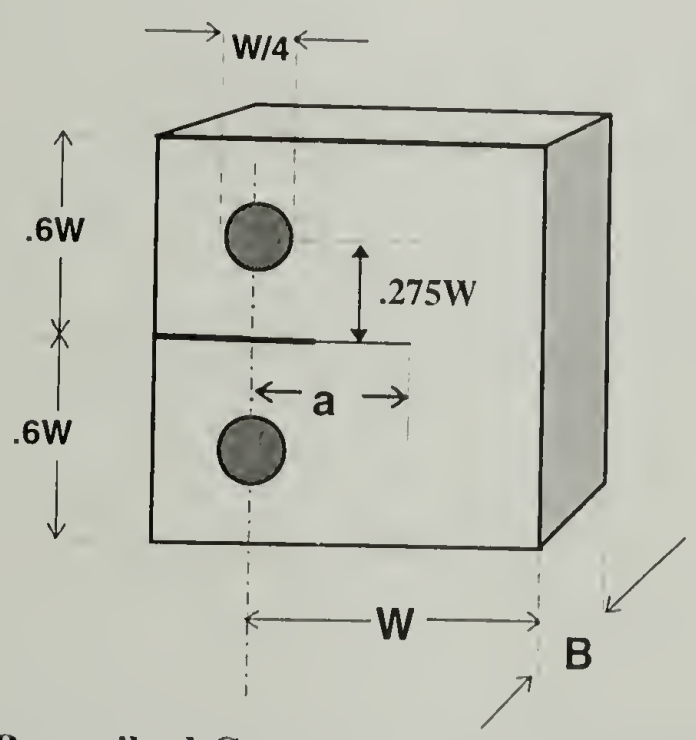


**Figure 6.103 Prescribed Compact Tension Specimen Geometry**

where **B** is the thickness of the plaque from which the specimens are cut,
**W** is the sample width such that W = 4 B[1],
**a** is the crack length (both the precut and the driven sharp crack).

[1]ASTM D5045 calls for W/B = 2 but allows for larger specimens in Appendix 2: for B < 12.7mm, W/B= 4 is allowed.

The crack length, **a**, should be produced such that $0.45 < \mathbf{a/W} < 0.55$. For the specimens evaluated in this section of the study, having a molded thickness of 0.25 inches, the following dimensions were utilized:

**B** = 0.25", **W** = 1.0", **a** = 0.5", hole diameter = 0.25".

### 6.6.3 Crack Tip Considerations

A state of plane strain is required for proper evaluation of a material using the Compact Tension specimen. This condition results when the crack tip is sufficiently sharp that the crack initiation energy is the same as the fracture energy for the material. When the crack is sufficiently sharp, a minimum toughness value will be obtained, characteristic of the energy to create new surface area from an existing sharp flaw in the material. Simply machining a cut into the specimen results in a blunt notch which gives artificially high fracture toughness values. Two methods are commonly used to sharpen the crack and improve the data: fatigue sharpening and wedge opening[7].

Fatigue sharpening is accomplished by fatiguing the specimen prior to actual testing. Fatigue loading will alternatively open and close the crack, causing repeated stretching and relief of the polymer ligaments at the crack tip. This cyclic stress will sharpen the crack through slow growth mechanisms, while allowing the bulk of the specimen to remain unchanged. Fatigue sharpening is effective for tough specimens. In this study, the two linear polymers of highest molecular weight were fatigue-sharpened by sinusoidal loading to stresses between 30% and 50% of the measured stress required to drive the blunt crack of a freshly machined specimen. Fatigue sharpening was not

effective for lower molecular weight PBT or c-PBTs because they tended to fracture as soon as the crack sharpened.

The second method of crack sharpening is accomplished by driving a wedge into a prepared specimen. Two types of wedges were attempted. A large wedge with a 17° rake angle was useful in producing controlled opening by inserting it into the precut crack and tapping it lightly with a hammer. The resulting crack could be made to jump forward a short distance by controlling the force of the hammer strike, but this method proved to be unsatisfactory at producing a controlled crack length

A more controllable wedge opening was accomplished by inserting a fresh razor blade into the precut crack and tapping the back of the blade lightly with a hammer. The length of the driven crack could be limited roughly by putting the uncracked end of the specimen in a vice and generating a compressive stress in this end to stop the running crack. With proper control, the crack could be driven a few millimeters before it stopped. Excessive driving force often resulted in a crack that was caused to deviate from the desired crack plane by the compressive stress.

Alternatively, some cracks were inserted by producing a temperature gradient, and thus a toughness gradient, in the specimen. The temperature gradient was generated by cooling the edge of the specimen containing the saw cut pre-crack in liquid nitrogen, while keeping the other edge relatively warm. Using a wedge to initiate fracture, cracks driven from the cold side were arrested when they entered the warmer material. This method proved more cumbersome and gave less reproducible crack lengths than the compression controlled cracks described earlier. Only those specimens which could be prepared with

sharp short cracks falling into the dimensional constraints of the ASTM criteria were evaluated in this study.

### 6.6.4 Double Grooved Double Cantilever Beam Specimen

The grooved double cantilever beam (DG DCB) specimen is similar to the compact tension specimen in that it is designed for Mode I crack opening in tension. The difference between these specimens lies in the stable crack growth possible in the DG DCB specimen. This specimen was first described by Berry[17] and used by Mai[24] to produce stable crack growth, although Mai's work resulted in a predominance of plane stress as determined from both the resulting surface topography and the high energies absorbed during fracture. The early descriptions have been modified to allow a wide net section for brittle crack propagation, guided by groves that are sufficiently sharp to prevent shear lip formation at the crack surfaces during fracture. This specimen has been used successfully to characterize brittle fracture in naturally brittle polymers[17] such as PMMA, PS, as well as in polycarbonate and other tough, ductile resins[18,25,26]. The geometry of the DG DCB specimen is shown below (with dimensions exaggerated for clarity of interpretation).

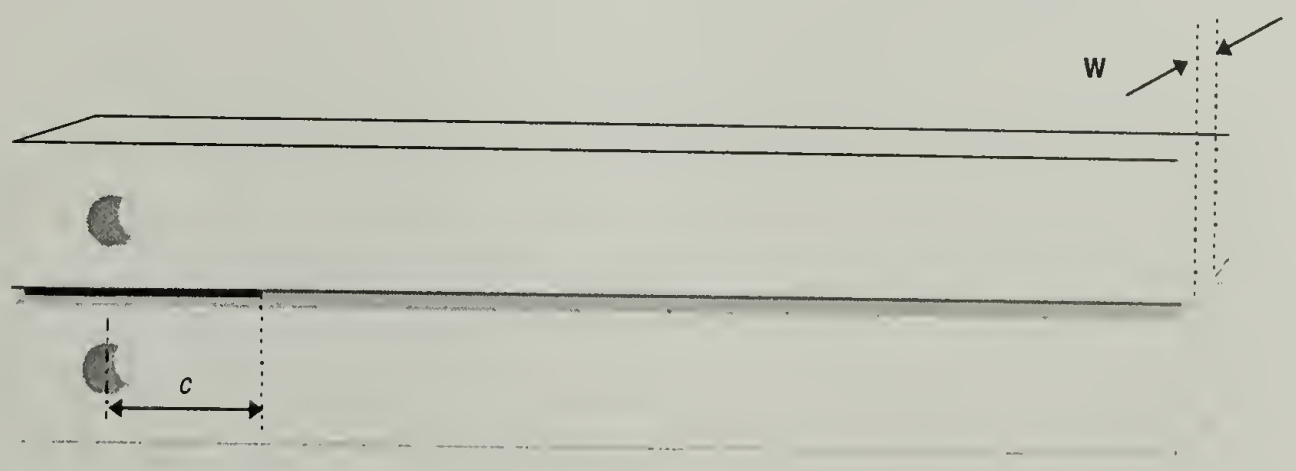


**Figure 6.104 Double Grooved Double Cantilever Beam Specimen Geometry. c = length of "starter crack" from the centers of the holes for pin loading.**

The specimen is cut from a molded plaque of material to dimensions of 3"x 8" by the nominal plaque thickness (generally 0.25" for the linear PBT resins). Side grooves are positioned along each long surface such that the two beams have equal moment of inertia. The grooves are inserted by multiple passes at increasing depth of cut using a slitting saw. The saw blade had been sharpened beforehand to produce a V-groove at the tip of the cut having a radius of 0.001". Final depths of the grooves were set by the toughness of the material, with tougher polymers requiring deeper grooves to produce crack growth at applied forces low enough to avoid a significant amount of anelastic deformation. Generally grooves were cut to a depth that left no more than half of the specimen thickness as a net section for cracking. A "pre-crack" was inserted at the loading end of the specimen by producing deeper, overlapping grooves resulting in a chevron shape cut with a sharp V-shaped loading front[17]. Two methods were employed to sharpen the saw cuts; tough polymers were fatigued, while the notches in the brittle polymers were nicked with a razor. The crack was then driven by pin-loading the specimen and pulling the arms apart at constant rate.

This specimen required a determination of both the crack length and the specimen compliance as a function of crack length. In a crystalline material, this required producing two identical specimens, one which is used for the fracture test and the second specimen for determining the compliance/crack length calibration. Increasing cut lengths are inserted into the calibration specimen, each followed by a compliance determination. A plot of crack length vs. compliance is then prepared which allows crack length determination in the fracture specimen by periodic reversal of the load for compliance

determination. Crack lengths are inferred from the calibrated specimen. Berry[17] has performed an analysis of this specimen and determined that $G_{Ic}$ may be determined from:

$$G_{Ic} = \frac{f^2}{2w} \cdot \frac{d\left(\delta/f\right)}{dc}$$

$$\text{or } G_{Ic} = n f \delta / 2 w c$$

where $f$ is the force, $\delta$ is the cross head displacement, $w$ is the net section containing the crack, and $c$ is the distance from the loading points to the crack front. A value for the empirical constant $n$ is determined from the relationship between crack length and force/displacement in the DG DCB specimen, i.e. $f/\delta = a\, c^{-n}$ by plotting:

$$log(f/\delta) = \alpha - n\, c$$

For injection molded VALOX 295 PBT, the constants were determined at different net sections as

$w = 0.13$ inches: $\alpha = 3.52$ and $n = 0.903$
$w = 0.08$ inches: $\alpha = 3.21$ and $n = 0.484$.

### 6.6.5 Outwater Dual Torsion Specimen

Although the dual torsion (DT) specimen in not one in which a single or "pure" mode of fracture is generated, this specimen has the distinct advantage of having fracture toughness determined without knowledge of the crack length. For opaque materials, or materials tested in hostile environments, this condition greatly simplifies the measurement. On first examination, the failure mode for this specimen may be thought to be a combination of Mode I and Mode III failure. This is because the level of shear stress generated may lead to a Mode III component. However, if the material is sufficiently brittle, the failure is primarily Mode I[10]. Evans[23] reports that a strong correspondence

exists between $K_c$ from this specimen and $K_{Ic}$ for a wide range of materials including steel, titanium , glass, aluminum oxide, and PMMA.

This specimen is simple to prepare and is self stabilizing in the loading fixtures. Therefore several measurements were made using this geometry. The specimen and its loading fixture are show below. The crack is guided by a pre-cut groove along the underside of the specimen, resulting in a reduced net section which contains the crack. A deeply notched support fixture (lower support block) was specially built for testing the range of PBT materials as the tougher specimens require greater displacement of the loading noses prior to the crack advancing.

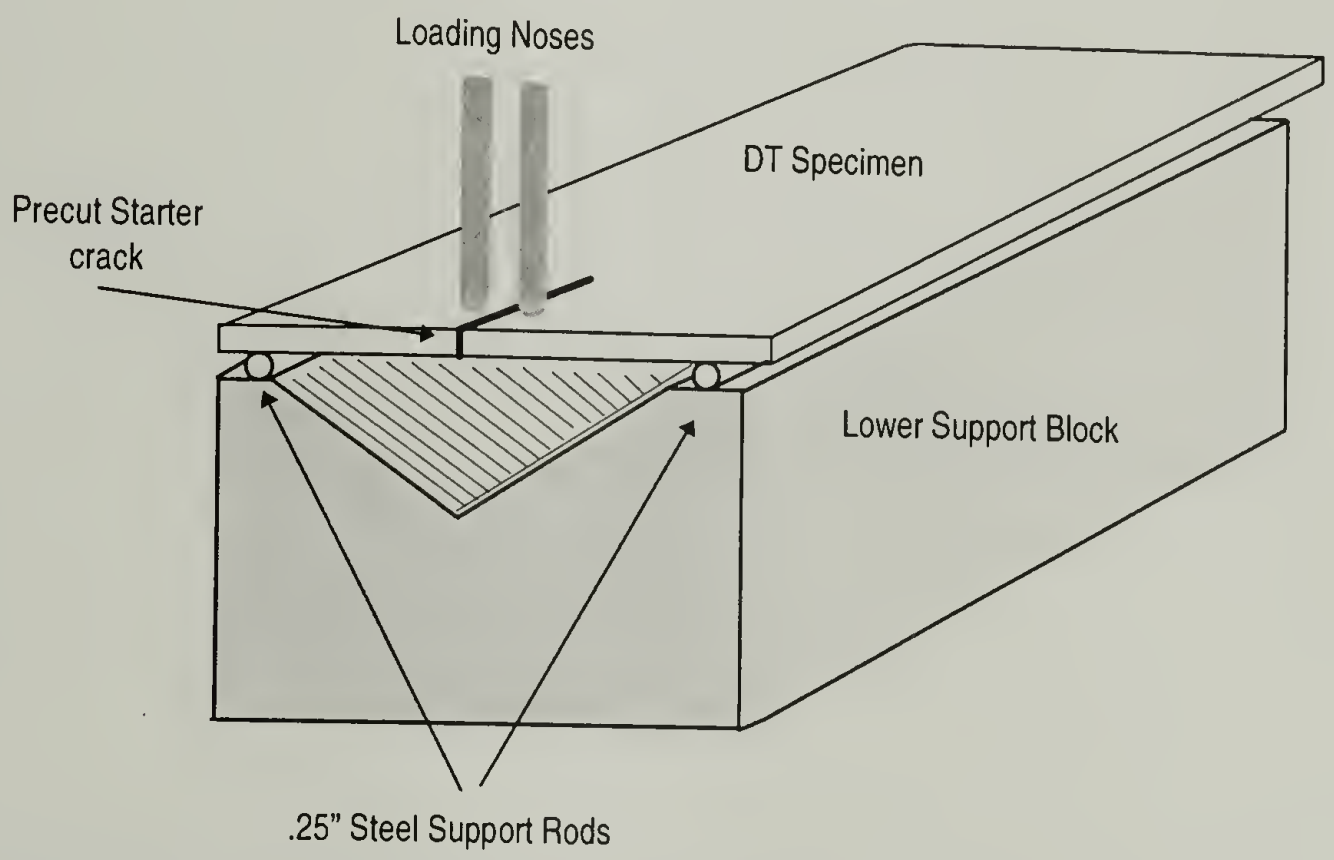


**Figure 6.105 Outwater Dual Torsion Fracture Specimen and Loading Fixtures**

This specimen geometry was first proposed by Kies and Clark[27], but the mathematical development of Kc and Gc were first published by Williams and Evans[19]. Their analysis provides the following expressions for fracture toughness and strain energy release rate in this geometry as:

$$G_c = \frac{3P^2 w_m{}^2}{2Wt^3 t_n G}$$

$$K_c = Pw_m \left( \frac{3(1+\nu)}{Wt^3 t_n} \right)$$

where $P$ = total applied load
$G$ = shear modulus of the material
$a$ = crack length
$t$ = thickness of the specimen
$t_n$ = net section thickness in the crack plane
$W$ = total width of the specimen
$w_m$ = moment arm (distance from the support rod to the loading nose).

$K_c$ is easily derived form $G_c$ by the relationship:

$$K_c = ( E\ G_c )^{1/2}$$

where E (Young's modulus ) and G (shear modulus) are related through Poisson's ratio:

$$E = 2\ G\ (1 + \nu).$$

The crack length falls out of the analysis because a linear relationship exists between the specimen compliance and the strain at all crack lengths. However, experimental values of crack toughness are found to be slightly dependent on the crack velocity for fast cracks. PMMA shows an independence of $K_c$ on velocity below $10^{-4}$ m/sec, with a 10% increase per decade of velocity as the crack velocity increases[19]. This specimen is therefore suited to failure time predictions and has been used successfully in both glasses[22,23] and polymers[20,21]. By slowly loading the PBT specimens, $K_c$ values were obtained which correlate well with values from the other specimen geometries.

### 6.6.6 Single Edge Notched Bending Specimen

The fourth specimen evaluated was selected for its ease of preparation. This allowed fracture characteristics to be evaluated on specimens that had been give heat

soaks for different periods of time beforehand. The single edge notched bending (SENB) specimen as described by ASTM D5043[11] gives single values of $K_c$ and $G_c$ if the pre-crack is sufficiently sharp to produce failure prior to plastic deformation.

Beams of polymer were prepared and loaded using the dimensions shown below. The linear PBT specimens were cut from injection molded plaques and tested such that the crack direction was the same as the flow direction from molding. The amorphous skins on the injection molded specimens were not removed prior to testing. These may have some effect in increasing the fracture toughness of the as-molded specimens[6]. Preparation of the specimens from the of cyclic PBTs was described earlier in Section 6.5.2. The same specimens were used for both SENB fracture and compression testing.

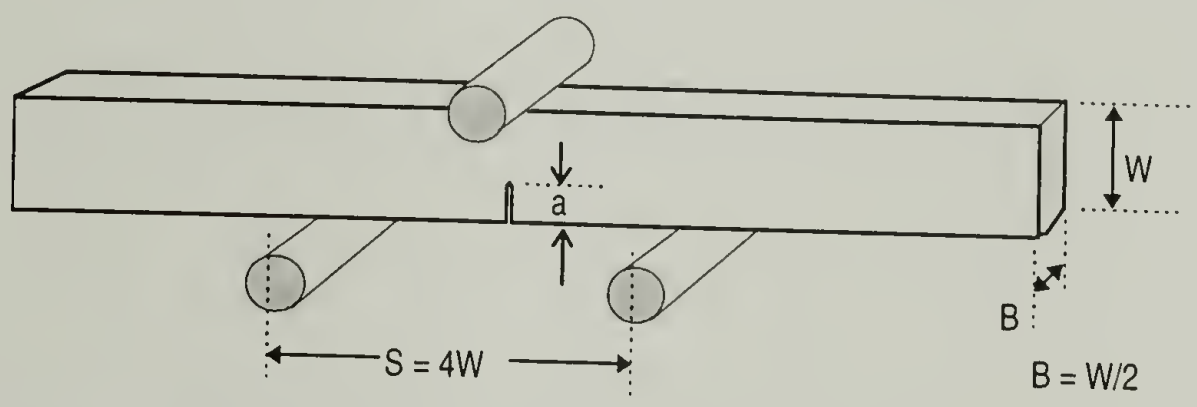


**Figure 6.106 Geometry of the Single Edge Notched Bending Specimen.**

The SENB specimen is very similar to the CT specimen described above and must meet the same criteria for pre-crack length, *a*, and specimen dimensions, *B* and *W*, to assure a valid test result. Pre-cracks were cut into each specimen using the sharpened slitting saw blade that was used to put side grooves in the DG DCB specimens and the lower guide groove in the DT specimens. Prior to testing, each crack was re-sharpened by a single sliding motion from a fresh razor blade as suggested by Liu and Donovan[28]. Specimens were then tested using an Instron Model 1115 at a crosshead rate of

0.02"/minute. Only specimens that fractured in the linear elastic loading region were considered to have resulted in valid tests results.

### 6.6.7 Results of Fracture Tests

A summary of the results of all fracture testing on unannealed specimens is given in Table 6.10 and a similar summary is given in Table 6.11 for specimens which were annealed for 15 hours at 150° C. Also included is the crystallinity level determined for each specimen since the toughness values were found to be correlated through the crystallinity levels. The c-PBT material listed in these tables was prepared using 0.3 mol % stannoxane and had an apparent linear molecular weight by GPC of just over 280,000 prior to any heat treatment and degradation. The c-PBT results, shown after conditioning at different heat soak times and temperatures, are presented in each table for comparison with the linear resin results.

It should be noted that there is a difference in the measured crystallinities of the different PBT specimens tested. The toughness is directly related to the crystallinity level of the polymer, as described in the general discussion of fracture in crystalline polymers in Section 6.6. While many factors influence the toughness of PBT (i.e., the presence of an amorphous skin, the crystal thickness, the number of intercrystalline tie chains, etc.), the toughness differences between the different linear PBTs is here simply presented in a plot of toughness as a function of crystallinity. In each such plot, the presentation has been greatly simplified by including only the average toughness value for each resin in the plot.

Figure 6.107 shows such a plot for the compact tension specimens. Data from both the unannealed specimens and annealed specimens are shown together in this plot,

with solid lines depicting the toughness vs. crystallinity difference before and after annealing. The two low molecular weight linear resins, VALOX 195 PBT and VALOX 295 PBT, gave valid test results prior to annealing. After annealing, all four of the linear resins gave valid test results.

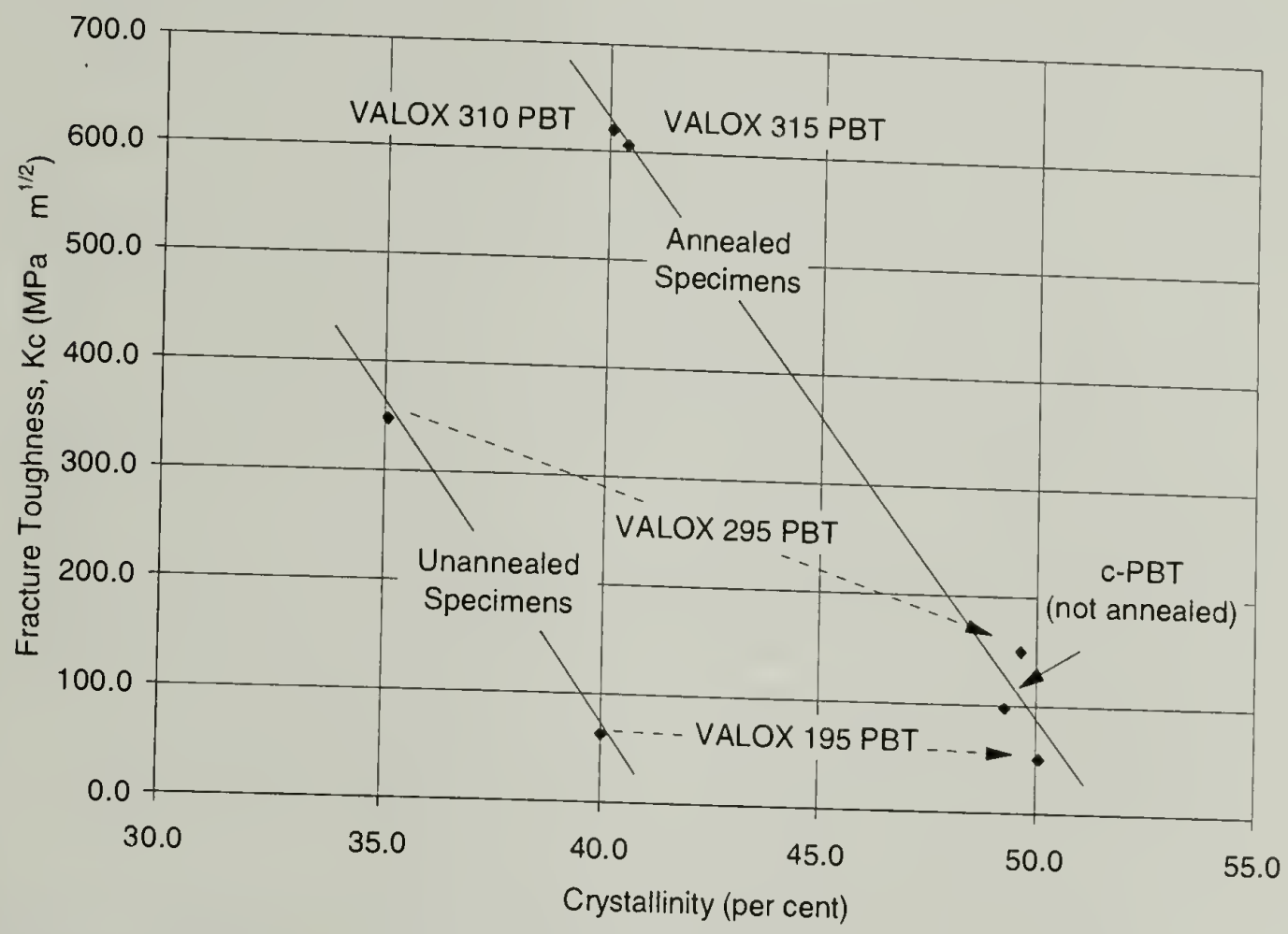


**Figure 6.107 Compact Tension fracture toughness vs. crystallinity.**

Annealing has the effect of increasing the crystallinity and lowering the toughness of PBT as seen by the shift in position indicated by the dotted lines for two resins. The fracture toughness of linear injection molded PBT is not simply a result of the level of crystallinity in the polymer. The unannealed and annealed data do not fall on the same line, presumable because of differences in toughness attributed to the amorphous skin[6], and possibly relating to crystal thickening on annealing. As described earlier in Section 6.6, crystal thickening has the effect of concentrating stress in the lower modulus glassy polymer when the material is put under load. No observations have been made of the morphological differences caused by annealing in these specimens. The single point for

c-PBT is found to lie on the line represented by annealed PBTs. This is not surprising as this specimen compression molded had no amorphous skin. The toughness of c-PBT prior to degradation is found to be between that of VALOX 195 PBT and VALOX 295 PBT.

**Table 6.10 Range for fracture results of un-annealed PBT resins.**

**Compact Tension Specimens**

| | % Crystallinity | Kc ($MPa \cdot m^{1/2}$) | Gc ($kJ/m^2$) |
|---|---|---|---|
| VALOX 195 PBT | 40.0 | 60 - 68 | 0.12 - 0.17 |
| VALOX 295 PBT | 35.1 | 320 - 370 | 4.2 - 5.6 |
| VALOX 310 PBT | 34.6 | Ductile | Ductile |
| VALOX 315 PBT | 33.1 | Ductile | Ductile |
| c-PBT | 49.3 | 80 - 110 | 0.23 - 0.54 |

**Dual Torsion Specimens**

| | % Crystallinity | Kc ($MPa \cdot m^{1/2}$) | Gc ($kJ/m^2$) |
|---|---|---|---|
| VALOX 195 PBT | 40.0 | 78 - 100 | 0.23 - 0.37 |
| VALOX 295 PBT | 35.1 | 370 - 390 | 5.6 - 6.1 |
| VALOX 310 PBT | 34.6 | 750 (Ductile) | 23 (Ductile) |
| VALOX 315 PBT | 33.1 | 1200 (Ductile) | 60 (Ductile) |
| c-PBT | 49.3 | 100 - 140 | 0.39 - 0.77 |

**Dual Cantilever Beam Specimens**

| | % Crystallinity | Kc ($MPa \cdot m^{1/2}$) | Gc ($kJ/m^2$) |
|---|---|---|---|
| VALOX 195 PBT | 40.0 | 70 - 130 | 0.18 - 0.61 |
| VALOX 295 PBT | 35.1 | 220 - 225 | 1.9 - 2.1 |
| VALOX 310 PBT | 34.6 | Ductile | Ductile |
| VALOX 315 PBT | 33.1 | Ductile | Ductile |
| c-PBT | 49.3 | No valid result | No valid result |

**Single Edge Notched Bending Specimens**

| | | % Crystallinity | Kc ($MPa \cdot m^{1/2}$) | Gc ($kJ/m^2$) |
|---|---|---|---|---|
| | VALOX 195 PBT | 40.0 | 40 - 60 | 0.06 - 0.13 |
| | VALOX 295 PBT | 35.1 | Ductile | Ductile |
| | VALOX 310 PBT | 34.6 | not tested | not tested |
| | VALOX 315 PBT | 33.1 | Ductile | Ductile |
| c-PBT | 2min @232C | 56.8 | 47 - 65 | 0.09 - 0.18 |
| c-PBT | 10min @250C | 43.2 | 120 - 165 | 0.12 - 0.21 |
| c-PBT | 20min @250C | 34.6 | 150 - 170 | 1.0 - 1.3 |
| c-PBT | 35min @250C | 36.3 | 140 - 160 | 0.9 - 1.2 |

**Table 6.11 Range for fracture results of linear PBT resins after annealing for 15 hours at 150° C. Also included are c-PBT specimens after compression molding at the conditions indicated.**

**Compact Tension Specimens**

| | % Crystallinity | Kc ($MPa \cdot m^{1/2}$) | Gc ($kJ/m^2$) |
|---|---|---|---|
| VALOX 195 PBT | 50.1 | 50 - 53 | 0.09 - 0.10 |
| VALOX 295 PBT | 49.6 | 140 - 160 | 0.8 - 1.1 |
| VALOX 310 PBT | 40.1 | 610 - 630 | 15 - 17 |
| VALOX 315 PBT | 40.4 | 560 - 660 | 12 - 17 |
| c-PBT | 49.3 | 80 - 110 | 0.23 - 0.54 |

**Dual Torsion Specimens**

| | % Crystallinity | Kc ($MPa \cdot m^{1/2}$) | Gc ($kJ/m^2$) |
|---|---|---|---|
| VALOX 195 PBT | 50.1 | 32 - 39 | 0.03 - 0.05 |
| VALOX 295 PBT | 49.6 | 80 - 110 | 0.23 -0.54 |
| VALOX 310 PBT | 40.1 | 450 | 7.2 |
| VALOX 315 PBT | 40.4 | 425 - 510 | 5.5 - 9.3 |
| c-PBT | 49.3 | 100 - 140 | 0.4 - 0.8 |

**Dual Cantilever Beam Specimens**

| | % Crystallinity | Kc ($MPa \cdot m^{1/2}$) | Gc ($kJ/m^2$) |
|---|---|---|---|
| VALOX 195 PBT | 50.1 | No valid result | No valid result |
| VALOX 295 PBT | 49.6 | No valid result | No valid result |
| VALOX 310 PBT | 40.1 | not tested | not tested |
| VALOX 315 PBT | 40.4 | No valid result | No valid result |
| c-PBT | 49.3 | No valid result | No valid result |

**Single Edge Notched Bending Specimens**

| | | % Crystallinity | Kc ($MPa \cdot m^{1/2}$) | Gc ($kJ/m^2$) |
|---|---|---|---|---|
| | VALOX 195 PBT | 50.1 | 32 - 38 | 0.04 - 0.05 |
| | VALOX 295 PBT | 49.6 | 130 - 165 | 0.6 - 1.0 |
| | VALOX 310 PBT | 40.1 | not tested | not tested |
| | VALOX 315 PBT | 40.4 | Ductile | Ductile |
| c-PBT | 2min @232C | 56.8 | 48 - 65 | 0.09 - 0.18 |
| c-PBT | 10min @250C | 43.2 | 125 - 165 | 0.12 - 0.21 |
| c-PBT | 20min @250C | 34.6 | 150 - 170 | 1.0 - 1.0 |
| c-PBT | 35min @250C | 36.3 | 140 - 160 | 0.9 - 1.2 |

Figure 6.108 shows analogous data from the Dual Torsion fracture specimens. The data follows the same trends, as seen for the Compact Tension fracture specimens. The same arguments for the changes in toughness with crystallinity also apply.

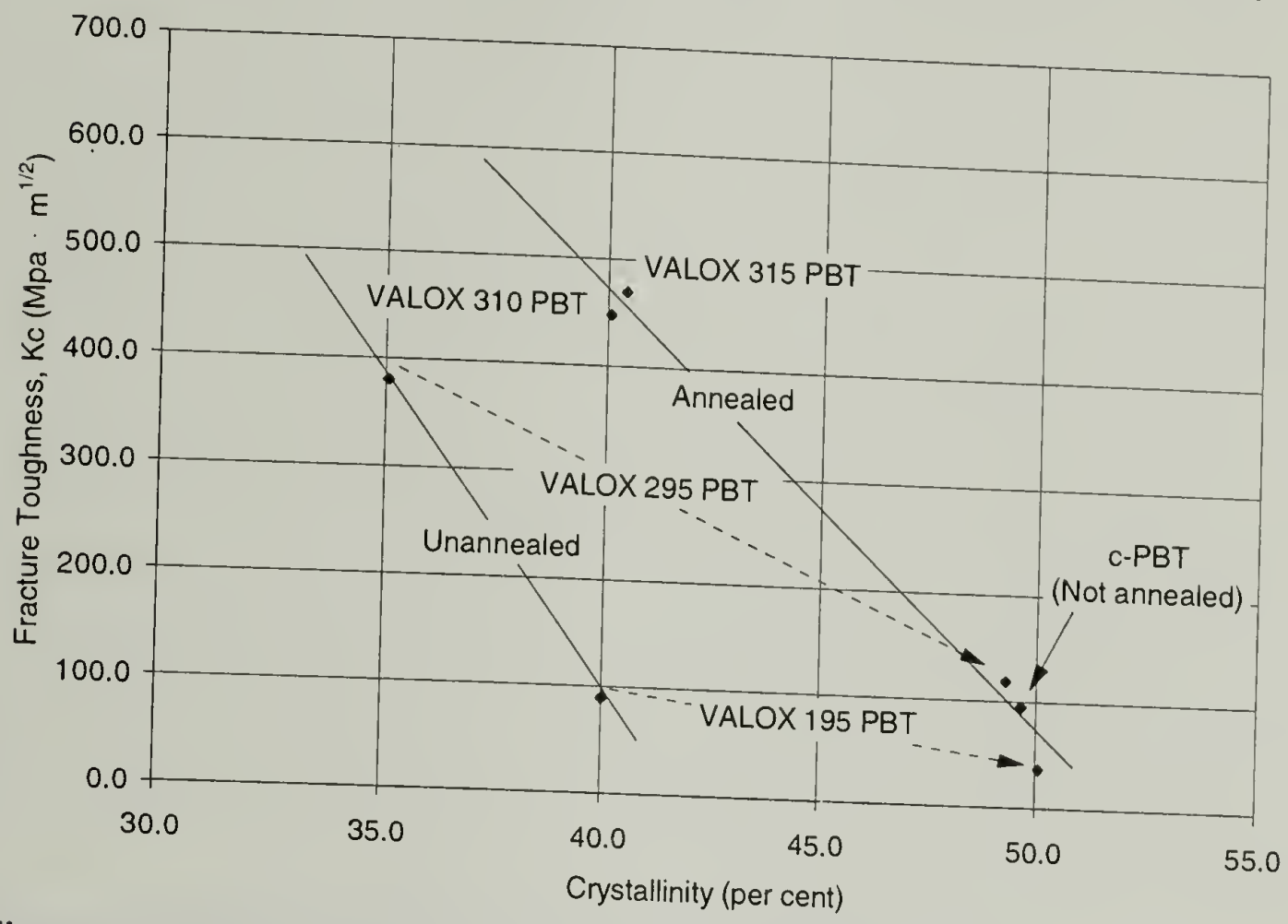


**Figure 6.108 Dual Torsion fracture results for PBT resins.**

The dual cantilever beam geometry was found to be the most difficult geometry for obtaining reproducible data over the range of toughness shown by the PBT resins under investigation. Only the two lowest molecular weight linear resins were found to produce valid measurements. VALOX 195 PBT resin gave results somewhat higher than the CT specimens, but in the same range as the DT specimens. VALOX 295 PBT resin produced results slightly below either the CT specimens or the DT specimens. The c-PBT specimen broke without a stable crack forming and no result was obtained for this polymer. DCB fracture data are included in Table 6.10 but are not plotted herein.

Figure 6.109 shows the results obtained using the Single Edge Notched Bending specimens. This geometry resulted in a significant amount of ductile deformation prior to

fracture for the two high molecular weight linear resins when test specimens were taken from the as-molded plaques as well as from plaques that had been annealed. VALOX 295 PBT showed ductile behavior prior to annealing, but produced acceptable results following the annealing treatment.

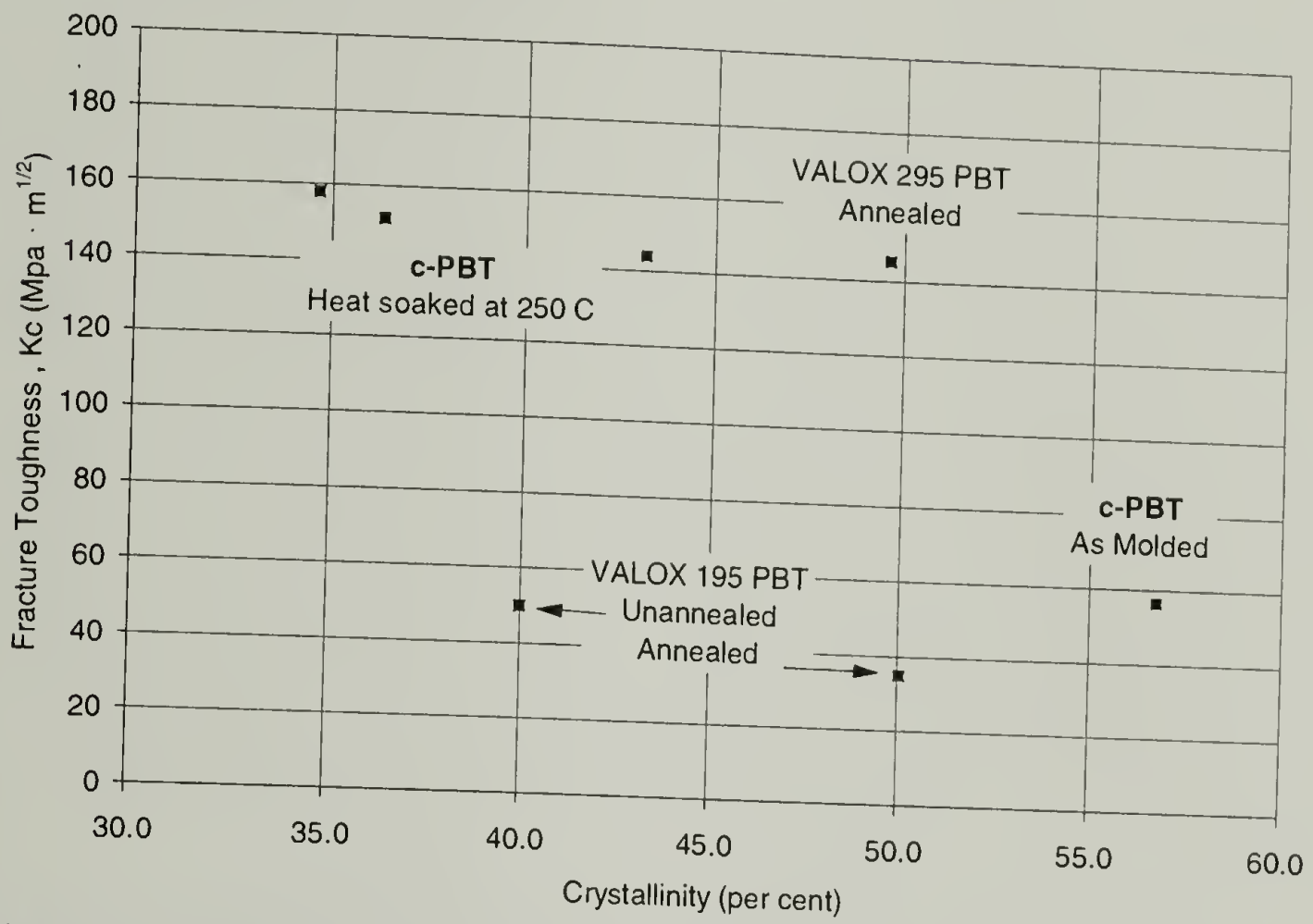


**Figure 6.109 Single Edge Notched Beam fracture results for c-PBT and linear PBT resins after various heat treatments.**

This geometry was amenable to producing useful fracture specimens from c-PBT that had been given different thermal conditioning treatments above the melt temperature. Prior to the melt conditioning, the c-PBT specimens were found to have a fracture toughness in the range of unannealed VALOX 195 PBT. On annealing, the specimens were found to have an increased toughness, more nearly equivalent to annealed VALOX 295 PBT. The increase in toughness following heat treatment for various times at 250° C is shown in Figure 6.110. All raw data from the testing is presented in this figure, as well as reproduced data from two different batches of c-PBT, designated as SMIII-26 and

SMIII-75. Each of these polymers was prepared by using 0.3 mol % stannoxane and pre-polymerizing the BTCs at 190° C for 20 minutes. The polymerization process was described in detail in Section 6.5.2. Following polymerization these specimens were compression molded by remelting and consolidation for 3 minutes at 232° C.

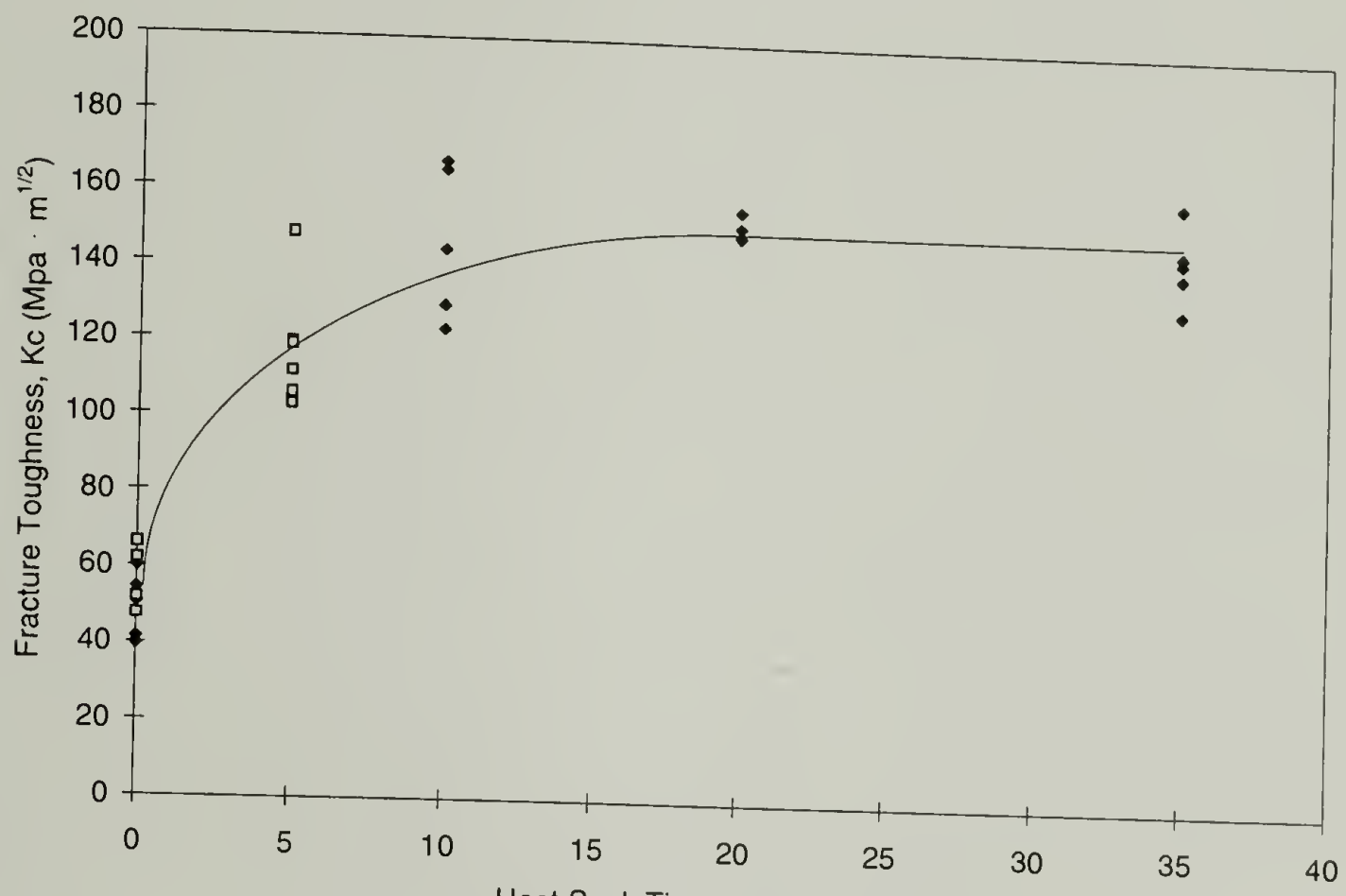


**Figure 6.110 Fracture toughness increase with extended time in the melt at 250° C for two different batches of c-PBT produced using 0.3 mol % stannoxane initiator. Filled diamonds are SMIII-75, open squares are SMIII-26.**

The thermal soak was found to degrade the c-PBT. Specimens at zero time were found to have an apparent $<M_w>$ of 280,000 while those which were thermally degraded for 30 minutes had a $<M_w>$ of about 85,000. This confirms the result reported earlier in Section 6.3.1.4 on the thermal stability of cyclic resins in rheology studies. If we assume that all residues of the stannoxane initiator are degraded by the thermal treatment, we find that a stannoxane initiator level of 0.3 mol % produces macrocyclic molecules with an

average of 3 to 4 tin residues which degrade to produce an average 3 to 4 linear chains based on a simply comparing the resulting molecular weights.

The results of all fracture testing are presented on a single graph is Figure 6.111. The data from unannealed specimens is seen to all fall within one band and the data from the annealed specimens are found to fall into a different band. The c-PBT fracture data, while decreasing in crystallinity and increasing in toughness with thermal conditioning and ring opening, does not follow the same trend as the linear resins. Linear PBT from degraded macrocyclic c-PBT exhibits a broader molecular weight distribution vs. the linear PBT resins, and shows a much reduced toughness vs. the linear resins.

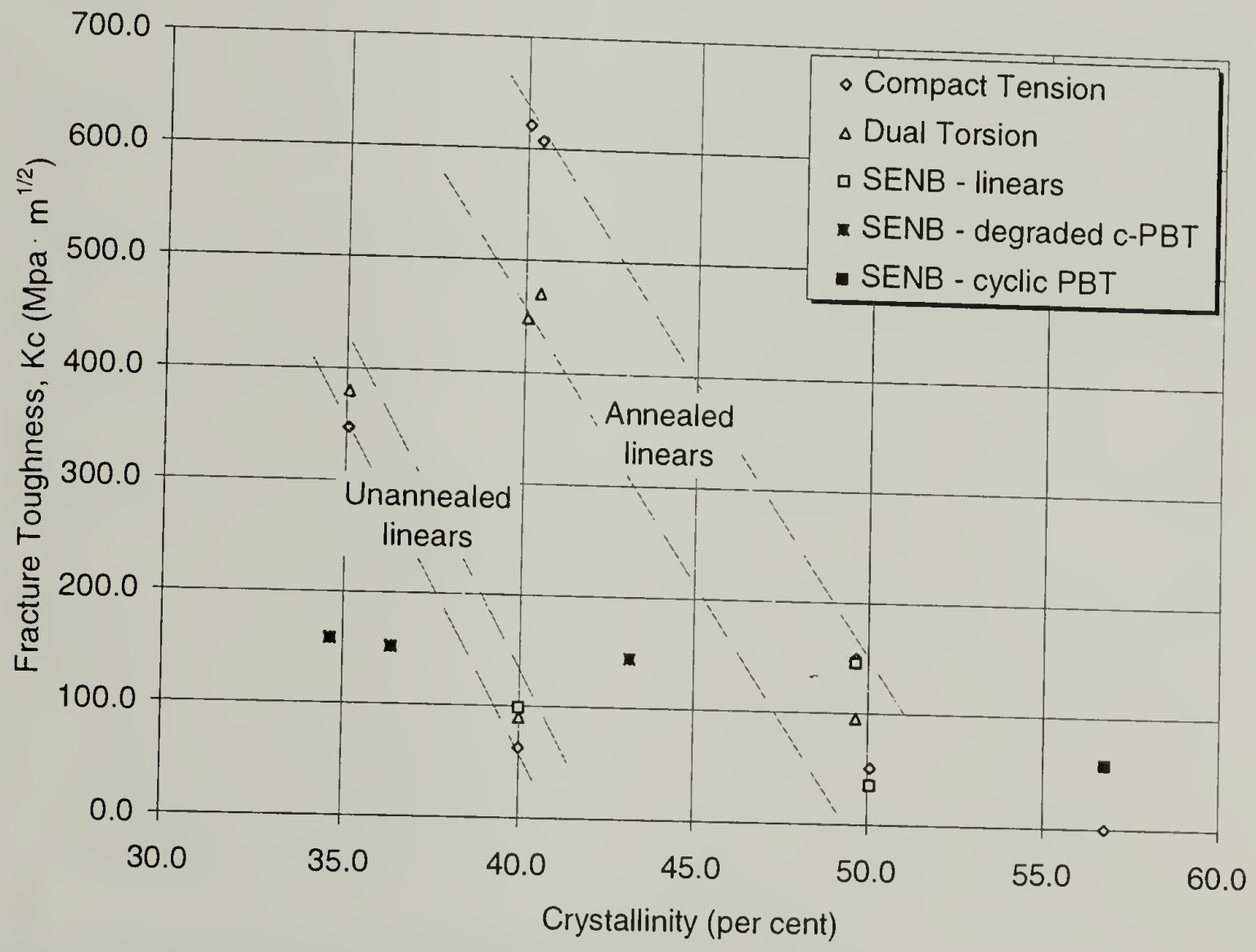


**Figure 6.111 Fracture Toughness testing results for all PBT resins using four different fracture specimens. Large solid data points represent c-PBT after various heat treatment conditions.**

Figure 6.111 validates that the different fracture geometries give reproducible results for PBT of the same chain topology. It also lends credence to the earlier claim that degrading the cyclic structures is not the best way to produce a viable PBT from cyclic oligomers. While increasing the toughness of the brittle nascent c-PBT through thermal degradation is of scientific value in helping to understand the behavior of cyclic and linear polymer chains, it does not result in producing a linear polymer of equivalent toughness to the commercial PBT resins. The recommendation in Section 5.3 for continuing this study with a new initiator, dibutyltin diethoxide, is reinforced by the results of the fracture studies on degraded macrocyclic c-PBT.

An estimate of the inherent fracture toughness of c-PBT can be made by applying the technique reported by Liu and Donovan for calculating the plastic zone size in nylons[28]. Based on work in ceramics, Evans[29] has proposed that the size of the plastic zone, $R_y$, should be proportional to the increase in critical fracture toughness resulting from plastic deformation, i.e.

$$\Delta K_{IC} = k\, R_y$$

where $k$ is a constant of proportionality and $\Delta K_{IC}$ is the increase in toughens over the inherent toughness without any plastic deformation. The size of the plastic zone ahead of a sharp crack tip under plane strain conditions is given by[30]

$$R_y = \frac{\pi^2}{8\Psi}\left(\frac{\sigma}{\sigma_y}\right)^2 c = \frac{\pi}{8\alpha\Psi}\frac{K^2}{\sigma_y^2}$$

where

$$K = \sigma\sqrt{\alpha\pi c}, \quad \alpha = \frac{\Omega}{\Psi}$$

$\Omega$ and $\Psi$ are geometric factors which account for the finite specimen and notch geometry.

In the SENB specimens under evaluation, this equation may be approximated by

$$R_y = \frac{K_{IC}^2}{4\sigma_y^2}$$

where the constants on the right hand side of the equation are reported in Tables 6.9 and 6.10. The theory of Evans assumes that the measured fracture toughness, $K_{IC}$, is the sum of the inherent toughness of the material, $K_0$, and the increased toughness due to the plastic zone, $\Delta K_{IC}$, as

$$K_{IC} = K_0 + \Delta K_{IC}.$$

Any increase in plastic zone size has a linear effect on the increase in fracture toughness. Values of $R_y$ were calculated and plotted vs. the respective $K_{IC}$ values for each specimen. While this type of analysis appears to be somewhat of a solipsism, it does provide an interesting conceptual result. Extrapolation to zero yield zone size should give an inherent toughness of the polymer, were it possible to initiate a fracture without first forming a plastic zone. Figure 6.113 shows this correlation for the linear VALOX PBT resins.

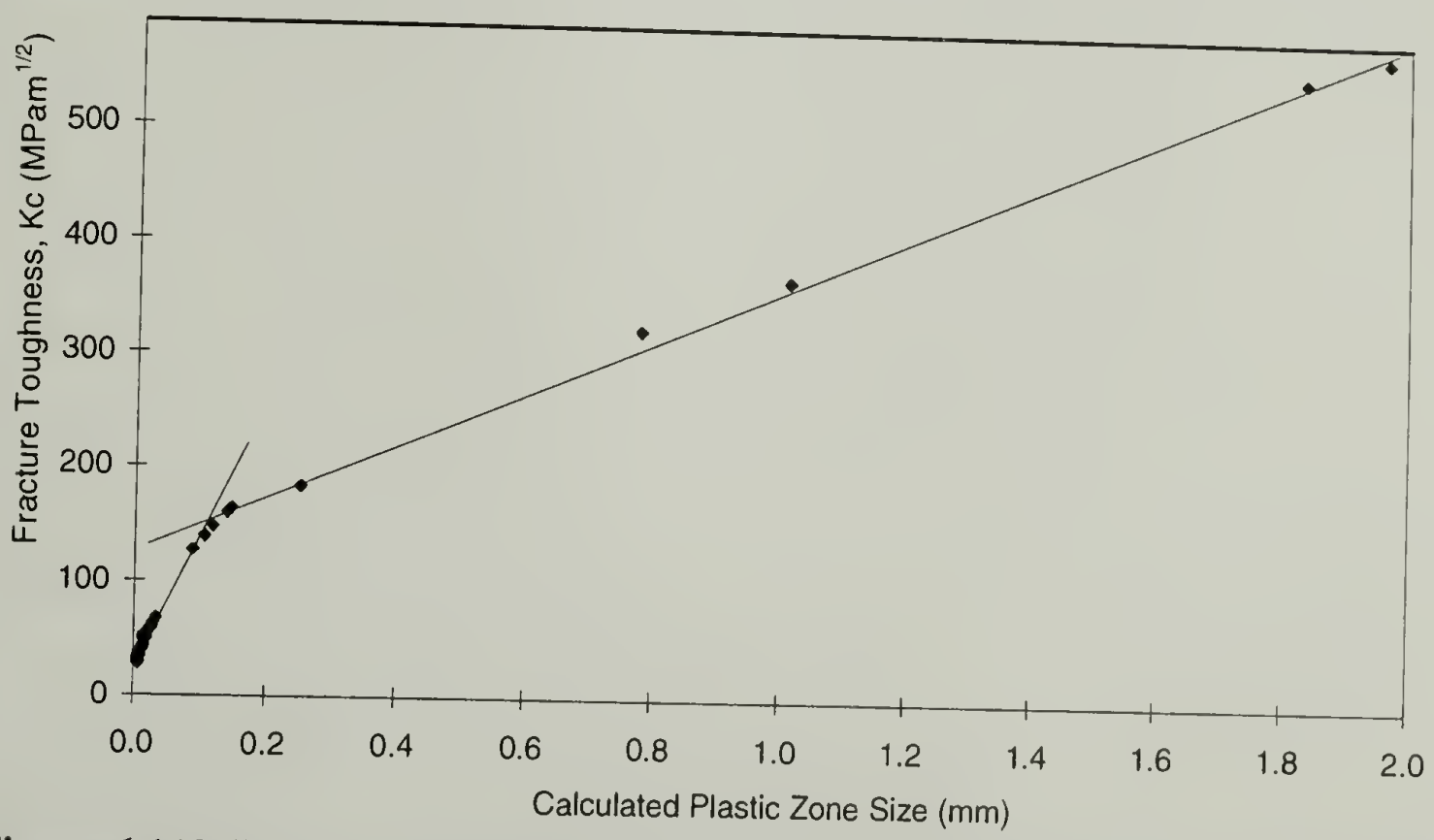


**Figure 6.112 Fracture toughness of linear VALOX PBT specimens as a function of yield zone size.**

Rather than the expected single correlation of plastic zone size vs. toughness, two distinct correlations exist for the linear resins. The data points on the upper line, having the lower slope, represent high molecular weight PBT resins, both annealed and unannealed. The points on the steeper slope represent VALOX 195 PBT. This resin was found to be below the critical molecular weight for entanglement in the rheology studies reported in Section 6.3.1.6, and its fracture toughness also suggests that this resin is incapable of supporting a stress (and thereby resisting fracture) to the same degree as the higher molecular weight linear PBT resins. The two lines predict a different "inherent toughness" for high molecular weight PBTs than for VALOX 195 PBT.

No supporting evidence has been found in the literature for this type of result. Liu's smallest calculated plastic zone sizes are reported for an amorphous nylon (iso/terephthalate acid / hexamethyl diamine) as 0.8 mm and for a nylon 6 as 0.15 mm. Both of these plastic zone radii are greater than the intersection of the slopes found for PBTs and thus show only a linear correlation associated with the tougher resins.

When this same analysis is done on the cyclic resins data, a non-linear result is found. Figure 6.113 shows that the data points representing macrocyclic PBTs, which have not been thermally degraded, all fall together on a linear slope. The slope of these data points is the same as that of the VALOX 195 PBT in Figure 6.112. The macrocyclic PBTs are believed to have lower fracture toughness' based on fewer interlamellar tie chains formed during crystallization. This result suggests that very low molecular weight linear resins also have fewer intercrystalline tie molecules, the absence of which decrease the "inherent toughness" of the PBT resin. When c-PBT is thermally degraded, its toughness increases, and the "inherent toughness" of the resin is also increases. This is

suggested by a decrease in the slope of the data in Figure 6.113 as the calculated plastic zone size increases.

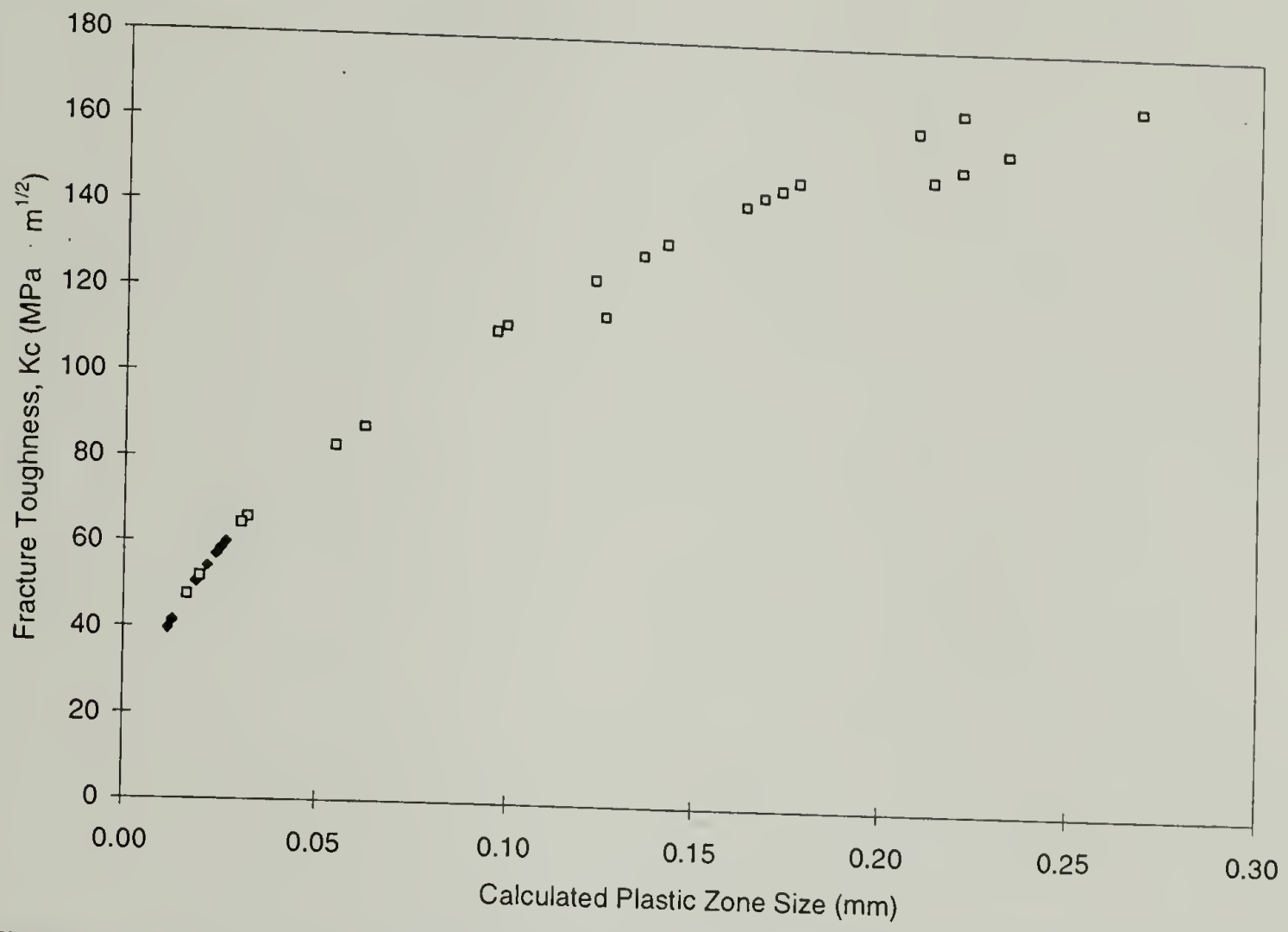


**Figure 6.113 Fracture toughness of c-PBT resins as a function of plastic zone size. Solid points represent c-PBT which has not been thermally degraded. The open points represent c-PBT after various heat soak times at 250° C.**

When the data from the two figures above are combined, a consistent picture of the toughening of c-PBT is found. Figure 6.114 shows the combine data near the transition zone. The c-PBT resins, when thermally degraded, produce a toughness nearly that of the commercial linear resins. The data from thermally degraded c-PBT shows that these resins are not as tough as the commercial resins, presumably because of a broader molecular weight distribution and the presence of some residual cyclic structure in the final degraded polymer. The slopes in this figure are the same as the slopes shown in Figure 6.112 for the linear PBT resins.

From the rheology studies, VALOX 195 PBT was found to be below the critical molecular weight for entanglement. This low entanglement density appears to allow VALOX 195 PBT to reach high crystallinity on cooling. The compressive yielding data suggests that the cyclic c-PBT has a lower tie chain density in the semi-crystalline polymer. This lower tie chain density appears to be related to the molecular dimensions of the cyclic resin during crystallization, and allows the c-PBT to also reach high levels of crystallinity. These two resins each fall on the steeper line which predicts a lower inherent toughness during brittle fracture.

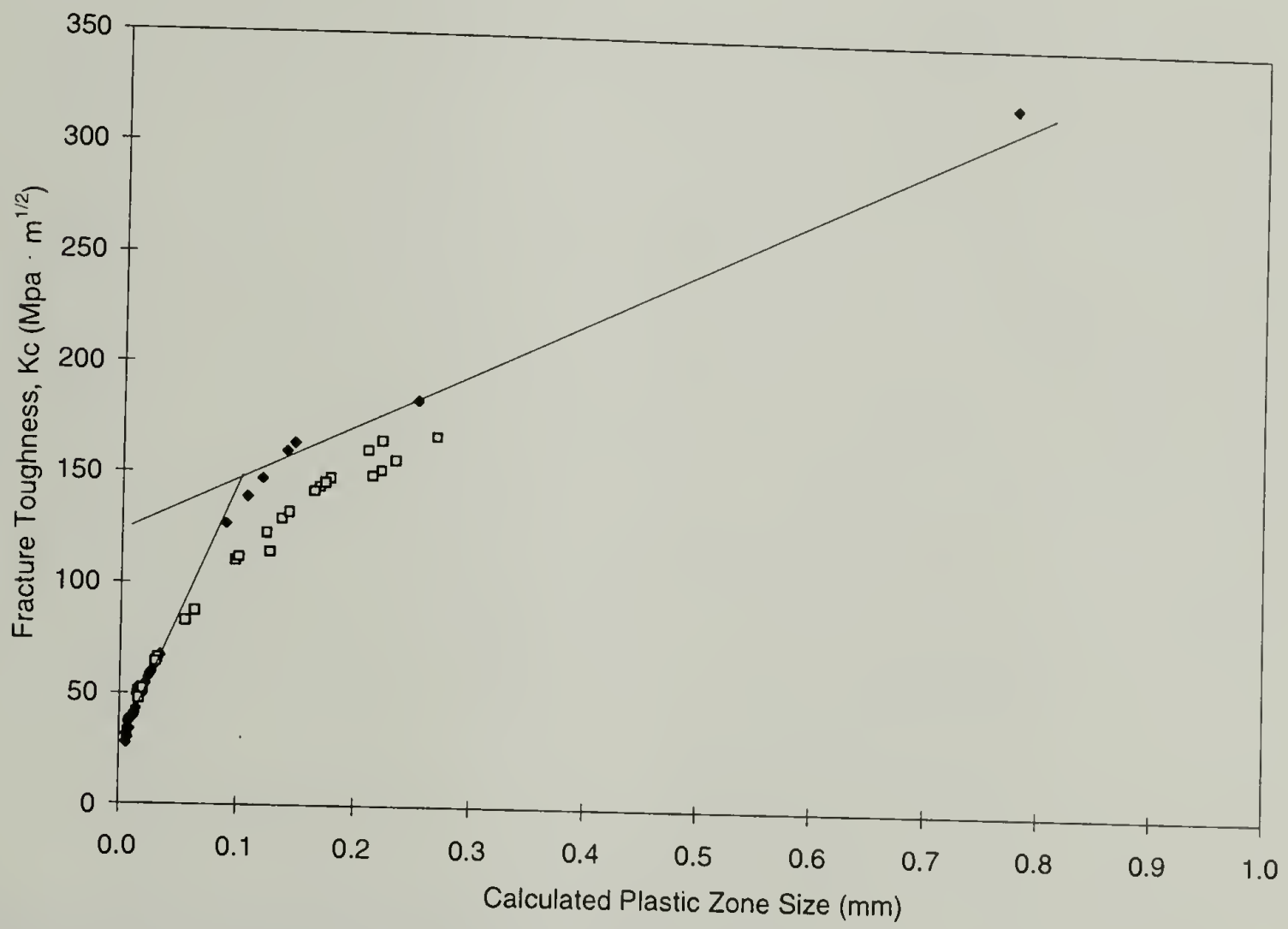


**Figure 6.114 Fracture toughness vs. plastic zone size using combined data from linear PBTs and c-PBTs. Solid data points represent linear VALOX PBT resins. Open data points represent thermally degraded c-PBT.**

The relationship between toughness and. yield zone size for the most brittle resins (VALOX 195 PBT and c-PBT) predicts that these resins have a lower inherent toughness

than any of the other PBT resins. The inherent toughness is a measure of the ability of the resin to resist fracture in the absence of any plasticity. The lower inherent toughness of VALOX 195 PBT and c-PBT appears to be the result of fewer tie chains in these two systems, compared to the higher molecular weight linear resins - both commercial linear resins and linear resins resulting from degradation of macrocyclic c-PBT. It appears that the toughness of PBT is not only related to the crystallinity of the resin. The crystallinity of the annealed VALOX 315 PBT and the unannealed VALOX 195 PBT are almost identical, while Figure 6.112 demonstrates that VALOX 315 has a 50 times larger yield zone radius and an order of magnitude increase in toughness.

High molecular weight linear PBTs have a higher inherent toughness which appears related to their ability to produce plastic deformation. The higher the molecular weight, the more plastic deformation takes place on loading, resulting in a ductile yield prior to failure. For low molecular weight linear PBT, and the c-PBT resins, this plastic deformation mechanism is less operative, and the polymer fails in a brittle manner, with very little plastic yielding at the crack tip. These resins have a lower inherent toughness, the result of fewer plastic deformation mechanisms. This may result from fewer intercrystalline tie chains in these resins. This hypothesis remains to be proven and more research will be required in this area to establish a reason for the apparent difference in the toughness between high and low molecular weight PBT resins.

This type of analysis can also give an estimate of the "inherent" strain energy to produce a brittle fracture. Figure 6.115 shows a plot of Gc vs. the calculated plastic zone size. The linear fit of this data predicts an intercept which represents the strain energy consumed exclusive of any plastic deformations, i.e. the inherent energy consumed in

creating new surfaces through breaking chemical bonds during fracture. This strain energy is predicted to be 0.02 KJ/m$^2$. (Only the most brittle fracture data are used in this figure to minimize data scatter and get a usable prediction of inherent energy.)

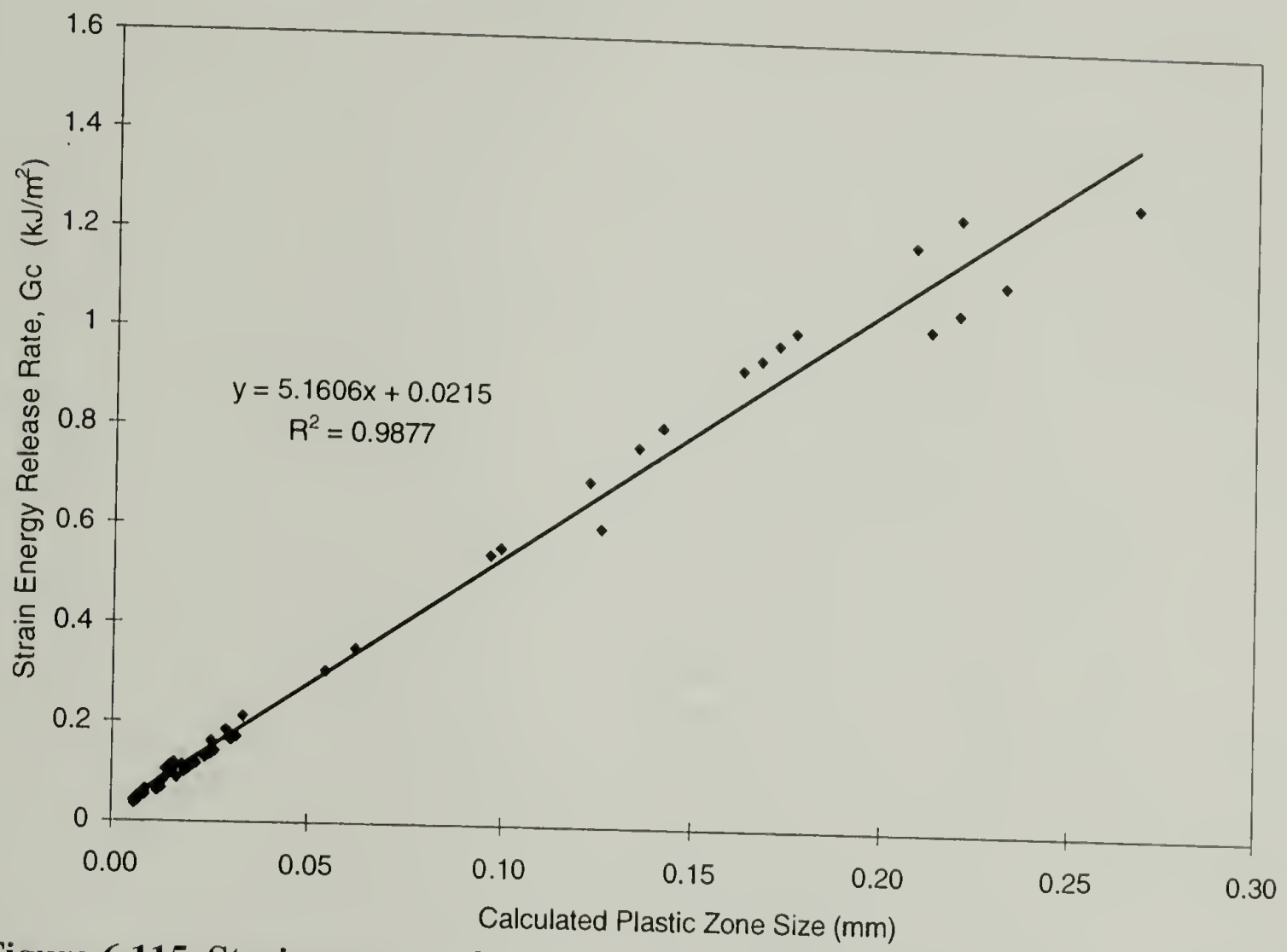


**Figure 6.115 Strain energy release rate as a function of calculated plastic zone size.**

A calculation of the energy associated with bond breaking can be performed following the methods of Berry[17]. The reported crystal lattice dimensions may be used to determine a cross-section for a PBT chain as 28.8 Å. Therefore, there would be 3.5 $E^{14}$ chains/cm$^2$ which cross any random plane in the solid structure. If only one third of these chains lie in the direction of applied stress, 1.2 $E^{14}$ chains would be broken by planar fracture through the solid. Using a C-C bond energy of 2.4 $E^{-19}$ cal / mol[31] gives a value of the Griffith surface energy, $\gamma$, for PBT of 0.0017 kJ/m$^2$. As shown earlier, $2\gamma$ = Gc, suggesting that 0.003 kJ/m$^2$ are consumed by a planar fracture of PBT. The inherent toughness predicted from the fracture test results is therefor about seven times higher than

predicted theoretically. A plausible explanation for this difference is that the fractal surface created by an actual fracture through the intercrystalline regions of PBT results in a much larger fracture area at the molecular level than is considered by bulk fracture techniques. In addition, significant elastic energy must be produced in bonds near the fracture surface prior to failure. On fracture, these bonds must dissipate much of this potential energy as vibrations, which are manifested as heat near the fracture surface. These energies are not easily measured but must account for a large amount of the excess fracture energy. The current result is much closer to the theoretical prediction of fracture energy than was reported by Berry. Further experimental work is needed to account for the excess energy consumed on fracture.

### 6.6.8 References for Fracture Toughness


1)Prentice, P., *Journal of Materials Science* **1985**, *20*, 1445-1454.
2)Keith, H. D.; Padden, F. J.; Vadimsky, R., *Journal of Polymer Science Part A-2* **1966**, *4*, 267-281.
3)Chang, E.; Kirsten, R.; Slagowski, E., *ACS Polymer Preprints* **1978**, *19*, 578.
4)Lustiger, A.; Markham, R. L., *Polymer* **1983**, *24*, 1647-1654.
5)Peterlin, A., *Journal of Polymer Science, Part A-2* **1969**, *7*, 1151-1163.
6)Hobbs, S. Y.; Pratt, C. F., *Journal of Applied Polymer Science* **1975**, *19*, 1701-1722.
7)Pook, L. P.; Smith, R. A. *Theoretical Background to Elastic Fracture Mechanics*; Smith, R. A., Ed.; Pergamon Press: Toronto, **1979**, pp. 29-68.
8)Smith, R. *Fracture Mechanics, Current Status, Future Prospects*; Smith, R., Ed.; Pergamon Press: Cambridge University, England,**1979**.
9)Yee, A.; Olsezwski, W.; Miller, S. *Plane Strain and the Brittleness of Plastics*; Deanin, R. and Crugnola, A., Ed.; American Chemical Society: Washington, DC, **1976**, pp. 97-111.
10)Pascoe, K. J. *7. General Fracture Mechanics*; Brostow, W. and Corneliussen, R., Ed.; Hanser Press, **1986**, pp. 119-143.
11)ASTM; D5043-96 *Plane Strain Fracture Toughness and Strain Energy Release Rate of Plastic Materials*, **1996**.
12)Young, R. *Introduction to Polymers*; 2nd ed.; Chapman and Hall: New York, **1983**.
13)Griffith, A., *Philosophical Transactions of the Royal Society* **1921**, *A 221*, 163-197.
14)Irwin, G., *Transactions of the American Society of Metals* **1948**, *40*, 147.
15)Orowan, E., *Rep. Prog. Phys.* **1948**, *12*, 185.
16)ASTM *Standard Test Method for Compressive Properties of Rigid Plastics*, 1996.
17)Berry, J. P., *Journal of Applied Physics* **1963**, *34*, 62.
18)Kambour, R. P.; Holik, a. S.; Miller, S., *Journal of Polymer Science: Polymer Physics Edition* **1978**, *16*, 91-104.
19)Williams, D. P.; Evans, A. G.,*Journal of Testing and Evaluation* **1973**, *1*, 264-270.
20)Beaumont, P. W. R.; Young, R. J., *Journal of Materials Science* **1975**, *10*.
21)Hine, P. J.; Duckett, R. A.; Ward, I. M., *Journal of Materials Science* **1984**, *19*, 3796-3805.
22)Evans, A. G., *Journal of Materials Science* **1972**, *7*, 1137-1136.
23)Evans, A. G., *International Journal of Fracture* **1972**, *9*, 267-275.
24)Mai, Y. W., *International Journal of Fracture* **1973**, *9*, 349.
25)Kambour, R. P.; Miller, S., *Journal of Material Science* **1976**, *11*, 823.
26)Kambour, R. P.; Smith, S. A., *Journal of Polymer Science: Polymer Physics Edition*, **1982**, *20*, 2069-2082.
27)Kies, J. A.; Clark, B. J. *Fracture - 1969*; Chapman and Hall, Ltd.: London, **1969**.
28)Liu, Y.; Donovan, J. A., *Polymer Engineering and Science* **1996**, *36*, 2345-2351.
29)Evans, A. G.; Ahmad, Z. B.; Gilbert, D. G.; Beaumont, P. W. R., *Acta Metall.* **1986**, *34*, 79.
30)Tetelman, A. S.; McEvily, A. J. *Fracture of Structural Materials*; John Wiley and Sons: New York, NY, **1967**.
31)*CRC Handbook of Chemistry and Physics*; 65 ed.; CRC Press, Inc.: Boca Raton, FL.

# CHAPTER 7
# CONCLUSIONS

The following conclusions are considered to be significant results of the research. Each conclusion is presented as a summary with reference to the section of the thesis where a full discussion may be found which leads to the conclusion. Each conclusion is important in understanding the unique characteristics of c-PBT. Following the conclusions are a series of significant findings resulting from this research.

- *c-PBT, polymerized at 190° C using the stannoxane initiator, produces an unexpected spherulitic morphology, one only previously reported for melt cooled linear PBT which had been slowly crystallized, isothermally crystallized at high temperatures, or crystallized from solution. This "usual" type spherulite is reported as only being formed by crystallization under conditions which allow a high degree of crystal perfection, i.e., slow crystallization rates. Finding this usual spherulite in c-PBT which was rapidly polymerized and crystallized leads to the conclusion that the cyclic PBT also crystallizes under conditions which lead to a high degree of crystal perfection, albeit the crystallization is extremely fast. The crystalline melting points for stannoxane-initiated c-PBT are higher than the melting points reported in the literature for linear PBT by 10° to 15° C after being isothermally crystallized under the same conditions. This implies that the crystals in c-PBT have a higher degree of perfection than those in linear PBT when the two variants are crystallized under the same conditions. (Sections 6.2.2 and 6.2.4.2)*

- *Crystallization of cyclic molecules produces a lower degree of intercrystalline tie-chains than crystallization of linear molecules of the same molecular weight. This*

*results in a faster rate of crystallization in fully polymerized systems (Section 6.2.5) and a solidified plastic with high modulus but lower yield stress (Section 6.5.3) and a lower fracture toughness (Section 6.6.7) for the cyclic polymers.*

- *Macrocyclic PBT has a significantly lower degree of melt entanglement than linear PBT of equivalent molecular weight. As polymerized at 190° C using stannoxane initiator, c-PBT has a significantly lower zero shear viscosity (by an order of magnitude) than would be predicted for a linear PBT resin. After thermal degradation, c-PBT is reduced in both molecular weight and viscosity. Following degradation of the resin, the correlation of molecular weight and viscosity falls very close to the predicted relationship for linear resins. The relationship of log viscosity vs. log apparent molecular weight for macrocyclic resins has a significantly lower slope than the same relationship for linear resins, suggesting a different degree of melt entanglement for the cyclic molecules. The relationship* $\eta = Mw^{2.6}$ *appears to hold over a wide range of molecular weights. ( Section 6.3.1.6)*

- *Ring expansion polymerization (using a cyclic oligomer and a cyclic initiator) appears to produce a simpler (less catenated and less knotted) cyclic molecule for research into the behavior of macrocyclic polymer vs. the previously reported methods involving bifunctional living polymerization with ring closure in dilute solution. (Section 6.3.1.6)*

- *By extrapolation, the crystalline regions of PBT are estimated to have twice the modulus of the glassy regions. Because the modulus is determined at low strains, this result is equally valid for macrocyclic and linear PBT resins. The modulus vs.*

*% crystallinity relationship is reported to be: Modulus (in GPa) = 0.0174 (% Crystallinity) + 1.59. (Section 6.5.3)*

- *Tie chain density determines the stress and strain where PBT deviates from elastic behavior. c-PBT, produced from stannoxane initiator, has a higher crystallinity than melt-cooled linear PBT with the mechanical result being that the cyclic polymer has a higher modulus, proportional to its crystallinity. However, c- PBT exhibits a 25 % lower yield stress at equivalent crystallinity (as determined by the stress where the strain has deviated from elastic behavior by 0.2 %). Fewer tie chains in the semi-crystalline structure of the cyclic resin vs. the linear resin, result in anelastic behavior at proportionally lower stresses. (Section 6.5.3)*
- *Macrocyclic PBT can be toughened through degradation of the cyclic structure. C-PBT produced from the stannoxane initiator is a very brittle polymer. However, its fracture toughness has been found to triple after only 10 minutes of thermal degradation at 250° C. This toughening is attributed a time-dependent degradation of the very high molecular weight cyclic molecular structure to a linear structure. On cooling from the melt, the degraded polymer is capable of producing a tougher PBT, apparently through increasing the number of intercrystalline tie chains in the semi-crystalline material. This degraded c-PBT is found to have a yield stress (see above conclusion) only 13 % below the linear PBT resin at equivalent crystallinity. (Sections 6.6.7 and 6.5.3)*
- *Macrocyclic PBT is inherently less tough than linear PBT based on its lower tie chain density. A calculated "inherent toughness" of PBT, in the absence of any plastic zone at the crack tip, has been determined to be 125 MPa·m$^{1/2}$. Below a critical*

*fracture toughness, this result is modified, and the "inherent toughness" decreases to only 20 to 30 MPa·m$^{1/2}$. The new finding suggests that resins that have fewer intercrystalline tie chains (both linear PBT below its critical molecular weight for melt entanglement, and high molecular weight cyclic PBT resins) have a less effective toughening mechanism to prevent fracture, which produces less plastic yielding at the crack tip. The theoretically predicted value of the Griffith fracture energy of PBT compares favorably with the results obtained in this study. (Section 6.6.7)*

The following findings, while not being significant conclusions, nevertheless are worth reporting in this section.

- Molecular weight of c-PBT is determined by the ratio of monomer concentration to the initiator concentration for both initiators used in this investigation. (Sections 5.1 and 5.2)
- The stannoxane initiator is unstable at temperatures above 220° C, leading to a degradation of the cyclic molecules when heated above the melt temperature of the crystalline c-PBT polymer. ( Sections 5.2 and 6.3.1.2)
- Between 170° C and 225° C, the nucleation time for crystallization of c-PBT polymer is faster when stannoxane initiator is used for the polymerization vs. using TBTE initiator. This appears to be based on the faster polymerization using the stannoxane initiator vs. the TBTE initiator. (Section 6.2.4.1)
- The stannoxane cyclic initiator produces a polymer that crystallizes much faster than does polymer produced by the TBTE linear initiator. Again, this is primarily a result of the rate of polymerization being at least an order of magnitude greater for the stannoxane initiator than the TBTE initiator. (Section 6.2.4.1)

- Polymerization of BTCs using stannoxane initiator produces a high degree of crystallinity at all temperatures investigated (170° C to 212° C). By contrast, BTCs polymerized with the TBTE initiator produce a highly crystalline polymer at the lower temperatures, but the crystallizability decreases as the temperature of isothermal polymerization and crystallization increases. (Section 6.2.4.1)
- At 170° C, polymer produced using TBTE initiator shows a significant decrease in crystallization rate when the polymer reaches about half of its ultimate crystallinity. This may be related to a slowing of the diffusion of cyclic oligomers which must reach an active polymerization site to react and form crystallizable high molecular weight polymer. At 170° C, crystallization is faster than polymerization when TBTE is used in the polymerization. (Section 6.2.4.1)
- In the temperature range of 210° C to 220° C, the time for TBTE to initiate polymerization and the time for the resultant PBT to begin to crystallize are about the same. At lower temperatures, where the degree of undercooling is greater and the polymerization rate is lower, the polymerization rate regulates, and limits, the crystallization rate. (Sections 6.2.4.1 and 6.3.2.4)
- At temperatures where PBT is relatively stable, thermal degradation of macrocyclic c-PBT (polymerized using 0.3 mol % stannoxane) decreases in molecular weight to 25 to 30 % of its original <Mw>, suggesting that there were an average of 3 to 4 stannoxane linkages in these polymers prior to degradation. (Section 6.3.1.4)

- The critical molecular weight for entanglement was determined to be about 55,000 Daltons for linear PBT resins based on GPC results using PS calibrants. (Section 6.3.1.6)
- Under isothermal crystallization conditions, low molecular weight c-PBT resins exhibit a high crystallization rate. Higher molecular weight c-PBT resins, with a higher viscosity under zero shear conditions, exhibit a lower rate of crystallization possibly stemming from a slower rate of diffusion. (Section 6.3.2)
- c-PBT produced using the stannoxane initiator was found to have a low concentration of end groups. The techniques used in preparation of the specimens are believed to have slightly degraded the cyclic resins, resulting in the formation of some hydroxyl end groups. The concentration of end groups was found to increase with time during collection of solution NMR data at 70° C over a four hour period, suggesting that residual water in the solvent was hydrolyzing the c-PBT during the experiment. (Section 6.4.3.2)
- Poisson's ratio for c-PBT produced from stannoxane initiator was found to be significantly lower than the Poisson's ratio of commercial linear PBT resins, suggesting a that there is less plastic deformation in the highly crystalline c-PBT resin. (Section 6.5.1)
- The mechanically determined Tg for cyclic PBT resins is the same as that of linear PBT resins. (Section 6.5.2)
- The fracture toughness results using four different geometry specimens were found to correlate well for the linear PBT resins. Crystallinity is a major determinant of the fracture toughness of linear PBT resins. (Section 6.6.7)

- c-PBT, produced with 0.3 mol % stannoxane initiator (Mw ~ 150,000), is found to have a fracture toughness similar to that of an annealed linear PBT of Mw ~ 90,000. Degradation of the c-PBT is found to increase its fracture toughness, but the resulting toughness is not equivalent to that of linear PBT at the same level of crystallinity. (Section 6.6.7)

Each of these conclusions and findings has merit to stand alone as an interesting or significant finding. Each conclusion helps to advance the understanding of the nature of PBT produced from cyclic oligomers, using a cyclic initiator. The polymers produced by this process are significantly different from the commercially available linear PBT resins. It remains to be proven however that these polymers are in fact truly macrocyclic in nature. Nevertheless, the preponderance of evidence compiled in this research points to the conclusion that these c-PBT resins, produced through a ring expansion polymerization, are truly cyclic macromolecules, and as such exhibit rheological and mechanical properties significantly different from the conventional linear analogues. In short, these differences appear understandable only in terms of the cyclic topology the molecules. *Quod erat demonstrandum.*

# CHAPTER 8

# RECOMMENDATIONS FOR FUTURE WORK

Several recommendations for further work have come out of the present research. These are listed in the order which they are discussed in the thesis.

1) ***Synthesize a Dibutyltin Diethoxide (DBDE) initiator and evaluate its effectiveness for producing high molecular weight, tough c-PBT.***

As discussed in Section 5.3, DBDE has not been synthesized, but is easily synthesized from dibutyltin chloride and ethanol. The condensation reaction should be nearly identical to the process for producing stannoxane as described in Section 5.1. Some adjustment may be needed in the reaction temperature, but this will become apparent on heating the components during the reaction. Characterization of the effectiveness of DBDE will include:

- Isothermal polymerization at 190° C to 210° C in the DSC to determine the rates of reaction vs. those when stannoxane initiator is used.
- Melting the polymer made with DBDE in the DSC following polymerization to determine both the melting point and the degree of crystallinity. Degree of crystallinity is expected to be high when polymerized at 190° C, but should decrease at higher polymerization temperatures.
- Tensile stress / strain tests on polymer produced by compression molding sheets of DBDE-initiated c-PBT at temperatures from 190° C to 210° C. Higher molding temperatures are expected to result in greater tensile elongations than were found for stannoxane-initiated c-PBTs.

- SENB fracture toughness characterization of polymer produced using DBDE to compare the toughness to that of commercial linear PBT resins.
- Fabrication of a composite structure from DBDE-initiated BTCs by infusing molten oligomer into a glass mat which has been solvent coated with the initiator.

*2) **Investigate the relationship between molecular weight and zero shear viscosity using cyclic polymers with much lower molecular weights than were produced in this study.***

- Prepare a series of c-PBT resins using stannoxane initiator at high concentrations to produce very low molecular weight cyclic polymers. Using from 0.6 mol % to 10.0 mol % stannoxane initiator should result in cyclic PBT with molecular weights ranging from 100,000 down to 20,000.
- Run low shear viscosity on these specimens at 250° C. Monitor the viscosity of the specimen as a function of time at temperature. Collect the specimens from the rheometer after 50 minutes of thermal degradation.
- Determine the apparent $<M_w>$ of the resins before and after the thermal exposure.
- Evaluate the relationship of viscosity vs. molecular weight at low molecular weights as compared to the linear resin relationships shown in this research.
- Determine the critical entanglement $<M_w>$ of cyclic PBT resins.

*3) **Produce definitive evidence of a macrocyclic structure in c-PBT produced by ring expansion polymerization. Two routes are suggested which may lead to a proof of the macrocyclic nature of such molecules through comparing the ratio of Mw/Rg for macrocyclic and linear PBT resins. In each case it is necessary to produce a non-crystalline specimen which could be readily dissolved in a benign good solvent for light scattering experiments, or could be deuterated and thus evaluated in solid state neutron scattering experiments.***

- The first route to producing amorphous polyester for evaluation would be to make copolymers of PBT and PET. When prepared using a high ratio of PET to PBT, such copolymers should possess a sufficiently low crystallinity that quenching could result in an essentially amorphous polymer.
- A second route to producing amorphous polyester would be to increase the length of the flexible segment until the polymer is sufficiently inhibited from crystallization. This second suggestion however reduces the correlation of the results with commercial linear polyesters.

# BIBLIOGRAPHY


Aklonis, J.J. and MacKnight, W.J., *Introduction to Polymer Viscosity*, 2nd Ed., Wiley-Interscience Publications, John Wiley & Sons, New York (1983).

Billmeyer, F.W., *Textbook of Polymer Science*, 2nd Ed., Wiley-Interscience Publications, John Wiley & Sons, New York (1971).

Brunelle, D.J., *New Methods of Polymer Synthesis*, Vol. 2, Chapter 6: Macrocycles for the Synthesis of High Molecular Weight Polymers, J.R. Ebdon and G.C. Eastmond, ed., Blackie Academic & Professional, London, (1996).

Crompton, T.R., *Analysis of Polymers, an Introduction*, Pergamon Press, Oxford (1989).

Flory, P.J., *Principles of Polymer Chemistry*, Cornell University Press, Ithaca (1953).

Fox, T.G, Gratch, S., Loshaek, S., *Rheology - Theory and Applications*, Chapter 12: Viscosity Relationships for Polymers in Bulk and in Concentrated Solution, Frederick R. Eirich, ed., Academic Press, New York (1956).

Khoury, F., and Passaglia, E., *Treatise on Solid State Chemistry, Vol. 3, Crystalline and Non-crystalline Solids*, Chapter 6: The Morphology of Crystalline Synthetic Polymers, N.B. Hannay, ed., Plenum Press, New York (1976).

Nielsen, L.E., *Mechanical Properties of Polymers and Composites*, Vol. 2, Marcel Dekker, New York (1974).

Nielsen, L.E., *Polymer Rheology*, Marcel Dekker, New York (1977).

Odian, G., *Principles of Polymerization*, 3d Ed., Wiley-Interscience Publications, John Wiley & Sons, New York (1991).

Pascoe, K.J., *Failure of Plastics*, Chapter 7: General Fracture Mechanics, W. Brostow and R. Corneliussen, ed., SPE Publications, Hanser Press (1986).

Porter, R.S., and Johnson, J.F., The Entanglement Concept in Polymer Systems, Chemical Reviews, Vol. 66, No. 1, pp. 1-20 (1966).

Rodrigues, F., *Principles of Polymer Systems*, McGraw-Hill New York (1970).

Semlyen, J.A., *Cyclic Polymers*, Elsevier Applied Science Publishers, London and New York (1986).

Young, R.J., *Introduction to Polymers*, Chapman and Hall, London (1981).